TRANS NOW
TRANSPORTATION NORTHWEST

Final Report
TNW2011-11

Research Project Agreement No. 61-8058

Mechanical Properties of High-Volume SCM Concretes

Hannesson (Lehman-PI)

Department of Civil and Environmental Engineering
University of Washington
Seattle, WA 98195

A report prepared for

Transportation Northwest (TransNow)
University of Washington
112 More Hall, Box 352700
Seattle, Washington 98195-2700

and

Washington State Department of Transportation

May 2011

TECHNICAL REPORT STANDARD TITLE PAGE

1. REPORT NO. TNW2011-11	2. GOVERNMENT ACCESSION NO.	3. RECIPIENT'S CATALOG NO.	
4. TITLE AND SUBTITLE Mechanical Properties of High-Volume SCM Concretes		5.REPORT DATE 5-11 6. PERFORMING ORGANIZATION CODE	
7. AUTHOR(S) Hannesson		8. PERFORMING ORGANIZATION REPORT NO. **TNW2011-11**	
9. PERFORMING ORGANIZATION NAME AND ADDRESS Transportation Northwest Regional Center X (TransNow) Box 352700, 112 More Hall University of Washington Seattle, WA 98195-2700		10. WORK UNIT NO. 11. CONTRACT OR GRANT NO. DTRT07-G-0010	
12. SPONSORING AGENCY NAME AND ADDRESS United States Department of Transportation Office of the Secretary of Transportation 1200 New Jersey Ave, SE Washington, D.C. 20590		13. TYPE OF REPORT AND PERIOD COVERED Final Research Report 14. SPONSORING AGENCY CODE	
15. SUPPLEMENTARY NOTES			
17. KEY WORDS cement, SCC, SCM		18. DISTRIBUTION STATEMENT	
19. SECURITY CLASSIF. (of this report) None	20. SECURITY CLASSIF. (of this page) None	21. NO. OF PAGES 240	22. PRICE

ABSTRACT

Portland cement production is a major source of CO2 emissions worldwide. More sustainable cement-based systems can be developed through the use of supplementary cementitious materials (SCMs) to partially replace cement content. Total cement replaced is often limited due to the slow strength gain that is typically observed in these systems.

This research seeks to develop self-consolidating concrete (SCC) containing high volumes of SCM that is applicable for composite construction. Possible composite components that this concrete would be applicable for include concrete filled tubes for structural columns and dual skin composite shear walls to resist gravity and seismic loadings. In these applications, an outside structural steel member is available to take initial loadings as the concrete develops strength. However, the time-dependent behavior of the concrete must be known to predict the performance of the composite system. Test results indicate that SCCs containing high volumes of SCMs (60-90%) have similar engineering properties (creep, shrinkage, strength, elastic modulus) as conventional SCC at later ages (≥ 28 day). The data show that effective combinations of fly ash and slag can be obtained.

Mechanical Properties of High-Volume SCM Concretes

Guðmundur Marteinn Hannesson

A thesis submitted in partial fulfillment of the requirements for the degree of

Master of Science in Civil Engineering

University of Washington

2010

Program Authorized to Offer Degree: Civil and Environmental Engineering

University of Washington

Graduate School

This is to certify that I have examined this copy of a master's thesis by

Guðmundur Marteinn Hannesson

and have found that it is complete and satisfactory in all respects,

and that any and all revisions required by the final

examining committee have been made.

Committee Members:

_____

Dawn Lehman

_____

Katherine Kuder

_____

Charles W. Roeder

_____

Jeffrey W. Berman

Date:_____

In presenting this thesis in partial fulfillment of the requirements for a master's degree at the University of Washington, I agree that the Library shall make its copies freely available for inspection. I further agree that extensive copying of this thesis is allowable only for scholarly purposes, consistent with "fair use" as prescribed in the U.S. Copyright Law. Any other reproduction for any purposes or by any means shall not be allowed without my written permission.

Signature _____

Date_____

Abstract

Portland cement production is a major source of CO_2 emissions worldwide. More sustainable cement-based systems can be developed through the use of supplementary cementitious materials (SCMs) to partially replace cement content. Total cement replaced is often limited due to the slow strength gain that is typically observed in these systems.

This research seeks to develop self consolidating concrete (SCC) containing high volumes of SCM that is applicable for composite construction. Possible composite components that this concrete would be applicable for include concrete filled tubes for structural columns and dual skin composite shear walls to resist gravity and seismic loadings. In these applications, an outside structural steel member is available to take initial loadings as the concrete develops strength. However, the time-dependent behavior of the concrete must be known to predict the performance of the composite system.

The research was performed in two phases. In the first Phase, four SCMs were investigated: two fly ash and two slag. Twenty binary mixes (cement and one SCM) were made with 20%, 40%, 60%, 80% and 100% cement replacement and one control mix (only Portland cement). In the second Phase, two SCMs were investigated: one fly ash and one slag. A total of 16 mixes with 60%, 80% and 90% cement replacement were prepared: one control mix, 6 binary mixes and 9 ternary mixes (cement and two SCM). The ternary mixes were made with three different ratios of fly ash to slag to get a wide range of $CaO/(SiO_2+Al_2O_3)$ ratio in the binder. Compressive strength, elastic modulus, creep and shrinkage of the mixes were evaluated with time.

Early age compressive strength (≤ 14 days) development of the SCM mixtures was normally less than the control. At later ages, mixes with as much as 60% cement replacement has strengths that exceeded the control. At higher replacement levels, performance varied significantly based on the SCM used.

The control mix had a constant elastic modulus after 7 days while the SCM mixes showed gradual increase in the elastic modulus (40% increase on average). The elastic modulus of

the control mix was higher than the SCM mixes at early-age. As the curing period was extended, the SCM mixes exhibited higher elastic modulus.

Both sealed and unsealed concrete mixes were tested for creep behavior. The sealed cylinders showed less creep than the unsealed cylinders. SCM concrete mix cured for 28 days exhibit comparable creep behavior as conventional concrete cured for 7 days.

Test results indicate that SCCs containing high volumes of SCMs (60-90%) have similar engineering properties (creep, shrinkage, strength, elastic modulus) as conventional SCC at later ages ($\geq$ 28 day). The data show that effective combinations of fly ash and slag can be obtained.

A modified Bolomey strength equation was used to evaluate SCM's efficiency. Second-order polynomial regression was used to relate equivalent cement content to SCM content. A reasonable, linear relationship between binder's $CaO/(SiO_2+Al_2O_3)$ ratio and the efficiency factor was observed, suggesting that the chemistry of the SCMs can be used to predict compressive strength development. Expressions form ACI and CEB were used to evaluate the elastic modulus and combined Maxwell and Bingham rheological model was used to model the creep behavior of the concrete mix.

Acknowledgement

The author gratefully acknowledges the support of Lafarge North America, especially Rob Shogren for his contribution to this research. He also wishes to express his sincere appreciation to the faculty and staff of the Department of Civil and Environmental Engineering at University of Washington and Seattle University for their support. The research was funded by the Transportation Northwest, a Regional University Transportation Center (UTC). The author gratefully acknowledges this support. Most importantly, this could not have happened without the encouragement and devotion of my family and friends, especially my wonderful wife Bergþóra.

Table of Contents

Abstract i

Acknowledgement iii

List of Figures ix

List of Tables xviii

Chapter 1: Introduction 1

1.1 Hydraulic Reaction 2

1.2 Pozzolanic Reaction 4

1.3 Structural Applications and Research Objective 4

1.4 Scope of Report 5

Chapter 2: Previous Research of SCM Concretes 6

2.1 Compressive Strength Equations 6

2.1.1 Bolomey Strength Equation 6

2.1.2 Féret Strength Equation 6

2.1.3 Abrams Strength Equation 7

2.1.4 Efficiency Factor (k-value) 7

2.2 Literature Review 8

2.2.1 Antiohos, Papadakis, Chaniotakis, & Tsimas, 2007 10

2.2.2 Antiohos, Papageorgiou, Papadakis, & Tsimas, 2008 14

2.2.3 Babu & Kumar, 2000 17

2.2.4 Carette, Bilodeau, Chevrier, & Malhotra, 1993 22

2.2.5 Das & Yudhbir, 2006 30

2.2.6 Han, Kim, & Park, 2003 33

2.2.7 Hwang, Noguchi, Tomosawa, 2004 39

2.2.8 Langley, Carette, & Malhotra, 1989 43

2.2.9 Naik & Singh, 1997 48

2.2.10 Naik, Singh, & Ramme, 1998 53

2.2.11 Nasser and Al-Manaseer, 1986 57

2.2.12 Obla, Hill, Thomas, Shashiprakash, & Perebatova, 2003 62

2.2.13 Oner, Akyuz, & Yildiz, 2005 65

2.2.14 Oner & Akyuz, 2007 71

2.2.15 Papadakis & Tsimas, 2002 – Part I 78

2.2.16 Papadakis, Antiohos, & Tsimas, 2002 – Part II 82

2.2.17 Pekmezci & Akyuz, 2004 84

2.2.18 Rajamane, Peter, Ambily, 2007 88

2.2.19 Ravina & Mehta, 1988 92

2.2.20 Sivasundaram, Carette, & Malhotra, 1991 98

2.2.21 Tikalsky, Carrasquillo, & Carrasquillo, 1989 106

2.2.22 Valente, Vigneri, Bressan, Pasqualini, Bianchini, & Liberatore, 2010 110

2.3 Summary 116

Chapter 3: Test Matrix and Setup 117

3.1 Overview of Phase I and II 117

3.1.1 Materials 118

3.1.2 Mix Proportions 119

3.1.3 Specimens Preparation and Curing 120

3.1.4 Test Matrix 121

3.2 Procedures and Setup 123

3.2.1 Initial Time of Set 123
3.2.2 Compressive Strength 125
3.2.3 Compressive Modulus of Elasticity 127
3.2.4 Creep and Shrinkage Monitoring 132
3.2.5 Active Silica 139
Chapter 4: Measured Engineering Response of High Volume SCM Concrete 145
4.1 Initial Time of Set and Air Content 146
4.2 Compressive Strength Behavior 147
4.2.1 Phase I 147
4.2.2 Phase II 152
4.3 Elastic Modulus 156
4.4 Creep and Shrinkage Response 159
4.4.1 Total Strain 160
4.4.2 Shrinkage Strain 161
4.4.3 Total, Drying and Basic Creep 163
Chapter 5: Analytical Expressions for Mechanical Properties 169
5.1 Compressive Strength 169
5.1.1 Equivalent Cement Content 169
5.1.2 Chemical Composition Effect 174
5.2 Modulus of Elasticity 186
5.3 Rheological Model for Creep 187
5.3.1 Creep model – Constant Stress 189
5.3.2 Relaxation model – Constant Strain 191
Chapter 6: Conclusions and Recommendations 192

6.1 Conclusions 192

6.1.1 Time of Set 192

6.1.2 Compressive Strength 192

6.1.3 Elastic Modulus 194

6.1.4 Creep and Shrinkage Strains 195

6.2 Recommendations for Further Research 195

Appendix A – Temperature and Humidity Report 202

Appendix B – Compressive Strength Data 204

Appendix C – Elastic Modulus Data 211

Appendix D – Creep and Shrinkage Data 217

Appendix E – Measured and Calculated strength from this research 222

Appendix F – Measured and Calculated Compressive Strength from Prior Research 229

List of Figures

Figure 1.1. Rate of hydration of the cement compounds (Mindess, Young, & Darwin, 2003) 3

Figure 1.2. Compressive strength development in paste of the cement compounds (Mindess, Young, & Darwin, 2003) 4

Figure 2.1. Number of research programs that have tested SCM mixes for compressive strength..... 9

Figure 2.2. Compression test results for (a) 20% and (b) 30% by weight cement replacement (Antiohos, Papadakis, Chaniotakis, & Tsimas, 2007) 12

Figure 2.3. Compressive strength results of quicklime-activated fly ash mortars reproduced from Antiohos, et al. 2008 16

Figure 2.4. Compressive strength at 28 day versus w/b at different replacement levels (Babu & Kumar, 2000) 19

Figure 2.5. Compressive strength at 28 day versus w/(c+k_eg) at different replacement levels (Babu & Kumar, 2000) 20

Figure 2.6. Compressive strength at 28 day versus w/(c+kg) at different replacement levels (Babu & Kumar, 2000) 21

Figure 2.7. Assessment of the reliability of the efficiencies evaluated (Babu & Kumar, 2000) 22

Figure 2.8. Compressive strength development of concrete made with ASTM Type I cement brand C1 (Carette, Bilodeau, Chevrier, & Malhotra, 1993) 26

Figure 2.9. Compressive strength development of concrete made with ASTM Type I cement brand C2 (Carette, Bilodeau, Chevrier, & Malhotra, 1993) 26

Figure 2.10. Observed and predicted compressive strength at 91 days for (a) 10% replacement, (b) 20% replacement, (d) 50% replacement and at 365 days for (c) 35% replacement (Das & Yudhbir, 2006)..... 32

Figure 2.11. Experimental and calculated relative compressive strength (Han, Kim, & Park, 2003) 38

Figure 2.12. Compressive strength development (Hwang, Noguchi, & Tomosawa, 2004) ... 41

Figure 2.13. Relationship between calculated and measured strength (Hwang, Noguchi, & Tomosawa, 2004), ... 42

Figure 2.14. Compressive strength development of the concrete mixes reproduced from Langley, et al. 1989. Figure A) show mixes with ASTM Type I cement and Figure B) shows mixes made with ASTM Type III cement ... 45

Figure 2.15. Elastic modulus development between 28 and 365 days of the concrete mix reproduced from Langley, et al. 1989. Figure A) shows mixes with ASTM Type I cement and Figure B) shows mixes made with ASTM Type III cement ... 46

Figure 2.16. Drying shrinkage strains of control and fly ash concrete after 7 days of curing (Langley, Carette, & Malhotra, 1989) ... 47

Figure 2.17. Creep strains of control and fly ash concrete after 28 day of curing (Langley, Carette, & Malhotra, 1989) ... 48

Figure 2.18. The 28 day compressive strength for the mixes as function of replacement (Note that the strength is represented in MPa; this is probably an error and is most likely either psi or kPa) (Naik & Singh, 1997) ... 51

Figure 2.19. Initial setting of the for the four different SCMs (Naik & Singh, 1997) ... 52

Figure 2.20. Final setting of the for the four different SCMs (Naik & Singh, 1997) ... 52

Figure 2.21. Compressive strength development of the concrete mixes (Naik, Singh, & Ramme, 1998) ... 55

Figure 2.22. Elastic modulus development of the concrete mixes (Naik, Singh, & Ramme, 1998) ... 56

Figure 2.23. Shrinkage behavior of the unsealed specimens with and without admixtures (Nasser & Al-Manaseer, 1986) ... 59

Figure 2.24. Creep strain behavior at different stress/strength behavior of the unsealed specimens with admixtures (Nasser & Al-Manaseer, 1986) ... 60

Figure 2.25. Creep strain behavior at different stress/strength behavior of the sealed specimens with admixtures (Nasser & Al-Manaseer, 1986) 60

Figure 2.26. Creep versus stress/strength ratio for the unsealed specimen with and without admixtures (Nasser & Al-Manaseer, 1986) 61

Figure 2.27. Creep versus stress/strength ratio for the sealed specimen with and without admixtures (Nasser & Al-Manaseer, 1986) 61

Figure 2.28. Compressive strength development of the concrete mixes reproduced from Obla, et al. 2003 64

Figure 2.29. Autogenous shrinkage behavior of SF and UFFA concrete (Obla, Hill, Thomas, Shashiprakash, & Perebatova, 2003) 65

Figure 2.30. Efficiency factor versus FA content at 28 days, by using Bolomey (left) and Féret (right) strength equations (Oner, Akyuz, & Yildiz, 2005) 69

Figure 2.31. Efficiency factor versus FA content at 180 days, by using Bolomey (left) and Féret (right) strength equations (Oner, Akyuz, & Yildiz, 2005) 69

Figure 2.32. Equivalent cement content versus FA content at 28 days, by using Bolomey (left) and Féret (right) strength equations (Oner, Akyuz, & Yildiz, 2005)..... 70

Figure 2.33. Equivalent cement content versus FA content at 180 days, by using Bolomey (left) and Féret (right) strength equations (Oner, Akyuz, & Yildiz, 2005)..... 70

Figure 2.34. Compressive strength development of concrete mixes with 175 kg/m^3 dosage of cement (Oner & Akyuz, 2007)..... 74

Figure 2.35. Compressive strength development of concrete mixes with 210 kg/m^3 dosage of cement (Oner & Akyuz, 2007)..... 74

Figure 2.36. Compressive strength development of concrete mixes with 245 kg/m^3 dosage of cement (Oner & Akyuz, 2007)..... 75

Figure 2.37. Compressive strength development of concrete mixes with 280 kg/m^3 dosage of cement (Oner & Akyuz, 2007)..... 75

Figure 2.38. Efficiency factor versus GGBS content at 28 days using the Bolomey equation (Oner & Akyuz, 2007) 76

Figure 2.39. Efficiency factor versus GGBS content at 28 days using the Féret equation (Oner & Akyuz, 2007) 76

Figure 2.40. Equivalent cement content versus GGBS content at 28 days, by using Bolomey (left) and Féret (right) strength equations (Oner & Akyuz, 2007) 77

Figure 2.41. Equivalent cement content versus GGBS content at 365 days, by using Bolomey (left) and Féret (right) strength equations (Oner & Akyuz, 2007) 77

Figure 2.42. Compressive strength of the SCM concrete at age: (a) 2 days, (b) 7 days, (c) 28 days and (d) 90 days. The negative values refers to cement replacement and positive values refers to aggregate replacement (Papadakis & Tsimas, 2002) 80

Figure 2.43. Compressive strength of slag concrete compared to the control mix (Papadakis & Tsimas, 2002) 81

Figure 2.44. Relationship between pozzolan amount and 28 day compressive strength (Pekmezci & Akyüz, 2004) 87

Figure 2.45.Equivalent cement content versus natural pozzolan content at 28 days, by using Bolomey (left) and Féret (right) strength equations (Pekmezci & Akyüz, 2004) 88

Figure 2.46. Relationship between the efficiency factor and fly ash fraction in the binder (Rajamane, Peter, & Ambily, 2007) 91

Figure 2.47. Relationship between calculated and measured strength reproduced from Rajamane, et al. 2007 92

Figure 2.48. Compressive strength development of concrete mixes using Class F fly ash as cement replacement (Ravina & Mehta, 1988) 96

Figure 2.49. Compressive strength development of concrete mixes using Class C fly ash as cement replacement (Ravina & Mehta, 1988) 97

Figure 2.50. Compressive strength development of the SCM concrete mixes that contained 155 kg/m^3 of cement (Sivasundaram, Carette, & Malhotra, 1991) 102

Figure 2.51. Compressive strength development of the SCM concrete mixes that contained 225 kg/m^3 of cement (Sivasundaram, Carette, & Malhotra, 1991) 102

Figure 2.52. Creep strain behavior of the SCM concrete mixes that contained 155 kg/m^3 of cement (Sivasundaram, Carette, & Malhotra, 1991) 105

Figure 2.53. Creep strain behavior of the SCM concrete mixes that contained 225 kg/m^3 of cement (Sivasundaram, Carette, & Malhotra, 1991) 105

Figure 2.54. Compressive strength development of concrete containing Class F fly ash (1 psi =6895 Pa) (Tikalsky, Carrasquillo, & Carrasquillo, 1989)..... 108

Figure 2.55. Compressive strength development of concrete containing Class C fly ash (1 psi =6895 Pa) (Tikalsky, Carrasquillo, & Carrasquillo, 1989)..... 108

Figure 2.56. Creep of the concrete (Tikalsky, Carrasquillo, & Carrasquillo, 1989) 109

Figure 2.57. Efficiency factor versus fly ash content for 28 day compressive strength (Valente, Vigneri, Bressan, Pasqualini, Bianchini, & Liberatore, 2010)..... 114

Figure 2.58. Efficiency factor versus fly ash content for 90 day compressive strength (Valente, Vigneri, Bressan, Pasqualini, Bianchini, & Liberatore, 2010)..... 114

Figure 2.59. Total equivalent cement content versus fly ash content at 28 and 90 day (Valente, Vigneri, Bressan, Pasqualini, Bianchini, & Liberatore, 2010)..... 115

Figure 3.1. Photograph of a rotary drum mixer 121

Figure 3.2. Photograph of casting of cylinders 121

Figure 3.3. Instruments needed for initial time of set 124

Figure 3.4. Compressive test setup 125

Figure 3.5. Photograph of the compressive strength set up 126

Figure 3.6. Photograph of the compressive apparatus at Lafarge North America..... 127

Figure 3.7. Photograph of the compressive test apparatus at University of Washington 127

Figure 3.8. Compressometer 128

Figure 3.9. Diagram of displacement..... 129

Figure 3.10. Photograph of Baldwin 300kip machine 130

Figure 3.11. Photograph of the elastic modulus setup 130

Figure 3.12. Typical stress-strain diagram for concrete and the points needed to determine the chord modulus of elasticity 131

Figure 3.13. Creep rig 133

Figure 3.14. Whittemore strain gauge and target 134

Figure 3.15. Target layout 135

Figure 3.16. Photograph of the target layout 135

Figure 3.17. Photograph of the creep rigs with the installed cylinders 136

Figure 3.18. Photograph of the shrinkage cylinders 137

Figure 3.19. Photograph of the Whittemore strain gauge 138

Figure 3.20. Hot plate 140

Figure 3.21. Filter apparatus 141

Figure 3.22. Reflux apparatus 141

Figure 3.23. Photograph of the evaporation setup 142

Figure 3.24. Photograph of the reflux setup 143

Figure 3.25. Photograph of the filter setup 143

Figure 4.1. The initial time of set of the binary SCM mixes (w/b = 0.35). 147

Figure 4.2. Strength development of the 20% SCM mixes and the Base I (w/b = 0.35)..... 149

Figure 4.3. Strength development of the 40% SCM mixes and the Base I (w/b = 0.35)..... 150

Figure 4.4. Strength development of the 60% SCM mixes and the Base I (w/b = 0.35)..... 150

Figure 4.5. Strength development of the 80% SCM mixes and the Base I (w/b = 0.35)..... 151

Figure 4.6. Strength development of the 100% SCM mixes and the Base I (w/b = 0.35).... 151

Figure 4.7. Compressive strength at 56 days versus cement replacement percentage 152

Figure 4.8. Comparison of Base I and Base II 154

Figure 4.9. Strength development of the 60% SCM mixes and the Base II (w/b = 0.40) 154

Figure 4.10. Strength development of the 80% SCM mixes and the Base II (w/b = 0.40) .. 155

Figure 4.11. Strength development of the 90% SCM mixes and the Base II (w/b = 0.40) .. 155

Figure 4.12. Strength development of the ternary mixes to the Base II (w/b = 0.40) 156

Figure 4.13. Elastic modulus of the 60% ternary SCM mixes and Base II (w/b = 0.40) 158

Figure 4.14. Elastic modulus of the 80% ternary SCM mixes and Base II (w/b = 0.40) 158

Figure 4.15. Elastic modulus of the 90% ternary SCM mixes and Base II (w/b = 0.40) 159

Figure 4.16. Total strain of the unsealed cylinders 161

Figure 4.17. Total strain of the sealed cylinders 161

Figure 4.18. Shrinkage strain of the unsealed cylinders since removal from fog room 162

Figure 4.19. Shrinkage strain of the sealed cylinders since removal from fog room 163

Figure 4.20. Elastic and creep strain of the unsealed cylinders since loading 164

Figure 4.21. Elastic and creep strain of the sealed cylinders since loading 165

Figure 4.22. Creep strain of the unsealed cylinders since loading (total creep) 165

Figure 4.23. Creep strain of the sealed cylinders since loading (basic creep) 166

Figure 4.24. Drying creep strain of the cylinders since loading 166

Figure 4.25. Creep coefficient of the unsealed cylinders since loading since loading 167

Figure 4.26. Creep coefficient of the sealed cylinders since loading since loading 168

Figure 5.1. Equivalent cement content versus cement replacement – Boardman FA (w/b = 0.35) 170

Figure 5.2. Equivalent cement content versus cement replacement – Centralia FA (w/b = 0.35) 170

Figure 5.3. Equivalent cement content versus cement replacement – Seattle SL (w/b = 0.35) 171

Figure 5.4. Equivalent cement content versus cement replacement – St. Mary's SL (w/b = 0.35) 171

Figure 5.5. Calculated versus measured compressive strength of the binary SCM (w/b = 0.35), using the Bolomey strength equation and calibrated kP expression (Table 5.1)..... 173

Figure 5.6. Measured and calculated strength using k-values from Table 5.2 174

Figure 5.7. Relationship between the total C/(S+A) ratio and the 28-day strength..... 176

Figure 5.8. Relationship between the total C/(S+A) ratio and the 56-day strength..... 176

Figure 5.9. Equivalent cement content versus the total C/(S+A) at an age of 28 days..... 177

Figure 5.10. Equivalent cement content versus the total C/(S+A) at an age of 56 days..... 178

Figure 5.11. Efficiency factor (k-value) versus the total C/(S+A) at an age of 7 days..... 179

Figure 5.12. Efficiency factor (k-value) versus the total C/(S+A) at an age of 14 days..... 179

Figure 5.13. Efficiency factor (k-value) versus the total C/(S+A) at an age of 28 days..... 180

Figure 5.14. Efficiency factor (k-value) versus the total C/(S+A) at an age of 56 days..... 180

Figure 5.15. The correlation between the slope, H(t), and time 181

Figure 5.16. Calculated versus measured compressive using proposed efficiency expression 182

Figure 5.17. Calculated versus measured compressive strength using proposed efficiency expression (separated with replacement percentage)..... 182

Figure 5.18. Calculated versus measured compressive strength from the prior research using proposed efficiency expression..... 183

Figure 5.19. Calculated versus measured compressive strength from the prior research using proposed efficiency expression without the data from Naik, et al. 1998..... 184

Figure 5.20. Calculated versus measured compressive strength from the prior research using proposed efficiency expression (separated with replacement percentage) 185

Figure 5.21. Calculated/Measured strength at 28 days versus w/b ratio from the prior research 185

Figure 5.22. Calculated versus measured elastic modulus by using the ACI equation, Eq. (5.2) 186

Figure 5.23. Calculated versus measured elastic modulus by using the CEM equation, Eq. (5.3) 187

Figure 5.24. One dimensional mechanical device 188

Figure 5.25. Comparison of test data and model for unsealed cylinders (total creep) 190

Figure 5.26. Comparison of test data and model for sealed cylinders (basic creep) 191

List of Tables

Table 2.1. Summary of reviewed papers that covered concrete containing SCM 9

Table 2.2. Mix proportions applied for preparing the fly ash intermixture (Antiohos, Papadakis, Chaniotakis, & Tsimas, 2007) 10

Table 2.3. Physical properties and chemical analysis (%) of cement and fly ash (Antiohos, Papadakis, Chaniotakis, & Tsimas, 2007) 11

Table 2.4. Efficiency factors of binary and ternary blended cements for 20% and 30% by weight of cement replacement (Antiohos, Papadakis, Chaniotakis, & Tsimas, 2007)..... 13

Table 2.5. Calculated and measured k-value of the intermixtures at 28 and 90 days (Antiohos, Papadakis, Chaniotakis, & Tsimas, 2007) 13

Table 2.6. Physical properties and chemical analysis (%) of cement and fly ash (Antiohos, Papageorgiou, Papadakis, & Tsimas, 2008) 15

Table 2.7. Mix proportions of specimens tested (% by weight of cementitious material) (Antiohos, Papageorgiou, Papadakis, & Tsimas, 2008) 15

Table 2.8. Compressive strength results of quicklime-activated fly ash mortars (Antiohos, Papageorgiou, Papadakis, & Tsimas, 2008) 16

Table 2.9. Efficiency factor (k-value) for cement-fly ash and cement-fly ash-quicklime mortars (Antiohos, Papageorgiou, Papadakis, & Tsimas, 2008) 17

Table 2.10. Details of the concrete evaluated (Babu & Kumar, 2000)..... 18

Table 2.11. Physical properties and chemical analysis (%) of cement and fly ashes (Carette, Bilodeau, Chevrier, & Malhotra, 1993) 24

Table 2.12. Mixture proportions and properties of fresh concrete (Carette, Bilodeau, Chevrier, & Malhotra, 1993) 24

Table 2.13. Compressive strength results of the mixes (Carette, Bilodeau, Chevrier, & Malhotra, 1993)..... 25

Table 2.14. Elastic modulus results of the mixes (Carette, Bilodeau, Chevrier, & Malhotra, 1993) 27

Table 2.15. Drying shrinkage test results after 7 days of curing (Carette, Bilodeau, Chevrier, & Malhotra, 1993) 28

Table 2.16. Drying shrinkage test results after 91 days of curing (Carette, Bilodeau, Chevrier, & Malhotra, 1993) 28

Table 2.17. Creep results of the concrete mixtures (Carette, Bilodeau, Chevrier, & Malhotra, 1993) 29

Table 2.18.The range of parameter used for model input (Das & Yudhbir, 2006) 30

Table 2.19. Compressive strength results of the mixes (Das & Yudhbir, 2006) 31

Table 2.20.The regression coefficients and correlation coefficient (R^2) at different days and cement replacements (Das & Yudhbir, 2006)..... 32

Table 2.21. Physical properties and chemical analysis (%) of cement and fly ash (Han, Kim, & Park, 2003)..... 34

Table 2.22. Mixture proportions and properties of fresh concrete (Han, Kim, & Park, 2003)35

Table 2.23. Compressive strength results of the mixes (Han, Kim, & Park, 2003)..... 36

Table 2.24. Physical properties of cement and fly ash (Hwang, Noguchi, & Tomosawa, 2004) 39

Table 2.25. Mixture proportions and properties of fresh concrete (Hwang, Noguchi, & Tomosawa, 2004)..... 40

Table 2.26. Physical properties and chemical analysis (%) of cements and fly ash (Langley, Carette, & Malhotra, 1989)..... 44

Table 2.27. Mixture proportions and properties of fresh concrete (Langley, Carette, & Malhotra, 1989)..... 44

Table 2.28. Compressive strength results of the mixes (Langley, Carette, & Malhotra, 1989) 45

Table 2.29. Elastic modulus results of the mixes (Langley, Carette, & Malhotra, 1989) 46

Table 2.30. Physical properties and chemical analysis (%) of cement and fly ash (Naik & Singh, 1997) 49

Table 2.31. Mixture proportions and properties of fresh concrete (Naik & Singh, 1997)..... 50

Table 2.32. Summary of times of setting for the different SCMs; hr:min (Naik & Singh, 1997) 51

Table 2.33. Physical properties and chemical analysis (%) of cements and fly ash (Naik, Singh, & Ramme, 1998) 54

Table 2.34. Mixture proportions and properties of fresh concrete (Naik, Singh, & Ramme, 1998) 54

Table 2.35. Compressive strength results of the mixes (Naik, Singh, & Ramme, 1998) 55

Table 2.36. Elastic modulus results of the mixes (Naik, Singh, & Ramme, 1998) 56

Table 2.37. Drying shrinkage results of the mixes (Naik, Singh, & Ramme, 1998) 56

Table 2.38. Physical properties and chemical analysis (%) of cement and fly ash (Nasser & Al-Manaseer, 1986) 58

Table 2.39. Mixture proportions and properties of fresh concrete (Nasser & Al-Manaseer, 1986) 58

Table 2.40. Physical properties and chemical analysis (%) of cements and fly ash (Obla, Hill, Thomas, Shashiprakash, & Perebatova, 2003) 63

Table 2.41. Mixture proportions and properties of fresh concrete (Obla, Hill, Thomas, Shashiprakash, & Perebatova, 2003) 63

Table 2.42. Compressive strength results of the mixes (Obla, Hill, Thomas, Shashiprakash, & Perebatova, 2003) 64

Table 2.43. Physical properties and chemical analysis (%) of cement and fly ash (Oner, Akyuz, & Yildiz, 2005) 66

Table 2.44. Mixture proportions and properties of fresh concrete (Oner, Akyuz, & Yildiz, 2005) 67

Table 2.45. Compressive strength results of the mixes (Oner, Akyuz, & Yildiz, 2005) 68

Table 2.46. Physical properties and chemical analysis (%) of cement and GGBS (Oner & Akyuz, 2007) 71

Table 2.47. Mixture proportions and properties of fresh concrete (Oner & Akyuz, 2007) 72

Table 2.48. Compressive strength results of the mixes (Oner & Akyuz, 2007) 73

Table 2.49. Physical properties and chemical analysis (%) of cement and SCMs (Papadakis & Tsimas, 2002) 79

Table 2.50. Mixture proportions of concretes, the minus refers to cement replacement and plus to aggregate replacement (Papadakis & Tsimas, 2002) 79

Table 2.51. Efficiency factor (k-value) for fly ashes and natural pozzolans (Papadakis & Tsimas, 2002) 81

Table 2.52. Comparison of calculated and measured activity index (Papadakis, Antiohos, & Tsimas, 2002) 83

Table 2.53. Calculated and Measured k-value, using Eq. (2.21) and data from Papadakis et al, et al. 2002 – Part I and II 84

Table 2.54. Physical properties and chemical analysis (%) of cement and natural pozzolan (Pekmezci & Akyüz, 2004) 85

Table 2.55. Mixture proportions and properties of fresh concrete (Pekmezci & Akyüz, 2004) 86

Table 2.56. Compressive strength results after 28 days of curing (Pekmezci & Akyüz, 2004) 86

Table 2.57. Physical properties and chemical analysis (%) of cement and fly ash (Rajamane, Peter, & Ambily, 2007) 89

Table 2.58. Mixture proportions and 7 and 28 day strength of the concrete (Rajamane, Peter, & Ambily, 2007) 90

Table 2.59. Physical properties and chemical analysis (%) of cement and fly ashes (Ravina & Mehta, 1988) 93

Table 2.60. Mixture proportions and properties of fresh concrete (Ravina & Mehta, 1988) . 94

Table 2.61. Compressive strength results of the mixes (Ravina & Mehta, 1988) 95

Table 2.62. Physical properties and chemical analysis (%) of cement and fly ashes (Sivasundaram, Carette, & Malhotra, 1991) 99

Table 2.63. Mixture proportions and properties of fresh concrete (Sivasundaram, Carette, & Malhotra, 1991)..... 100

Table 2.64. Compressive strength results of the mixes (Sivasundaram, Carette, & Malhotra, 1991) 101

Table 2.65. Elastic modulus results of the mixes (Sivasundaram, Carette, & Malhotra, 1991) 103

Table 2.66. Creep results of the concrete mixtures..... 104

Table 2.67. Physical properties and chemical analysis (%) of cements and fly ashes (Tikalsky, Carrasquillo, & Carrasquillo, 1989) 107

Table 2.68.The basic mixture proportions of the concrete (Tikalsky, Carrasquillo, & Carrasquillo, 1989) 107

Table 2.69. Physical properties and chemical analysis (%) of cement and fly ash (Valente, Vigneri, Bressan, Pasqualini, Bianchini, & Liberatore, 2010) 111

Table 2.70. Mixture proportions and properties of fresh concrete (Valente, Vigneri, Bressan, Pasqualini, Bianchini, & Liberatore, 2010) 112

Table 2.71. Compressive strength results of the mixes (Valente, Vigneri, Bressan, Pasqualini, Bianchini, & Liberatore, 2010)..... 113

Table 3.1. Physical properties and chemical analysis (%) of cement, fly ash (FA) and slag (SL) in Phase I 119

Table 3.2. Physical properties and chemical analysis (%) of cement, fly ash (FA) and slag (SL) in Phase II 119

Table 3.3. Mix proportions of the specimens in Phase I and II 120

Table 3.4. Phase I: Binary mixes and test overview 122

Table 3.5. Phase II: Binary and ternary mixes and test overview..... 123

Table 4.1. Mixture proportions and name convention of Phase I..... 145

Table 4.2. Mixture proportions and name convention of Phase II..... 146

Table 4.3.The air content in the mixes and the initial time of set with fly ash (FA) or slag (SL) as cement replacement..... 147

Table 4.4. Compressive strength of SCC, with standard deviation, with fly ash (F) or slag (S) as cement replacement (w/b = 0.35) 149

Table 4.5. Compressive strength of SCC, with standard deviation, with fly ash (F) or slag (S) as cement replacement (w/b = 0.40) 153

Table 4.6. Elastic modulus of SCC, with standard deviation, with Boardman fly ash (BF) and Seattle slag (SS) as cement replacement (w/b = 0.40)..... 157

Table 4.7. Stress/Strength ratio in the creep test..... 160

Table 4.8. Creep results of the concrete mixtures..... 163

Table 5.1. Coefficients of second-order polynomial regression and R^2 values for Bolomey strength equations (FA = fly ash and SL = slag) 172

Table 5.2. Measured and calculated k-values using Eq. (2.21) at an age of 28 days 174

Table 5.3. Slope at each age, standard error, R^2-value and number of data points 178

Table 5.4. Material constants for creep model..... 190

Chapter 1: Introduction

Cement production is one of the major sources of CO_2 emissions in the world. According to the European Cement Association, cement production was responsible for 2.83 billion tons of CO_2 emissions (roughly 2.3% of the total emissions) worldwide in 2008 (CEMBUREAU, 2009). Portland cement has so far been the primary content in the binder of concrete. Therefore, lowering the amount of cement in the binder could reduce concrete's carbon footprint (Mehta, 2009; Malhotra, 2006). Materials that are commonly used as cement replacement in concrete are fly ash and slag.

Fly ash is a by-product material that is widely available in the world. Fly ash is the inorganic, noncombustible residue of powdered coal after burning in power plants. The molten particles are swept out of the furnace with the stack gases and collected by electrostatic precipitators. Fly ash is employed in a wide variety of construction applications (Mindess, Young, & Darwin, 2003). Slag is residue from metallurgical processes, either from production of metals from ore or refinement of impure metals. The slag used in concrete typically come from the blast furnace production of iron from ore.

Slag can be used in large quantities as a supplementary cementitious material (SCM) because of its inherent cementitious properties. Fly ash; however, is limited by the amount of calcium oxide in the binder with which it can react (Mindess, Young, & Darwin, 2003). Even so, a concrete with 100% Class C fly ash for binder was used in a commercial cast-in-place application. This concrete was used in the foundation walls and footings, the floor slab, two structural load-bearing beams, and various nonstructural elements such as architectural panels. The structure has now been operational for over a year (Cross, Stephens, & Berry, 2010).

SCMs are commonly used in concrete because they improve both durability and the interface with aggregate. SCMs also reduce porosity in the concrete. Using fly ash as SCM in a concrete mix increases the workability of fresh concrete because the fly ash particles are more spherically shaped than cement, which results in less water demand. However, there is a high material variability associated with SCM which affects their efficiency and concrete containing SCMs tends to have slower strength development especially at high cement

replacement rates, since the Portland cement reaction (hydraulic) is much faster than the SCM reaction (mostly pozzolanic).

1.1 Hydraulic Reaction

The hydraulic reaction of Portland cement consists mostly of a reaction of four compounds: tricalcium silicate (C_3S), dicalcium silicate (C_2S), tricalcium aluminate (C_3A) and tetracalcium aluminoferrite (C_4AF). The Bogue calculation (ASTM C 150, 2009) can be used to approximate the amount of each compound. The C_3S and C_2S react with water (H) and form calcium-silicate-hydrate (C-S-H) and calcium hydroxide (CH). The reactions are expressed as follows:

$$2C_3S + 11H \rightarrow C\text{-}S\text{-}H + 3CH \tag{1.1}$$

$$2C_2S + 9H \rightarrow C\text{-}S\text{-}H + CH \tag{1.2}$$

C-S-H makes up over one half of the volume of a hydrated paste and is the most important component. The CH crystals occupy about 20-25 % of the paste's solid volume. CH contributes slightly to the binder's strength but is more soluble than C-S-H. CH is considered to be the weakness in the binder's strength.

The C_3A compound reacts with water and gypsum ($C\bar{S}H_2$) and forms ettringite ($C_6A\bar{S}_3H_{32}$):

$$C_3A + 3C\bar{S}H_2 + 26H \rightarrow C_6A\bar{S}_3H_{32} \tag{1.3}$$

Ettringite causes expansion in the cement paste, but it can contribute to early strength. If not enough gypsum is available to react with C_3A, the C_3A will react with water alone which leads to a flash set. Gypsum is thus often added to cement to prevent a flash set. If too much gypsum is added, then more ettringite will be formed long after setting, which may disrupt the paste sufficiently enough to lower the compressive strength of the paste or even, in extreme cases, cause cracking.

The C_4AF reaction forms similar hydration products as C_3A, with or without gypsum. The reaction is slower and seldom causes a flash set. The rates of hydration for the cement compounds are shown in Figure 1.1. It can be seen that C_3A and C_3S are the most reactive compounds, whereas C_2S reacts slower.

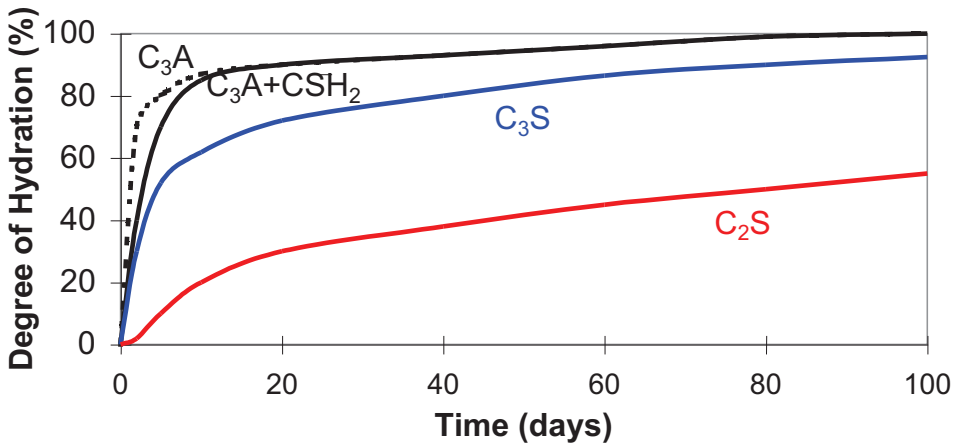

Figure 1.1. Rate of hydration of the cement compounds (Mindess, Young, & Darwin, 2003)

Rates of reactions do not necessarily have a direct impact on strength development. Figure 1.2 displays the compressive strength development of the cement compound. Clearly, the calcium silicate compounds provide the majority of the strength development in Portland cement. C_3S provides most of the early strength and both C_3S and C_2S contribute equally to final strength. The C_3A reacts instantly with minimal contribution to the early age strength.

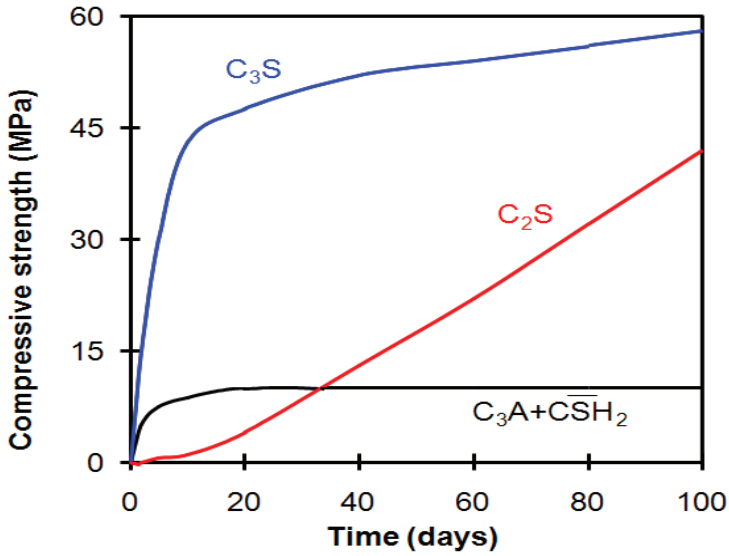

Figure 1.2. Compressive strength development in paste of the cement compounds (Mindess, Young, & Darwin, 2003)

1.2 Pozzolanic Reaction

The pozzolanic reaction of SCMs consists mostly of a reaction of two compounds, amorphous or glassy silica (S) and aluminum oxide (A). S is the major component of SCMs and reacts with water (H) and CH, which is formed from the hydration of the calcium silicates. The principal pozzolanic reaction is thus:

$$S + CH + H \rightarrow C\text{-}S\text{-}H \tag{1.4}$$

Small quantities of reactive aluminum oxide in SCMs can substitute for silica as part of the C-S-H. When SCMs have appreciable quantities of reactive aluminum oxide, a separate set of secondary reactions can occur, leading to formation of calcium-aluminates-hydrates (C-A-H):

$$CH + A + H \rightarrow C\text{-}A\text{-}H \tag{1.5}$$

C-A-H and C-S-H have similar crystal structures and therefore contribute equally to the paste strength. Calcium hydroxide, produced by the hydration of Portland cement, is consumed by the pozzolanic reaction. The pozzolanic reaction can thus only take place after the hydraulic reaction starts. The primary pozzolanic reaction, Eq. (1.4), has kinetics similar to the slow rate hydration of C_2S, Eq.(1.2). Hence, adding SCMs to the binder has a similar effect as raising the C_2S content in cement. Therefore, the pozzolanic reaction has a more significant impact on the long-term strength and less significant impact on the early strength. Since the pozzolanic reaction results in an overall increase in solid volume, the paste porosity will eventually be reduced, resulting in higher strength and durability compared with plain paste of comparable reaction.

1.3 Structural Applications and Research Objective

The aim of this research is to minimize Portland cement content and, therefore, the embedded carbon content in self consolidating concrete (SCC) for structural applications by

maximizing the SCM content. SCC has advantages in reinforced concrete and composite construction by facilitating rapid construction. Possible composite components include concrete filled tubes for structural columns and dual skin composite shear walls to resist gravity and seismic loadings. An advantage of using a high-volume SCM concrete in these applications is that early strength is not required from the concrete, since the steel jacket is capable of supporting the initial construction loads and formwork is not removed (as would be required for a reinforced concrete component). Therefore, concrete containing high volume of SCMs can be more readily used in composite constructions, even though a low early strength (≤ 14 days) is often associated with such concrete.

1.4 Scope of Report

Chapter 2 provides a summary of the experimental research that has been performed on concrete mixes that contains high volume of fly ash and slag. Only research data that focuses on compressive strength, elastic modulus, shrinkage, creep and time of set will be covered in this chapter.

Chapter 3 presents an overview of the materials that were used in the concrete mixes in addition to test setup and test procedure for the mixes that were tested for mechanical properties.

Chapter 4 presents the results of the material testing program. The tests were performed in two phases. Phase I had a water-binder-ratio of 0.35 and Phase II had a water-binder-ratio of 0.40. In the first Phase compressive strength, initial time of set and air content were measured. In the second Phase elastic modulus, creep and shrinkage strains as well as compressive strength were measured.

Chapter 5 provides analytical expressions to determine compressive strength and elastic modulus of the concrete mixes. A creep model was used to model the creep behavior of the concrete mixes.

Chapter 6 concludes the report with a brief summary of the tests performed, observations, research conclusions, and recommendations for future research of concrete that contains high volume of SCMs.

Chapter 2: Previous Research of SCM Concretes

This chapter provides a summary of the experimental research that has been performed on concrete mixes that contains high volume of fly ash and slag. Only research data that focuses on compressive strength, elastic modulus, shrinkage, creep and time of set will be covered in this chapter. For each research program, the objective, material and mix design, experimental results and conclusions are provided. A brief summary about compressive strength equations and efficiency factor (k-value) concept is provided prior the research summaries. Some of these expressions have been applied to the prior research results and this research program. Section 2.1 provides the compressive strength equations

2.1 Compressive Strength Equations

Equations to estimate the expected strength for specific concrete mix containing SCM have been proposed. Some equations are function of activation energy, which is the minimum energy required for a chemical reaction to take place (Han, Kim, & Park, 2003). Others have linked the compressive strength to the SCM's fineness, the amount of CaO, loss of ignition, and ratio of potassium to alumina (Das & Yudhbir, 2006). Common strength equations in design depend primarily on the water-to-binder ratio (w/b). The most common equations include Bolomey (1922), Féret (1892) and Abrams (1918) strength equations (Brandt, 1995).

2.1.1 Bolomey Strength Equation

The Bolomey strength equation is time dependant and is expressed as:

$$f_c' = K_B\left(\frac{1}{w/c} - a(t)\right) \tag{2.1}$$

where K_B (MPa) is the Bolomey coefficient and depends on mix design and age, $a(t)$ is a coefficient depending mainly on time and curing, f'_c is the compressive strength of concrete (MPa), c is cement mass in concrete (kg/m^3) and w is the water mass in concrete (kg/m^3).

2.1.2 Féret Strength Equation

The Féret strength equation is time dependant and is expressed as:

$$f_c' = K_F \left(\frac{V_c}{V_c + V_w + V_a} \right)^2 \quad \textbf{(2.2)}$$

where K_F (MPa) is the Féret coefficient and depends on mix design and age, f'_c is the compressive strength of concrete (MPa), V_c is cement volume in concrete (m^3/m^3), V_w is the water volume in concrete (m^3/m^3) and V_a is the air volume in concrete (m^3/m^3).

2.1.3 Abrams Strength Equation

The Abrams strength equation is time dependant and is expressed as:

$$f_c' = \frac{A_1}{B_1^{w/c}} \quad \textbf{(2.3)}$$

where A_1 and B_1 are empirical constants that depend on mix design and age, f'_c is the compressive strength of concrete (MPa), c is cement mass in concrete (kg/m^3) and w is the water mass in concrete (kg/m^3).

K_B, $a(t)$, K_F, A_1 and B_1 are all evaluated using a linear regression of experimental data.

2.1.4 Efficiency Factor (k-value)

The efficiency factor (*k*-value) is defined as the portion of the SCM that can be considered equivalent to Portland cement (Papadakis & Tsimas, 2002). Therefore, a value of k = 1 indicates that, in terms of the compressive strength performance, the SCM is equivalent to cement. A value of k less than one indicates that the performance of the SCM is inferior to cement. The quantity of the SCM is multiplied by the *k* value to estimate the equivalent cement content, which can be added to the Portland cement content to determine of the resulting effective w/b ratio, required cement content, etc. The *k*-value is usually associated with the compressive strength, but can also be used to quantify other parameters such as chloride penetration (Papadakis & Tsimas, 2002).

It has been shown that the Bolomey strength equation can be simplified in many cases by substituting $a(t) = -0.5$, for structural grade concrete (Rajamane, Peter, & Ambily, 2007).

Structural concrete, according to the ACI, shall not have strength less than 17.2 MPa (2500 psi) (ACI Committee 318, 2008). The modified Bolomey equation using the concept of the efficiency factor, will be:

$$f_c' = K_B\left(\frac{1}{w/(c+kP)} - 0.5\right) \tag{2.4}$$

where the *k*-value is the efficiency factor of the SCMs and is both dependent on time and replacement percentage. The variable *P* is the SCM mass in the concrete (kg/m^3). Using the product of *k*-value and *P* as the effective binder portion of the SCM, the Féret and Abrams equations can be converted similarly to:

$$f_c' = \left(\frac{V_c + kV_p}{V_c + kV_p + V_w + V_a}\right)^2 \tag{2.5}$$

$$f_c' = \frac{A_1}{B_1^{w/(c+kP)}} \tag{2.6}$$

where the *k*-value is the efficiency factor of the SCMs and *P* the SCM mass as before, V_p is the SCM content in the concrete (m^3/m^3). Thus, both kP and kV_p are considered to be the equivalent cement content.

2.2 Literature Review

Considerable amount of research has been done on concrete that contains SCMs. Table 2.1 summarizes the research that were reviewed. All the research provided compressive strength data on the concrete that contained SCM, except the research performed by Nasser, et al. (Nasser & Al-Manaseer, 1986). Many authors have focused on the efficiency factor (k-value) concept. Others focused more at the mechanical and durability properties, including shrinkage and creep, of the SCM concretes. Only one research program (Naik & Singh, 1997) performed a comprehensive study on time of set with various fly ash and replacements. Figure 2.1 provides a histogram with the number of research programs that

have tested SCM mixes for compressive strength and the SCM percentage of the total binder. Most common percentage levels were on the order of 20-50%.

Table 2.1. Summary of reviewed papers that covered concrete containing SCM

Reference	Year	%	Experimental data					
			Compressive strength	Efficiency factor	Elastic Modulus	Shrinkage Strain	Creep Strain	Time of set
Antiohos, et al.	2007	20-30	X	X				
Antiohos, et al.	2008	20	X	X				
Babu, et al.	2000	0-80	X	X				
Carette, et al.	1993	58	X			X	X	
Das, et al.	2006	0-50	X					
Han, et al.	2003	0-30	X					
Hwang, et al.	2004	0-49	X					
Langley, et al.	1989	55-56	X		X	X	X	
Naik, et al.	1997	0-100	X					X
Naik, et al.	1998	0-40	X		X	X		
Nasser, et al.	1986	20				X	X	
Obla, et al.	2003	0-11	X			X		
Oner, et al.	2005	0-37	X	X				
Oner, et al.	2007	0-61	X	X				
Papadakis, et al. – I	2002	0-20	X	X				
Papadakis, et al. – II	2002	0-20	X	X				
Pekmezci, et al.	2004	0-29	X	X				
Rajamane, et al.	2007	0-49	X	X				
Ravina, et al.	1988	0-60	X					
Sivasundaram, et al.	1991	58	X		X		X	
Tikalsky, et al.	1987	0-35	X			X	X	
Valente, et al.	2010	0-35	X	X				

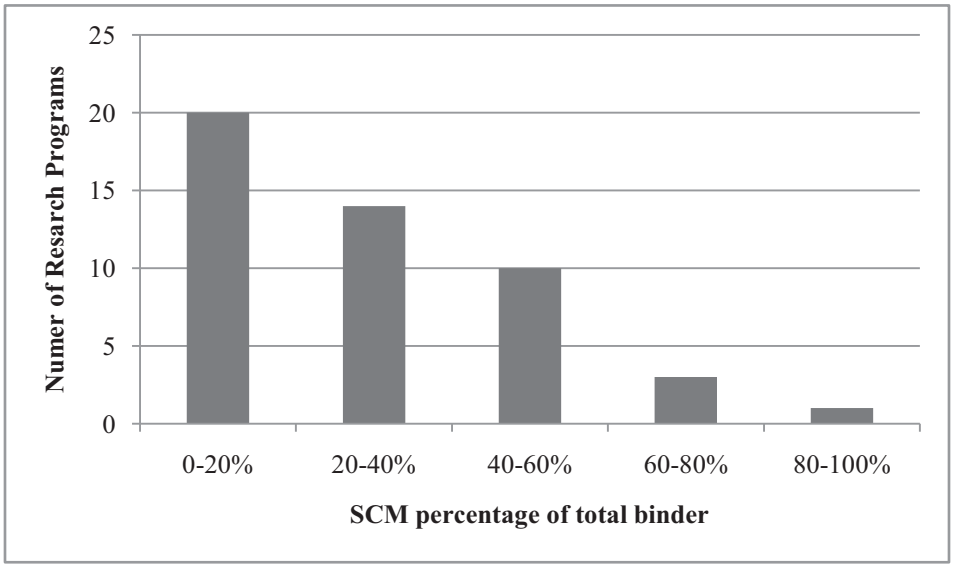

Figure 2.1. Number of research programs that have tested SCM mixes for compressive strength

2.2.1 Antiohos, Papadakis, Chaniotakis, & Tsimas, 2007

Improving the performance of ternary blended cements by mixing different types of fly ashes

2.2.1.1 Research Objective

Antiohos, et al. examined ways to improve concrete's strength mixtures that incorporate SCM. Two types of fly ash were used, differing in their calcium content. Additionally the authors sought to optimize Class C/Class F ratio and cement replacement for best performance. The results show the importance of the active silica content in ternary based systems. This factor has considerable impact of strength development in fly ash-cement mixes.

2.2.1.2 Material and Mix Design

CEM Type I cement and two different Class C fly ashes (T_f and T_k) were selected to study. The difference between the Class C ashes was primarily the active silica content. Class F fly ash (T_m) was blended with the Class C ashes to produce ternary mix. Table 2.2 shows the new fly ash intermixtures that were prepared by using various dosages of Class C fly ashes (T_f and T_k) and Class F fly ash (T_m).

Table 2.2. Mix proportions applied for preparing the fly ash intermixture (Antiohos, Papadakis, Chaniotakis, & Tsimas, 2007)

Intermixture	T_f	T_k	T_m
T_1	50	0	50
T_2	0	50	50
T_3	25	0	75
T_4	0	25	75

Table 2.3 shows the physical properties and chemical analysis of the cement and fly ashes that were used in the research. Specimens were prepared by replacing 20 and 30% by weight. All of the specimens were cast into 40x40x160 mm prisms and all of them had w/b ratios of 0.5. One control mix was prepared with 100% cement in the binder.

Table 2.3. Physical properties and chemical analysis (%) of cement and fly ash (Antiohos, Papadakis, Chaniotakis, & Tsimas, 2007)

Compounds	Shorthand notation	CEM Type I	T_m	T_f	T_k	T_1	T_2	T_3	T_4
Silicon Dioxide (SiO_2)	S	20.3	51.4	36.9	29.7	44.1	42.2	48.0	46.6
Aluminum Oxide (Al_2O_3)	A	4.8	16.7	13.5	13.9	15.7	15.7	15.9	15.9
Iron Oxide (Fe_2O_3)	F	3.8	8.8	7.1	6.5	8.8	7.1	8.9	7.8
$K_2O + Na_2O$	K+N	0.5	2.3	1.4	1.8	1.7	1.5	2.0	1.9
Sulphur Trioxide (SO_3)	$\bar{S}$	2.6	1.5	5.1	5.1	3.2	3.5	2.4	2.6
Calcium Oxide (CaO)	C	65.0	13.8	29.8	34.1	21.5	23.9	18.0	19.3
Magnesium Oxide (MgO)	M	1.6	2.3	2.7	3.6	2.5	2.8	2.4	3.0
Loss on Ignition	LOI	2.3	4.9	4.4	4.0	4.6	4.5	4.7	4.7
Specific gravity (g/cm^3)	SG	3.13	2.59	2.83	2.93	2.70	2.76	2.65	2.68
Active Silica	γ	--	61	79	81	69	57	67	41
Blaine specific surface (m^2/kg)	Blaine	376	560	545	560	550	560	550	560
Activity Index, 7 day (%)	7 AI	--	--	--	--	--	--	--	--
Activity Index, 28 day (%)	28 AI	--	--	--	--	--	--	--	--

2.2.1.3 Experimental Results

2.2.1.3.1 Compressive Strength

Compressive strength development of the different 20% replacement mixtures is shown in Figure 2.2(a). The control mix (100% cement) had higher strength than all of the 20% SCM mixes up to 7 days. This is expected since fly ash does not contribute much to early strength development. However, after two days of curing the 20% SCM mixes started to develop strength at a faster rate than the control mix. Furthermore after 28 days of curing, all the 20% SCM mixes were either approaching or outperforming the control mix. At 28 day the T_1 ternary mix has the highest strength. The binary mixes, T_f and T_m, had lower strength values. The authors point out that this demonstrates that synergy between the ashes has taken place.

At age of 90 days, the improvement in strength performance of the 20% SCMs can be detected. At this stage of hydration, the fly ash contributes more to the strength than the hydration of the cement that has been replaced. The T_1 mixture exhibited a slight superiority amongst all intermixtures tested suggesting that a 50:50 ratio of Class C to Class F gives the best mechanical properties. The authors suggested that T_1 ternary mixture superior performance is most likely associated (assuming that fineness of all ashes is similar) with the greater amount of reactive silica contained in T_f, which has important role in strength development, especially after the first month of SCM mixes.

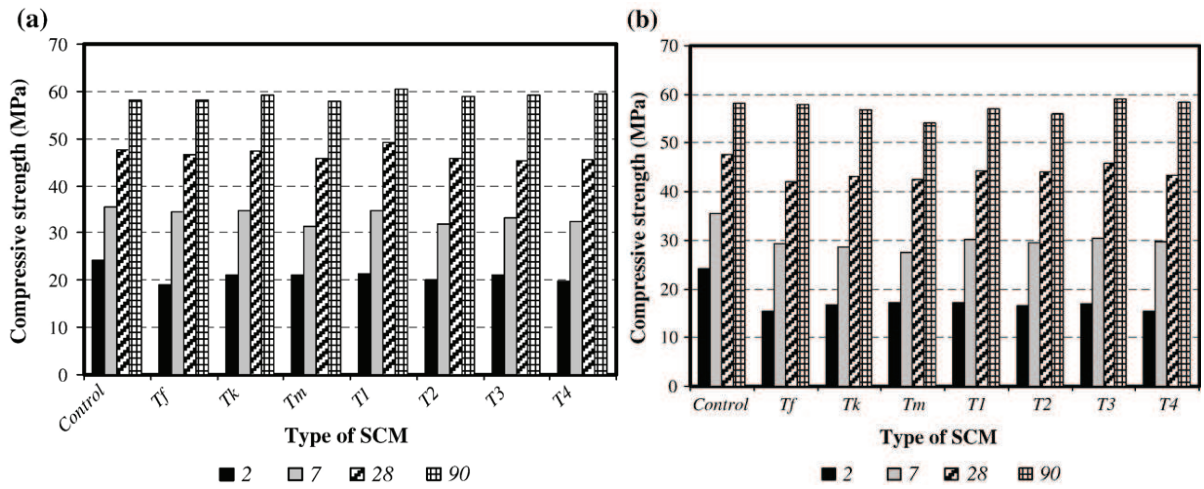

Figure 2.2. Compression test results for (a) 20% and (b) 30% by weight cement replacement (Antiohos, Papadakis, Chaniotakis, & Tsimas, 2007)

Compressive Strength development of the different 30% replacement mixtures is shown in Figure 2.2(b). Although strength development of the binary and ternary mixes at 7 days was further retarded due to the increased cement replacement, the ternary mixtures had clearly beneficial effects both on early and later strength of the 30% SCM mixes. Contrariwise to the results obtained for 20% SCM mixes, the most efficient blends is the ones with a substantial participation of low-calcium ash T_m, that is, T_3 and T_4 blends, which performs slightly better. The authors suggest that it is due to the excess of active silica.

2.2.1.3.2 Efficiency Factor

The modified Bolomey strength equation was used to evaluate the efficiency factor (k-value) of the SCMs compared to the control mix. Table 2.4 summarizes the efficiency factors for the mixes. The efficiency factors were below unity during early hydration stages, but at later ages they reached and/or exceeded unity.

Table 2.4. Efficiency factors of binary and ternary blended cements for 20% and 30% by weight of cement replacement (Antiohos, Papadakis, Chaniotakis, & Tsimas, 2007)

Day	T_f	T_k	T_m	T_1	T_2	T_3	T_4
	20% replacement						
2	0.67	0.81	0.81	0.82	0.73	0.80	0.73
7	0.92	0.94	0.72	0.94	0.76	0.84	0.78
28	0.92	0.97	0.88	**1.09**	0.87	0.85	0.86
90	**0.99**	**1.06**	**0.97**	**1.15**	**1.05**	**1.06**	**1.09**
	30% replacement						
2	0.63	0.68	0.71	0.71	0.68	0.70	0.63
7	0.73	0.70	0.65	0.76	0.73	0.78	0.75
28	0.76	0.80	0.78	0.85	0.84	0.92	0.81
90	**0.99**	0.94	0.82	**0.95**	0.90	**1.03**	**1.01**

The authors used an analytical expression to relate the active silica content of artificial pozzolans with the k-value of their respective cementitous systems (Papadakis, Antiohos, & Tsimas, 2002):

$$k = \left(\gamma_s \frac{f_{s,p}}{f_{c,p}}\right)\left(1 - a(t)\frac{w}{c}\right) \tag{2.7}$$

where γ_S is the ratio of active silica to the total silica in the SCM, $f_{S,P}$ and $f_{C,P}$ are the weight fraction of the silica in SCM and cement, respectively, *a(t)* is the same as in Eq. (2.1), c is cement content in concrete (kg/m^3) and *w* is the water content in concrete (kg/m^3).

The idea for this expression was to enable a first approximation of the future performance of SCM mixes knowing primarily the amount of silica present in the amorphous Phase of the SCMs. Table 2.5 shows the calculated and measured k-value at 28 and 90 days.

Table 2.5. Calculated and measured k-value of the intermixtures at 28 and 90 days (Antiohos, Papadakis, Chaniotakis, & Tsimas, 2007)

Intermixture	28 day		90 day	
	Calculated	Measured	Calculated	Measured
T_1	1.08	0.9	1.15	1.1
T_2	0.87	0.87	1.05	1.06
T_3	0.85	0.95	1.06	1.16
T_4	0.86	0.87	1.09	1.06

2.2.1.4 Conclusions

From this research the following conclusions were made

1. The effect of blending different ashes into ternary mixes resulted in improvements in compressive strength throughout the curing period when compared to the binary mixes.

2. It was found that for 20% SCMs equal contribution from each fly ash (50:50 ratio) was the most effective, while the 30% SCMs were depended on their active silica content

3. Previously reported expression, correlating the active silica of the artificial pozzolans with k-value of binary mixes, proved to be valid for ternary mixes as well. Using such expression can lead to relatively safe approximation of the future compressive strength.

2.2.2 Antiohos, Papageorgiou, Papadakis, & Tsimas, 2008

Influence of quicklime addition on the mechanical properties and hydration degree of blended cements containing different fly ash

2.2.2.1 Research Objective

Antiohos, et al. studied the mechanical properties of fly ash-cement systems with the addition of quicklime. In this research, two fly ashes (high and moderate calcium content) were chemically activated by adding industrially-produced quicklime.

2.2.2.2 Material and Mix Design

The authors selected CEM Type I cement and two different fly ashes, one with high calcium content (T_D) and one with lower calcium content (T_M). Table 2.6 shows the physical properties and chemical analysis of the cement and fly ashes that were used in the research.

Table 2.6. Physical properties and chemical analysis (%) of cement and fly ash (Antiohos, Papageorgiou, Papadakis, & Tsimas, 2008)

Compounds	Shorthand notation	CEM Type I	T_D	T_M
Silicon Dioxide (SiO_2)	S	21.5	29.7	51.4
Aluminum Oxide (Al_2O_3)	A	4.9	13.9	16.7
Iron Oxide (Fe_2O_3)	F	3.8	6.5	8.8
$K_2O + Na_2O$	K+N	--	--	--
Sulphur Trioxide (SO_3)	$\bar{S}$	1.4	5.1	1.5
Calcium Oxide (CaO)	C	65.5	34.1	13.8
Magnesium Oxide (MgO)	M	2.2	3.6	2.3
Loss on Ignition	LOI	2.3	4.0	4.9
Specific gravity (g/cm^3)	SG	3.13	2.72	2.59
Active Silica	γ_s	--	81	61
Blaine specific surface (m^2/kg)	Blaine	412	560	555
Activity Index, 7 day (%)	7 AI	--	--	--
Activity Index, 28 day (%)	28 AI	--	--	--

Specimens were prepared by replacing 20% of cement (by weight). All of the specimens were cast into 40x40x160 mm prisms. All of them had w/b ratio constant at 0.5. One control mix was prepared with 100% cement in the binder. The other mixes used either one of the fly ashes and a specified portion of quicklime. Table 2.7 shows the mix proportions of the tested specimens.

Table 2.7. Mix proportions of specimens tested (% by weight of cementitious material) (Antiohos, Papageorgiou, Papadakis, & Tsimas, 2008)

Mix no.	Cement (%)	FA (%)	Quicklime (%)
Ref	100.0	0.0	0.0
T_D	80.0	20.0	0.0
T_D-Q3	80.0	19.4	0.6
T_D-Q6	80.0	18.8	1.2
T_M	80.0	20.0	0.0
T_M-Q5	80.0	19.0	1.0
T_M-Q15	80.0	17.0	3.0

2.2.2.3 Experimental Results

2.2.2.3.1 Compressive Strength

Table 2.8 summarizes the compressive strength results of all the mixes. Figure 2.3 shows the data in graphical from for better comparison. It can be seen that with small quicklime replacement (3%) of T_D ash resulted in a small strength increase at all ages and most importantly during the early ages. When the quicklime addition increased to 6% (by weight of fly ash), the strength was slightly less than the mortar containing 3% quicklime but it had higher strength at all ages than T_D ash alone. The authors argue that based on these results a

3% quicklime addition is the optimum addition, but they point out that only two replacement levels were examined and the optimum addition could be in between.

The effect of quicklime on the strength development of the lower-lime ash (T_M) is contrary what was observed with the T_D ash. The quick lime addition did not accelerate the strength but instead it caused decrease of the compressive strength of all examined blends at almost all ages. The authors suggest that the decrease in strength results from the reactive silica present in the pore solution was decreased due to fly ash replacement, and therefore insufficient to react completely with the remaining of hydrated lime.

Table 2.8. Compressive strength results of quicklime-activated fly ash mortars (Antiohos, Papageorgiou, Papadakis, & Tsimas, 2008)

Mix no	%	Measured Strength (MPa)			
		2 day	7 day	28 day	90 day
Ref	0	24.2	35.6	47.7	58.1
T_D	20	23.0	34.5	47.7	58.4
T_D-Q3	20	23.6	35.4	49.6	61.5
T_D-Q6	20	23.4	35.3	48.8	60.8
T_M	20	21.1	31.4	45.9	57.8
T_M-Q5	20	22.2	31.3	45.4	56.8
T_M-Q15	20	20.2	30.8	44.8	56.2

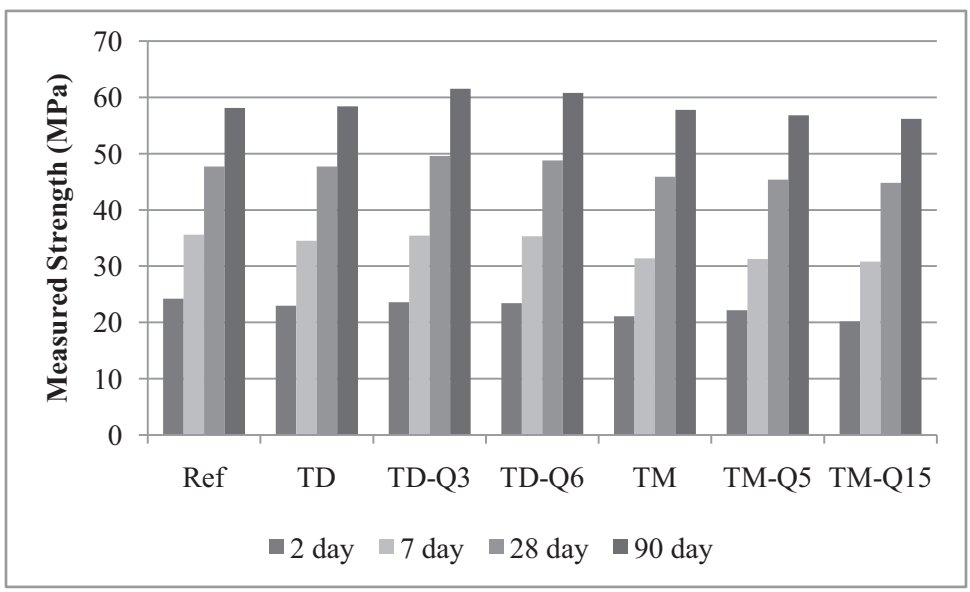

Figure 2.3. Compressive strength results of quicklime-activated fly ash mortars reproduced from Antiohos, et al. 2008

2.2.2.3.2 Efficiency Factor

The modified Bolomey strength equation was used to evaluate the efficiency (k-value) of the SCMs compared to the control mix. Table 2.9 shows the efficiency factors of the SCM mortars in the research.

Table 2.9. Efficiency factor (k-value) for cement-fly ash and cement-fly ash-quicklime mortars (Antiohos, Papageorgiou, Papadakis, & Tsimas, 2008)

Mix no	2 day	7 day	28 day	90 day
T_D	0.93	0.92	1.00	1.01
T_D-Q3	1.04	1.01	1.12	1.21
T_M	0.81	0.72	0.88	0.97
T_M-Q5	0.88	0.74	0.85	0.91
T_M-Q15	0.75	0.68	0.81	0.87

The k-value of T_D ash with quicklime addition reaches unity very quickly and it easily exceeds it with curing time, furthermore it has higher k-value than T_D ash alone. The k-value of the T_M ash with quicklime addition has negative impact on the k-value when it is compared to the k-value of T_M ash alone, except the 5% quicklime addition at very early period of hydration (up to 7 days)

2.2.2.4 Conclusions

From this research the following conclusions were made

1. The addition of industrially produced quicklime on fly ash-Portland cement pastes had positive influence mainly on the strength development and reaction rate of high lime fly ash.

2. Conversely, when quicklime replaced an ash with lower lime content, it resulted in decrease in strength.

2.2.3 Babu & Kumar, 2000

Efficiency of GGBS in concrete

2.2.3.1 Research Objective

Babu and Kumar examined the cementitious efficiency of ground granulated blast-furnace slag (GGBS) in concrete at the various replacement percentages. The efficiency concept was

used to establish the variation of the strength as a function of water-to-cementitious materials ratio relations of the GGBS binary concretes.

2.2.3.2 Material and Mix Design

For the evaluation of the efficiency of the GGBS, this research used prior data. Table 2.10 presents the range of data that was used for evaluation of the efficiency factor. This data concludes total of 175 mixes, thereof 70 mixes with 100% ASTM type I Portland cement. The GGBS in these mixes had quantities of SiO_2 from 31.1-38.6% and quantities of CaO from 32.8-43.9%. The replacement percentages range from 10-80%.

Table 2.10. Details of the concrete evaluated (Babu & Kumar, 2000)

Slag no	%	w/b range	Slump range (mm)	28-day strength range (MPa)	Average efficiency
1	0	0.23-0.83	40-170	19.7-106	--
2	10	0.26-0.38	150	58.5-105	1.29
3	30	0.26-0.55	100-150	49.1-105	1.02
4	50	0.30-0.80	35-190	21.2-89.3	0.84
5	60	0.26-0.50	150	43.4-80.0	0.78
6	65	0.46-0.75	100	23.0-57.5	0.75
7	70	0.41-0.61	45-65	32.5-62.5	0.73
8	80	0.50	--	29.5-32.5	0.70

2.2.3.3 Experimental Results

2.2.3.3.1 Evaluation of Efficiency

To evaluate the efficiency of the GGBS, Δw concept was used. The Δw concept attempts to have a uniform w/b ratio for the binary concretes and control concrete (w/c) by applying the efficiency factor (k-value) at any particular strength (similar to the modified Bolomey strength equation, Eq. (2.4)).

The authors found at by using a single efficiency value (general efficiency factor, k_e), at all replacements did not lead to a good correlation. Better correlation was found, by using "percentage efficiency factor (k_p)" to correct the "overall efficiency factor (k)". The relationship between the efficiency factors is: $k = k_e + k_p$

Figure 2.4 shows the 28 day compressive strength versus w/b ratio for different replacement levels. From the figure it can be seen that SCM mixes up to 30% replacement are all slightly

above the control mixes (100% Portland cement) and all the other replacement levels were below the control mixes.

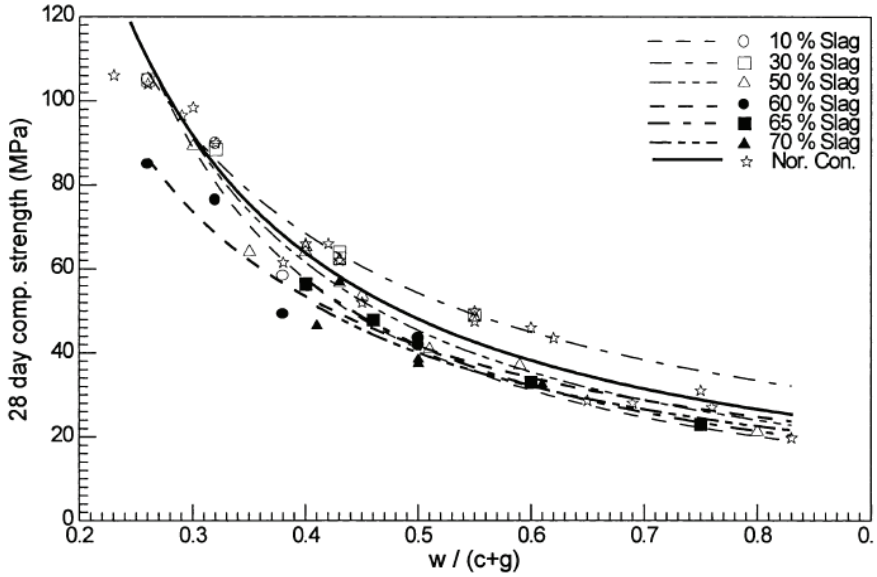

Figure 2.4. Compressive strength at 28 day versus w/b at different replacement levels (Babu & Kumar, 2000)

The w/b ratio was modified by applying the k_e concept, that is replacing w/(c+g) with w/(c+k_eg), where g is the amount of GGBS. After several trials with k_e-value, the authors found that a single value of 0.9 to minimize the strength differential of the 28 day strength of the binary and control mixes. Figure 2.5 shows the 28 day compressive strength versus w/(c+k_eg) ratio at different replacement levels.

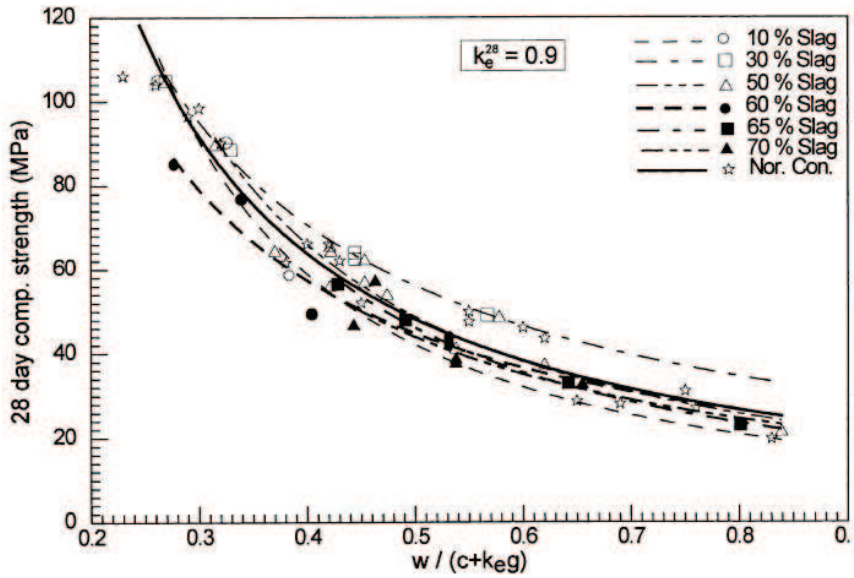

Figure 2.5. Compressive strength at 28 day versus w/(c+k_eg) at different replacement levels (Babu & Kumar, 2000)

It was observed that k_e-value did not result with an equivalent w/(c+k_eg) ratio for all replacement levels. Therefore, k_p-value was added to find w/b ratio of the GGBS mixes that approximated better the control mix. This value was found to vary between +0.39 and -0.20 for replacement levels between 10% and 80%. This resulted in k-value, which is the sum of k_e and k_p, that varies from 1.29-0.70 for the replacements levels between 10-80%. Figure 2.6 shows the 28 day compressive strength versus w/(c+kg) ratio at different replacement levels. This shows by adopting k = k_e + k_p results with a w/b ratio for the GGBS mixes that is consistent with the control mix

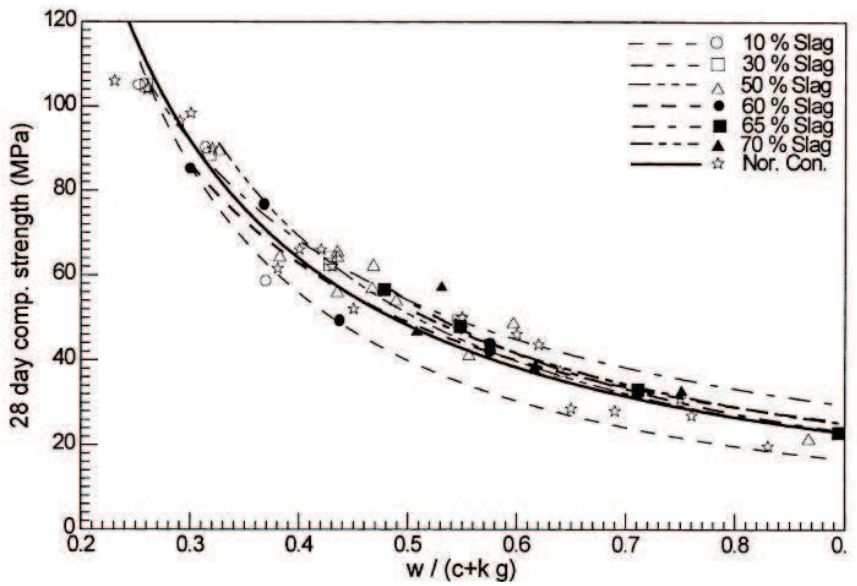

Figure 2.6. Compressive strength at 28 day versus w/(c+kg) at different replacement levels (Babu & Kumar, 2000)

Figure 2.7 shows best fit of the corrected w/b ratio to strength relations of the GGBS concretes in comparison to that of the control concretes. The regression coefficient for GGBS concretes as well as control concretes was found to be 0.94 at 28 days. The evaluation also showed that the slag concretes based on the k-value, will need an increase of 8.6% for 50% replacement and 19.5% for 65% replacement in the total cementitious materials for achieving strength equivalent to that of normal concrete at 28 days.

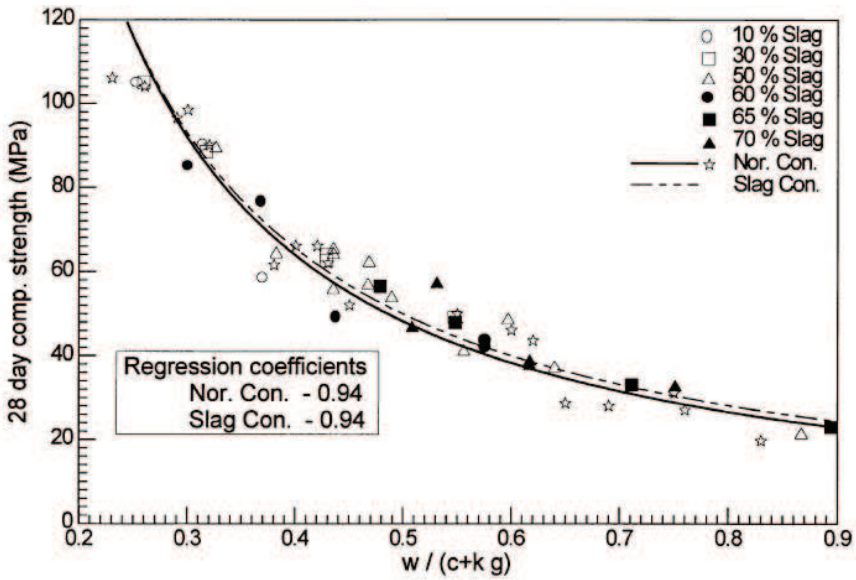

Figure 2.7. Assessment of the reliability of the efficiencies evaluated (Babu & Kumar, 2000)

2.2.3.4 Conclusions

From this research the following conclusions were made

1. Evaluating the efficiency of GGBS in the same way as fly ash and silica fume was found to be appropriate. This research used overall strength efficiency factor (k) which was the sum of the general efficiency factor (k_e) and the percentage efficiency factor (k_p). The k_e value was 0.9, the k_p-value varied from +0.39 to -0.20 and k-value varied from 1.29 to 0.70 for replacement levels from 10-80%.

2. The overall strength prediction of concrete varying from 20-100 MPa with replacement levels from 10-80% by this method resulted in regression coefficient of 0.94, which was also the same for the control concrete.

3. To obtain equal strength as the control concrete at 28 day at 50% and 65% replacement level, an additional 8.5% and 19.5% increase in the total cementitious material is required.

2.2.4 Carette, Bilodeau, Chevrier, & Malhotra, 1993

Mechanical Properties of Concrete Incorporating High Volumes of Fly Ash from Sources in the U.S.

2.2.4.1 Research Objective

Carette, et al. researched the impact of increasing the replacement level of fly ash in concrete. The authors point out that replacement levels in current practice is limited to approximate 25% by weight, but the authors want to test concrete with 60% replacement by weight to contribute to cleaner environment.

2.2.4.2 Material and Mix Design

Two ASTM Type I Portland cements were selected from sources in the U.S. for this research. The difference between the cement brands were that one was low C_3A alkali type (C1) and the other was high C_3A alkali type (C2). Eight fly ashes were selected from sources in the U.S. to cover a wide range of chemical compositions. Two of the ashes had high CaO content (F5 and F3), one ash had an intermediate CaO content (F8) and the rest had low CaO content. Table 2.11 shows the physical properties and chemical analysis of the cements and fly ashes that were used in the research.

Sixteen mixtures were made with different binder materials. For all the mixtures, the w/b ratio was at 0.33 and the cement replacement was 58%. The proportioning and the properties of the mixes are summarized in Table 2.12. For determination of elastic modulus, compressive strength and creep characteristics, 152x305 mm cylinders were cast and for determination of drying shrinkage 76x102x390 mm prisms were cast.

Table 2.11. Physical properties and chemical analysis (%) of cement and fly ashes (Carette, Bilodeau, Chevrier, & Malhotra, 1993)

Compounds	Shorthand notation	C1	C2	F1	F2	F3	F4	F5	F6	F7	F8
Silicon Dioxide (SiO_2)	S	21.2	19.2	49.0	53.6	46.2	48.9	46.4	54.5	47.3	55.4
Aluminum Oxide (Al_2O_3)	A	4.8	5.8	26.7	27.4	15.6	21.1	15.3	31.5	25.4	18.5
Iron Oxide (Fe_2O_3)	F	3.7	2.0	12.3	7.7	7.7	16.6	7.4	6.3	13.8	6.4
$K_2O + Na_2O$	K+N	0.3	1.5	2.6	2.8	7.4	3.8	2.7	0.6	2.1	4.0
Sulphur Trioxide (SO_3)	$\bar{S}$	2.3	3.5	0.8	0.4	1.7	1.9	1.5	0.4	0.9	0.9
Calcium Oxide (CaO)	C	65.0	63.5	2.4	2.9	14.9	4.5	19.3	1.2	1.8	9.5
Magnesium Oxide (MgO)	M	1.2	2.5	1.0	1.0	4.3	1.1	5.5	0.9	1.5	2.2
Loss on Ignition	LOI	1.1	2.6	2.8	1.5	0.5	1.0	0.5	1.5	2.2	0.3
Specific gravity (g/cm^3)	SG	3.14	3.14	2.35	2.23	2.45	2.45	2.46	2.34	2.43	2.41
Active Silica	γ_s	--	--	--	--	--	--	--	--	--	--
Blaine specific surface (m^2/kg)	Blaine	371	376	273	221	239	318	263	238	327	355
Activity Index, 7 day (%)	7 AI	--	--	--	--	--	--	--	--	--	--
Activity Index, 28 day (%)	28 AI	--	--	85	85	88	91	101	85	85	--

Table 2.12. Mixture proportions and properties of fresh concrete (Carette, Bilodeau, Chevrier, & Malhotra, 1993)

Mixture no.	Cement brand	Fly ash source	%	Cement (kg/m^3)	SCM[1] (kg/m^3)	Water (kg/m^3)	w/b	FAg[2] (kg/m^3)	CAg[3] (kg/m^3)	SP[4] (mL/m^3)	AEA[5] (%)	Slump (mm)	Air (%)
1	C1	F1	58	152	211	119	0.33	1192	641	300	3.8	140	5.6
2	C2	F1	58	152	211	120	0.33	1196	643	210	4.5	165	5.2
3	C1	F2	58	153	212	120	0.33	1191	639	470	3.9	230	4.9
4	C2	F2	58	153	212	120	0.33	1192	639	400	4.7	180	5.9
5	C1	F3	58	152	211	119	0.33	1197	643	80	1.4	135	5.9
6	C2	F3	58	153	213	120	0.33	1206	648	45	2	125	5.6
7	C1	F4	58	152	212	119	0.33	1200	645	265	3.6	180	5.3
8	C2	F4	58	152	211	118	0.33	1195	642	135	3.4	150	5.8
9	C1	F5	58	152	211	119	0.33	1200	646	170	1.9	170	5.5
10	C2	F5	58	152	211	119	0.33	1201	646	85	2.1	140	5.3
11	C1	F6	58	152	210	118	0.33	1189	640	475	3.5	75	5.8
12	C2	F6	58	152	210	119	0.33	1188	639	340	4.3	150	5.5
13	C1	F7	58	152	211	119	0.33	1195	642	285	2.4	180	5.3
14	C2	F7	58	152	211	118	0.33	1193	641	210	3.7	145	5.8
15	C1	F8	58	152	210	118	0.33	1194	641	220	2.7	165	5.2
16	C2	F8	58	151	209	119	0.33	1187	638	150	2.8	160	5.9

[1]Fly ash, [2]Fine Aggregate, [3]Coarse Aggregate, [4]Superplasticizer, [5]Air-entraining admixture

2.2.4.3 Experimental Results

2.2.4.3.1 Compressive Strength

The compressive data is presented in Table 2.13 and illustrated in Figure 2.8 and Figure 2.9. The compressive strength of the concrete mixes made with cement C2 had higher early-strength (≤ 7 days) than the mixes with cement C1. At 28 and 91 days, Cement C2 had still higher strength for concrete mixes made with low- and intermediate-calcium fly ash. However the concrete mixes made with high-calcium fly ash (F3 and F5) and cement C1 showed higher strength than mixes made with C2, at these days. The strength data available showed that mixes made with cement C1 between 91 days and 1 year had always greater strength development than mixes made with cement C2. As a result, the difference in strength after 1 year with different types of cement was very small.

The authors state that the relative performance of the fly ashes in concrete depends on the brand of cement used (high or low alkali type). In addition, the age of test is an important factor influencing the relative performance of the various cementing materials.

Table 2.13. Compressive strength results of the mixes (Carette, Bilodeau, Chevrier, & Malhotra, 1993)

Mixture no.	Cement brand	Fly ash source	Measured Strength (MPa)				
			1 day	7 days	28 days	91 day	365 days
1	C1	F1	5.6	18.8	28.8	39.7	52.0
2	C2	F1	10.3	24.9	39.3	50.9	57.9
3	C1	F2	4.9	18.3	29.5	40.6	56.8
4	C2	F2	10.5	21.2	32.5	45.0	58.8
5	C1	F3	9.7	23.9	38.1	45.6	53.2
6	C2	F3	13.9	26.3	37.2	45.0	51.3
7	C1	F4	3.1	22.5	34.3	44.3	56.3
8	C2	F4	11.5	24.8	37.4	45.6	55.2
9	C1	F5	4.1	23.0	38.5	48.9	63.1
10	C2	F5	9.1	27.6	41.4	48.8	61.2
11	C1	F6	5.8	18.2	27.8	39.5	54.7
12	C2	F6	10.8	22.6	35.0	45.8	58.7
13	C1	F7	5.6	19.0	30.1	39.1	--
14	C2	F7	10.3	21.9	36.9	44.7	--
15	C1	F8	5.1	21.6	38.1	48.9	--
16	C2	F8	8.4	26.5	42.2	50.4	--

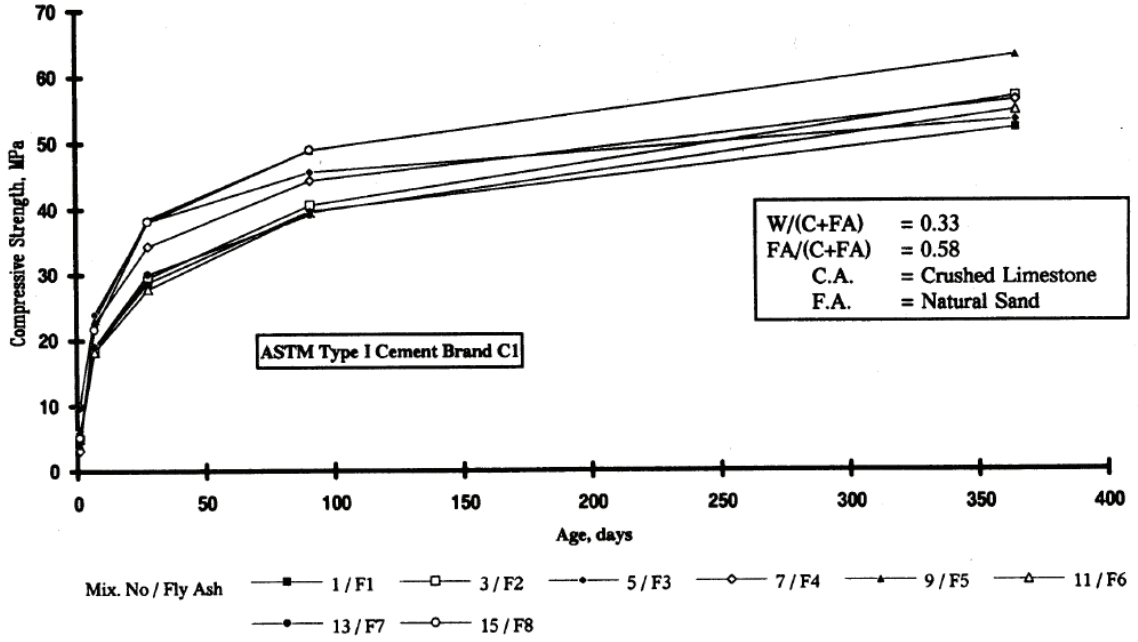

Figure 2.8. Compressive strength development of concrete made with ASTM Type I cement brand C1 (Carette, Bilodeau, Chevrier, & Malhotra, 1993)

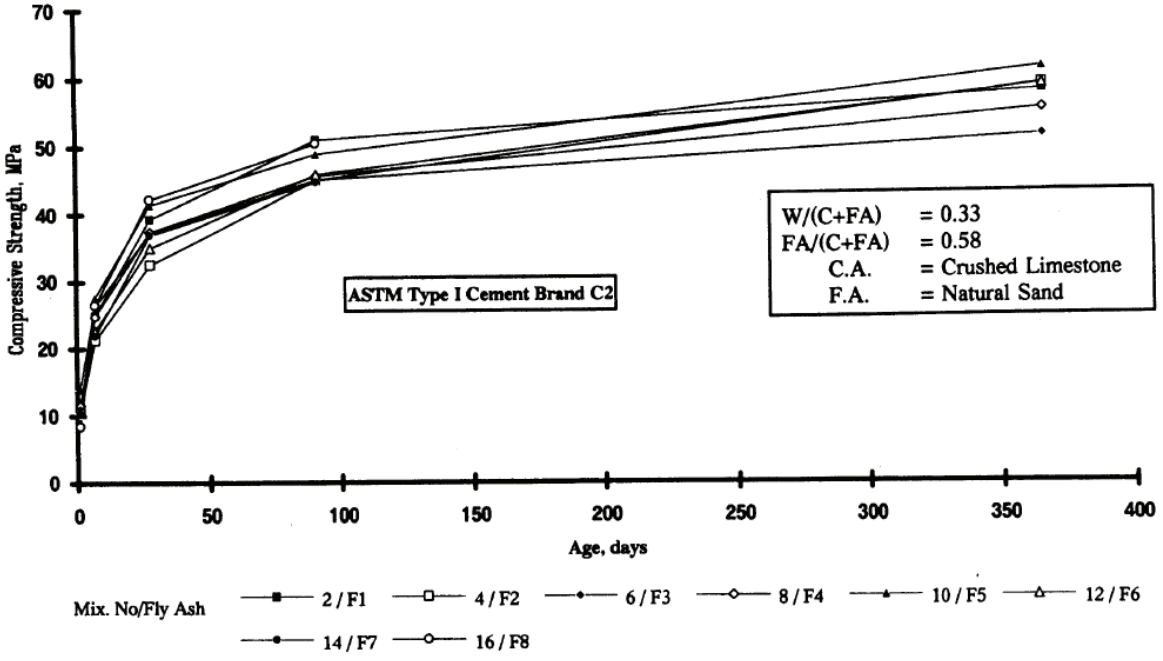

Figure 2.9. Compressive strength development of concrete made with ASTM Type I cement brand C2 (Carette, Bilodeau, Chevrier, & Malhotra, 1993)

2.2.4.3.2 Elastic Modulus

The researchers also measured the elastic modulus of the concrete mixes. The modulus values are presented in Table 2.14. Elastic modulus data for the control mix was not provided. Similar to the compressive strength results, the elastic modulus of the concrete mixes made with cement C2 had higher modulus values at 28 days than the mixes with cement C1. The elastic modulus values at 91 days and 1 year appears not to be depended of type of cement.

Table 2.14. Elastic modulus results of the mixes (Carette, Bilodeau, Chevrier, & Malhotra, 1993)

Mixture no.	Cement brand	Fly ash source	Elastic modulus (GPa)		
			28 days	91 day	365 days
1	C1	F1	33.0	39.2	42.4
2	C2	F1	35.8	41.0	42.6
3	C1	F2	32.1	38.6	43.3
4	C2	F2	33.6	37.1	41.2
5	C1	F3	37.7	39.7	40.6
6	C2	F3	37.6	39.8	39.8
7	C1	F4	35.9	40.7	43.4
8	C2	F4	36.4	39.7	41.4
9	C1	F5	34.9	40.0	44.6
10	C2	F5	39.5	41.5	45.6
11	C1	F6	32.8	40.4	43.6
12	C2	F6	36.2	40.4	43.6
13	C1	F7	33.5	36.6	--
14	C2	F7	35.9	40.1	--
15	C1	F8	36.8	42.0	--
16	C2	F8	39.4	41.7	--

2.2.4.3.3 Drying shrinkage and Creep Strain

Shrinkage was also monitored for the binary mixes. The shrinkage results after 7 and 91 days of curing are presented in Table 2.15 and Table 2.16, respectively. The concrete mixes that were cured for 7 days before drying and made with cement C2 show slightly more shrinkage strain than compared mixes with cement type C1. This trend does not exist for concrete cured for 91 days before drying; overall the shrinkage strains were similar. The drying shrinkage strain of the 7 day cured concretes at the end of 224 days range from 400 to 600 μ strains, whereas for the 91 day curing these values ranged from 350 to 450 μ strains.

Table 2.17 shows the creep behavior of the mixes. Only partial data was available, but from the data presented, concrete made with cement C1 have somewhat higher specific creep

strains than concrete made with cement C2 (specific creep strain is defined as the creep strain per unit of stress). The creep strains ranged from 277 to 364 μ strains after 196 days of loading under constant 12.2 MPa.

Table 2.15. Drying shrinkage test results after 7 days of curing (Carette, Bilodeau, Chevrier, & Malhotra, 1993)

Mixture no.	Cement brand	Fly ash source	Drying shrinkage strain (10^{-6}) - cured for 7 days						
			7 days	14 days	28 days	56 days	112 days	224 days	448 days
1	C1	F1	139	241	341	387	380	418	433
2	C2	F1	245	330	422	493	536	582	589
3	C1	F2	210	291	366	419	411	437	450
4	C2	F2	231	344	440	515	557	584	606
5	C1	F3	181	263	352	422	419	458	497
6	C2	F3	121	231	352	394	437	472	507
7	C1	F4	160	274	344	404	433	472	511
8	C2	F4	241	287	387	433	479	518	539
9	C1	F5	170	233	305	376	419	433	457
10	C2	F5	181	288	362	430	475	515	536
11	C1	F6	192	245	326	369	426	461	--
12	C2	F6	220	362	411	475	564	606	--
13	C1	F7	184	217	323	411	444	468	--
14	C2	F7	223	316	429	507	539	603	--
15	C1	F8	181	262	352	437	504	578	--
16	C2	F8	224	305	401	482	546	567	--

Table 2.16. Drying shrinkage test results after 91 days of curing (Carette, Bilodeau, Chevrier, & Malhotra, 1993)

Mixture no.	Cement brand	Fly ash source	Drying shrinkage strain (10^{-6}) - cured for 91 days					
			7 days	14 days	28 days	56 days	112 days	224 days
1	C1	F1	124	163	224	302	355	397
2	C2	F1	125	177	217	270	319	362
3	C1	F2	106	156	203	281	326	373
4	C2	F2	110	160	238	284	351	380
5	C1	F3	71	167	210	284	352	415
6	C2	F3	82	153	210	259	337	401
7	C1	F4	139	170	210	255	309	365
8	C2	F4	71	135	199	252	316	373
9	C1	F5	60	145	206	241	298	365
10	C2	F5	132	188	206	316	262	430
11	C1	F6	110	196	245	305	383	464
12	C2	F6	132	210	284	351	411	500
13	C1	F7	135	181	241	266	333	369
14	C2	F7	85	128	177	263	319	366
15	C1	F8	132	188	274	291	341	--
16	C2	F8	103	156	245	274	319	--

Table 2.17. Creep results of the concrete mixtures (Carette, Bilodeau, Chevrier, & Malhotra, 1993)

Mixture no.	Cement brand	Fly ash source	Age at Loading (day)	Applied Stress (MPa)	Inelastic Strain (10^{-6})	Duration of loading (day)	Creep Strain (10^{-6})	Specific Creep Strain (10^{-6}/MPa)
1	C1	F1	130	12.2	325	196	332	27.2
3	C1	F2	126	12.2	327	196	364	29.8
4	C2	F2	127	12.2	317	196	283	23.2
7	C2	F4	127	12.2	315	196	300	24.6
11	C1	F6	127	12.2	320	196	357	29.3
12	C2	F6	126	12.2	310	196	289	23.7
13	C1	F7	132	12.2	327	196	287	23.5
14	C2	F7	133	12.2	325	196	277	22.7

2.2.4.4 Conclusions

From this research the following conclusions were made:

1. High-volume fly ash concrete with good overall mechanical properties can be produced with fly ashes and cements covering a wide range of chemical compositions and fineness.

2. Compressive strength of 50-60 MPa was achieved for all concretes at age of 91 days. The use of cement C2 resulted in considerably higher early-age strength than those obtained with the use of cement C1.

3. The values of modulus of elasticity for the mixes were of the order of 40 GPa at 90 days.

4. There was no clear relation between the amount of drying shrinkage and type of fly ash in the concretes. With increase of curing the shrinkage strains reduced in all cases. The drying shrinkage strain of the 7 day cured concretes at the end of 224 days range from 400 to 600 μ strains, whereas for the 91 day curing these values range from 350 to 450 μ strains.

5. The creep strains of the concrete mixes that were tested show low creep strains. They were usually of the order of 300 μ strains.

2.2.5 Das & Yudhbir, 2006

A simplified model for prediction of pozzolanic characteristics of fly ash, based on chemical composition

2.2.5.1 Research Objective

Das and Yudhbir proposed an equation to estimate the strength development of concrete that contains fly ash as cement replacement. The equation predicts concrete strength based on chemical composition, since the chemical compositions varies greatly between sources.

2.2.5.2 Material and Mix Design

Regular Portland cement was used and fly ashes with wide a range of chemical compositions were selected. The equation that predicts compressive strength is based on 4 parameters; ratio of potassium to alumina (K/A)*10, calcium oxide (CaO), Loss of Ignition (LOI) and fineness. Table 2.18 presents minimum, maximum and average value of the parameters that was used for evaluation of the compressive strength equation. Four different cement replacement levels were tested; 10%, 20%, 35% and 50%. For determination of compressive strength, the mixes were cast in cubes according to ASTM C 1949. Compressive strength was determined at 28, 90 and 365 days

Table 2.18.The range of parameter used for model input (Das & Yudhbir, 2006)

	Min	Max	Ave.
(K/A)*10	0.72	1.20	1.00
CaO	1.40	16.80	5.80
LOI	1.20	8.20	3.50
Fineness	3415	4420	3913

2.2.5.3 Experimental Results

2.2.5.3.1 Compressive Strength

The compressive data is presented in Table 2.19. The compressive strength values of the 10% cement replacement mixes had very similar strength as the control mixes at all ages. The 20%, 35% and 50% mixes all exhibit lower strength at age 28 and 91 days. At age 356 days some of the mixes are exceeding the base mix while others show lower strength values.

Table 2.19. Compressive strength results of the mixes (Das & Yudhbir, 2006)

Sl. no.	Compressive strength (N/mm^2)														
	Control mortar			Fly ash replacement											
				10% replacement			20% replacement			35% replacement			50% replacement		
	Curing period (days)			Curing period (days)			Curing period (days)			Curing period (days)			Curing period (days)		
	28	91	365	28	91	365	28	91	365	28	91	365	28	91	365
1	35.37	43.16	48.47	32.54	39.71	47.50	29.00	40.14	49.44	23.35	36.26	47.02	18.04	32.37	42.17
2	34.61	43.85	45.23	37.38	46.04	51.11	31.84	42.54	48.40	23.19	37.27	43.87	21.81	34.64	39.35
3	35.37	43.16	48.47	33.60	44.46	50.90	32.90	43.59	54.77	26.53	40.14	51.86	24.41	38.41	47.50
4	33.37	41.37	44.40	33.04	34.34	45.74	29.37	39.30	45.74	24.03	36.82	46.62	15.35	26.06	33.75
5	35.51	42.68	46.75	33.38	42.68	50.49	31.25	41.40	52.83	24.50	38.84	51.89	19.53	32.44	45.81
6	38.34	46.40	47.78	31.82	38.51	44.92	26.84	35.27	42.05	20.70	35.27	39.66	13.42	23.20	31.54
7	36.47	43.02	44.06	32.83	39.58	43.62	28.45	37.86	44.50	23.71	36.14	41.42	16.41	28.83	40.53
8	36.47	43.02	44.06	32.10	40.87	45.82	29.54	40.44	47.14	26.99	41.73	53.31	16.41	30.12	44.94
9	33.37	41.37	44.40	33.04	41.78	46.62	27.03	36.82	46.18	18.69	28.96	40.85	15.35	28.13	38.63
10	33.37	41.37	44.40	35.04	44.27	48.40	29.03	38.47	46.62	22.03	33.92	43.07	15.35	27.72	34.19
11	35.99	44.20	48.54	29.87	40.22	44.17	24.11	35.36	43.69	17.28	28.73	37.38	11.88	22.10	31.07
12	34.61	43.85	45.23	33.57	43.41	45.68	27.69	35.96	42.52	21.81	34.20	44.33	18.34	31.57	42.07
13	33.37	41.37	44.40	33.04	41.37	44.85	25.70	35.58	41.74	17.02	27.30	33.75	11.68	20.69	26.64
14	33.99	43.37	45.64	31.27	37.30	43.36	25.49	34.26	42.45	18.70	29.92	38.80	12.24	22.12	28.30
15	33.37	41.37	44.40	30.37	40.54	45.29	24.03	33.51	41.30	16.02	26.06	35.52	9.34	16.55	27.53
16	35.99	44.20	48.54	31.31	41.99	47.08	26.63	38.01	46.60	20.52	34.47	46.60	16.92	31.82	44.66
17	32.82	38.20	40.47	30.19	38.20	43.71	27.90	38.58	46.14	21.33	32.85	40.88	14.11	24.45	34.81
18	34.68	41.65	45.09	30.17	39.56	45.09	27.40	37.48	46.90	20.12	32.48	42.84	13.87	25.40	36.98
19	33.85	39.78	43.16	29.45	39.78	44.89	26.75	35.41	41.00	19.64	29.44	37.12	12.53	20.29	30.65
20	32.82	38.20	40.47	28.23	37.05	43.31	24.62	32.47	40.47	17.72	26.74	35.62	12.47	19.86	29.55
21	34.68	41.65	45.09	25.32	33.73	36.07	20.12	27.90	31.11	11.45	18.74	23.00	6.94	13.74	18.49
22	32.82	38.20	40.47	28.23	35.91	41.69	21.33	29.79	36.83	16.74	25.97	34.40	10.17	17.19	26.71
23	33.37	40.68	45.44	29.70	37.43	42.26	22.69	29.70	36.80	15.68	24.41	32.72	9.68	17.09	23.17
24	33.37	40.68	45.44	32.37	37.83	44.53	24.03	36.61	41.80	19.69	29.70	37.26	12.35	20.75	30.44
25	38.34	46.40	47.78	28.75	38.05	34.40	27.22	34.80	38.23	18.78	26.45	31.06	9.97	18.10	23.41
26	33.37	40.68	45.44	31.37	39.87	44.53	25.36	35.80	40.89	18.02	30.10	37.71	12.35	22.78	29.08
27	35.51	42.68	46.75	30.18	33.29	42.07	23.44	30.30	39.27	15.27	23.90	30.39	9.94	17.07	21.97
28	35.99	44.20	48.54	31.31	40.66	47.08	25.19	35.80	41.26	15.84	26.96	33.49	9.36	18.12	26.70
29	33.99	43.37	45.64	29.57	38.60	45.64	24.81	33.39	41.54	18.02	26.02	34.23	11.22	19.08	26.02
30	35.99	45.78	47.78	33.11	43.49	50.65	27.71	41.66	50.17	21.60	32.51	45.87	13.32	23.35	34.88
31	35.99	45.78	47.78	30.23	38.92	44.44	22.67	32.96	37.27	15.84	26.10	33.45	9.00	16.48	22.94
32	35.99	45.78	47.78	29.87	40.29	44.44	23.03	33.42	37.75	14.40	24.26	29.15	8.28	15.57	21.02
33	35.51	42.68	46.75	32.67	39.27	44.88	24.15	29.88	40.67	14.56	23.47	28.98	9.94	17.50	22.91

2.2.5.3.2 Application of Prediction Model

The authors proposed a prediction equation to predict a concrete strength with fly ash as replacement. The proposed equation is expressed as follows:

$$CS = c_1\left((K/A) * 10\right)^{c_2} + c_3(CaO)^{c_4} + c_5(LOI)^{c_6} + c_7\left(\frac{Fineness}{1000}\right)^{c_8} \quad \textbf{(2.8)}$$

where CS is the compressive strength (N/mm^2), c_1-$c_8$are coefficients determined by least squares technique. Table 2.20shows the regression coefficients and correlation coefficient at different days and cement replacements for this research. It was observed that coefficient $c_4 \approx 0.0$ for all replacements and all days. The coefficient c_5 has always negative value, which indicates that LOI has negative impact on the compressive strength. It can also be seen that

the R^2 is more than 0.85 for 20%, 35% and 50% cement replacement, but less than 0.85 for 10% cement replacement. Figure 2.10 shows the relationship between calculated and measured strength values.

Table 2.20.The regression coefficients and correlation coefficient (R^2) at different days and cement replacements (Das & Yudhbir, 2006)

Coeff.	10% replacement			20% replacement			35% replacement			50% replacement		
	28 d	90 d	365 d	28 d	90 d	365 d	28 d	90 d	365 d	28 d	90 d	365 d
c_1	4.40	2.67	0.19	1.04	0.13	0.20	1.60	1.60	1.68	0.64	0.38	0.66
c_2	0.00	0.00	6.50	1.30	6.95	7.05	1.89	2.18	3.32	3.28	4.66	4.97
c_3	4.42	1.87	8.13	4.01	5.69	5.85	0.00	11.72	12.33	9.23	2.64	2.00
c_4	0.00	0.00	0.00	0.00	0.00	0.00	0.00	0.00	0.00	0.00	0.04	0.00
c_5	-7.10	-3.96	-4.13	-5.84	-4.41	-5.54	-1.87	-3.34	-2.18	-7.96	-9.75	-2.36
c_6	0.21	0.32	0.37	0.34	0.47	0.47	0.69	0.65	0.85	0.35	0.42	0.89
c_7	27.39	33.45	36.67	24.35	30.00	36.78	16.62	16.39	20.35	10.41	25.99	23.63
c_8	0.14	0.19	0.15	0.22	0.23	0.24	0.31	0.44	0.44	0.45	0.37	0.45
R^2	0.714	0.641	0.693	0.885	0.882	0.877	0.861	0.894	0.876	0.919	0.932	0.900

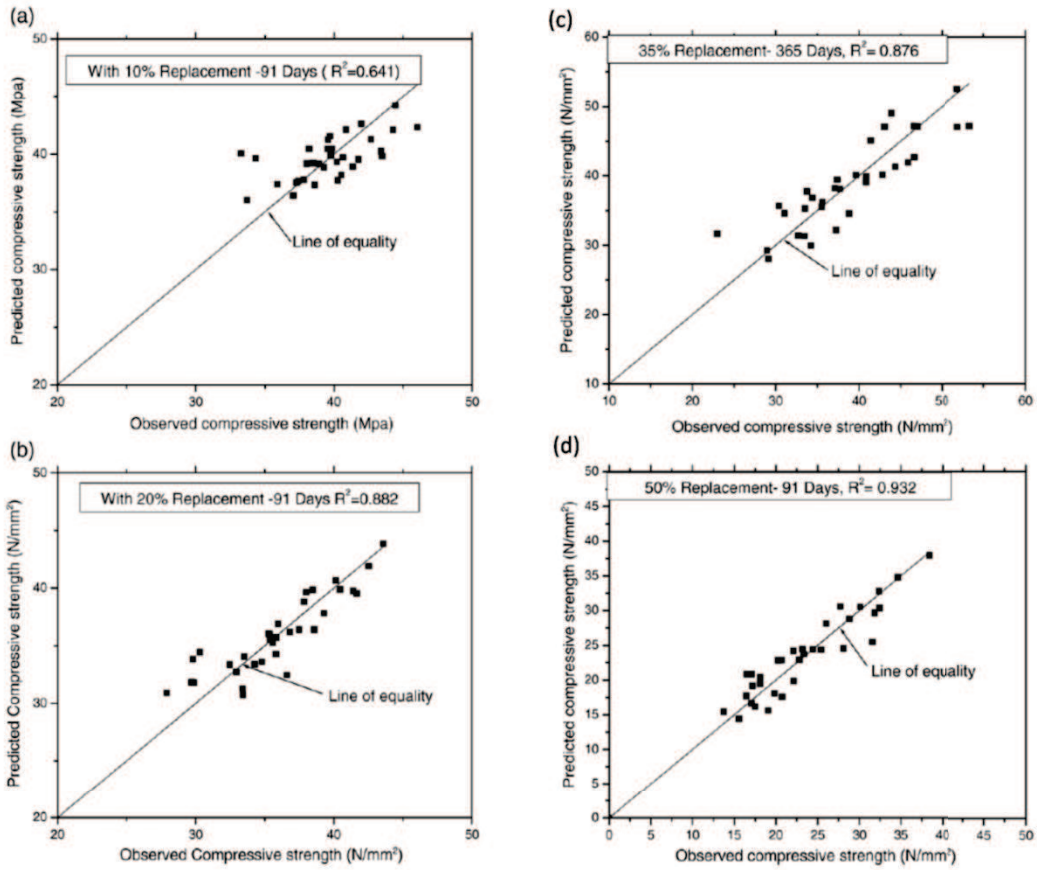

Figure 2.10. Observed and predicted compressive strength at 91 days for (a) 10% replacement, (b) 20% replacement, (d) 50% replacement and at 365 days for (c) 35% replacement (Das & Yudhbir, 2006)

2.2.5.4 Conclusions

From this research the following conclusions were made:

1. Linear power equation was modeled to predict compressive strength based on four parameters; ratio of potassium to alumina (K/A)*10, calcium oxide (CaO), Loss of Ignition (LOI) and fineness. Coefficients of the equation were determined by least square technology

2. It was observed that the R^2 was more than 0.85 for replacement of 20% and higher. The R^2 value got closer one with higher replacement levels. The equation did worst prediction for the 10% replacement.

2.2.6 Han, Kim, & Park, 2003

Prediction of compressive strength of fly ash concrete by new apparent activation energy function

2.2.6.1 Research Objective

Han, et al. produced a data inventory of fly ash concrete for various w/b ratio and fly ash replacement levels. Using the results, the authors proposed a new prediction model to estimate the compressive strength development of fly ash concrete.

2.2.6.2 Material and Mix Design

ASTM Type II Portland cement and one Class F fly ash were used in this research. Since the chemical composition for the cement weren't provided, typical values according to ASTM C 150 were used. Table 2.21 shows the physical properties and chemical analysis of the cement and fly ash that were used in the research.

Table 2.21. Physical properties and chemical analysis (%) of cement and fly ash (Han, Kim, & Park, 2003)

Compounds	Shorthand notation	ASTM Type II*	Class F Fly ash
Silicon Dioxide (SiO_2)	S	20.6	55.1
Aluminum Oxide (Al_2O_3)	A	4.4	34.9
Iron Oxide (Fe_2O_3)	F	3.3	3.7
$K_2O + Na_2O$	K+N	0.7	1.2
Sulphur Trioxide (SO_3)	$\bar{S}$	2.7	--
Calcium Oxide (CaO)	C	62.9	3.6
Magnesium Oxide (MgO)	M	2.2	1.2
Loss on Ignition	LOI	2.7	--
Specific gravity (g/cm^3)	SG	3.15	2.06
Active Silica	γ_s	--	--
Blaine specific surface (m^2/kg)	Blaine	370	332
Activity Index, 7 day (%)	7 AI	--	--
Activity Index, 28 day (%)	28 AI	--	--

*Typical values for ASTM Type II – no chemical composition given

Twenty-four mixtures were made with different w/b ratios and different replacement levels, thereof 6 mixes that were prepared as control mixes (100% Portland cement). The highest replacement level was 30%. The proportioning and the properties of the mixes are summarized in Table 2.22. The binder content in the mixes ranged from 231-600 kg/m^3 and the water content from 162-198 kg/m^3. For determination of the compressive test, the specimens were cast in 100x200 mm cylinders and cured till testing.

Table 2.22. Mixture proportions and properties of fresh concrete (Han, Kim, & Park, 2003)

Mixture no.	%	Cement (kg/m^3)	SCM[1] (kg/m^3)	Water (kg/m^3)	w/b	FAg[2] (kg/m^3)	CAg[3] (kg/m^3)	SP[4] (%)	Slump (mm)
WC60-0	0	330	0	198	0.60	788	963	0.0	74
WC60-10	10	297	33	198	0.60	781	955	0.0	49
WC60-20	20	264	66	198	0.60	775	947	0.0	53
WC60-30	30	231	99	198	0.60	768	938	0.0	50
WC55-0	0	350	0	193	0.55	787	962	0.0	55
WC55-10	10	315	35	193	0.55	780	953	0.0	38
WC55-20	20	280	70	193	0.55	773	945	0.0	35
WC55-30	28	254	100	193	0.55	766	936	0.0	34
WC40-0	0	420	0	168	0.40	703	1054	1.2	209
WC40-10	10	378	42	168	0.40	696	1044	1.2	182
WC40-20	20	336	84	168	0.40	688	1032	1.5	197
WC40-30	30	294	126	168	0.40	680	1020	1.7	189
WC35-0	0	480	0	168	0.35	683	1025	1.5	193
WC35-10	10	432	48	168	0.35	675	1012	1.5	218
WC35-20	20	384	96	168	0.35	666	999	1.5	190
WC35-30	30	336	144	168	0.35	657	986	1.8	179
WC32-0	0	520	0	166	0.32	638	1042	1.8	215
WC32-10	10	468	52	166	0.32	629	1027	1.8	216
WC32-20	20	416	104	166	0.32	621	1013	2.0	214
WC32-30	30	364	156	166	0.32	612	998	2.3	207
WC27-0	0	600	0	162	0.27	569	1056	2.0	217
WC27-10	10	540	60	162	0.27	560	1039	2.0	179
WC27-20	20	480	120	162	0.27	550	1022	2.3	175
WC27-30	30	420	180	162	0.27	541	1005	3.0	171

[1]Fly ash, [2]Fine Aggregate, [3]Coarse Aggregate, [4]Superplasticizer

2.2.6.3 Experimental Results

2.2.6.3.1 Compressive Strength

The compressive data is presented in Table 2.23. The early compressive strength of fly ash concrete tends to be less than the control mixes but the long-term compressive strength of fly ash concrete is larger than the control mix. The mixes with 10% replacement showed higher strength after 90 days, whereas mixes with 20% and 30% replacement showed higher strength than the control at 180 and 365 days, respectively.

Table 2.23. Compressive strength results of the mixes (Han, Kim, & Park, 2003)

Mixture no.	%	Measured Strength (MPa)					
		3 days	7 days	28 days	90 days	180 days	365 days
WC60-0	0	15.4	23.6	32.9	38.6	41.6	42.5
WC60-10	10	13.1	21.8	33.8	40.3	45.4	47.6
WC60-20	20	10.2	18.0	28.0	37.2	41.6	44.8
WC60-30	30	7.2	13.5	25.0	36.0	40.1	43.2
WC55-0	0	18.7	26.6	36.1	40.2	46.3	46.5
WC55-10	10	16.0	25.4	38.3	45.8	49.6	51.8
WC55-20	20	14.6	22.6	33.8	43.5	50.0	52.1
WC55-30	28	12.7	18.3	30.9	39.3	47.0	48.2
WC40-0	0	34.0	43.6	49.7	56.3	60.4	61.9
WC40-10	10	31.5	42.1	50.3	57.5	62.8	66.5
WC40-20	20	29.4	38.0	48.0	56.5	61.4	65.4
WC40-30	30	24.2	33.7	42.8	53.5	57.6	61.3
WC35-0	0	45.0	49.1	56.3	59.7	66.6	68.8
WC35-10	10	39.5	50.2	55.7	64.3	72.4	74.8
WC35-20	20	34.1	44.9	56.0	61.3	71.4	75.3
WC35-30	30	27.0	39.1	51.8	59.5	68.9	73.9
WC32-0	0	45.9	52.2	62.1	63.3	71.2	71.4
WC32-10	10	43.4	51.9	61.7	65.3	75.4	77.6
WC32-20	20	39.6	46.6	58.6	66.1	78.1	78.9
WC32-30	30	28.8	36.5	44.2	57.7	67.5	72.8
WC27-0	0	56.5	61.2	71.8	73.8	82.0	83.4
WC27-10	10	49.9	56.6	67.7	75.4	85.2	87.4
WC27-20	20	44.0	50.5	65.0	72.8	81.3	85.2
WC27-30	30	34.5	40.0	51.9	60.4	70.8	78.6

2.2.6.3.2 Application of Prediction Model

The authors proposed a model to predict a concrete strength with fly ash as replacement. The proposed model is expressed as follows:

$$\frac{S}{S_{28}} = R_u \left\{ 1 - \frac{1}{\sqrt{1 + A\left[e^{-\frac{E_0}{RT}e^{-\alpha t}} + e^{-\frac{E_0}{RT}e^{-\alpha t_0}}(t - t_0)\right]}} \right\} \quad \textbf{(2.9)}$$

where S is the compressive strength (MPa), S_{28} is the 28-day compressive strength at each curing temperature (MPa), R_u is the limiting relative compressive strength with $R_u = S_u/S_{28}$, S_u is the limiting compressive strength (MPa), A is a constant, R is gas constant and equal to 8.3144 J/K mol, T is curing temperature (K), E_0 is initial apparent activation energy (J/mol),

α is a constant, t is age (days), and t_0 is age when the strength development is assumed to begin (days). The authors suggested that t_0 should be taken as zero and $A = 10^7$. Therefore this equation involves three unknown parameters, R_u, E_0 and α. Regression results were used to calibrate the three unknown parameters. The authors found that α did not vary with fly ahs replacement and was independent of w/b ratio. Therefore, all the data could be average using α = 0.000615.

Estimation of the limiting relative compressive strength (R_u) was divided into two groups depending on the w/b ratio:

w/b ≤ 0.40 $$R_u = 1.166 + 0.008FA \quad \textbf{(2.10)}$$

w/b > 0.40 $$R_u = 1.313 + 0.013FA \quad \textbf{(2.11)}$$

where FA is the fly ash replacement ratio (%). Estimation of the initial apparent activation energy (E_0) was divided into the same groups depending on the w/b ratio:

w/b ≤ 0.40 $$E_0 = 39720 + 119FA \quad \textbf{(2.12)}$$

w/b > 0.40 $$E_0 = 42920 + 90FA \quad \textbf{(2.13)}$$

where FA is the fly ash replacement ratio (%) like before. To estimate the 28 day compressive strength (S_{28}), the authors used the modified Bolomey strength equation, Eq. (2.4). Figure 2.11 shows the regression curves and experimental results for the relative compressive strength (normalized for the 28 day) according to the w/b ratio.

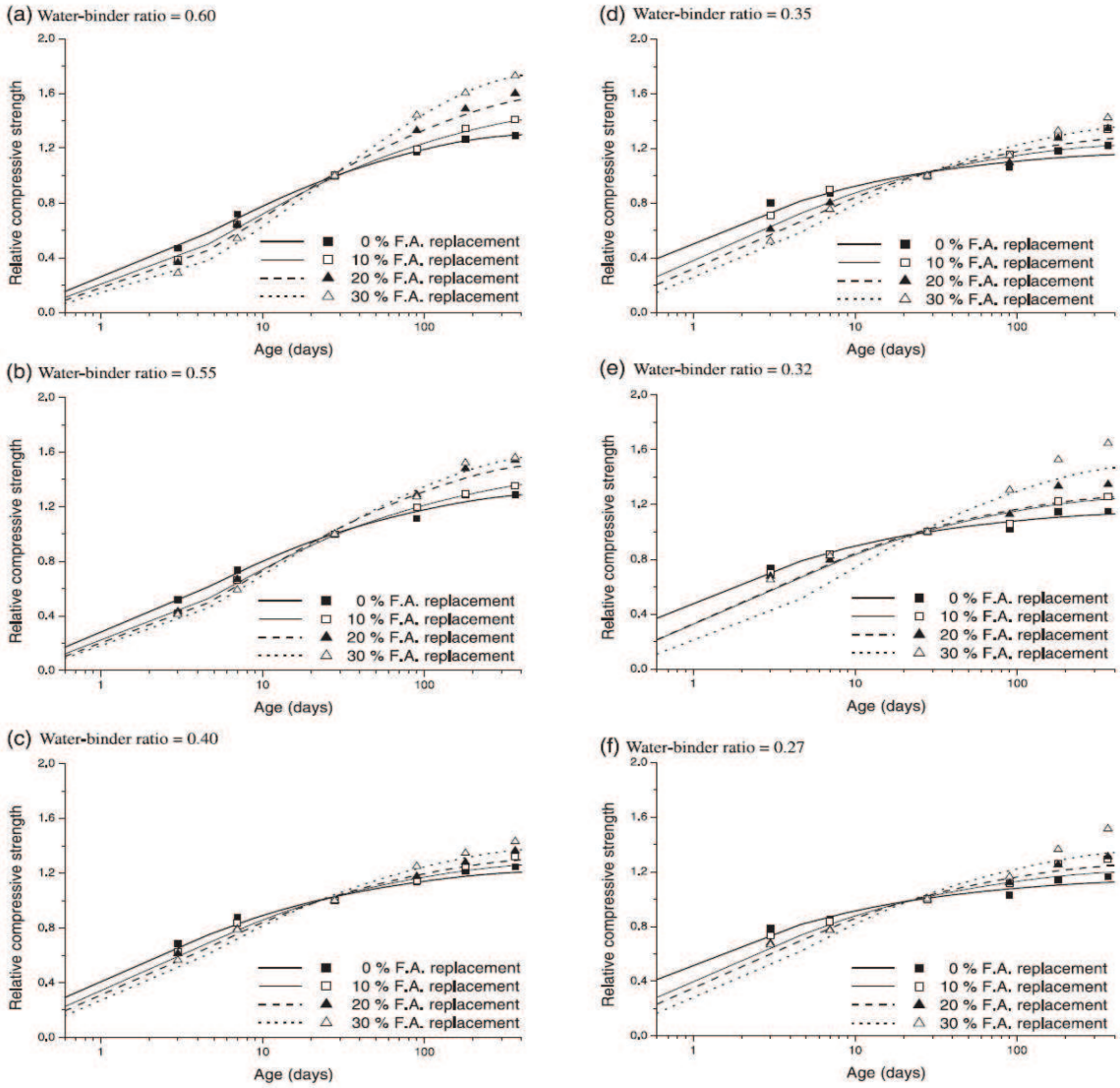

Figure 2.11. Experimental and calculated relative compressive strength (Han, Kim, & Park, 2003)

2.2.6.1 Conclusions

From this research the following conclusions were made:

1. Fly ash replacement mix increases the long-term strength although the strength development is delayed with an increase cement replacement.

2. Fly ash replacement ratio and w/b ratio was used to determine the initial apparent activation energy and the limiting relative compressive strength. However, the constant α was found independent of both fly ash replacement and w/b ratio.

3. The proposed prediction model does a decent job of predicting the compressive strength of concrete that contains fly ash as cement replacement.

2.2.7 Hwang, Noguchi, Tomosawa, 2004

Prediction model of compressive strength development of fly-ash concrete

2.2.7.1 Research Objective

Hwang, et al. proposed an equation to estimate the strength development of concrete that contains fly ash as cement replacement. Furthermore the aim is to establish a technique of proportioning concrete with high volume of fly ash.

2.2.7.2 Material and Mix Design

Twenty-one mixes were designed with different w/b ratios and different replacement levels, thereof 5 mixes that were prepared as control mixes (100% Portland cement). Table 2.24 shows the physical properties of the cement and fly ash that were used in the research.

Table 2.24. Physical properties of cement and fly ash (Hwang, Noguchi, & Tomosawa, 2004)

Compounds	Shorthand notation	Cement	Fly ash
Specific gravity (g/cm^3)	SG	3.16	2.27
Blaine specific surface (m^2/kg)	Blaine	337	389

The proportioning and the properties of the mixes are summarized in Table 2.25. The highest replacement level in this research was 49%. The binder content in the mixes ranged from 250-629 kg/m^3 and the water content remained constant at 175 kg/m^3. For determination of the compressive test, the specimens were cast in 100x200 mm cylinders and cured till testing.

Table 2.25. Mixture proportions and properties of fresh concrete (Hwang, Noguchi, & Tomosawa, 2004)

Mix name	%	Cement (kg/m^3)	SCM[1] (kg/m^3)	Water (kg/m^3)	w/b	FAg[2] (kg/m^3)	CAg[3] (kg/m^3)	AEA[4] (%)	Slump (mm)	Air (%)
PL35	0	500	0	175	0.35	760	991	1.7	21.3	3.1
EX35-20	21	500	129	175	0.28	608	991	2.5	20.4	1.6
PL40	0	438	0	175	0.40	811	991	1.6	22.8	3.6
EX40-10	14	438	69	175	0.35	730	991	1.8	21.8	1.6
EX40-20	24	438	137	175	0.30	649	991	2.0	21.1	1.9
EX40-30	32	438	206	175	0.27	568	991	2.5	19.7	1.5
PL50	0	350	0	175	0.50	884	991	1.5	19.5	3.3
EX50-10	18	350	75	175	0.41	795	991	1.4	18.0	2.3
EX50-20	30	350	150	175	0.35	707	991	1.7	18.1	2.3
EX50-30	39	350	224	175	0.30	607	991	2.1	11.5	2.3
IN50-10	10	315	35	175	0.50	871	991	1.4	19.5	2.7
IN50-20	20	280	70	175	0.50	842	991	1.4	19.0	2.6
IN50-30	30	245	105	175	0.50	845	991	1.8	20.0	3.6
PL60	0	291	0	175	0.60	914	991	1.4	18.1	2.3
EX60-10	21	291	79	175	0.47	839	991	1.5	20.5	1.7
EX60-20	35	291	158	175	0.39	732	991	1.6	18.5	1.6
EX60-30	45	291	237	175	0.33	653	991	2.2	11.6	2.0
PL70	0	250	0	175	0.70	948	991	1.5	18.1	3.0
EX70-10	25	250	82	175	0.53	870	991	1.5	19.5	1.5
EX70-20	40	250	164	175	0.42	758	991	1.7	19.8	2.2
EX70-30	49	250	245	175	0.35	676	991	1.9	18.7	1.6

[1]Fly ash, [2]Fine Aggregate, [3]Coarse Aggregate, [4]Air-entraining admixture

2.2.7.3 Experimental Results

2.2.7.3.1 Compressive Strength

The compressive strength development for selected mixes is presented in Figure 2.12. The early-age compressive strength of the cement replacement mixes (IN) were less than the control mixes (PL) but the long-term compressive strength IN mixes were larger. The sand addition mixes (EX) exhibited higher strength than the control mix which is expected since the EX mix have higher binder content.

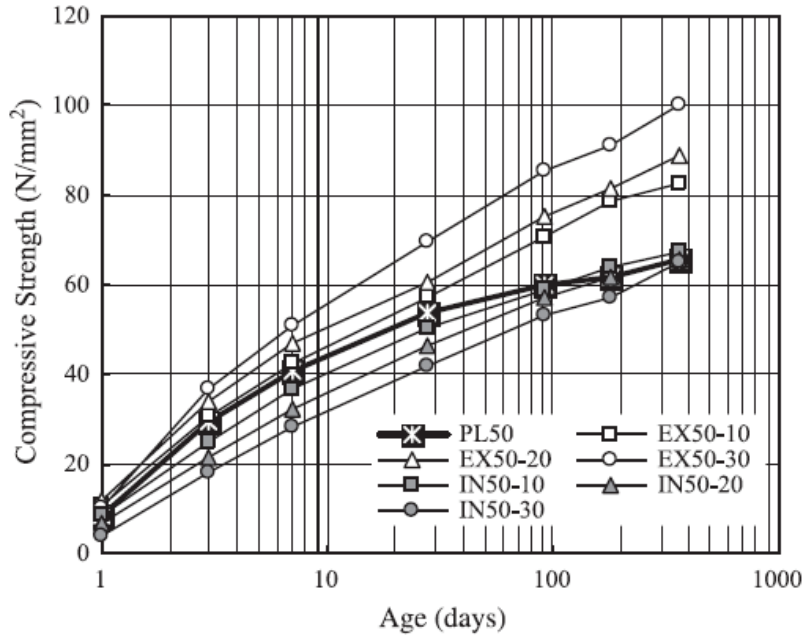

Figure 2.12. Compressive strength development (Hwang, Noguchi, & Tomosawa, 2004)

2.2.7.3.2 Application of Prediction Model

The authors proposed a prediction equation to predict a concrete strength with fly ash as replacement. The proposed equation is expressed as follows:

$$f_c(t) = \left(\frac{t}{a + bt}\right)\left(\frac{\alpha_1 \alpha_2 FA + C}{W}\right) + B \quad \textbf{(2.14)}$$

where f_c (t) is the compressive strength at day t (N/mm^2), t is the age (days), W is the water content (kg/m^3), C is the cement content (kg/m^3) and B is an experimental constant. a and b are experimental constants, α_1 is function of FA/C, α_2 is function of specific surface area by Blaine, FA is the fly ash content (kg/m^3). The coefficients a, b and B are independent of the fly ash properties and can thus be calibrated with the control mix alone. Following expression was used to evaluate $\alpha_{1:}$

$$\alpha_1 = k_1(t)\exp\{k_2(t)(FA/C)\} \quad \textbf{(2.15)}$$

where k_1(t) and k_2(t) are functions of age and can be determine with following expression:

$$k_1(t) = m_1\{1 - exp(-m_2) + m_3\} \quad \textbf{(2.16)}$$

$$k_2(t) = n_1\{1 - exp(-n_2) + n_3\} \quad \textbf{(2.17)}$$

where m_1, m_2, m_3, n_1, n_2, n_3 are experimental coefficients. They were found to be m_1 = 1.55, m_2 = 0.0075, m_3 = 0.156, n_1 = -0.750, n_2 = 0.01 and n_3 = -0.371. To estimated α_2 the following expression was used:

$$\alpha_2 = k_3 \cdot Blaine + 0.71 \quad \textbf{(2.18)}$$

where Blaine is the specific surface area by Blaine (cm^2/g) and k_3 is an experimental coefficient, $k_3 = 1.14x10^{-4}$

Figure 2.13 shows the relationship between calculated and measured strength values, for this research and a few others.

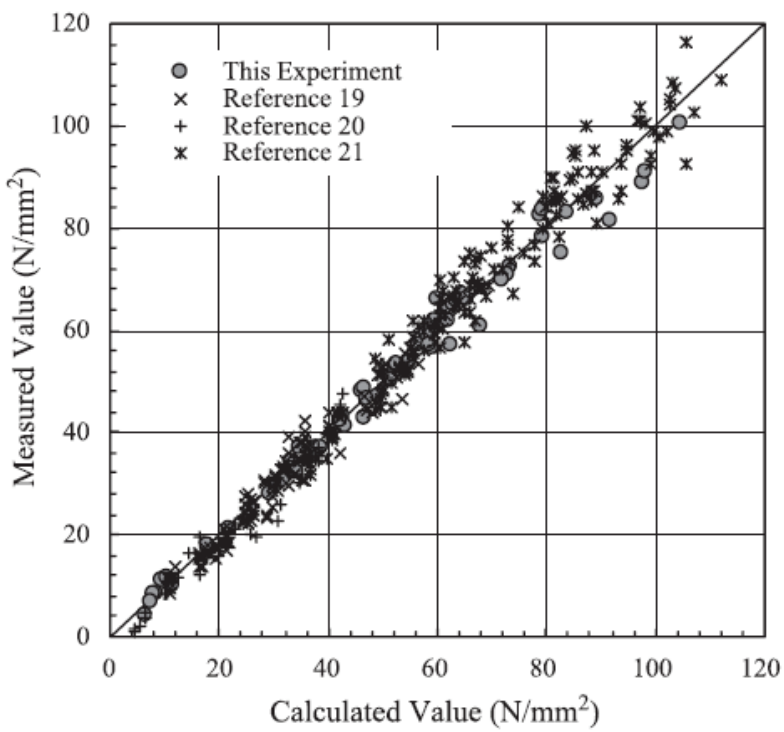

Figure 2.13. Relationship between calculated and measured strength (Hwang, Noguchi, & Tomosawa, 2004),

2.2.7.4 Conclusions

From this research the following conclusions were made:

1. An equation was derived to estimate the compressive strength development of concrete containing fly ash.

2. This equation is capable of explaining the increase in early-strength when fine aggregate is replaced with fly ash as well as the decrease in early-strength and increase in long-term strength when fly ash is used as cement replacement.

3. The equation takes also into account the effect of fly ash's Blaine specific surface area on the strength.

2.2.8 Langley, Carette, & Malhotra, 1989

Structural Concrete Incorporating High Volumes of ASTM Class F fly ash

2.2.8.1 Research Objective

Langley, et al. examined the major engineering properties of concrete that contains 56 % Class F fly ash as cement replacement.

2.2.8.2 Material and Mix Design

Two types of Portland cements were selected, ASTM Type I and ASTM Type III in additio, ASTM Class F fly ash was selected as the SCM. Table 2.26 shows the physical properties and chemical analysis of the cements and fly ash that were used.

Table 2.26. Physical properties and chemical analysis (%) of cements and fly ash (Langley, Carette, & Malhotra, 1989)

Compounds	Shorthand notation	ASTM Type I	ASTM Type III	Fly ash
Silicon Dioxide (SiO_2)	S	20.2	20.3	45.2
Aluminum Oxide (Al_2O_3)	A	5.3	5.6	20.7
Iron Oxide (Fe_2O_3)	F	2.7	2.0	24.8
$K_2O + Na_2O$	K+N	1.3	1.3	3.0
Sulphur Trioxide (SO_3)	$\bar{S}$	4.3	5.4	--
Calcium Oxide (CaO)	C	61.7	62.2	1.6
Magnesium Oxide (MgO)	M	1.7	1.4	1.0
Loss on Ignition	LOI	--	--	--
Specific gravity (g/cm^3)	SG	--	--	--
Active Silica	γ_s	--	--	--
Blaine specific surface (m^2/kg)	Blaine	380	579	351
Activity Index, 7 day (%)	7 AI	--	--	--
Activity Index, 28 day (%)	28 AI	--	--	96

Thirteen mixes were made with different w/b ratios (0.28 to 0.49). There were 6 control mixes with 100% Portland cement. Nine mixes were made with ASTM Type I cement and four mixes were made with ASTM Type III. The cement replacement was 55-56 % by weight. The binder content varied from 225-400 kg/m^3 and water varied from 102-132 kg/m^3. The proportioning and the properties of the mixes are summarized in Table 2.27. For determination of elastic modulus, compressive strength, drying- and creep characteristics, 150x300 mm cylinders were cast.

Table 2.27. Mixture proportions and properties of fresh concrete (Langley, Carette, & Malhotra, 1989)

Cement Type	Mix no.	%	Cement (kg/m^3)	SCM[1] (kg/m^3)	Water (kg/m^3)	w/b	FAg[2] (kg/m^3)	CAg[3] (kg/m^3)	AEA[4] (mL/m^3)	Slump (mm)	Air (%)
I	1	55	180	220	110	0.28	760	1110	180	120	6.0
	1C	0	340	0	132	0.39	855	1020	40	140	5.5
	2	56	150	190	102	0.30	795	1100	215	200	6.6
	2C	0	340	0	132	0.39	855	1020	40	200	6.9
	3	56	150	190	111	0.33	760	1135	115	100	6.0
	3C	0	295	0	132	0.45	885	995	115	110	6.6
	4	56	150	190	119	0.35	750	1100	190	210	6.9
	4C	0	290	0	132	0.46	800	1020	85	210	6.4
	5	56	100	125	110	0.49	880	1100	165	100	3.6
III	6	56	150	190	102	0.30	795	1100	225	205	6.5
	6C	0	340	0	132	0.39	855	1020	40	210	6.4
	7	56	150	190	119	0.35	750	1100	170	210	6.6
	7C	0	290	0	132	0.46	800	1020	140	220	6.9

[1]Fly ash, [2]Fine Aggregate, [3]Coarse Aggregate, [4]Air-entraining admixture

2.2.8.3 Experimental Results

2.2.8.3.1 Compressive Strength

The compressive data is presented in Table 2.28. The strength data for selected mixes up to 365 days are presented in Figure 2.14. As expected, the early strength (≤ 7 days) of the control mixes was higher than the SCM mixes. However, a very rapid strength gain occurs in the mixes that had fly ash as replacement between days 7 and 28 and again from 28 to 91 days. At 91 days, all of the SCM mixes have higher strength than the control mixes. The early age of a concrete that contains ASTM Type I cement alone is comparable to concrete made with ASTM Type III and a high volume of fly ash.

Table 2.28. Compressive strength results of the mixes (Langley, Carette, & Malhotra, 1989)

Cement Type	Mix no.	Measured Strength (MPa)					
		1 days	3 days	7 days	28 days	91 days	365 days
I	1	13.7	22.4	34.2	57.1	75.2	--
	1C	27.3	35.6	44.6	52.3	54.0	--
	2	0.6	17.7	26.0	49.1	63.0	79.0
	2C	10.2	32.2	40.4	50.7	57.3	60.6
	3	16.5	17.2	25.8	46.1	61.8	--
	3C	2.7	31.0	38.7	47.2	51.3	--
	4	20.5	15.5	20.5	37.5	53.0	69.0
	4C	4.0	30.5	34.9	44.7	49.1	52.2
	5	--	8.6	12.1	23.0	37.9	--
III	6	30.5	22.0	30.0	48.5	64.0	84.1
	6C	5.7	42.4	49.0	59.0	59.0	66.8
	7	30.7	16.7	23.8	37.5	53.7	63.7
	7C	--	37.5	41.1	46.1	51.0	53.2

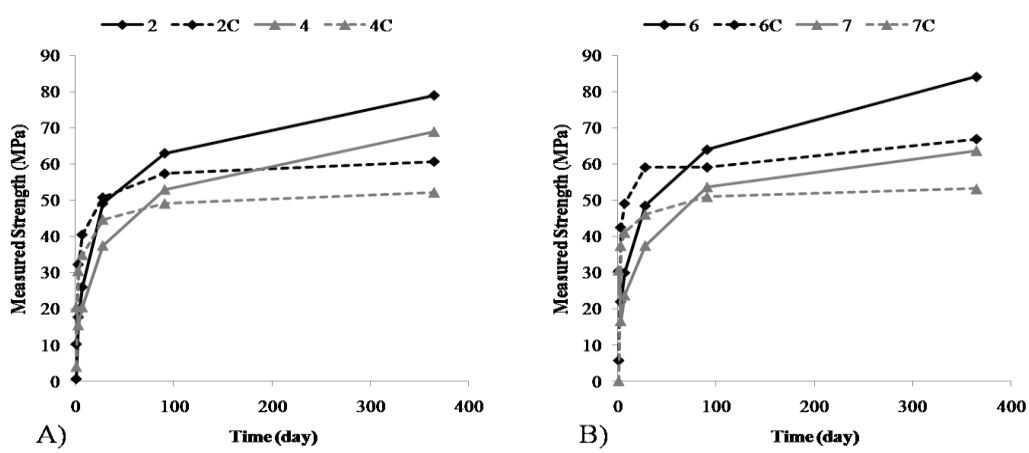

Figure 2.14. Compressive strength development of the concrete mixes reproduced from Langley, et al. 1989. Figure A) show mixes with ASTM Type I cement and Figure B) shows mixes made with ASTM Type III cement

2.2.8.3.2 Elastic Modulus

The elastic modulus data is presented in Table 2.29. Figure 2.15 shows the elastic modulus development of selected mixes. All of the fly ash concrete show considerable increase in elastic modulus between 28 and 365 days and substantially larger values than control concretes at 365 days. The elastic modulus for the fly ash concrete ranged from 43.1 to 46.6 GPa.

Table 2.29. Elastic modulus results of the mixes (Langley, Carette, & Malhotra, 1989)

Cement Type	Mix no.	Elastic Modulus (GPa)	
		28 days	365 days
I	1	36.1	--
	1C	31.5	--
	2	35.1	46.6
	2C	36.8	38.2
	3	33.8	--
	3C	28.9	--
	4	31.6	--
	4C	34.9	34.4
	5	27.9	--
III	6	32.7	46.1
	6C	32.2	36.3
	7	32.1	43.1
	7C	32.6	34.8

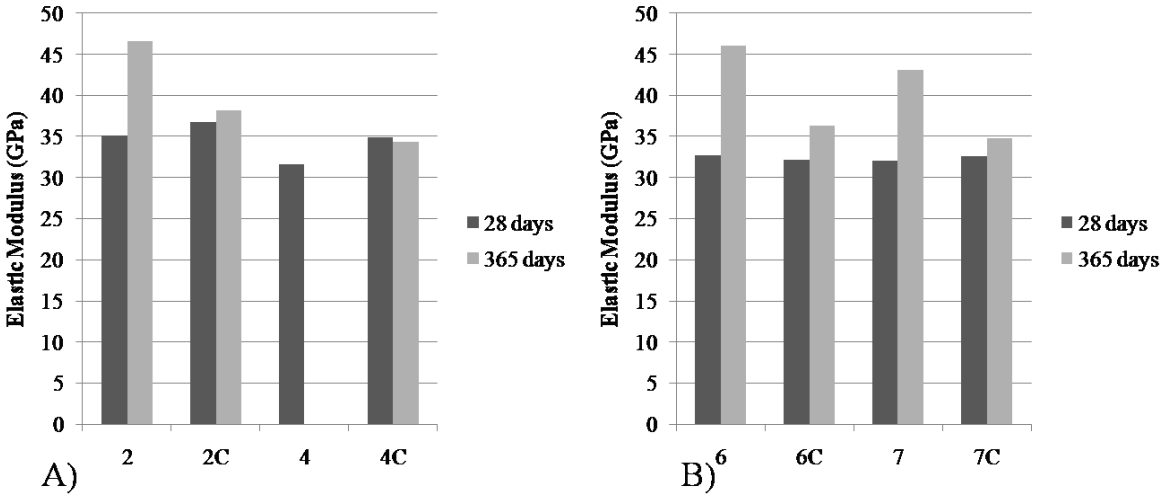

Figure 2.15. Elastic modulus development between 28 and 365 days of the concrete mix reproduced from Langley, et al. 1989. Figure A) shows mixes with ASTM Type I cement and Figure B) shows mixes made with ASTM Type III cement

2.2.8.3.3 Drying Shrinkage and Creep

The concrete specimens were cured for 7 days prior to air drying. The results are shown Figure 2.16. The fly ash concrete showed lower total shrinkage strains at the end of the test (approximately 15 months). Figure 2.17 shows the long-term creep deformation of the fly ash and control concrete. The specimens were cured for 28 days prior loading. After about 250 days of loading it was observed that the creep of fly ash concrete is significantly less than the creep of the control concrete.

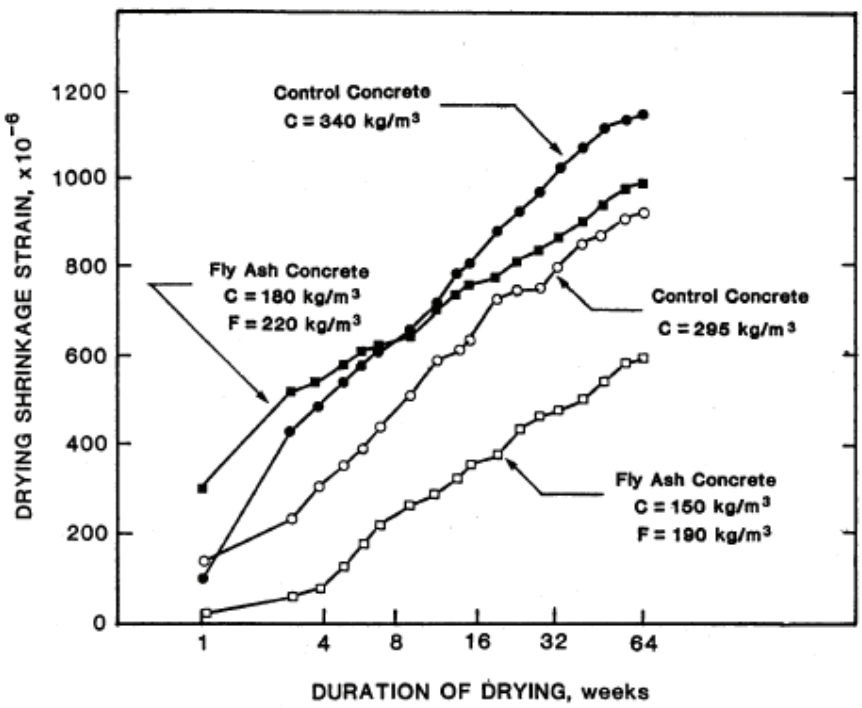

Figure 2.16. Drying shrinkage strains of control and fly ash concrete after 7 days of curing (Langley, Carette, & Malhotra, 1989)

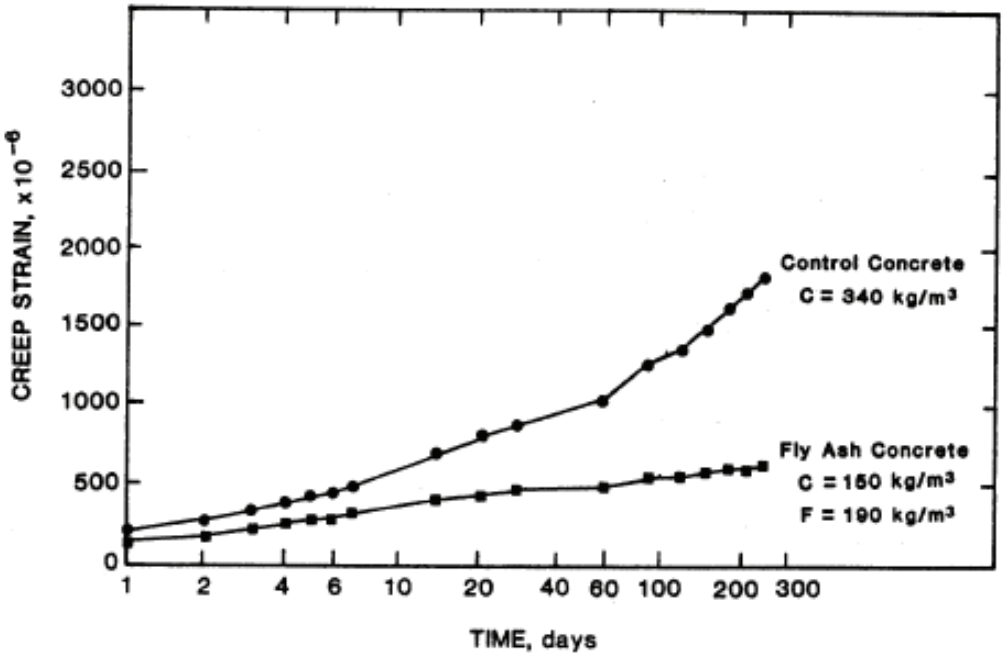

Figure 2.17. Creep strains of control and fly ash concrete after 28 day of curing (Langley, Carette, & Malhotra, 1989)

2.2.8.4 Conclusions

From this research the following conclusions were made:

1. Concrete that has high volume of ASTM Class F fly ash can reach strength of about 60 MPa at 120 days. The amount of Class F fly ash to achieve maximum strength has not been determined, but the authors point out that extensive data indicates that it should be in the range of 55-60%.

2. This research indicates that concrete with high volume of fly ash has better mechanical performance, such as elastic modulus, drying- and creep strains, than concrete made only with Portland cement.

3. The early-age concrete that contains ASTM Type I cement alone is comparable to concrete made with ASTM Type III and high volume of fly ash.

2.2.9 Naik & Singh, 1997

Influence of Fly Ash on Setting and Hardening Characteristic of Concrete Systems

2.2.9.1 Research Objective

Naik and Singh examined the setting and hardening characteristics of concrete that contains Class C fly ash from number of sources.

2.2.9.2 Material and Mix Design

ASTM Type I Portland cement was selected and four fly ashes, all Class C, were used. Table 2.30 shows the physical properties and chemical analysis of the cement and fly ashes that were used in the research.

Table 2.30. Physical properties and chemical analysis (%) of cement and fly ash (Naik & Singh, 1997)

Compounds	Shorthand notation	ASTM Type I	P-4 Fly ash	DPC Fly ash	Columbia Fly ash	Weston Fly ash
Silicon Dioxide (SiO_2)	S	20.7	32.9	32.2	44.8	30.0
Aluminum Oxide (Al_2O_3)	A	4.4	19.4	18.4	22.8	17.6
Iron Oxide (Fe_2O_3)	F	2.4	5.4	5.8	4.2	4.9
$K_2O + Na_2O$	K+N	0.9	2.2	1.7	0.7	2.7
Sulphur Trioxide (SO_3)	$\overline{S}$	--	--	--	--	--
Calcium Oxide (CaO)	C	57.5	28.9	23.9	17.0	27.9
Magnesium Oxide (MgO)	M	1.6	4.8	5.1	5.1	6.2
Loss on Ignition	LOI	1.1	0.7	5.6	0.3	0.2
Specific gravity (g/cm^3)	SG	3.16	2.78	2.58	2.62	2.68
Active Silica	γ_s	--	--	--	--	--
Blaine specific surface (m^2/kg)	Blaine	351	--	--	--	--
Activity Index, 7 day (%)	7 AI	--	--	79	82	87
Activity Index, 28 day (%)	28 AI	--	105	85	99	97

A total of 34 mixes were prepared, with cement replacement up to 100%, and tested for initial and final time of set. Four of the thirty-four mixes were prepared as control mixes with only Portland cement as binder. The binder content in the mixes varied from 345 to 488 kg/m^3, the water content varied from 135 to 176 kg/m^3 and the w/b ratio in the mixes varied from 0.34-0.37. The proportioning and the properties of the mixes are summarized in Table 2.31. For determination of compressive strength the concrete mixes were cast in 150x300 mm cylinders and for the testing of time of set the concrete mixes were placed in 150x150x600 mm molds.

Table 2.31. Mixture proportions and properties of fresh concrete (Naik & Singh, 1997)

Mix name	%	Cement (kg/m^3)	SCM[1] (kg/m^3)	Water (kg/m^3)	w/b	FAg[2] (kg/m^3)	CAg[3] (kg/m^3)	Slump (mm)	Air (%)
P-4 FA	0	360	0	169	0.47	815	1070	200	2.3
	10	324	45	162	0.44	815	1070	--	1.2
	20	288	91	162	0.43	815	1077	175	0.8
	30	252	135	167	0.43	815	1084	200	0.6
	40	216	180	135	0.34	833	1084	215	1.0
	50	180	224	167	0.41	815	1084	215	1.0
	60	144	270	155	0.37	815	1084	150	0.6
	70	108	315	167	0.39	815	1084	100	2.1
	80	72	360	155	0.36	815	1084	150	1.1
	90	37	405	167	0.38	815	1084	180	0.7
	100	0	488	155	0.32	815	1084	180	0.6
DCP FA	0	371	0	158	0.42	840	1110	200	2.3
	10	334	46	157	0.41	840	1110	75	2.0
	30	257	138	156	0.39	830	1100	140	1.6
	50	174	218	176	0.45	802	1040	165	1.3
	70	108	315	154	0.35	812	1077	125	1.5
	90	36	403	153	0.35	807	1070	200	1.0
Columbia FA	0	360	0	151	0.44	850	1080	110	1.4
	10	326	46	152	0.41	854	1085	170	1.8
	30	254	136	152	0.39	854	1085	190	0.1
	50	180	165	150	0.37	845	1075	190	1.3
	70	768*	310	164	0.40	816	1055	170	0.3
	90	35	394	150	0.35	820	1053	170	1.1
Weston FA	0	360	0	151	0.44	850	1080	110	1.4
	20	290	90	148	0.39	855	855	100	1.8
	40	215	180	170	0.43	840	1060	190	1.6
	60	144	270	158	0.38	840	1072	190	0.4
	80	71	352	144	0.34	832	1054	195	1.5
	100	0	437	155	0.35	825	1050	--	--

* Most likely that this is a typo, should probably be 168

[1]Fly ash, [2]Fine Aggregate, [3]Coarse Aggregate

2.2.9.3 Experimental Results

2.2.9.3.1 Compressive Strength

The compressive strength data for concrete mixes at age of 28 day is shown in Figure 2.18. The scale of this figure is likely an error; it should most likely be either psi or kPa. However, this data suggest that cement replacement up to 50-60 % gives the best compressive strength by using Class C fly ash as SCM.

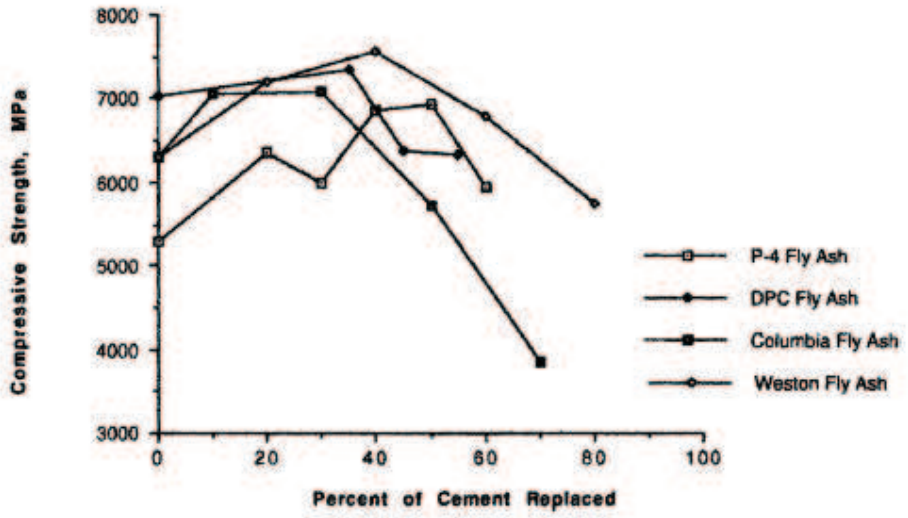

Figure 2.18. The 28 day compressive strength for the mixes as function of replacement (Note that the strength is represented in MPa; this is probably an error and is most likely either psi or kPa) (Naik & Singh, 1997)

2.2.9.3.2 Time of Set

The initial and final setting from this research is presented in Table 2.32. Figure 2.19 and Figure 2.20 show graphically the initial and final setting, respectively. Both the source of fly ash and the replacement level effect both the initial and final setting. In general a large delay occurs in both initial and final setting up 70% cement replacement when compared to the control mix. Beyond 70% replacement, time of set decreases relative to the control mix. At replacement higher than 80%, flash set occurs for the DCP and P-4 fly ash mixes.

Table 2.32. Summary of times of setting for the different SCMs; hr:min (Naik & Singh, 1997)

%	P-4 FA		DCP FA		Columbia FA		Weston FA	
	Initial set	Final set	Initial set	Final set	Initial set	Final set	Initial set	Final set
0	4:35	5:55	4:35	6:00	4:20	5:45	4:20	5:45
10	5:05	6:30	5:00	6:50	6:35	8:20	--	--
20	7:20	9:05	6:15	8:10	--	--	5:25	7:20
30	8:30	10:15	7:30	9:30	10:00	12:35	--	--
40	10:40	12:25	9:20	11:40	--	--	7:05	9:55
50	10:25	13:25	9:40	12:30	12:30	15:40	--	--
60	10:10	13:30	4:45	12:10	--	--	8:00	10:45
70	6:30	9:55	2:30	3:35	12:30	21:40	--	--
80	2:40	3:55	1:30	1:45	--	--	5:50	11:50
90	1:30	1:50	--	--	4:30	7:25	--	--
100	0:40	0:50	--	--	--	--	--	--

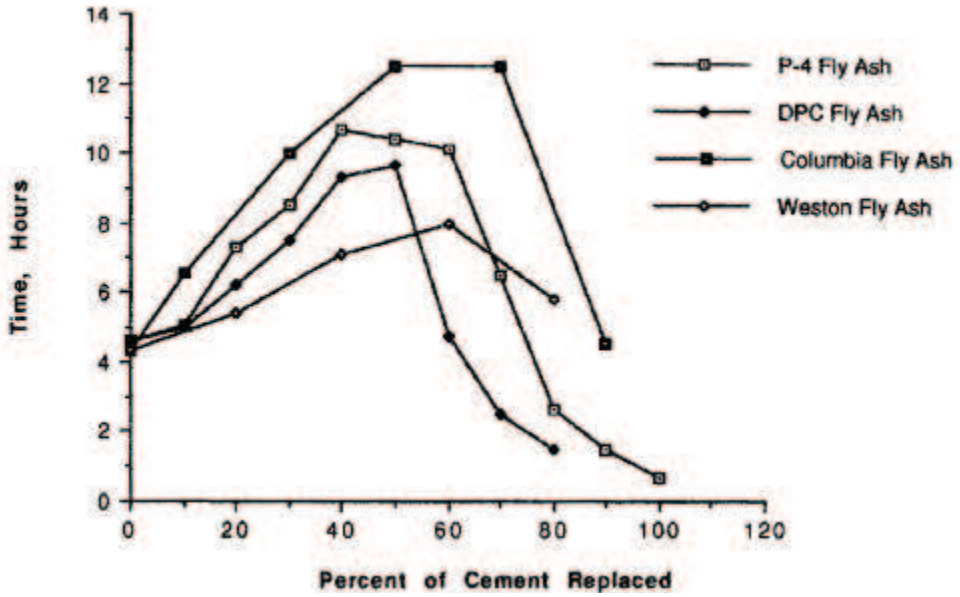

Figure 2.19. Initial setting of the for the four different SCMs (Naik & Singh, 1997)

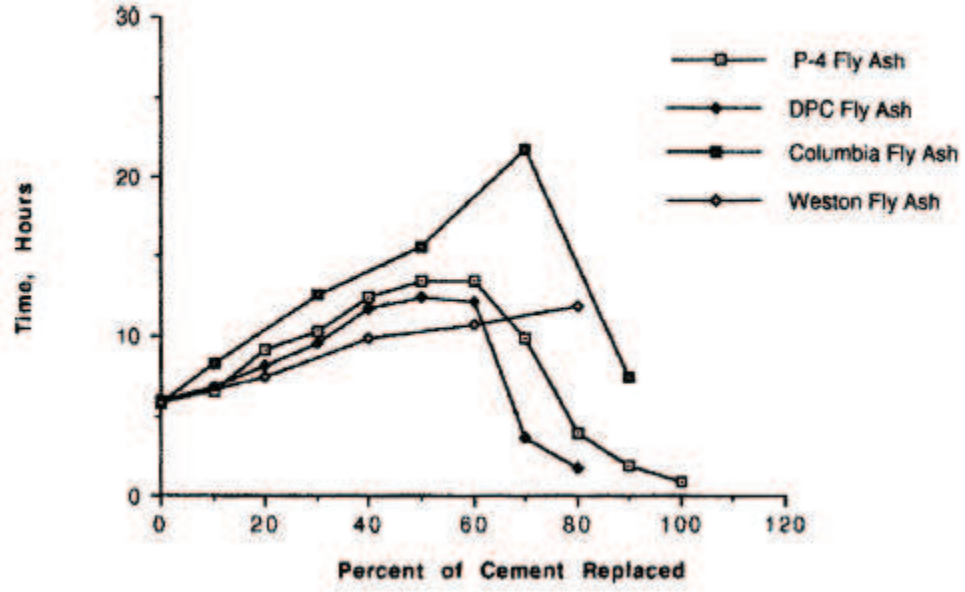

Figure 2.20. Final setting of the for the four different SCMs (Naik & Singh, 1997)

The authors state that the delay in time of set is associated with dilution effect resulting from cement replacements with fly ash. Additionally, the authors argue, that fly ash properties themselves also contributed to the variations in the time of set. The authors suggest that the flash set at high replacement ratios might be attributed to the fact that the concentration of gypsum in the mixture becomes low.

2.2.9.4 Conclusions

From this research the following conclusions were made:

1. Both initial and final setting is influenced by the amount and source of fly ash used.
2. In general, delay occurs in both initial and final set times for 70% fly ash replacement went up when compared to the control mix. Beyond the peak delay, the setting characteristics reverse, that is, the SCM mixtures set faster than the control. For some sources of fly ash flash set occurred at replacement higher than 80%.
3. Retarding or accelerating admixture can be used to control the setting characteristics of the SCM mixes.
4. The SCM mixes showed higher compressive strength than the control mix up to 70% even though significant delay was in most cases associated with that replacement level. Therefore, setting characteristic of SCM concretes should not be taken as sole parameter when selecting fly ash and replacement for particular application.

2.2.10 Naik, Singh, & Ramme, 1998

Mechanical Properties and Durability of Concrete Made with Blended Fly Ash

2.2.10.1 Research Objective

Naik, et al. hypothesized that a blend of Class F and Class C fly ashes should produce a rate of hydration reaction in between that of a concrete with Class F fly ash mixture and Portland cement mixture. Furthermore, the authors believe that the concrete containing the blended fly ash should have improved microstructure, which should lead to better mechanical properties and durability. These theories were examined experimentally through testing of the compressive strength and elastic modulus.

2.2.10.2 Material and Mix Design

ASTM Type I Portland cement was selected and two types of fly ashes, Class C and Class F, were chosen as the SCM. Table 2.33 shows the physical properties and chemical analysis of the cement and fly ashes that were used in the research.

Table 2.33. Physical properties and chemical analysis (%) of cements and fly ash (Naik, Singh, & Ramme, 1998)

Compounds	Shorthand notation	ASTM Type I	Class C Fly ash	Class F Fly ash
Silicon Dioxide (SiO_2)	S	21.1	34.2	48.4
Aluminum Oxide (Al_2O_3)	A	3.9	19.3	27.0
Iron Oxide (Fe_2O_3)	F	2.9	5.8	6.6
$K_2O + Na_2O$	K+N	1.8	1.3	1.5
Sulphur Trioxide (SO_3)	$\bar{S}$	3.7	3.1	0.6
Calcium Oxide (CaO)	C	74.7	29.2	8.5
Magnesium Oxide (MgO)	M	2.0	5.0	2.0
Loss on Ignition	LOI	1.0	0.5	2.8
Specific gravity (g/cm^3)	SG	3.11	2.59	2.24
Active Silica	γ_s	--	--	--
Blaine specific surface(m^2/kg)	Blaine	385	--	--
Activity Index, 7 day (%)	7 AI	--	--	--
Activity Index, 28 day (%)	28 AI	--	107	82

Five mixes were made, one control mix (100% Portland cement), one with only Class C fly ash (35% cement replacement) and three with blended fly ashes (40% cement replacement). The blended ashes had three different Class C/Class F ratios; 25:75, 50:50 and 75:25. The binder content varied from 265.5-398 kg/m^3 and water varied from 107-133 kg/m^3. The proportioning and the properties of the mixes are summarized in Table 2.34. For determination of elastic modulus and compressive strength, 150x300 mm cylinders were cast. In addition 75x100x400 mm prisms were cast for determination of drying shrinkage.

Table 2.34. Mixture proportions and properties of fresh concrete (Naik, Singh, & Ramme, 1998)

Mix no.	%	Cement (kg/m^3)	FA-C[1] (kg/m^3)	FA-F[2] (kg/m^3)	Water (kg/m^3)	w/b	FAg[3] (kg/m^3)	CAg[4] (kg/m^3)	AEA[5] (mL/m^3)	Slump (mm)	Air (%)
C1	0	356	0.0	0.0	107	0.30	836	1044	460	165	5.8
C2	35	259	139.0	0.0	133	0.33	677	1172	350	160	5.2
B1	40	227	115.5	38.5	119	0.31	827	1032	385	185	5.7
B2	40	227	76.5	76.5	120	0.32	830	1035	425	210	5.2
B3	40	225	37.5	112.5	107	0.29	810	1020	500	215	5.7

[1]Class C Fly ash,[2]Class F Fly ash,[3]Fine Aggregate, [4]Coarse Aggregate,[5]Air-entraining admixture

2.2.10.3 Experimental Results

2.2.10.3.1 Compressive Strength

The compressive data is presented in Table 2.35 and illustrated in Figure 2.21. The B1 mix has highest strength values throughout the test. The B3 mix had lower strength than the mix with Class C ash alone (C2). All the SCM mixes show higher strength value than the control

mix (C1) from day 7, except the B3 mix. But the strength of the B3 mix exceeds the strength of the C1 mix after 28 days of curing.

Table 2.35. Compressive strength results of the mixes (Naik, Singh, & Ramme, 1998)

Mix no.	Measured Strength (MPa)				
	1 day	7 day	28 day	91 day	365 day
C1	18.3	28.4	33.7	33.8	--
C2	12.3	36.5	47.4	55.7	70.6
B1	19.4	46.4	58.9	69.4	76.1
B2	15.3	38.1	51.2	61.1	63.8
B3	9.5	27.3	38.9	45.3	52.0

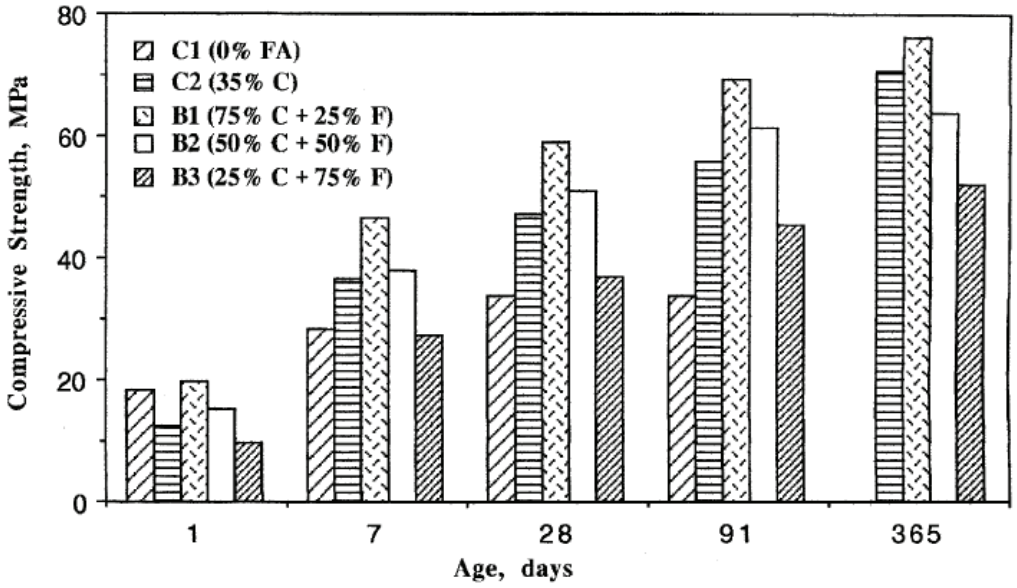

Figure 2.21. Compressive strength development of the concrete mixes (Naik, Singh, & Ramme, 1998)

2.2.10.3.2 Elastic Modulus

The elastic modulus data is presented in Table 2.36 and illustrated in Figure 2.22. Prior to 28 days, the control mix shows the highest elastic modulus. Furthermore the control mix has more consistent elastic modulus throughout the testing. The control mix has considerably higher modulus at day one, but at day 7 and beyond the difference decreased significantly. Similar to the compressive strength, the B3 mix had the lowest modulus values. After 28 days of curing, modulus values of the SCM mix does not increase significantly with the exception of the C2 mix, which exhibits a large increase in modulus between 91 and 365 days.

Table 2.36. Elastic modulus results of the mixes (Naik, Singh, & Ramme, 1998)

Mix no.	Elastic Modulus (MPa)				
	1 day	7 day	28 day	91 day	365 day
C1	24.5	29.1	30.3	31.7	--
C2	13.4	22.8	25.4	34.1	46.2
B1	11.8	27.8	29.3	34.8	34.5
B2	13.9	24.6	29.8	29.3	33.1
B3	7.9	17.0	21.4	29.0	29.6

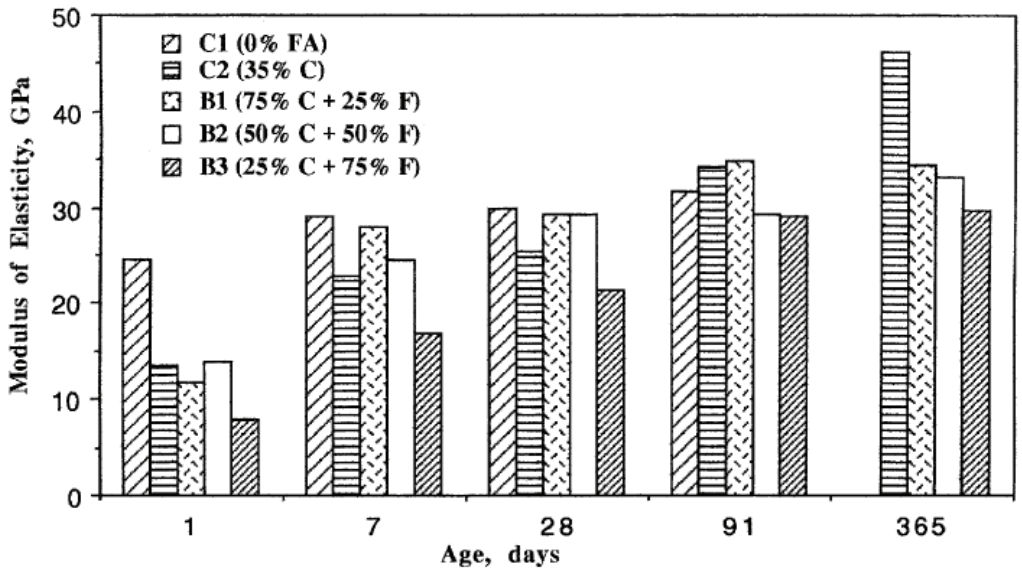

Figure 2.22. Elastic modulus development of the concrete mixes (Naik, Singh, & Ramme, 1998)

2.2.10.3.3 Drying Shrinkage

The drying shrinkage data is presented in Table 2.37. The blended fly ash mixes were tested for drying shrinkage strains. The B1 and B2 mixes show very similar drying shrinkage whereas the B3 mix, which had the most Class F fly ash, showed noticeably poorer performance, in particular the log-term shrinkage.

Table 2.37. Drying shrinkage results of the mixes (Naik, Singh, & Ramme, 1998)

Mix no.	Drying Shrinkage μ strain						
	4 day	7 day	14 day	28 day	56 day	112 day	224 day
B1	--	--	362	408	426	574	417
B2	--	186	286	321	445	454	497
B3	221	290	371	--	516	1383	1487

2.2.10.4 Conclusions

From this research the following conclusions were made:

1. The effect of blending Class C and Class F fly ashes together showed significant change on both mechanical and durability performance. In general, replacing the Class C ash with Class F up to 50% showed the best performance.

2. The B1 mix showed always the highest compressive strength, followed by the B2 mix from 7 to 91 days.

3. Elastic modulus of the control concrete was higher than the SCM concretes up to day 28. After 28 days of curing all mixes showed similar elastic modulus, except the C2 mix which exhibits large increase between 91 and 365 days.

4. The drying shrinkage of the B1 and B2 mixes were similar, while the B3 mix (which had the most Class F fly ash) showed poorer results.

2.2.11 Nasser and Al-Manaseer, 1986

Creep of Concrete Containing Fly Ash and Superplasticizer at Different Stress/Strength Ratios

2.2.11.1 Research Objective

Nasser and Al-Manaseer investigated what influence fly ash and superplasticizer has on creep behavior of concrete at different stress/strength ratios.

2.2.11.2 Material and Mix Design

ASTM Type I Portland cement was selected and one Class C fly ash was used as the SCM. Table 2.38 shows the physical properties and chemical analysis of the cement and fly ash that were used in the research.

Table 2.38. Physical properties and chemical analysis (%) of cement and fly ash (Nasser & Al-Manaseer, 1986)

Compounds	Shorthand notation	ASTM Type I	Class C Fly ash
Silicon Dioxide (SiO_2)	S	21.2	46.8
Aluminum Oxide (Al_2O_3)	A	4.1	21.9
Iron Oxide (Fe_2O_3)	F	2.3	3.9
$K_2O + Na_2O$	K+N	0.7	3.6
Sulphur Trioxide (SO_3)	$\bar{S}$	2.6	0.8
Calcium Oxide (CaO)	C	62.8	12.4
Magnesium Oxide (MgO)	M	4.6	2.9
Loss on Ignition	LOI	1.4	0.6
Specific gravity (g/cm^3)	SG	--	2.36
Active Silica	γ_s	--	--
Blaine specific surface (m^2/kg)	Blaine	--	--
Activity Index, 7 day (%)	7 AI	--	--
Activity Index, 28 day (%)	28 AI	--	75

Two mixes were prepared; one control mix with 100% Portland cement in the binder and the one with 20% FA as cement replacement. Both mixes had binder content of 219 kg/m^3 and water content of 131 kg/m^3, therefore the w/b ratio was equal to 0.60 for both mixes. The proportioning and the properties of the mixes are summarized in Table 2.39. For determination of compressive strength, shrinkage- and creep strain. The concrete mixes were cast using 76.2x288.6 mm cylinders

Table 2.39. Mixture proportions and properties of fresh concrete (Nasser & Al-Manaseer, 1986)

Mix no.	Cement (kg/m^3)	SCM[1] (kg/m^3)	Water (kg/m^3)	w/b	FAg[2] (kg/m^3)	CAg[3] (kg/m^3)	AEA[4] (L/m^3)	SP[5] (L/m^3)
Mix 1	219	--	131	0.60	703	831	0.28	--
Mix 2	175	44	131	0.60	703	831	0.20	1.61

[1]Fly ash, [2]Fine Aggregate, [3]Coarse Aggregate, [4]Air-entraining admixture,[5]Superplasticizer

2.2.11.3 Experimental Results

2.2.11.3.1 Creep and Shrinkage

Shrinkage was determined from the same mix that was used to determine creep strain. Without providing any data, the authors state that shrinkage of the sealed specimens was negligible. However, as shown in Figure 2.23 both unsealed specimens with and without the admixtures had very similar shrinkage behavior

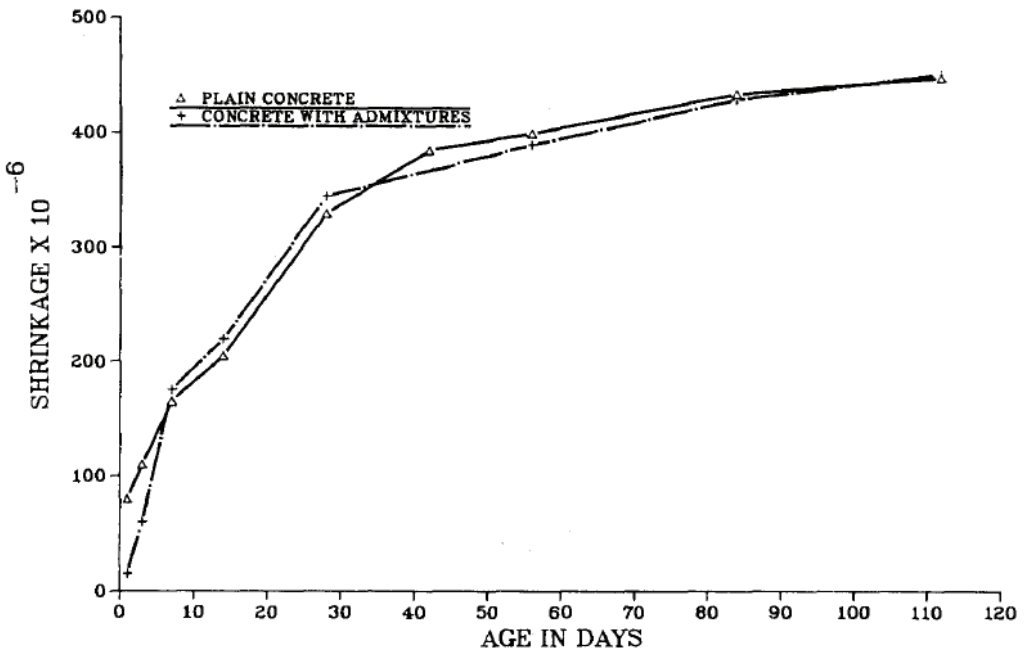

Figure 2.23. Shrinkage behavior of the unsealed specimens with and without admixtures (Nasser & Al-Manaseer, 1986)

The creep strain behavior was determined at stress/strength ratios between 10 to 60% loaded after 28 days of curing. Figure 2.24 and Figure 2.25 exhibit the creep strain behavior for the sealed and unsealed specimens with admixture, respectively. As expected the specimen that were under higher load showed higher creep strain and it was also anticipated that the unsealed specimen would exhibit higher creep strain than the sealed specimens.

Figure 2.26 and Figure 2.27 display the creep strain as days 28 and 84 versus stress/strength for the sealed and unsealed specimens with and without admixture, respectively. The creep strain was found to vary linearly with increased stress/strength ratio. The creep strain of the unsealed concretes with admixtures was higher (average of 72% higher) than unsealed concrete without admixture. This difference was observed to decrease with increasing stress/strength ratio. However, the variation of the creep strains of the sealed specimens with and without admixture was found to be small. On average creep strain of the unsealed specimens was 4.21 times larger than that of the sealed specimens for concrete with admixtures, compared to 2.48 for concrete without the admixtures.

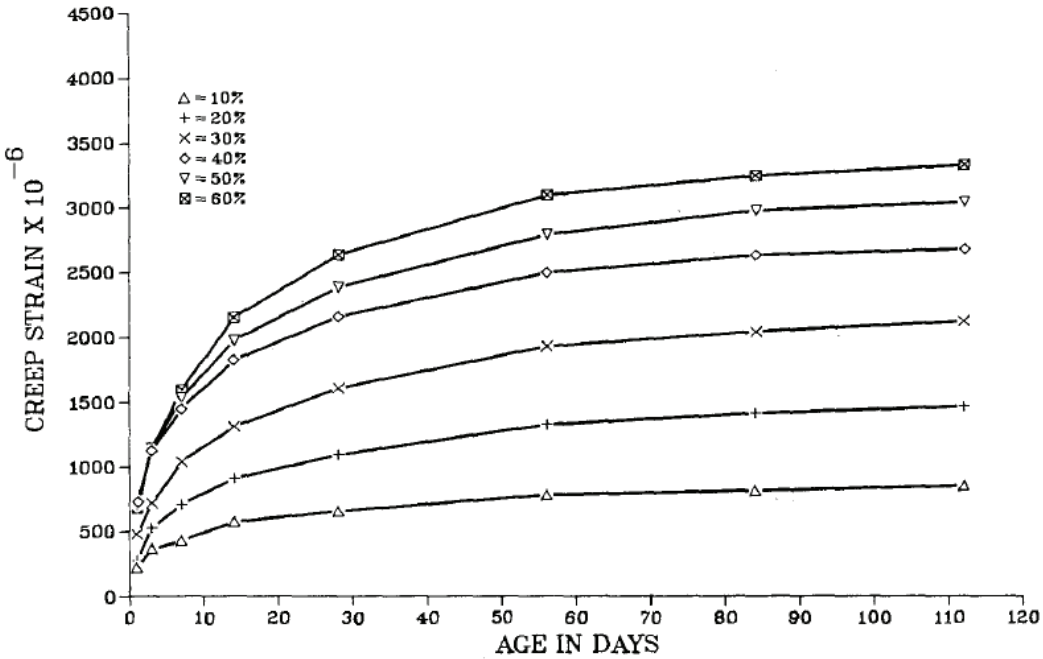

Figure 2.24. Creep strain behavior at different stress/strength behavior of the unsealed specimens with admixtures (Nasser & Al-Manaseer, 1986)

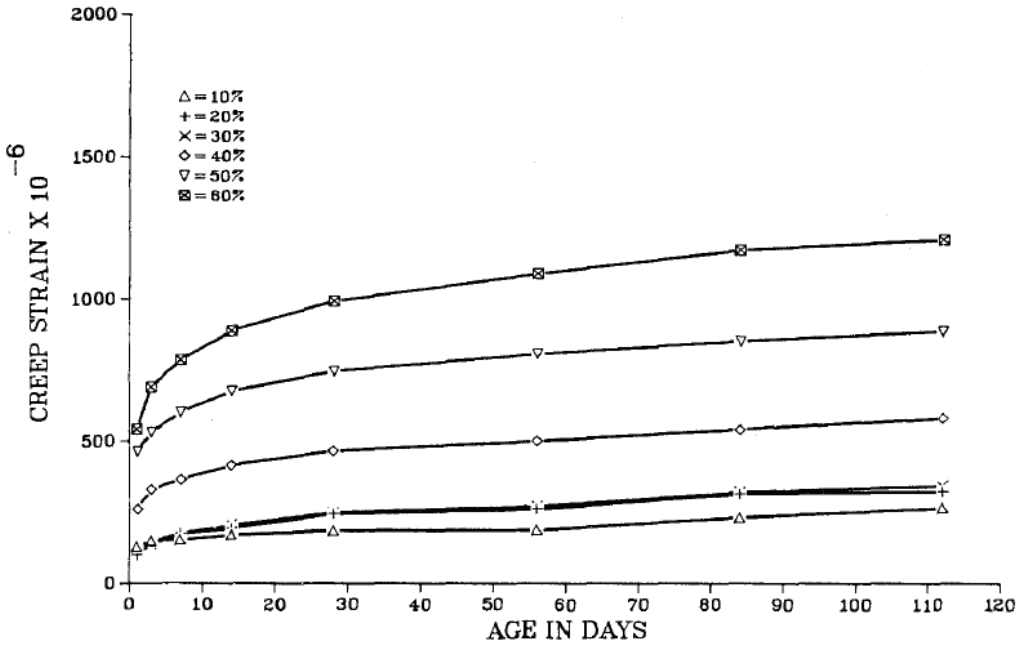

Figure 2.25. Creep strain behavior at different stress/strength behavior of the sealed specimens with admixtures (Nasser & Al-Manaseer, 1986)

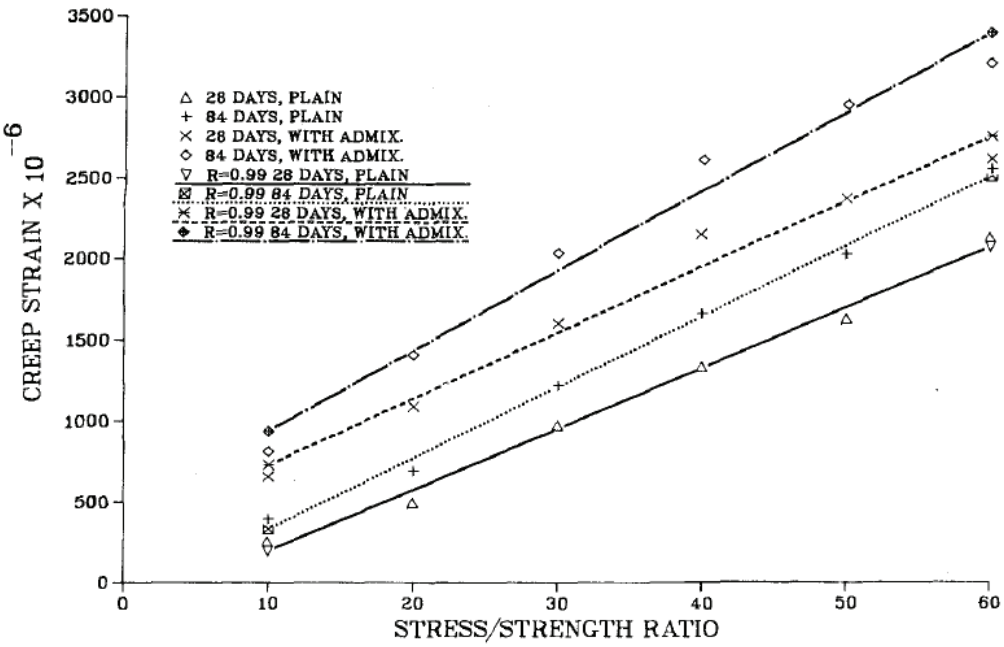

Figure 2.26. Creep versus stress/strength ratio for the unsealed specimen with and without admixtures (Nasser & Al-Manaseer, 1986)

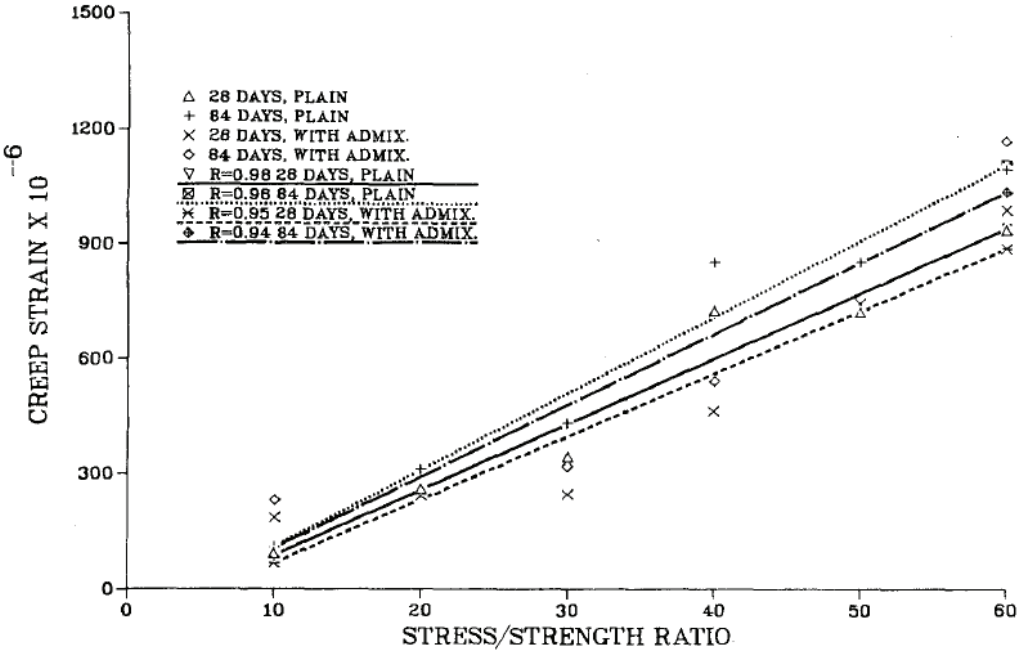

Figure 2.27. Creep versus stress/strength ratio for the sealed specimen with and without admixtures (Nasser & Al-Manaseer, 1986)

2.2.11.4 Conclusions

From this research the following conclusions were made:

1. The shrinkage strain behavior for concrete with or without admixtures was found to be very similar for both sealed and unsealed specimens.

2. It was observed that creep strain of specimens with or without admixtures varied approximately linearly with increasing stress/strength ratio.

3. The creep strain of the unsealed concretes with admixtures was found to be 72% higher than unsealed concrete without admixture.

2.2.12 Obla, Hill, Thomas, Shashiprakash, & Perebatova, 2003

Properties of Concrete Containing Ultra-Fine Fly Ash

2.2.12.1 Research Objective

Obla, et al. investigated use of ultra-fine fly ash in concrete (UFFA). Prior investigations on use of fly ash in concrete have shown that the parameters can be improved by reducing its particle size. This was the first research program to conduct comprehensive study on this type of fly ash.

2.2.12.2 Material and Mix Design

ASTM Type I Portland cement was selected and ultra fine fly ashes (UFFA) and silica fume (SF) were chosen as the SCM. According to ASTM C 618, based on chemical composition, the fly ash is classified as Class F. Table 2.40 shows the physical properties and chemical analysis of the cement and fly ash that were used in the research.

Table 2.40. Physical properties and chemical analysis (%) of cements and fly ash (Obla, Hill, Thomas, Shashiprakash, & Perebatova, 2003)

Compounds	Shorthand notation	ASTM Type I	UFFA
Silicon Dioxide (SiO_2)	S	20.9	50.7
Aluminum Oxide (Al_2O_3)	A	4.6	27.2
Iron Oxide (Fe_2O_3)	F	3.5	3.1
$K_2O + Na_2O$	K+N	--	--
Sulphur Trioxide (SO_3)	$\bar{S}$	2.8	1.0
Calcium Oxide (CaO)	C	64.3	11.8
Magnesium Oxide (MgO)	M	1.2	2.5
Loss on Ignition	LOI	1.3	0.3
Specific gravity (g/cm^3)	SG	3.15	2.57
Active Silica	γ_s	--	--
Blaine specific surface(m^2/kg)	Blaine	370	800
Activity Index, 7 day (%)	7 AI	--	--
Activity Index, 28 day (%)	28 AI	--	127

Six mixes were prepared, one control mix (100% Portland cement), one with 8% silica fume as the SCM and four with 8-11% UFFA as the SCM. The difference between the UFFA mixes was primarily the amount of High-Range Water Reducer (HRWR) admixture, which varied from 524 to 818 mL/100 kg. The binder content in the mixes varied from 360 to 374 kg/m^3, the water content varied from 120 to 143 kg/m^3 and the w/b ratio in the mixes varied from 0.32-0.40. The proportioning and the properties of the mixes are summarized in Table 2.41. For determination of compressive strength the concrete mixes were cast in 102x203 mm cylinders.

Table 2.41. Mixture proportions and properties of fresh concrete (Obla, Hill, Thomas, Shashiprakash, & Perebatova, 2003)

Mix no.	%	Cement (kg/m^3)	UFFA[1] (kg/m^3)	SF[2] (kg/m^3)	Water (kg/m^3)	w/b	HRWR[3] (mL/100 kg)	Slump (mm)	Air (%)
360 C	0	360	0	0	142	0.39	655	200	6.4
360 SF8	8	331	0	29	143	0.40	1047	190	5.0
360 UF12.1	11	331	43	0	141	0.38	524	185	5.6
360 UF8	8	331	29	0	130	0.36	589	165	5.4
360 UF12.2	11	331	43	0	129	0.34	655	210	5.4
360 UF12.3	11	331	43	0	120	0.32	818	190	6.5

[1]Ultra Fine Fly ash, [2]Silica Fume, [3]High-Range Water Reducer

2.2.12.3 Experimental Results

2.2.12.3.1 Compressive Strength

The compressive data from this research is presented in Table 2.42 and shown graphically in Figure 2.28. Both the SF mix and the UFFA mixes showed higher strengths than the control mix. When the 8% replacement mixes are compared, the 360 SF8 mix shows higher early

strength (between 7 and 28 days) than 360 UF8 mix, but at later ages (90 days and beyond) the strength of both mixes was similar. When the replacement of the UFFA is increased to 11%, it exhibit higher strength than the others.

Table 2.42. Compressive strength results of the mixes (Obla, Hill, Thomas, Shashiprakash, & Perebatova, 2003)

Mix no.	Measured Strength (MPa)					
	1 day	3 day	7 day	28 day	90 day	180 day
360 C	13.9	25.1	33.6	39.2	46.3	47.9
360 SF8	13.4	26.4	40.8	47.9	53.9	56.6
360 UF12.1	12.7	31.1	36.8	45.1	53.6	63.2
360 UF8	14.2	29.3	36.9	44.8	54.6	55.9
360 UF12.2	15.0	30.8	41.6	50.7	56.9	62.9
360 UF12.3	24.7	37.1	49.3	57.3	60.5	63.7

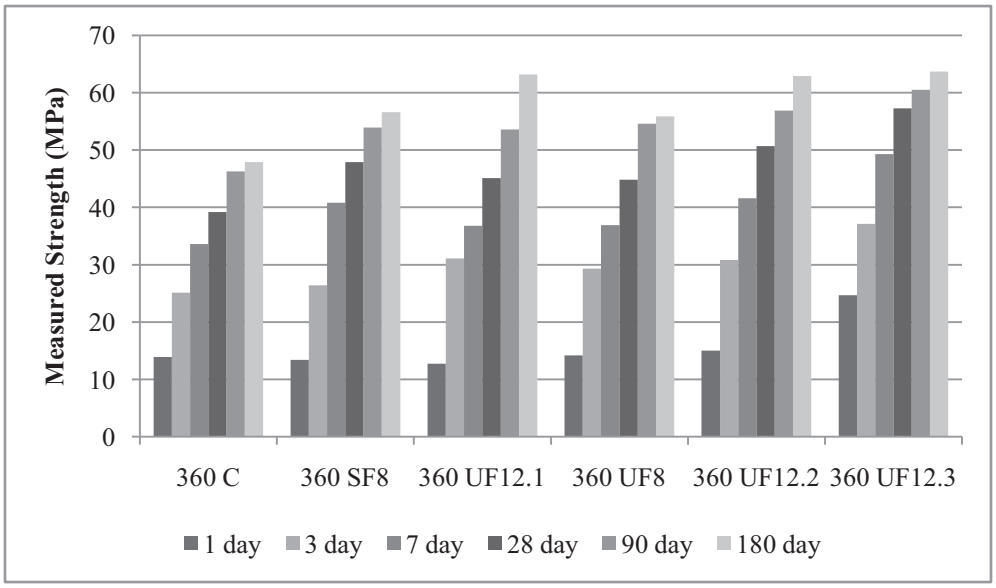

Figure 2.28. Compressive strength development of the concrete mixes reproduced from Obla, et al. 2003

2.2.12.3.2 Autogeneous Shrinkage

The autogeneous shrinkage of a UFFA mix and SF mix were compared to the control mix is shown in Figure 2.29. The SF mix has much higher rate of increase in autogeneous shrinkage at early ages than the UFFA mix and the control mix. The authors suggest this high rate is due to rapid stress development in the SF mix at early age, when the material is still relatively week. Furthermore the authors state that elastic modulus and drying shrinkage values were very similar, without showing any data to support that.

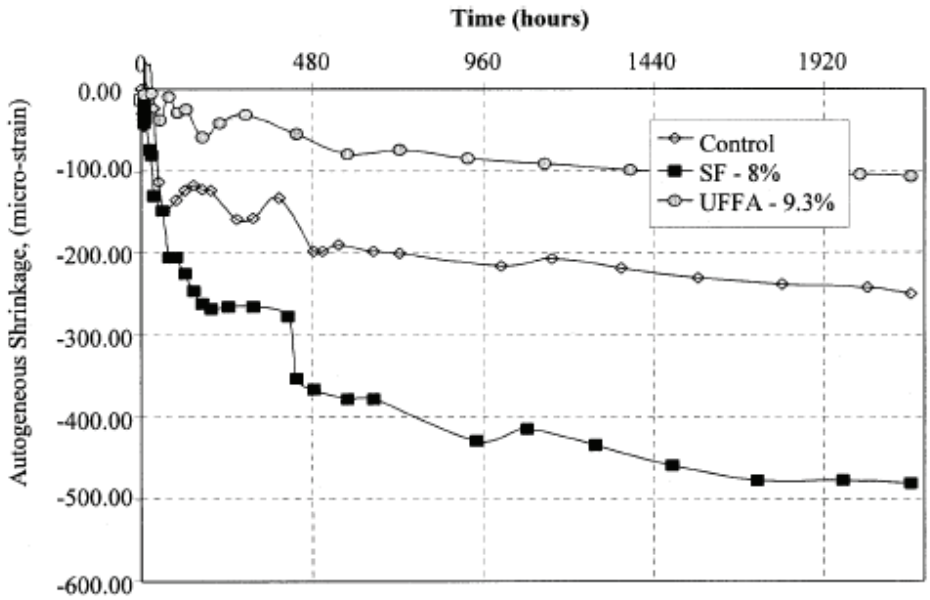

Figure 2.29. Autogenous shrinkage behavior of SF and UFFA concrete (Obla, Hill, Thomas, Shashiprakash, & Perebatova, 2003)

2.2.12.4 Conclusions

From this research the following conclusions were made:

1. The UFFA fly ash can produce compressive strength that is comparable to highly reactive pozzolan such as SF, even though the FA is classified as Class F. However, only the concrete with 11% UFFA reach a similar early-age compressive strength as the 8% SF replacement concrete.

2. The UFFA mix shows less autogenous shrinkages than both the SF mix and the control mix.

2.2.13 Oner, Akyuz, & Yildiz, 2005

An experimental study strength development of concrete containing fly ash and optimum usage of fly ash in concrete

2.2.13.1 Research Objective

Oner, et al. looked at optimizing amount of fly ash to achieve the maximum strength. Efficiency of the fly ash was evaluated using the modified Bolomey and Féret strength equations and the strength values.

2.2.13.2 Material and Mix Design

ASTM Type I Portland cement was selected and Class F fly ash was chosen as the SCM. Table 2.43shows the physical properties and chemical analysis of the cement and FA that were used in the research.

Table 2.43. Physical properties and chemical analysis (%) of cement and fly ash (Oner, Akyuz, & Yildiz, 2005)

Compounds	Shorthand notation	ASTM Type I	Class F Fly ash
Silicon Dioxide (SiO_2)	S	20.7	57.6
Aluminum Oxide (Al_2O_3)	A	4.9	25.2
Iron Oxide (Fe_2O_3)	F	3.0	6.5
$K_2O + Na_2O$	K+N	0.9	4.3
Sulphur Trioxide (SO_3)	$\bar{S}$	2.3	0.2
Calcium Oxide (CaO)	C	61.8	2.1
Magnesium Oxide (MgO)	M	1.4	2.5
Loss on Ignition	LOI	3.2	1.7
Specific gravity (g/cm^3)	SG	3.1	2.09
Active Silica	γ_s	--	--
Blaine specific surface (m^2/kg)	Blaine	351	336
Activity Index, 7 day (%)	7 AI	--	--
Activity Index, 28 day (%)	28 AI	--	--

A total of 28 concrete mixes were prepared. Four control mixes (100% Portland cement) were prepared. The cement content in the FA mix was 200, 240, 280 and 320 kg/m^3, the total binder content in the mixes varied from 230-505 kg/m^3, the water content varied from 216-255 kg/m^3 and the w/b ratio of the mixes varied from 0.50-0.94. The mixes had five different cement replacements, 13%, 20%, 25%, 30%, 33% and 37%. The proportioning and the properties of the mixes are summarized in Table 2.44. For determination of compressive strength, the mixes were cast in 150 mm cubes.

Table 2.44. Mixture proportions and properties of fresh concrete (Oner, Akyuz, & Yildiz, 2005)

Mix name	%	Cement (kg/m^3)	SCM[1] (kg/m^3)	Water (kg/m^3)	w/b	FAg[2] (kg/m^3)	CAg[3] (kg/m^3)	Slump (mm)	Air (%)
C250FA00	0	250	0	218	0.87	1285	555	120	1.6
C200FA30	13	200	30	216	0.94	1293	558	120	1.6
C200FA50	20	200	50	219	0.88	1266	547	115	1.8
C200FA65	25	200	65	221	0.83	1246	538	115	1.9
C200FA85	30	200	85	224	0.79	1225	529	120	1.8
C200FA100	33	200	100	229	0.76	1203	519	125	1.8
C200FA115	37	200	115	232	0.74	1184	511	125	1.7
C300FA00	0	300	0	225	0.75	1242	536	120	1.6
C240FA35	13	240	35	223	0.81	1251	540	120	1.6
C240FA60	20	240	60	225	0.75	1221	527	115	1.8
C240FA80	25	240	80	228	0.71	1195	516	115	1.9
C240FA100	29	240	100	231	0.68	1176	508	120	1.7
C240FA120	33	240	120	236	0.66	1146	495	120	1.8
C240FA140	37	240	140	240	0.63	1122	484	125	1.8
C350FA00	0	350	0	232	0.66	1197	517	120	1.7
C280FA40	13	280	40	230	0.72	1208	522	115	1.7
C280FA70	20	280	70	232	0.66	1174	507	120	1.8
C280FA95	25	280	95	236	0.63	1142	493	115	1.9
C280FA120	30	280	120	240	0.60	1114	481	120	1.8
C280FA140	33	280	140	245	0.58	1088	470	125	1.8
C280FA165	37	280	165	249	0.56	1058	457	125	1.8
C400FA00	0	400	0	239	0.60	1154	498	120	1.7
C320FA50	14	320	50	237	0.64	1159	501	115	1.8
C320FA80	20	320	80	240	0.60	1122	484	115	2.0
C320FA105	25	320	105	243	0.57	1096	473	115	2.0
C320FA135	30	320	135	247	0.54	1062	458	120	1.9
C320FA160	33	320	160	251	0.52	1032	446	125	1.9
C320FA185	37	320	185	255	0.50	1009	436	125	1.8

[1]Fly ash, [2]Fine Aggregate, [3]Coarse Aggregate

2.2.13.3 Experimental Results

2.2.13.3.1 Compressive Strength

The compressive data from this research is presented in Table 2.45. From the strength data, it can be seen, for a given age and cement content, an optimum fly ash content can be found to achieve maximum strength. It can also be seen that the 28 day strength of the binary fly ash mixes, were lower strength than the comparable control mix with equivalent w/b ratio. However, at 180 day strength the fly ash mixes exceeded the control mix.

Table 2.45. Compressive strength results of the mixes (Oner, Akyuz, & Yildiz, 2005)

Mix name	Measured strength (MPa)	
	28 day	180 day
C250FA00	23.1	26.6
C200FA30	21.3	25.0
C200FA50	22.4	26.7
C200FA65	22.9	27.2
C200FA85	22.7	27.1
C200FA100	21.4	25.7
C200FA115	20.0	24.2
C300FA00	29.5	34.2
C240FA35	27.1	32.2
C240FA60	29.2	34.6
C240FA80	29.6	35.3
C240FA100	29.8	35.6
C240FA120	28.5	34.2
C240FA140	26.9	32.6
C350FA00	35.7	41.4
C280FA40	33.0	38.9
C280FA70	35.6	42.2
C280FA95	36.2	43.3
C280FA120	36.5	43.4
C280FA140	35.5	42.5
C280FA165	33.6	40.8
C400FA00	41.5	48.0
C320FA50	39.3	46.3
C320FA80	41.4	49.3
C320FA105	42.5	50.7
C320FA135	42.7	50.9
C320FA160	41.2	49.7
C320FA185	39.5	48.3

2.2.13.3.2 Efficiency Factor

The modified Bolomey and Féret strength equations were used to evaluate the efficiency (k-value) of the FA and control mixes. Figure 2.30 and Figure 2.31 show the relationship between the efficiency factor and FA content by using the Bolomey and Féret strength equation at 28 day and 180 day, respectively. From these figures it can be seen as the FA content increases the efficiency of the FA decreases linearly.

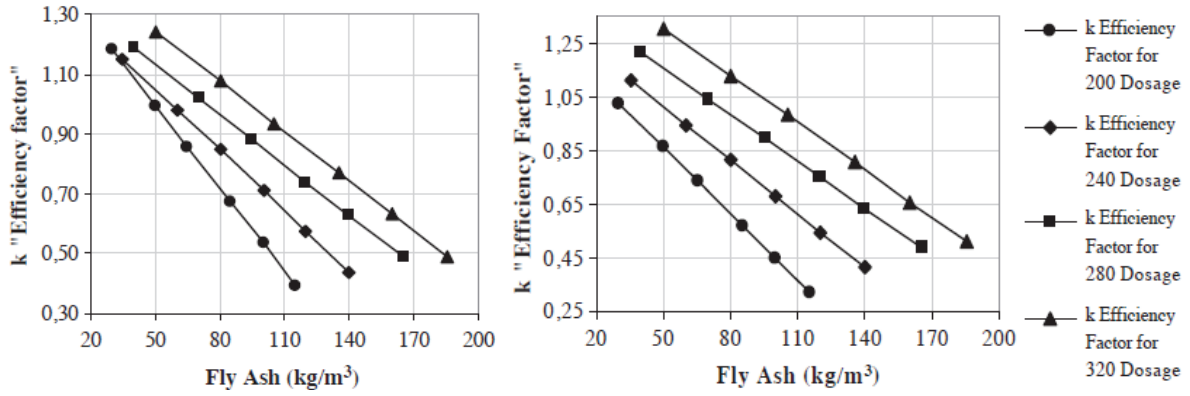

Figure 2.30. Efficiency factor versus FA content at 28 days, by using Bolomey (left) and Féret (right) strength equations (Oner, Akyuz, & Yildiz, 2005)

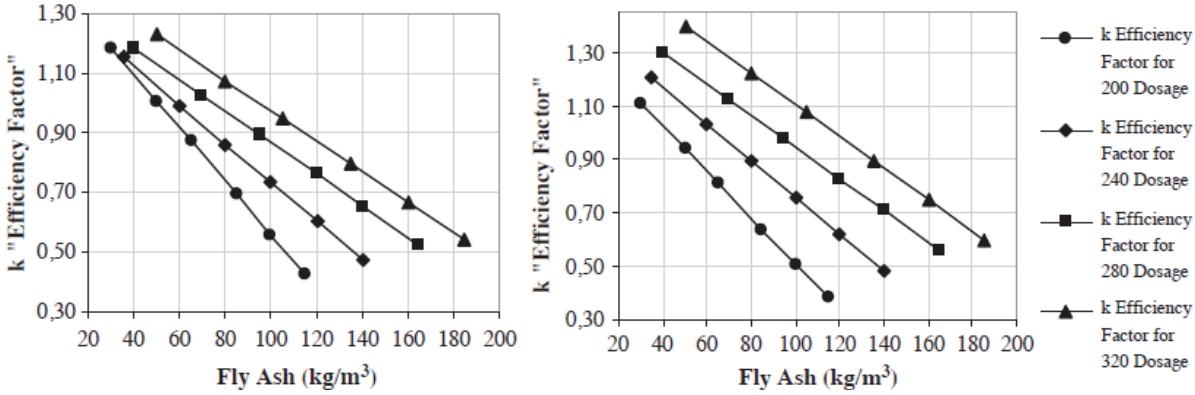

Figure 2.31. Efficiency factor versus FA content at 180 days, by using Bolomey (left) and Féret (right) strength equations (Oner, Akyuz, & Yildiz, 2005)

Equivalent cement content (C') of the FA can be calculated by multiplying the efficiency factor to the FA content. Figure 2.32 and Figure 2.33 present C' versus FA content at 28 and 365 days, respectively. The straight line on these figures represent when the FA is essentially equivalent to cement. From these figures it can be seen that C' increases with time, because the efficiency of the FA increases with age.

It was observed that the C' versus FA plots show a 2nd order polynomial relation, which passes through the origin. To find the optimum amount of FA, the derivative of the 2nd order polynomials was taken. The optimum amount of FA was found to be approximately 30% of the total binding material, beyond that amount some of the FA will remain unreacted and will serve as fine aggregate in the concrete mix.

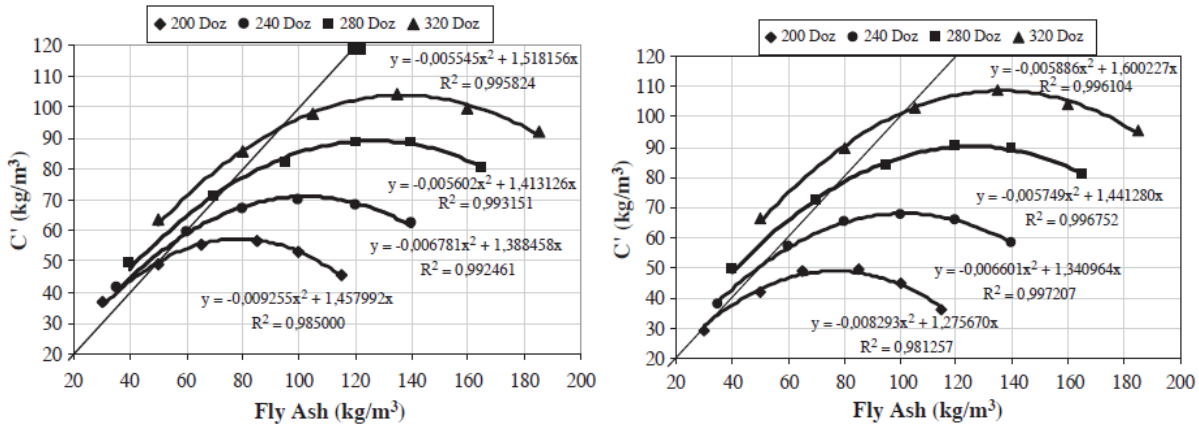

Figure 2.32. Equivalent cement content versus FA content at 28 days, by using Bolomey (left) and Féret (right) strength equations (Oner, Akyuz, & Yildiz, 2005)

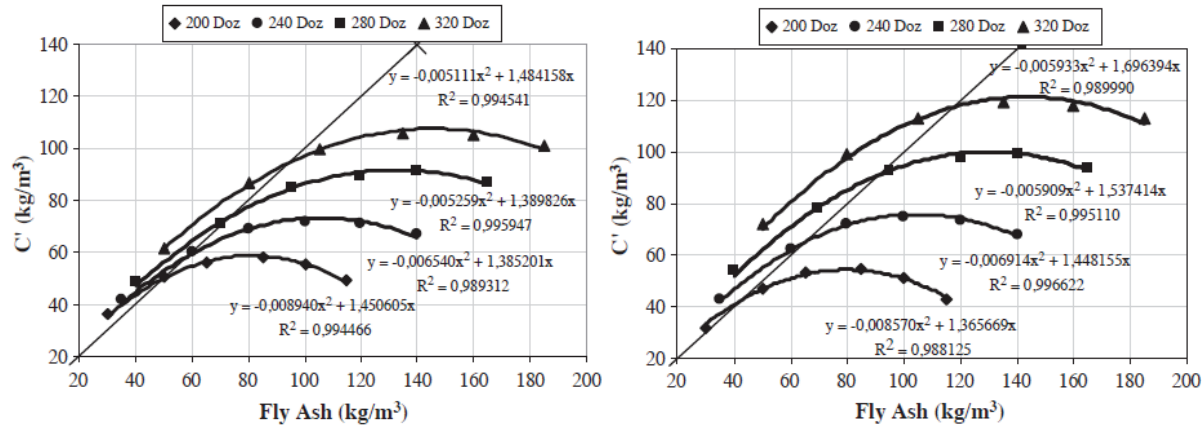

Figure 2.33. Equivalent cement content versus FA content at 180 days, by using Bolomey (left) and Féret (right) strength equations (Oner, Akyuz, & Yildiz, 2005)

2.2.13.4 Conclusions

From this research the following conclusions were made:

1. It was observed that the 28 day strength of the FA mixes exhibit lower strength than the control mix, but at 180 day the FA mixes had strength higher than the control mix. The reason is that pozzolanic reaction is slower than the hydraulic reaction.

2. The compressive strength of the FA concrete increases as the FA content increases up to an optimum point, after that is reached, the strength starts to decrease with increased FA content.

3. The optimum point was found to be approximately 30% of the total binding material. After reaching the optimum point some of the FA will remain unreacted and serve as fine aggregate in the concrete mix.

2.2.14 Oner & Akyuz, 2007

An experimental study on optimum usage of GGBS for the compressive strength of concrete

2.2.14.1 Research Objective

Oner, et al. looked for the optimum amount of ground granulated blast-furnace slag (GGBS) to achieve the maximum compressive strength. The efficiency of the GGBS was evaluated using the modified Bolomey and Féret strength equations and the strength values.

2.2.14.2 Material and Mix Design

ASTM Type I Portland cement was selected and grade 100 GGBS was chosen as the SCM. Table 2.46shows the physical properties and chemical analysis of the cement and GGBS that were used in the research.

Table 2.46. Physical properties and chemical analysis (%) of cement and GGBS (Oner & Akyuz, 2007)

Compounds	Shorthand notation	ASTM Type I	GGBS
Silicon Dioxide (SiO_2)	S	20.7	39.2
Aluminum Oxide (Al_2O_3)	A	4.9	10.2
Iron Oxide (Fe_2O_3)	F	3.0	2.0
$K_2O + Na_2O$	K+N	0.9	1.4
Sulphur Trioxide (SO_3)	$\overline{S}$	2.3	--
Calcium Oxide (CaO)	C	61.8	32.8
Magnesium Oxide (MgO)	M	1.4	8.5
Loss on Ignition	LOI	3.2	1.0
Specific gravity (g/cm^3)	SG	3.10	2.87
Active Silica	γ_s	--	--
Blaine specific surface (m^2/kg)	Blaine	351	425
Activity Index, 7 day (%)	7 AI	--	75
Activity Index, 28 day (%)	28 AI	--	96

Total of 32 concrete mixes were prepared. Eight of the mixes were prepared as control mixes (100% Portland cement). The cement content in the GGBS mix was 175, 210, 245 and 280 kg/m^3, the total binder content in the mixes varied from 175-720 kg/m^3 and the water content varied from 209-295 kg/m^3. The w/b ratio of the mixes varied from 0.41-1.19 and the mixes

had cement replacement from 0-61%. The proportioning and the properties of the mixes are summarized in Table 2.47. For determination of compressive strength, the mixes were cast in 150 mm cubes.

Table 2.47. Mixture proportions and properties of fresh concrete (Oner & Akyuz, 2007)

Mixture no.	%	Cement (kg/m^3)	SCM[1] (kg/m^3)	Water (kg/m^3)	w/b	FAg[2] (kg/m^3)	CAg[3] (kg/m^3)	Air (%)	Slump (mm)
C250GGBS00.0	0	250	0	219	0.88	732	1111	1.6	120
C175GGBS00.0	0	175	0	209	1.19	768	1166	1.4	115
C175GGBS37.5	18	175	37.5	215	1.01	748	1135	1.5	120
C175GGBS75.0	30	175	75	218	0.87	731	1109	1.6	115
C175GGBS125.0	42	175	125	223	0.74	707	1073	1.8	120
C175GGBS175.0	50	175	175	230	0.66	681	1033	1.8	120
C175GGBS225.0	56	175	225	238	0.60	654	991	1.7	120
C175GGBS275.0	61	175	275	248	0.55	624	948	1.6	125
C300GGBS00	0	300	0	225	0.75	708	1075	1.6	120
C210GGBS00.0	0	210	0	214	1.02	751	1140	1.5	120
C210GGBS45.0	18	210	45	219	0.86	729	1106	1.5	115
C210GGBS90.0	30	210	90	224	0.75	707	1072	1.7	115
C210GGBS150.0	42	210	150	231	0.64	677	1027	1.8	120
C210GGBS210.0	50	210	210	240	0.57	645	979	1.8	120
C210GGBS270.0	56	210	270	251	0.52	611	927	1.7	120
C210GGBS330.0	61	210	330	261	0.48	578	877	1.6	125
C350GGBS00	0	350	0	232	0.66	684	1037	1.7	120
C245GGBS00.0	0	245	0	218	0.89	735	1114	1.4	120
C245GGBS52.5	18	245	52.5	225	0.76	708	1073	1.7	115
C245GGBS105.0	30	245	105	230	0.66	683	1036	1.7	120
C245GGBS175.0	42	245	175	239	0.57	647	982	1.8	115
C245GGBS245.0	50	245	245	250	0.51	609	924	1.9	125
C245GGBS315.0	56	245	315	263	0.47	569	864	1.9	125
C245GGBS385.0	61	245	385	279	0.44	526	799	1.8	125
C400GGBS00	0	400	0	239	0.60	659	999	1.7	120
C280GGBS00.0	0	280	0	224	0.80	716	1087	1.5	120
C280GGBS60.0	18	280	60	231	0.68	686	1041	1.7	115
C280GGBS120	30	280	120	236	0.59	659	999	1.8	115
C280GGBS200	42	280	200	247	0.51	617	936	1.9	115
C280GGBS280	50	280	280	263	0.47	570	866	2.0	120
C280GGBS360	56	280	360	278	0.43	525	796	2.0	120
C280GGBS440	61	280	440	295	0.41	477	723	1.8	125

[1]Ground granulated blast-furnace slag, [2]Fine Aggregate, [3]Coarse Aggregate

2.2.14.3 Experimental Results

2.2.14.3.1 Compressive Strength

The compressive data from this research is presented in Table 2.48and shown graphically in Figure 2.34 through Figure 2.37. The concrete mixes with same amount of cement are plotted together. This is not a fair comparison; the fly ash is added to the binder instead of replacing the cement. The authors state that the early-age strength of the GGBS mixes exhibit lower

strength than the control mix, but as the curing period was extended the GGBS mixes had strength higher than the control mix. However, the compressive strength data presented prove otherwise.

Table 2.48. Compressive strength results of the mixes (Oner & Akyuz, 2007)

Mixture no.	Measured Strength (MPa)						
	7 day	14 day	28 day	63 day	119 day	180 day	365 day
C250GGBS00.0	15.3	17.6	22.7	23.2	23.7	24.6	25.9
C175GGBS00.0	9.2	9.7	13.0	13.3	13.6	14.1	14.5
C175GGBS37.5	12.7	13.4	18.1	19.3	20.0	20.5	21.4
C175GGBS75.0	16.4	17.4	23.5	26.8	28.1	29.0	30.5
C175GGBS125.0	18.6	20.2	27.0	31.7	34.8	36.2	38.4
C175GGBS175.0	19.1	20.6	27.8	33.1	36.5	38.2	40.8
C175GGBS225.0	18.5	20.1	27.2	32.9	36.1	38.0	40.9
C175GGBS275.0	17.1	18.5	25.1	30.4	33.7	35.8	38.7
C300GGBS00	19.9	22.7	28.9	29.8	30.4	31.5	33.1
C210GGBS00.0	12.4	13.7	17.5	18.0	18.3	18.8	19.8
C210GGBS45.0	16.7	18.3	23.6	25.0	26.7	27.6	28.9
C210GGBS90.0	21.2	23.1	30.0	33.0	35.8	37.1	39.1
C210GGBS150.0	23.9	26.1	34.0	40.0	43.4	45.2	47.9
C210GGBS210.0	24.4	26.6	34.9	40.9	45.4	47.4	50.5
C210GGBS270.0	24.1	26.3	34.5	40.7	45.3	47.5	50.7
C210GGBS330.0	22.2	24.3	31.8	37.8	42.4	44.7	47.9
C350GGBS00	24.9	27.8	35.0	35.9	36.5	37.9	40.0
C245GGBS00.0	16.1	17.9	22.6	23.0	23.5	24.3	25.6
C245GGBS52.5	20.8	22.9	29.0	30.3	33.0	34.3	36.2
C245GGBS105.0	25.6	28.3	36.1	39.2	42.5	44.3	46.9
C245GGBS175.0	29.6	32.4	41.4	47.7	51.7	54.0	57.4
C245GGBS245.0	30.1	33.0	42.3	48.5	53.5	56.0	59.7
C245GGBS315.0	29.5	32.4	41.5	48.1	53.7	56.3	60.2
C245GGBS385.0	26.6	29.2	37.5	43.5	49.0	51.7	55.2
C400GGBS00	29.1	32.6	40.4	41.5	42.4	44.0	46.3
C280GGBS00.0	19.6	21.9	27.5	28.3	28.9	29.8	31.2
C280GGBS60.0	24.0	26.7	33.7	35.2	37.8	39.1	41.1
C280GGBS120	29.8	33.1	41.8	45.9	49.1	51.0	53.8
C280GGBS200	33.8	37.5	47.5	54.5	58.3	60.8	64.5
C280GGBS280	34.4	38.1	48.4	55.3	59.9	62.6	66.7
C280GGBS360	33.3	37.0	47.0	54.9	59.9	62.8	67.2
C280GGBS440	30.2	33.5	42.7	49.6	55.2	58.3	62.4

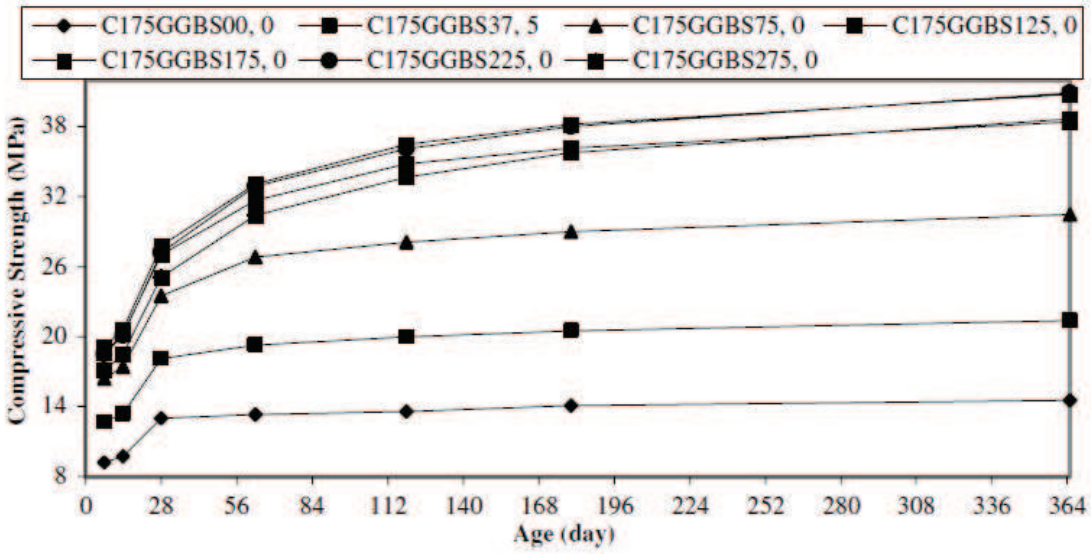

Figure 2.34. Compressive strength development of concrete mixes with 175 kg/m^3 dosage of cement (Oner & Akyuz, 2007)

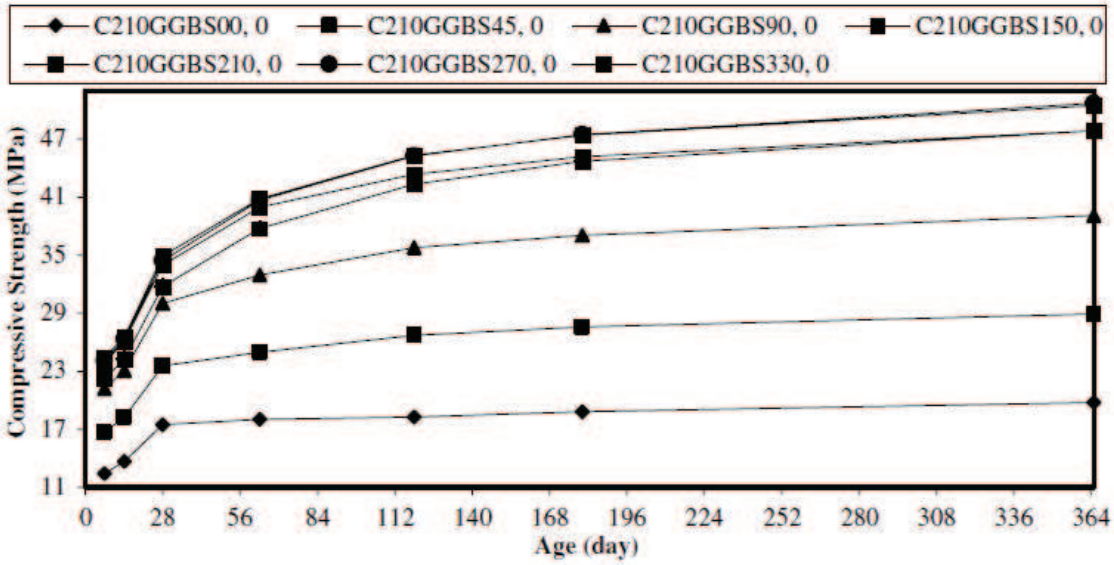

Figure 2.35. Compressive strength development of concrete mixes with 210 kg/m^3 dosage of cement (Oner & Akyuz, 2007)

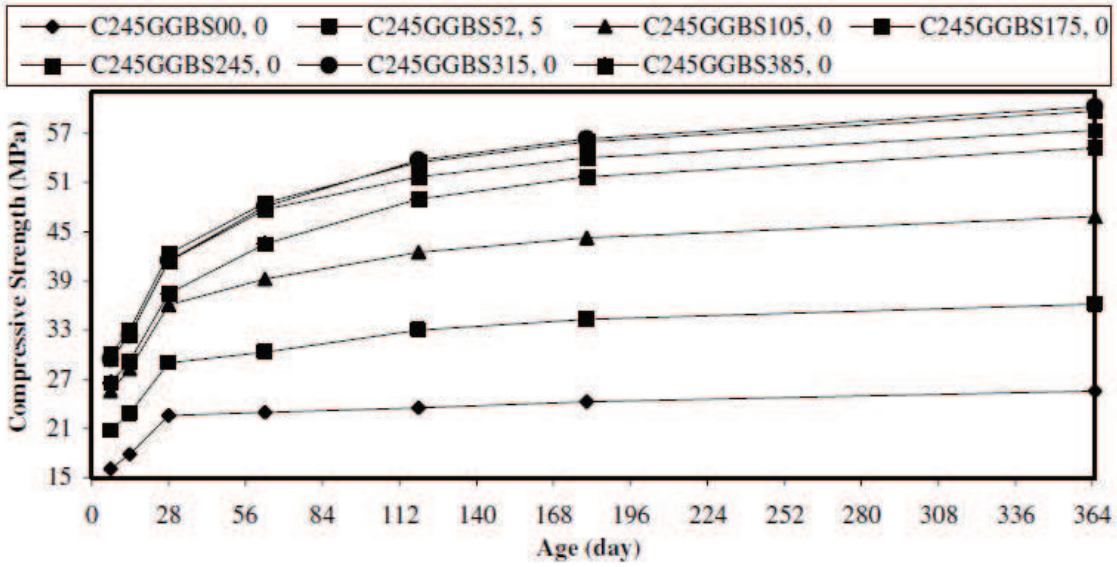

Figure 2.36. Compressive strength development of concrete mixes with 245 kg/m^3 dosage of cement (Oner & Akyuz, 2007)

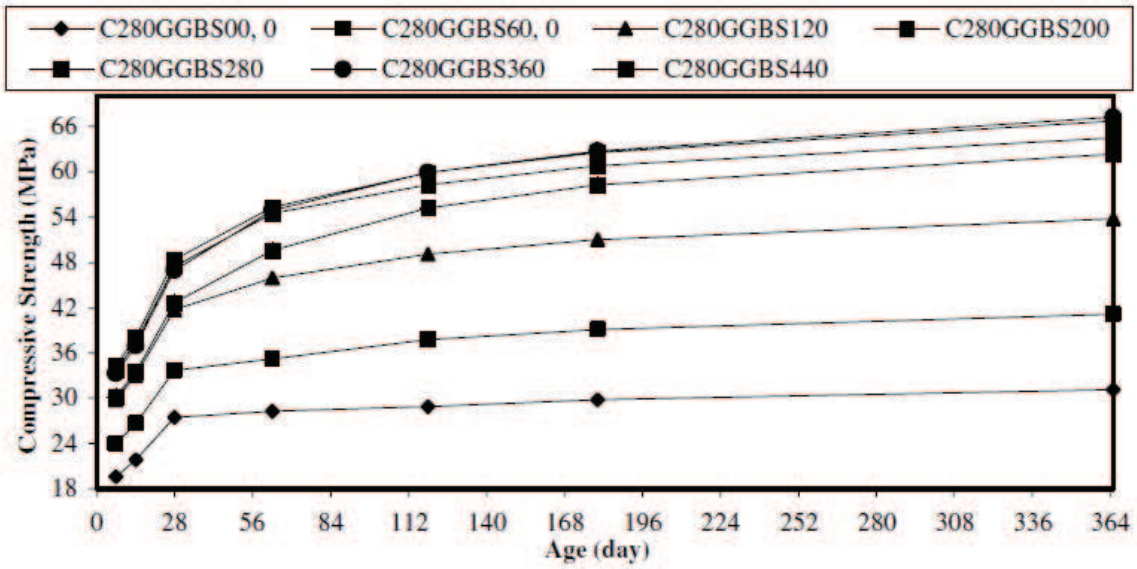

Figure 2.37. Compressive strength development of concrete mixes with 280 kg/m^3 dosage of cement (Oner & Akyuz, 2007)

2.2.14.3.2 Efficiency Factor

The modified Bolomey and Féret strength equations were used to evaluate the efficiency (k-value) of the GGBS compared to the control mixes. Figure 2.38 and Figure 2.39 show the relationship between the efficiency factor and GGBS content at 28 day by using the Bolomey

and Féret strength equation, respectively. From these figures it can be seen as the GGBS content increases the efficiency of the GGBS decreases linearly.

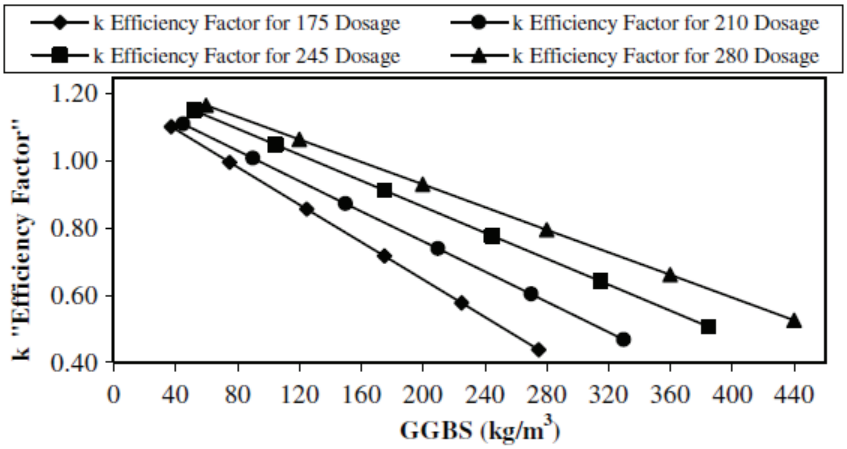

Figure 2.38. Efficiency factor versus GGBS content at 28 days using the Bolomey equation (Oner & Akyuz, 2007)

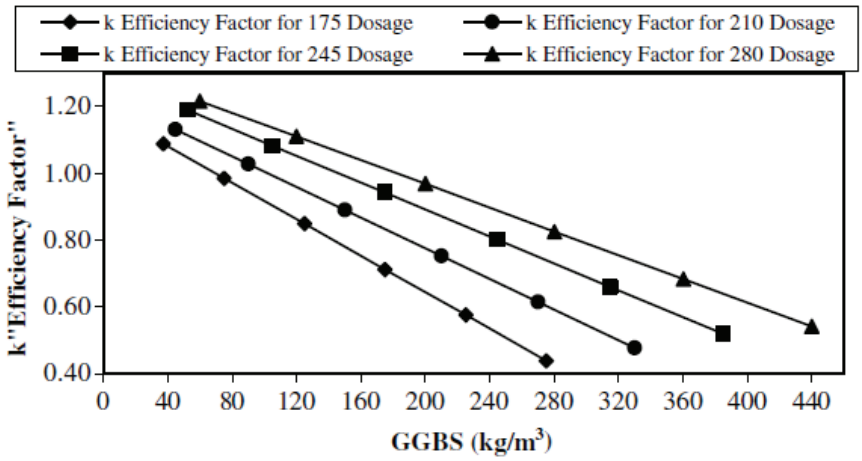

Figure 2.39. Efficiency factor versus GGBS content at 28 days using the Féret equation (Oner & Akyuz, 2007)

Equivalent cement content (C') of the GGBS can be calculated by multiplying the efficiency factor to the GGBS content. Figure 2.40 and Figure 2.41 present C' versus GGBS content at 28 and 365 days, respectively. The straight line on these figures represent when GGBS is behaving same as cement. From these figures it can be seen that C' increases with time, because the efficiency of the GGBS increases with age, which was anticipated since pozzolanic reaction is slower than the hydraulic reaction.

It was observed that all the C' versus GGBS had 2nd order polynomial relation, which passed through the origin. To find the optimum amount of GGBS, the derivative of these functions was taken. The optimum amount of GGBS was found to be approximately 55-59% of the total binding material, beyond that amount some of the GGBS will remain unreacted and will serve as fine aggregate in the concrete mix.

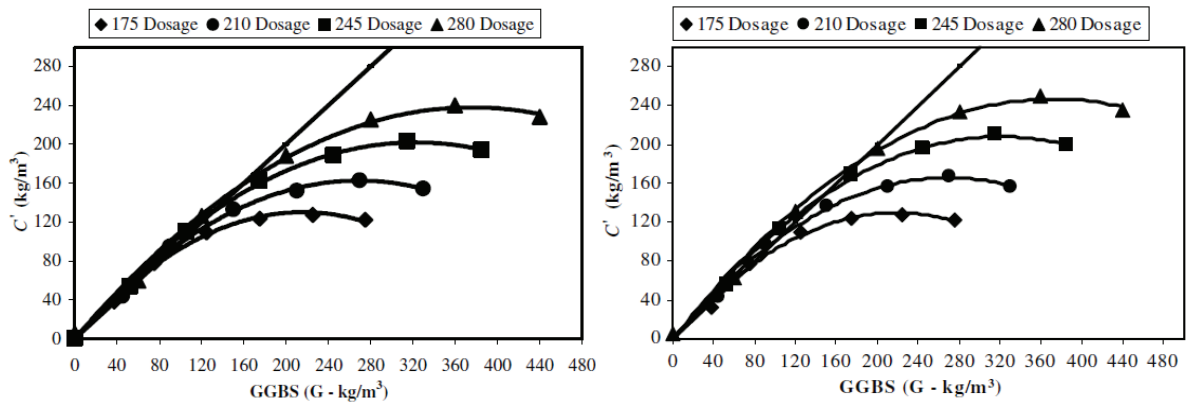

Figure 2.40. Equivalent cement content versus GGBS content at 28 days, by using Bolomey (left) and Féret (right) strength equations (Oner & Akyuz, 2007)

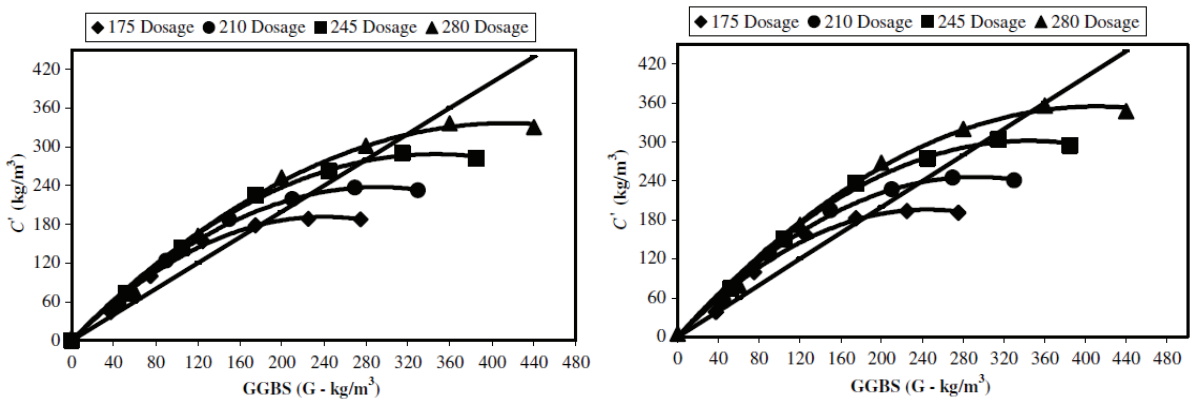

Figure 2.41. Equivalent cement content versus GGBS content at 365 days, by using Bolomey (left) and Féret (right) strength equations (Oner & Akyuz, 2007)

2.2.14.4 Conclusions

From this research the following conclusions were made:

1. The authors state that the early-age strength of the GGBS mixes exhibit lower strength than the control mix, but as the curing period was extended the GGBS mixes had strength higher than the control mix. However, the compressive strength data presented prove otherwise.

2. The compressive strength of the GGBS concrete increases as the GGBS content increases up to an optimum point, after that is reached, the strength starts to decrease with increased GGBS content.

3. The optimum point was found to be approximately 55-59% of the total binder content. After reaching the optimum point some of the GGBS will remain unreacted and serve as fine aggregate in the concrete mix.

2.2.15 Papadakis & Tsimas, 2002 – Part I

Supplementary cementing materials in concrete Part I: efficiency and design

2.2.15.1 Research Objective

Papadakis and Tsimas examined the efficiency of artificial materials and natural pozzolans by replacing either the cement or aggregate. The modified Bolomey strength equation was used to determine the efficiency of the SCM.

2.2.15.2 Material and Mix Design

CEM Type I Portland cement was used. For SCMs four artificial materials and two natural pozzolans were selected. Three of the four artificial materials were fly ash; one had low-calcium content (FL), one had high-calcium content (FH) and one had both high-calcium and high-sulfur content (FHS). The fourth artificial material was nickel slag (SL). The two natural pozzolans were volcanic turf; one with low-calcium content (ME) and one with high-calcium content (DE). Table 2.49shows the physical properties and chemical analysis of the cement and SCMs.

Table 2.49. Physical properties and chemical analysis (%) of cement and SCMs (Papadakis & Tsimas, 2002)

Compounds	Shorthand notation	CEM Type I	FL	FH	FHS	SL	ME	DE
Silicon Dioxide (SiO_2)	S	20.7	44.9	33.4	31.3	36.2	58.2	22.3
Aluminum Oxide (Al_2O_3)	A	4.8	18.5	17.4	15.9	10.3	14.2	1.0
Iron Oxide (Fe_2O_3)	F	3.9	7.9	5.6	5.4	40.2	4.3	1.0
$K_2O + Na_2O$	K+N	0.6	2.5	2.0	1.6	0.8	3.5	0.4
Sulphur Trioxide (SO_3)	$\bar{S}$	2.5	3.9	5.6	7.9	0.2	1.2	1.2
Calcium Oxide (CaO)	C	64.7	14.9	25.2	27.4	5.1	7.4	45.9
Magnesium Oxide (MgO)	M	2.1	2.2	3.1	3.0	3.1	1.4	1.5
Loss on Ignition	LOI	--	--	--	--	--	--	--
Specific gravity (g/cm^3)	SG	--	--	--	--	--	--	--
Active Silica (%)	γ_s	--	70	75	73	5	50	50
Blaine specific surface (m^2/kg)	Blaine	--	--	--	--	--	--	--
Activity Index, 7 day (%)	7 AI	--	--	--	--	--	--	--
Activity Index, 28 day (%)	28 AI	--	99	91	100	--	81	75

Four mixes were made for each SCM, two with cement replacement and two with fine aggregate replacement. In both cases 10% and 20% were replaced with SCM by weight. One control mix was made without any SCM. The binder content varied from 350-420 kg/m^3 and the water was kept constant at 175 kg/m^3, therefore the w/b ratio varied from 0.42-0.50.The proportioning and the properties of the mixes are summarized in Table 2.50. For determination of compressive strength, the mixes were cast in 150 mm cubes.

Table 2.50. Mixture proportions of concretes, the minus refers to cement replacement and plus to aggregate replacement (Papadakis & Tsimas, 2002)

Specimen	%	Cement (kg/m^3)	SCM[1] (kg/m^3)	Water (kg/m^3)	w/b	Aggregate (kg/m^3)
Control	0	350	0	175	0.50	1900
P(+10)	9	350	35	175	0.45	1865
P(+20)	17	350	70	175	0.42	1830
P(-10)	10	315	35	175	0.50	1900
P(-20)	20	280	70	175	0.50	1900

[1]Fly ash

2.2.15.3 Experimental Results

2.2.15.3.1 Compressive Strength

The compressive strength of the three fly ash and the two natural pozzolans is presented in Figure 2.42. Generally, it was observed that for mixes when the SCM replaces the aggregate, the SCM mixes exhibited higher strength than the control mix. This strength increase is mainly because of higher C-S-H content since the SCM is reacting with available calcium hydroxide. The strength is lower at early age, with the SCMs replacement concrete. After 90

days, the fly ashes concretes had higher strength than the control mix. The selected concretes with the natural pozzolans never exceed the control mix; the authors suggest that the reason is primarily due to lower active silica content. Figure 2.43 shows the compressive strength development of the slag concrete, the strength was almost the same as the control mix regardless whether the slag was ground or not.

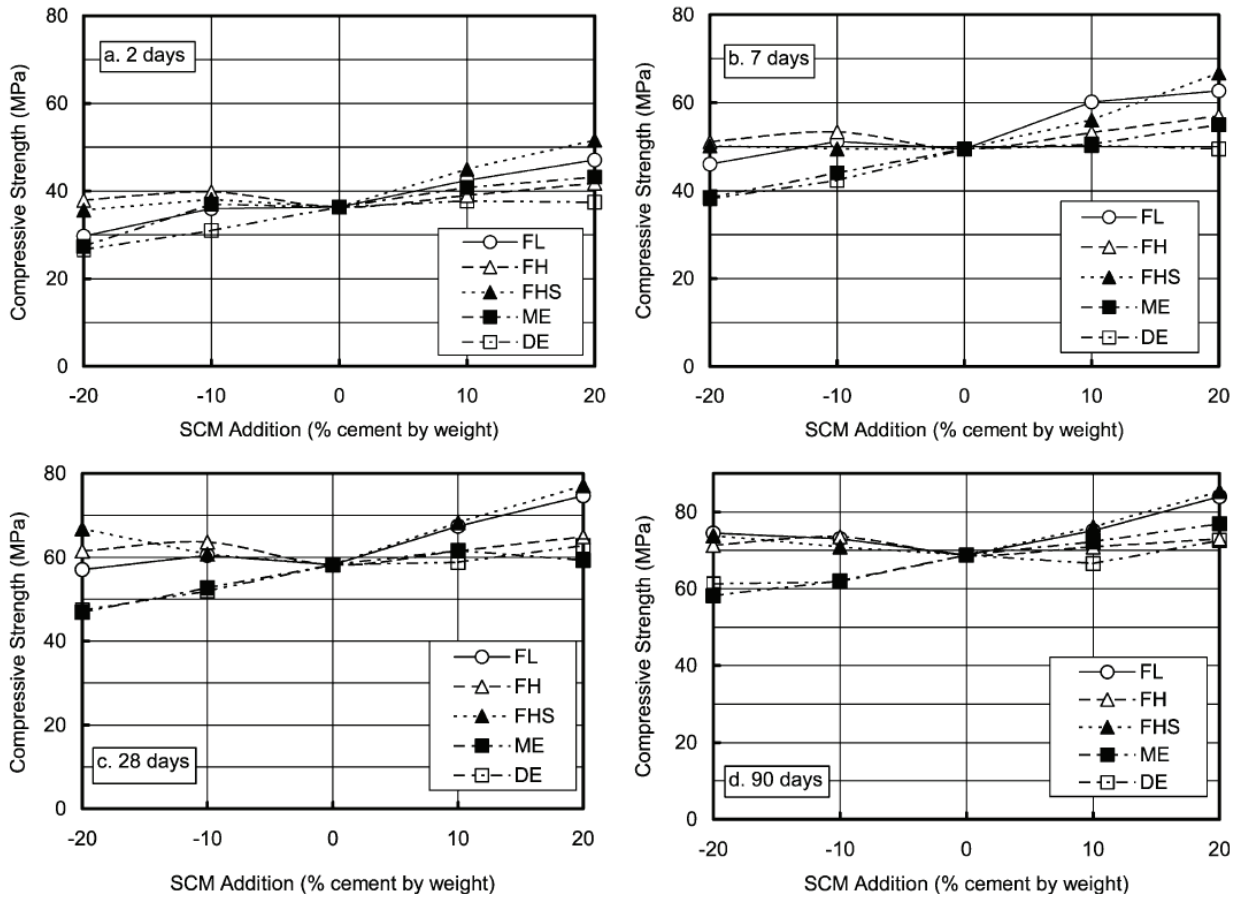

Figure 2.42. Compressive strength of the SCM concrete at age: (a) 2 days, (b) 7 days, (c) 28 days and (d) 90 days. The negative values refers to cement replacement and positive values refers to aggregate replacement (Papadakis & Tsimas, 2002)

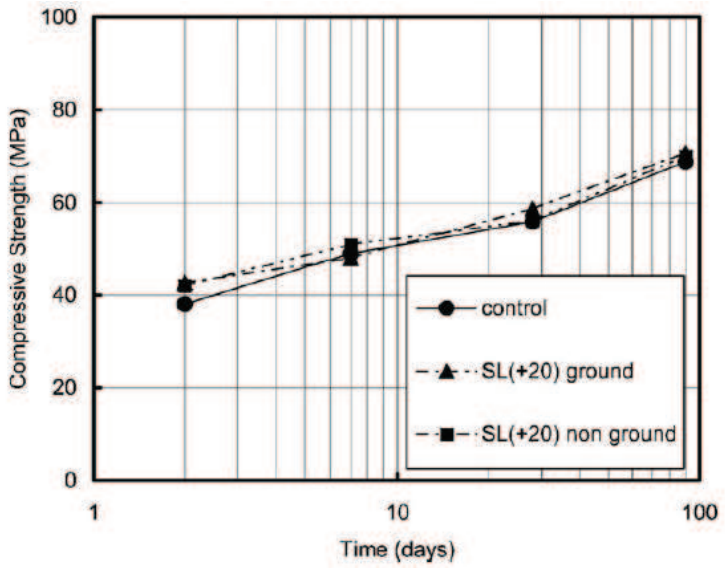

Figure 2.43. Compressive strength of slag concrete compared to the control mix (Papadakis & Tsimas, 2002)

2.2.15.3.2 Efficiency Factor

The modified Bolomey strength equation was used to evaluate the efficiency (k-value) of the SCMs compared to the control mix. Table 2.51 shows the efficiency factors of the SCMs in the research.

Table 2.51. Efficiency factor (k-value) for fly ashes and natural pozzolans (Papadakis & Tsimas, 2002)

SCM	2 days	7 days	28 days	90 days
FL	0.8	1.0	1.1	1.2
FH	0.8	0.9	0.9	0.9
FHS	1.0	1.0	1.4	1.2
ME	0.4	0.3	0.3	0.3
DE	0.2	0.2	0.2	0.2

The fly ashes have efficiency factor of approximately one at early age and is greater than one for an extended curing period, with the exception of the FH. The natural pozzolans never reach unity and exhibit much lower value than the fly ash and are therefore less efficient. The k-value of the SL was calculated to be 0-0.1. The reason for the low values for the SL and the natural pozzolans is correlated to their low active silica value.

2.2.15.4 Conclusions

From this research the following conclusions were made:

1. To compare the performance of SCM to Portland cement, an efficiency factor can be used. The efficiency factor (k-value) is the part of the SCM that is considered to be equivalent to cement.

2. When the SCM replaced the aggregate, the concrete had higher strength than the control mix. However, when the SCM replaced the cement, the early-age strength was lower than the control mix but when the curing period was extended all the fly ash exhibit strength higher than the control mix.

3. The fly ash had higher k-value than the natural pozzolans and the nickel slag. The reason is primarily due the fact that in this research the fly ash has higher active silica content.

2.2.16 Papadakis, Antiohos, & Tsimas, 2002 – Part II

Supplementary cementing materials in concrete Part II: A fundamental estimation of the efficiency factor

2.2.16.1 Research Objective

Papadakis, et al. investigated the relation between the active silica content and efficiency factor. The efficiency factor was used to predict the activity index.

2.2.16.2 Material and Mix Design

This paper uses original material and mix design data as well as the experimental results previous work (Papadakis & Tsimas, 2002).

2.2.16.3 Experimental Results

2.2.16.3.1 Activity Index

Activity index (AI) is measured by testing a compressive strength of mortar with SCM replacement and compared to a control with 100% Portland cement at days 7 and 28. Twenty percent replacement is used to determine AI of FA and fifty percent replacement is used to determine AI of SL. The authors proposed a prediction equation to predict the activity index of SCM; assuming a cement replacement of 25%. The proposed equation is expressed as follows:

$$AI = 1 + 0.25(k - 1)/(1 - 0.5a(t) \quad \textbf{(2.19)}$$

where AI is the activity index of SCM, k is the efficiency factor of the SCM and a(t) is coefficient depending mainly on time and curing (from Bolomey equation). Table 2.52 shows the comparison of measured AI and calculated by Eq. (2.19). Very good agreement between the calculated and measured values was observed. Therefore, Eq. (2.19) can be rearranged to calculate the efficiency factor for a given AI:

$$k = 1 + 4(AI - 1)(1 - 0.5a(t)) \quad \textbf{(2.20)}$$

Eq. (2.20) can be used to approximate the efficiency factor for 25% cement replacement.

Table 2.52. Comparison of calculated and measured activity index (Papadakis, Antiohos, & Tsimas, 2002)

SCM	28 day		90 day	
	Calculated	Measured	Calculated	Measured
FL	1.03	0.99	1.06	0.97
FH	0.97	0.91	0.97	0.96
FHS	1.13	1.00	1.06	0.99
ME	0.77	0.81	0.80	0.83
DE	0.73	0.75	0.77	0.80

2.2.16.3.2 Active silica

The *k*-value for equivalent strength was correlated to the active silica content of the SCM through analytical expressions. Using the active silica content of the SCM, a first approximation of the *k*-value can be obtained and the strength of a concrete incorporating artificial SCM can be predicted. The following relationship for the *k*-value was derived:

$$k = \left(\gamma_S \frac{f_{s,p}}{f_{c,p}}\right)\left(1 - a(t)\frac{w}{c}\right) \quad \textbf{(2.21)}$$

where γ_S is the ratio of active silica to the total silica in the SCM, $f_{S,P}$ and $f_{C,P}$ are the weight fraction of the silica in SCM and cement, respectively, *a(t)* is the same as in Eq. (2.1), *c* is cement content in concrete (kg/m^3) and *w* is the water content in concrete (kg/m^3).

It was found and verified by experimental comparison that the expression is valid only for artificial SCMs (fly ash, slag), but the *k*-value was overestimated for natural SCMs. The authors suggest that the reason for this exception is either the C-S-H component is weaker or that the active silica measurement is not applicable to natural pozzolans. Table 2.53 presents the measured and calculated k-values.

Table 2.53. Calculated and Measured k-value, using Eq. (2.21) and data from Papadakis et al, et al. 2002 – Part I and II

SCM	Measured k-value				Calculated k-values			
	2 days	7 days	28 days	90 days	2 days	7 days	28 days	90 days
FL	0.8	1.0	1.1	1.2	0.7	1.0	1.1	1.3
FH	0.8	0.9	0.9	0.9	0.6	0.8	0.9	1.1
FHS	1.0	1.0	1.4	1.2	0.5	0.7	0.8	1.0
ME	0.4	0.3	0.3	0.3	0.7	0.9	1.1	1.2
DE	0.2	0.2	0.2	0.2	0.3	0.3	0.4	0.5

2.2.16.4 Conclusions

From this research the following conclusions were made:

1. Relating the efficiency factor to the activity index was found to be valid. However, using that approach is only valid for certain amount of SCM in the concrete.

2. An expression relating the efficiency factor (k-value) to the active silica content of SCM was derived. This approach was found to be valid for artificial SCMs (fly ash, slag). However, the *k*-value was overestimated for natural SCMs. It may result from a weaker C-S-H component in the natural SCMs or that the active silica measurement is not applicable to natural pozzolans.

2.2.17 Pekmezci & Akyuz, 2004

Optimum usage of a natural pozzolan for the maximum compressive strength of concrete

2.2.17.1 Research Objective

Pekmezci and Akyuz looked for the optimum amount of natural pozzolan to achieve the maximum strength. Furthermore, optimum efficiency of the natural pozzolan was determined by using the Bolomey and Féret strength equations.

2.2.17.2 Material and Mix Design

ASTM Type I Portland cement was selected and natural pozzolan, which was volcanic turf, was chosen as the SCM. Table 2.54 shows the physical properties and chemical analysis of the cement and natural pozzolan that were used in the research.

Table 2.54. Physical properties and chemical analysis (%) of cement and natural pozzolan (Pekmezci & Akyüz, 2004)

Compounds	Shorthand notation	ASTM Type I	Volcanic Turf
Silicon Dioxide (SiO_2)	S	20.5	64.0
Aluminum Oxide (Al_2O_3)	A	5.3	12.5
Iron Oxide (Fe_2O_3)	F	2.7	4.0
$K_2O + Na_2O$	K+N	--	--
Sulphur Trioxide (SO_3)	$\bar{S}$	3.3	0.2
Calcium Oxide (CaO)	C	63.4	3.4
Magnesium Oxide (MgO)	M	3.0	2.5
Loss on Ignition	LOI	1.1	11.0
Specific gravity (g/cm^3)	SG	3.15	2.25
Active Silica	γ_s	--	--
Blaine specific surface (m^2/kg)	Blaine	342	435
Activity Index, 7 day (%)	7 AI	--	--
Activity Index, 28 day (%)	28 AI	--	92

A total of 15 concrete mixes were prepared. Three of the mixes were control mixes (100% Portland cement) with cement contents of 300, 350 and 402 kg/m^3. The total binder content in the SCM mixes varied from 290-460 kg/m^3 and the water content varied from 215-253 kg/m^3. The w/b ratio of the mixes varied from 0.54-0.81 and the mixes had cement replacement from 0-29%. The proportioning and the properties of the mixes are summarized in Table 2.55. For determination of compressive strength, the mixes were cast in 50 mm cubes.

Table 2.55. Mixture proportions and properties of fresh concrete (Pekmezci & Akyüz, 2004)

Mixture no.	%	Cement (kg/m^3)	SCM[1] (kg/m^3)	Water (kg/m^3)	w/b	FAg[2] (kg/m^3)	CAg[3] (kg/m^3)	Slump (mm)	Air (%)
C300T00	0	300	0	234	0.78	899	879	70	0.7
C250T40	14	250	40	235	0.81	893	873	70	0.9
C250T50	17	245	49	218	0.74	912	892	60	0.9
C250T75	23	244	74	228	0.72	884	864	70	1.0
C250T100	29	254	102	237	0.67	849	830	80	1.1
C350T00	0	350	0	238	0.68	872	853	90	0.7
C300T40	12	300	40	238	0.70	871	852	70	0.6
C300T50	14	300	50	237	0.68	865	846	70	0.7
C300T75	20	296	74	236	0.64	853	834	70	0.8
C300T100	25	299	99	242	0.61	828	810	75	0.8
C400T00	0	402	0	217	0.54	875	856	80	0.9
C350T40	10	350	40	234	0.60	852	833	75	0.8
C350T50	12	351	50	233	0.58	849	830	90	0.7
C350T75	18	352	75	245	0.57	806	787	85	1.1
C350T100	22	357	103	253	0.55	789	771	90	0.6

[1]Natural Pozzolan, [2]Fine Aggregate, [3]Coarse Aggregate

2.2.17.3 Experimental Results

2.2.17.3.1 Compressive Strength

The 28 day compressive data is presented in Table 2.56 and shown graphically in Figure 2.44. From the strength data, it can be seen, for given cement content, an optimum natural pozzolan content can be found to achieve maximum strength.

Table 2.56. Compressive strength results after 28 days of curing (Pekmezci & Akyüz, 2004)

Mixture no.	Measured Strength (MPa)
	28 day
C300T00	26.8
C250T40	24.8
C250T50	29.2
C250T75	25.4
C250T100	26.6
C350T00	30.9
C300T40	32.9
C300T50	33.4
C300T75	34.4
C300T100	34.0
C400T00	42.1
C350T40	40.2
C350T50	40.8
C350T75	41.8
C350T100	42.2

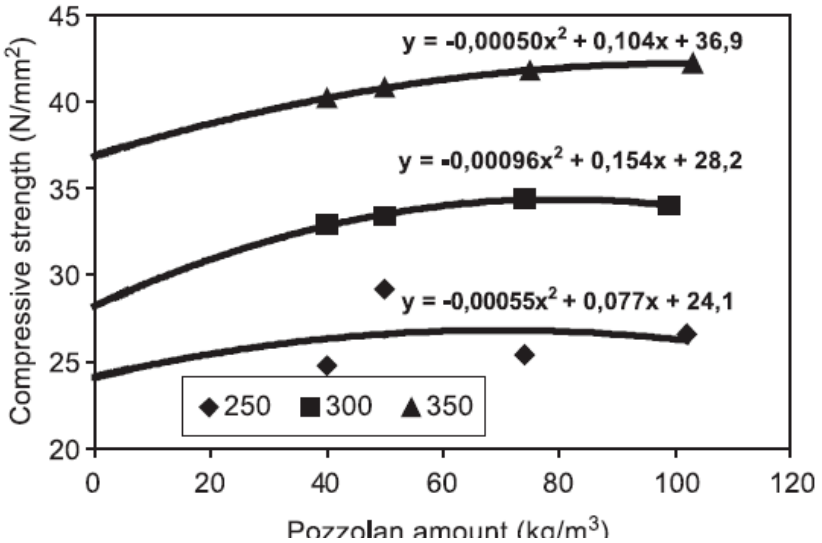

Figure 2.44. Relationship between pozzolan amount and 28 day compressive strength (Pekmezci & Akyüz, 2004)

2.2.17.3.2 Efficiency Factor

The modified Bolomey and Féret strength equations were used to evaluate the efficiency (k-value) of the natural pozzolan compared to the control mix. Equivalent cement content (C') of the natural pozzolan can be calculated by multiplying the efficiency factor to the natural pozzolan content. Figure 2.45 presents C' versus natural pozzolan content at 28 day by using the Bolomey and Féret equation. The straight line on these figures represent when natural pozzolan is behaving same as cement.

It was observed that all the C' versus natural pozzolan relation had an approximately 2nd order polynomial relation, which passed through the origin. The optimum amount of natural pozzolan was computed by taking the derivative of the 2nd order equation and setting it equal to zero. The optimum amount of natural pozzolan was found to be approximately 22% of the total binding material, beyond that amount some of the natural pozzolan will remain unreacted and will serve as fine aggregate in the concrete mix.

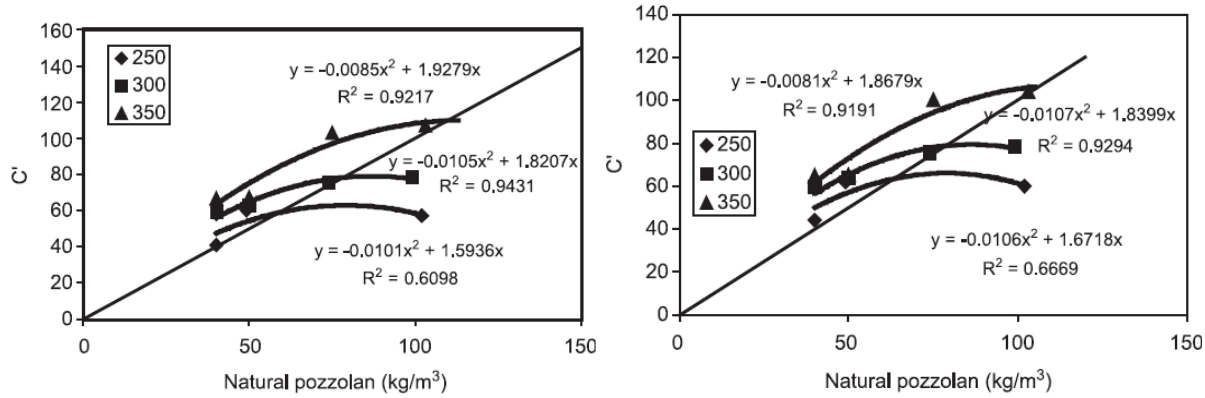

Figure 2.45.Equivalent cement content versus natural pozzolan content at 28 days, by using Bolomey (left) and Féret (right) strength equations (Pekmezci & Akyüz, 2004)

2.2.17.4 Conclusions

From this research the following conclusions were made:

1. The compressive strength of the natural pozzolan concrete increases as the natural pozzolan content increases up to an optimum point, after that is reached, the strength starts to decrease with increased natural pozzolan content.

2. The optimum percentage was found to be approximately 22% of the total binding material. After reaching the optimum point some of the natural pozzolan will remain unreacted and serve as fine aggregate in the concrete mix.

2.2.18 Rajamane, Peter, Ambily, 2007

Prediction of compressive strength of concrete with fly ash as sand replacement material

2.2.18.1 Research Objective

Rajamane, et al. developed an equation to predict the 7 and 28 day compressive strength of concrete with fly ash used as sand replacement.

2.2.18.2 Material and Mix Design

Ordinary Portland cement (OPC) was selected and Class F fly ash was chosen as the SCM. Table 2.57 shows the physical properties and chemical analysis of the cement and fly ash.

Table 2.57. Physical properties and chemical analysis (%) of cement and fly ash (Rajamane, Peter, & Ambily, 2007)

Compounds	Shorthand notation	OPC	Class C Fly ash
Silicon Dioxide (SiO_2)	S	--	59.0
Aluminum Oxide (Al_2O_3)	A	--	--
Iron Oxide (Fe_2O_3)	F	--	--
$K_2O + Na_2O$	K+N	--	0.8
Sulphur Trioxide (SO_3)	$\bar{S}$	--	--
Calcium Oxide (CaO)	C	--	1.0
Magnesium Oxide (MgO)	M	--	0.3
Loss on Ignition	LOI	--	1.0
Specific gravity (g/cm^3)	SG	3.15	2.20
Active Silica	γ_s	--	--
Blaine specific surface (m^2/kg)	Blaine	295	310
Activity Index, 7 day (%)	7 AI	--	--
Activity Index, 28 day (%)	28 AI	--	--

A total of 28 concrete mixes were prepared. One mix was the control mixes (no fly ash). Three sand replacement levels of 20%, 40% and 60% were used. The FA percentage of total binder content varied from 0-49%. Resulting that sand to fly ash ratio ranging from 1.0 to 1.6. The w/b ratio varied from 0.20 to 0.43. The proportioning and the properties of the mixes are summarized in Table 2.58. For determination of compressive strength, the mixes were cast in 100 mm cubes; Table 2.58 presents the compressive strengths at 7 and 28 days.

Table 2.58. Mixture proportions and 7 and 28 day strength of the concrete (Rajamane, Peter, & Ambily, 2007)

Mixture no.	%	w/b	m[1]	p_s[2] (%)	Measured Strength (MPa)	
					7 day	28 day
S0	0	0.35	0.0	0	35.2	46.1
S1	17	0.25	1.0	20	44.2	65.2
S2	17	0.42	1.0	20	25.6	35.9
S3	17	0.38	1.0	20	29.2	41.5
S4	29	0.21	1.0	40	49.2	70.2
S5	29	0.43	1.0	40	23.1	30.2
S6	29	0.32	1.0	40	32.5	46.2
S7	38	0.25	1.0	60	38.9	59.1
S8	38	0.38	1.0	60	25.1	34.9
S9	38	0.34	1.0	60	28.1	42.2
S10	19	0.24	1.2	20	44.6	69.4
S11	19	0.40	1.2	20	24.6	36.4
S12	19	0.36	1.2	20	28.6	43.1
S13	32	0.20	1.2	40	55.1	71.0
S14	32	0.41	1.2	40	24.8	35.1
S15	32	0.30	1.2	40	34.2	45.6
S16	42	0.23	1.2	60	46.1	59.1
S17	42	0.35	1.2	60	28.2	39.5
S18	42	0.32	1.2	60	29.4	44.6
S19	24	0.23	1.6	20	48.3	62.9
S20	24	0.38	1.6	20	24.9	36.2
S21	24	0.34	1.6	20	32.6	45.9
S22	39	0.24	1.6	40	37.9	62.7
S23	39	0.37	1.6	40	23.1	37.5
S24	39	0.34	1.6	40	30.0	42.1
S25	49	0.20	1.6	60	44.9	65.9
S26	49	0.36	1.6	60	24.9	34.1
S27	49	0.28	1.6	60	30.7	49.2

[1]Fly ash addition factor, [2]Sand replacement

2.2.18.3 Experimental Results

2.2.18.3.1 Application of Prediction Model

The authors proposed a prediction equation to predict a concrete strength with fly ash as sand replacement. The proposed equation is expressed as follows:

$$f_c = K_B \left(\frac{1 + m * p_s * s * k}{wc} - 0.5 \right) \quad \textbf{(2.22)}$$

where f_c is the compressive strength (MPa), m is the fly ash addition factor (>1), p_s is the sand replacement level, s is the sand proportion in the mix, k is the efficiency factor and K_B

(MPa) is the Bolomey coefficient, Eq.(2.1), and depends on mix design and age. The coefficient K_B is independent of the fly ash properties and can thus be calibrated with the control mix alone. The authors say that the efficiency factor has logarithmic relationship with the fly ash fraction in the binder, the relationship is:

$$k = a + b \cdot \log(P) \tag{2.23}$$

where a and b are experimental coefficients and P is the percentage of fly ash in binder (%). The relationship between fly ash and efficiency factor is shown in Figure 2.46. The authors were able to predict the compressive strength of the specimens, by using the logarithmic relationship of the efficiency factor and Eq. (2.22). Figure 2.47 shows the relationship between calculated and measured strength values, for this research and published literature with fly ash as sand replacement (Rafat, 2003; Dhir, McCarthy, & Title, 1994; Mangaraj & Krishnamoorthy, 1994).

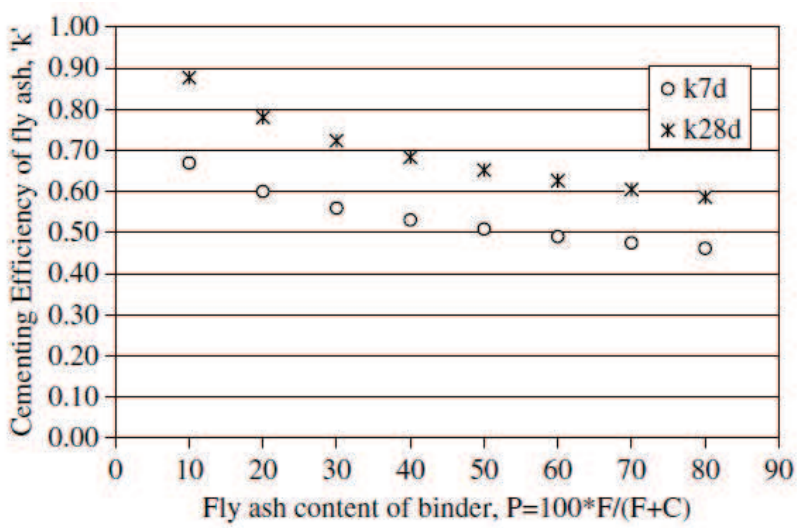

Figure 2.46. Relationship between the efficiency factor and fly ash fraction in the binder (Rajamane, Peter, & Ambily, 2007)

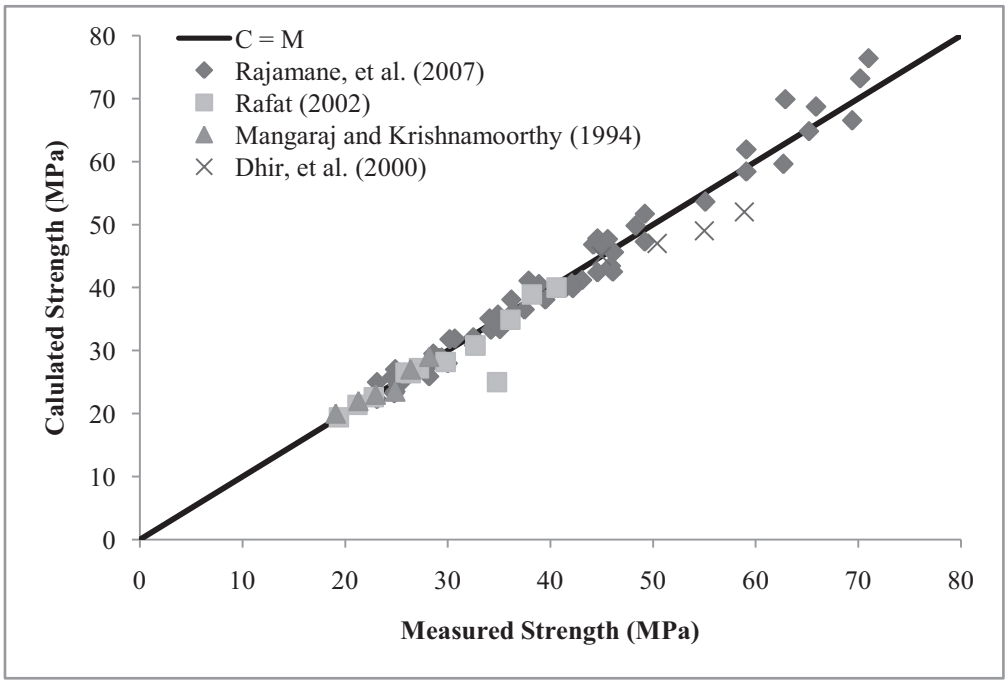

Figure 2.47. Relationship between calculated and measured strength reproduced from Rajamane, et al. 2007

2.2.18.4 Conclusions

From this research the following conclusions were made:

1. An equation was derived to estimate the compressive strength of concrete that has fly ash as sand replacement.

2. The equation uses the k-value from the modified Bolomey strength equation and the Bolomey coefficient to calibrate the mix based on the control mix without any fly ash.

3. The equation accounts for different values of sand replacement as well as if the added FA quantity is more than the replaced sand.

2.2.19 Ravina & Mehta, 1988

Compressive strength of low cement/high fly ash concrete

2.2.19.1 Research Objective

Ravina and Mehta investigated the compressive strength of concrete mixes with cement replacement of 35 to 50% using Class F and Class C fly ashes. Their target was to reach compressive strength over 14 MPa (2000 psi) at 28 day.

2.2.19.2 Material and Mix Design

ASTM Type I Portland cement was selected and two Class F (FA1 and FA2) and two Class C (FA3 and FA4) fly ashes were chosen as SCMs. The chemical composition for the cement was not provided, so typical values according to ASTM C 150 were used. Table 2.59shows the physical properties and chemical analysis of the cement and FA that were used in the research.

Table 2.59. Physical properties and chemical analysis (%) of cement and fly ashes (Ravina & Mehta, 1988)

Compounds	Shorthand notation	ASTM Type I*	FA1	FA2	FA3	FA4
Silicon Dioxide (SiO_2)	S	20.5	52.2	68.4	45.8	39.5
Aluminum Oxide (Al_2O_3)	A	5.3	27.4	17.2	22.3	19.5
Iron Oxide (Fe_2O_3)	F	2.7	9.2	3.7	7.4	5.7
$K_2O + Na_2O$	K+N	--	0.8	1.4	0.5	1.9
Sulphur Trioxide (SO_3)	$\bar{S}$	3.3	0.5	0.5	1.6	1.8
Calcium Oxide (CaO)	C	63.4	4.4	5.6	19.0	24.7
Magnesium Oxide (MgO)	M	3.0	1.0	1.6	5.0	3.4
Loss on Ignition	LOI	1.1	3.5	0.3	0.2	0.2
Specific gravity (g/cm^3)	SG	3.15	2.31	2.3	2.46	2.58
Active Silica	γ_s	--	--	--	--	--
Blaine specific surface(m^2/kg)	Blaine	351	351	244	480	377
Activity Index, 7 day (%)	7 AI	--	--	--	--	--
Activity Index, 28 day (%)	28 AI	--	--	--	--	--

*Typical values for ASTM Type I – no chemical composition given

A total of 19 concrete mixes were prepared. Three were control mixes (100% Portland cement). The cement content in the FA mix was 105, 120 and 135 kg/m^3, the total binder content in the mixes varied from 120-300 kg/m^3, the water content varied from 140-180 kg/m^3 and the w/b ratio of the mixes varied from 0.47-1.5. The fly ash percentage of the total binder varied from 0 to 60%. The proportioning and the properties of the mixes are summarized in Table 2.60. For determination of compressive strength, the mixes were cast in 76.2x152.4 mm cylinders.

Table 2.60. Mixture proportions and properties of fresh concrete (Ravina & Mehta, 1988)

Mixture no.	%	Cement (kg/m^3)	SCM[1] (kg/m^3)	Water (kg/m^3)	w/b	FAg[2] (kg/m^3)	CAg[3] (kg/m^3)
Reference	0	210	0	170	0.81	900	1155
Control - A	0	135	0	180	1.33	950	1140
A-FA1	34	135	70	160	0.78	895	1165
A-FA2	34	135	70	155	0.76	895	1160
A-FA3	34	135	70	155	0.76	900	1170
A-FA4	34	135	70	155	0.76	900	1170
A2-FA1	51	135	140	150	0.55	830	1180
A2-FA2	51	135	140	150	0.55	830	1180
Control - B	0	120	0	180	1.50	960	1145
B-FA1	43	120	90	155	0.74	900	1165
B-FA2	43	120	90	155	0.74	895	1165
B-FA3	43	120	90	155	0.74	905	1180
B-FA4	43	120	90	150	0.71	905	1180
B2-FA1	60	120	180	140	0.47	805	1180
B2-FA2	60	120	180	140	0.47	805	1180
C-FA1	50	105	105	155	0.74	900	1170
C-FA2	50	105	105	155	0.74	900	1170
C-FA3	50	105	105	155	0.74	900	1180
C-FA4	50	105	105	155	0.74	900	1180

[1]Fly ash, [2]Fine Aggregate, [3]Coarse Aggregate

2.2.19.3 Experimental Results

2.2.19.3.1 Compressive Strength

The compressive data from this research is presented in Table 2.61. Figure 2.48 and Figure 2.49 exhibit the compressive strength development of the concrete mixes by using Class F and Class C fly ash as cement replacement, respectively. For an extended curing period (around 180 days) most of the SCM mixes exceeded the reference mix. The authors argue that it was expected that FA1 would perform better than FA2 even though they were both classified as Class F, since the FA1 was finer and contained less quartz.

Eventually, all the SCM mixes reach the target strength of 14 MPa, but at different ages. In general, the SCM mixes that contained Class C fly ash reached the design strength earlier than the mixes that contained Class F fly ash. However, doubling the amount of Class F fly ash (A2 and B2 mixes) and keeping the cement content constant, resulted in a strength development that was comparable to the mixes that contained Class C fly ash.

Table 2.61. Compressive strength results of the mixes (Ravina & Mehta, 1988)

Mixture no.	Measured Strength (MPa)					
	7 day	14 day	28 day	56 day	180 day	400 day
Reference	10.9	12.9	15.3	17.8	20.4	20.5
Control - A	3.6	4.0	5.3	5.9	6.3	--
A-FA1	6.0	7.6	9.6	13.6	18.3	25.0
A-FA2	5.5	6.6	8.8	12.5	15.2	18.0
A-FA3	7.5	9.9	11.9	17.9	20.4	20.9
A-FA4	7.8	10.1	12.5	17.8	19.7	20.4
A2-FA1	8.7	10.3	13.1	19.9	29.8	--
A2-FA2	7.6	8.9	11.2	15.5	24.3	--
Control - B	2.4	2.9	4.0	4.8	4.9	--
B-FA1	4.5	5.3	7.4	11.2	16.4	24.0
B-FA2	4.8	5.9	7.9	11.9	15.3	23.4
B-FA3	6.6	9.0	10.4	16.6	19.3	25.5
B-FA4	5.1	7.2	9.0	14.8	16.3	18.0
B2-FA1	7.1	9.0	10.1	16.6	23.1	31.6
B2-FA2	6.9	8.9	9.6	15.2	19.6	27.3
C-FA1	3.7	4.4	5.8	10.3	15.6	21.9
C-FA2	--	4.6	6.1	9.8	14.1	20.8
C-FA3	5.3	6.7	8.5	14.6	19.4	27.8
C-FA4	4.7	5.6	7.3	12.9	14.9	19.8

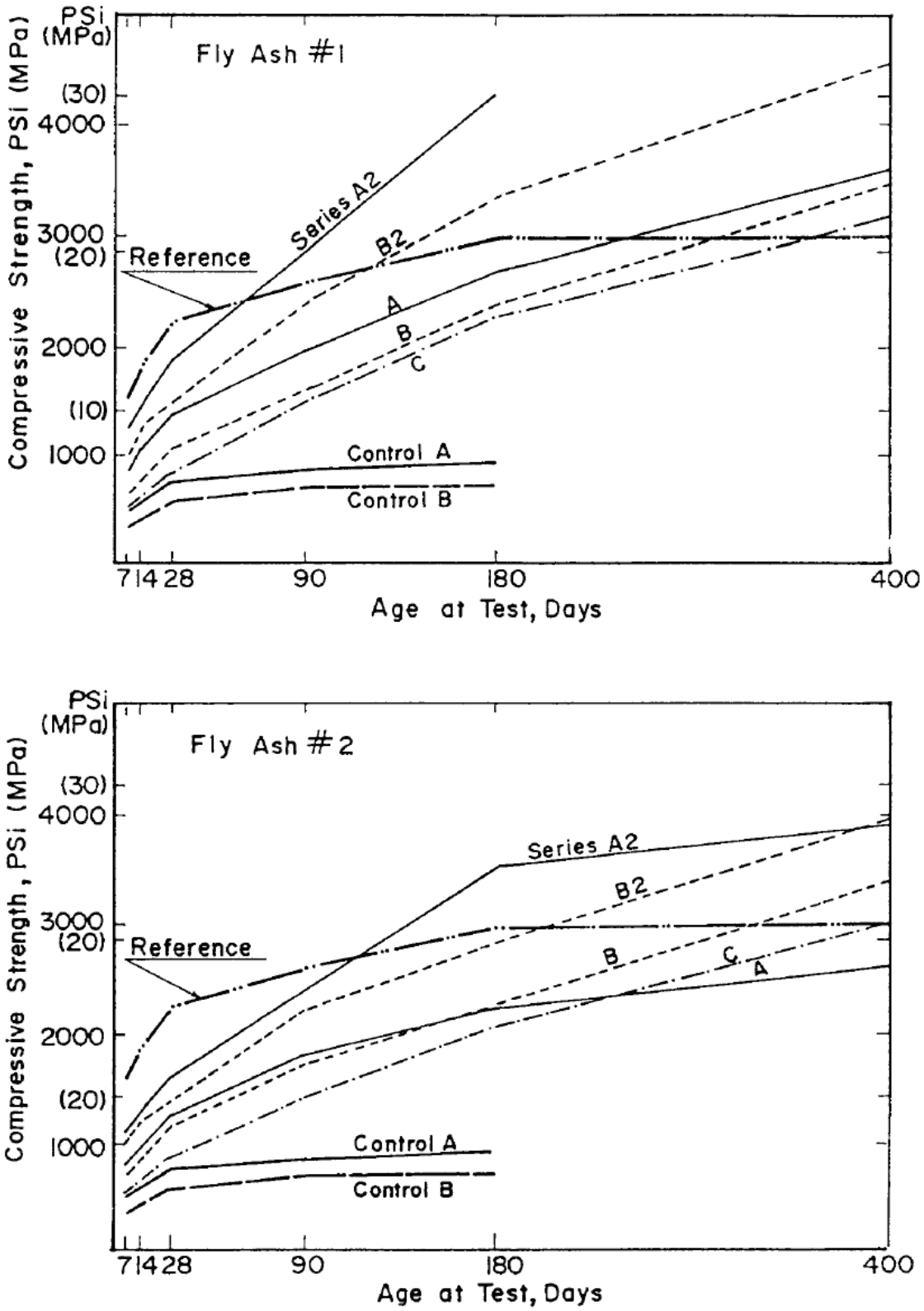

Figure 2.48. Compressive strength development of concrete mixes using Class F fly ash as cement replacement (Ravina & Mehta, 1988)

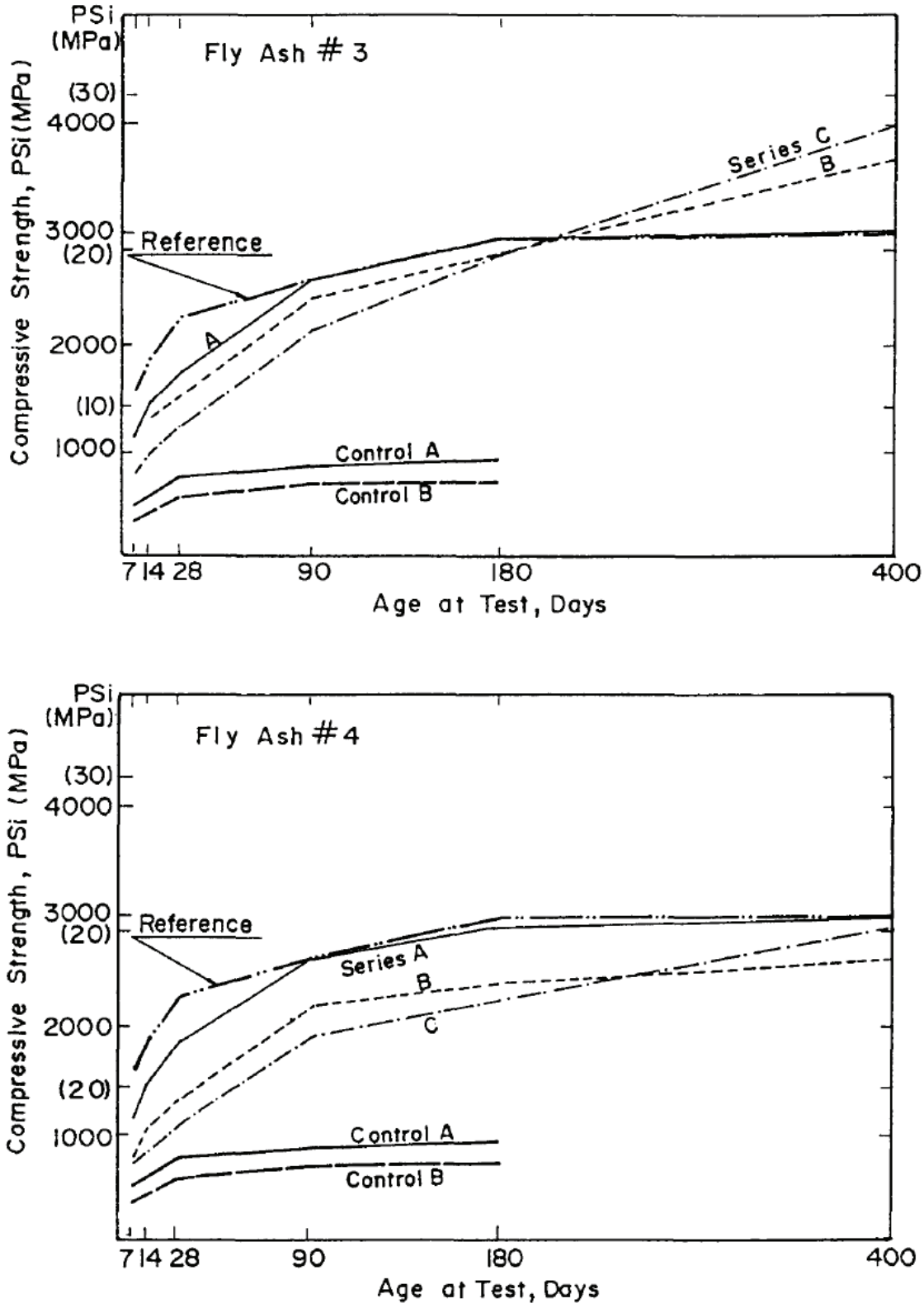

Figure 2.49. Compressive strength development of concrete mixes using Class C fly ash as cement replacement (Ravina & Mehta, 1988)

2.2.19.4 Conclusions

From this research the following conclusions were made:

1. It was possible to achieve the design strength of 14 MPa with fly ash concrete that contained 40-50% cement replacement.

2. In general mixes with Class C fly ash reached the design strength earlier than mixes with Class F fly ash. However, for given amount of cement doubling the amount of Class F fly ash resulted in a strength development that was comparable to the mixes that contained Class C fly ash.

3. The authors state that fly ash could be used when early strengths are not needed.

2.2.20 Sivasundaram, Carette, & Malhotra, 1991

Mechanical Properties, Creep and Resistance to Diffusion of Chloride Ions of Concretes Incorporating High Volumes of ASTM Class F Fly Ashes from Seven Different Sources

2.2.20.1 Research Objective

Sivasundaram, et al. examined the behavior of concretes that contain 58% Class F fly ash as cement replacement. Fly ash from seven different sources was selected to get wide range of data.

2.2.20.2 Material and Mix Design

ASTM Type I Portland cement was selected and seven Class F fly ashes were selected as SCM to cover a wide range of chemical compositions. Table 2.62 shows the physical properties and chemical analysis of the cement and fly ashes that were used in the research.

Table 2.62. Physical properties and chemical analysis (%) of cement and fly ashes (Sivasundaram, Carette, & Malhotra, 1991)

Compounds	Shorthand notation	ASTM Type I	FA1	FA2	FA3	FA4	FA5	FA6	FA7
Silicon Dioxide (SiO_2)	S	21.5	47.1	38.3	45.1	55.7	55.6	62.1	48.2
Aluminum Oxide (Al_2O_3)	A	4.0	23.0	12.8	22.2	20.4	23.1	21.4	24.9
Iron Oxide (Fe_2O_3)	F	2.6	20.4	39.7	15.7	4.6	3.5	3.0	18.9
$K_2O + Na_2O$	K+N	1.2	3.7	1.7	2.1	5.7	2.2	1.0	-
Sulphur Trioxide (SO_3)	$\overline{S}$	3.1	0.7	1.3	1.4	0.4	0.3	0.2	0.8
Calcium Oxide (CaO)	C	62.7	1.2	4.5	3.8	10.7	12.3	11.0	2.8
Magnesium Oxide (MgO)	M	3.7	1.2	0.4	0.9	1.5	1.2	1.8	1.1
Loss on Ignition	LOI	1.4	2.9	0.9	9.7	0.4	0.3	0.7	3.7
Specific gravity (g/cm^3)	SG	3.15	2.53	2.96	2.38	1.90	2.05	2.11	2.54
Active Silica	γ_s	--	--	--	--	--	--	--	--
Blaine specific surface (m^2/kg)	Blaine	417	289	198	448	215	326	240	307
Activity Index, 7 day (%)	7 AI	--	90	86	88	68	86	69	--
Activity Index, 28 day (%)	28 AI	--	98	92	94	73	95	77	--

Total of 26 mixes were made with different w/b ratios, from 0.21 to 0.49. One mix was prepared as control mix (100% Portland cement). The total binder content varied from 200-545 kg/m^3 and the water content varied from 99-150 kg/m^3. All the fly ash mixes had 58% cement replacement. The proportioning and the properties of the mixes are summarized in Table 2.63. For determination of elastic modulus, compressive strength and creep characteristics, 152x305 mm cylinders were cast.

Table 2.63. Mixture proportions and properties of fresh concrete (Sivasundaram, Carette, & Malhotra, 1991)

Mixture series	Fly ash source	Batch	%	Cement (kg/m^3)	SCM[1] (kg/m^3)	Water (kg/m^3)	w/b	FAg[2] (kg/m^3)	CAg[3] (kg/m^3)	SP[4] (L/m^3)	AEA[5] (mL/m^3)	Slump (mm)	Air (%)
1	1	A	58	228	315	117	0.22	640	1139	15.9	978	200	3.3
		B	58	229	316	117	0.21	642	1142	15.8	735	200	2.8
		C	58	154	211	112	0.31	683	1216	4.3	239	140	5.0
		D	58	151	208	111	0.31	674	1199	4.7	347	100	5.7
		E	58	225	311	117	0.22	632	1124	15.7	1287	200	4.1
2	2	A	58	224	310	116	0.22	646	1149	14.5	800	200	4.0
		B	58	219	301	113	0.22	630	1120	14.2	781	200	5.4
		C	58	149	205	108	0.31	675	1200	3.3	310	195	6.6
		D	58	150	206	109	0.31	679	1207	3.3	311	125	7.0
		E	58	211	291	150	0.30	559	993	--	752	75	9.1
3	3	C	58	154	211	118	0.32	679	1209	14.5	719	200	3.5
		D	58	155	212	119	0.32	683	1215	14.6	884	200	3.5
4	4	A	58	224	309	120	0.23	588	1045	21.5	1596	200	4.6
		B	58	222	306	119	0.23	583	1036	21.9	1583	200	4.7
		C	58	153	210	112	0.31	654	1162	5.4	429	200	5.0
		D	58	153	211	112	0.31	656	1166	5.4	430	200	5.0
5	5	A	58	223	307	117	0.22	597	1062	22.7	1909	200	4.8
		B	58	222	306	117	0.22	596	1057	22.7	1902	225	4.7
		C	58	151	208	110	0.31	656	1166	4.6	551	175	6.4
		D	58	154	211	112	0.31	665	1182	4.3	447	140	5.3
6	6	A	58	212	292	126	0.25	573	1016	41.2	1513	200	6.8
		B	58	215	296	127	0.25	579	1028	41.6	1530	200	5.8
		C	58	152	208	115	0.32	660	1174	11.2	284	200	4.9
		D	58	148	204	112	0.32	646	1147	11.2	277	200	6.3
7	7	C	58	154	211	113	0.31	797	1196	6.1	--	200	1.3
8	Control	A	0	200	0	98.6	0.49	880	1121	32.4	285	100	6.6

[1]Fly ash, [2]Fine Aggregate, [3]Coarse Aggregate, [4]Superplasticizer, [5]Air-entraining admixture

2.2.20.3 Experimental Results

2.2.20.3.1 Compressive Strength

The compressive data is presented in Table 2.64. Figure 2.50 and Figure 2.51 show the compressive strength development of the mixes that had cement contents of 155 kg/m^3 and 225 kg/m^3, respectively. All the SCM mixes showed higher compressive strength when the cement content was increased, except FA5 concrete. The long-term strength is lowest for the mixes made with FA4 and FA6. When the Pozzolanic activity index (Table 2.62) is examined all the ashes showed high activity index (AI). Again, the FA4 and FA6 show the lowest AI, which may result in lower long-term strength of the mixes made with those ashes.

Table 2.64. Compressive strength results of the mixes (Sivasundaram, Carette, & Malhotra, 1991)

Mixture series	Fly ash source	Batch	Measured Strength (MPa)					
			1 day	3 day	7 day	28 day	91 day	365 day
1	FA1	A	13.8	--	34.8	54.7	69.9	83.4
		B	--	--	--	55.4	--	--
		C	6.4	--	19	31.2	43.9	52.2
		D	--	--	--	28.9	--	--
		E	14	--	33.4	53.1	67.6	78.7
2	FA2	A		21.1	33	53	67.3	80.6
		B	--	--	--	48.2	--	--
		C	4.2	--	15.9	26.9	35.5	42.7
		D	--	--	--	24.5	--	--
		E	--	9.1	10.4	17.8	23.2	28
3	FA3	C	--	14	21	36.4	49.1	58.7
		D	--	--	--	33.6	--	--
4	FA4	A	--	13.5	21.9	34.8	45.4	50.8
		B	--	--	--	30	--	--
		C	2.8	--	17.8	28.2	35.9	39.1
		D	--	--	--	28.1	--	--
5	FA5	A	--	19.1	25.4	40.8	48.3	54.8
		B	--	--	--	40.3	--	--
		C	6.7	--	23.1	40.7	48.5	54.1
		D	--	--	--	42	--	--
6	FA6	A		15.9	19.6	32.3	41.5	48.1
		B	--	--	--	30.4	--	--
		C	--	12.3	15.6	27.2	32.9	36.6
		D	--	--	--	20	--	--
7	FA7	C	--	16.9	22.1	37.5	50.6	--
8	Control	A	5.6	--	23.4	29.9	34.9	38.5

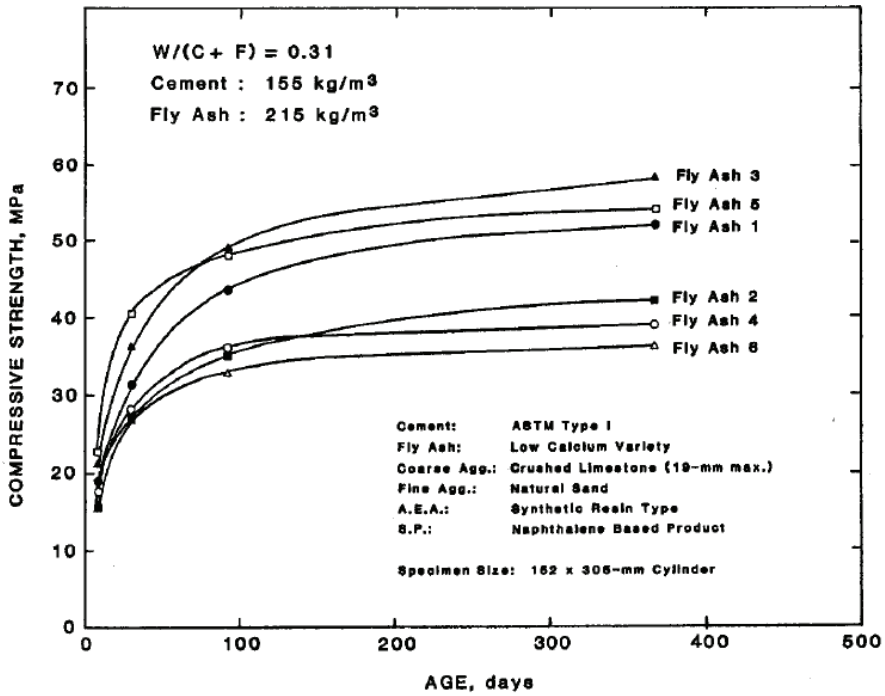

Figure 2.50. Compressive strength development of the SCM concrete mixes that contained 155 kg/m^3 of cement (Sivasundaram, Carette, & Malhotra, 1991)

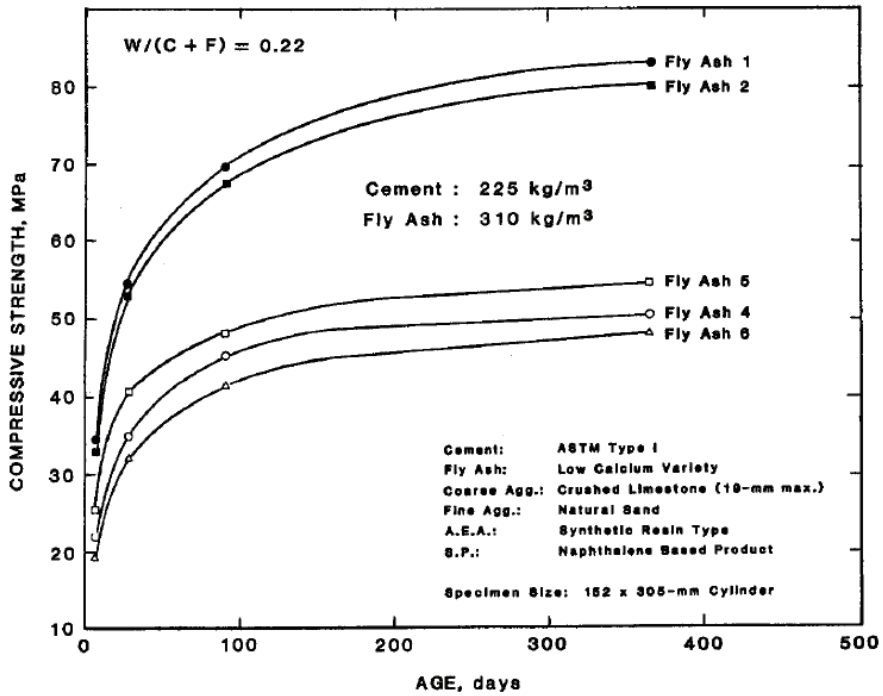

Figure 2.51. Compressive strength development of the SCM concrete mixes that contained 225 kg/m^3 of cement (Sivasundaram, Carette, & Malhotra, 1991)

2.2.20.3.2 Elastic Modulus

The elastic modulus was also measured and the data are presented in Table 2.65. Elastic modulus test was performed on the concrete at 28 and 125 days. Generally, the SCM concrete mixes that developed higher compressive strength had higher long-term elastic modulus values. The concrete mix made with FA4 showed the opposite behavior, the mix with more cement content showed less elastic modulus than the mix with lower cement content, but the authors suggest that experimental error might be the reason for this result.

Similar to the compressive strength behavior, the concrete mix made with FA5 showed equivalent elastic modulus even though the cement content was increased. All of the elastic modulus values are high compared to the strength values and the authors suggest that it is the result of the unhydrated fly ash particles acting as fine aggregate.

Table 2.65. Elastic modulus results of the mixes (Sivasundaram, Carette, & Malhotra, 1991)

Mixture series	Fly ash source	Batch	Elastic Modulus (GPa) 28 day	125 day
1	FA1	A	--	--
		B	41.0	45.2
		C	--	--
		D	34.9	38.9
		E	--	--
2	FA2	A	--	--
		B	37.9	44.5
		C	--	--
		D	27.4	34.4
		E	--	--
3	FA3	C	--	--
		D	32.9	38.5
4	FA4	A	--	--
		B	30.8	36.4
		C	--	--
		D	35.9	39.4
5	FA5	A	--	--
		B	37.2	41.3
		C	--	--
		D	38.1	41.6
6	FA6	A	--	--
		B	33.2	37.8
		C	--	--
		D	25.0	--
7	FA7	C	--	--
8	Control	A	--	--

2.2.20.3.3 Creep Strain

Table 2.66 summarizes the creep response of the mixes. Figure 2.52 and Figure 2.53 exhibit the creep strain behavior of the mixes that had cement content of 155 kg/m^3 and 225 kg/m^3, respectively. The creep strains of all the SCM concretes, with 155 kg/m^3 and 225 kg/m^3 cement content, appear to be very low. The highest creep strain was 501x10^{-6}. The concrete mixes that had higher binder content, exhibit higher creep strain. The author argue that overall the creep strains of the SCM mixes are lower than conventional concrete. The authors suggest that the low creep strains are results of large portion of fly ash remaining unreacted in the concrete and thus acting as a fine aggregate, providing higher resistance against creep.

Table 2.66. Creep results of the concrete mixtures

Mixture series	Fly ash source	Batch	Age at loading (day)	Applied Stress (MPa)	Stress/ Strength[1]	Loading Duration (days)	Inelastic strain (10^{-6})	Creep Strain (10^{-6})
1	FA 1	B	149	24.1	0.32	365	560	310
		D	133	11.3	0.28	365	302	211
2	FA 2	B	149	24.1	0.37	365	570	402
		D	139	11.3	0.33	365	337	352
3	FA 3	D	144	11.4	0.24	365	305	252
4	FA 4	B	144	11.4	0.28	365	352	304
		D	134	11.4	0.33	365	300	243
5	FA 5	B	149	11.4	0.23	365	295	211
		D	135	11.3	0.23	365	274	156
6	FA 6	B	144	11.4	0.3	365	360	501

[1]Compressive strength at day of loading

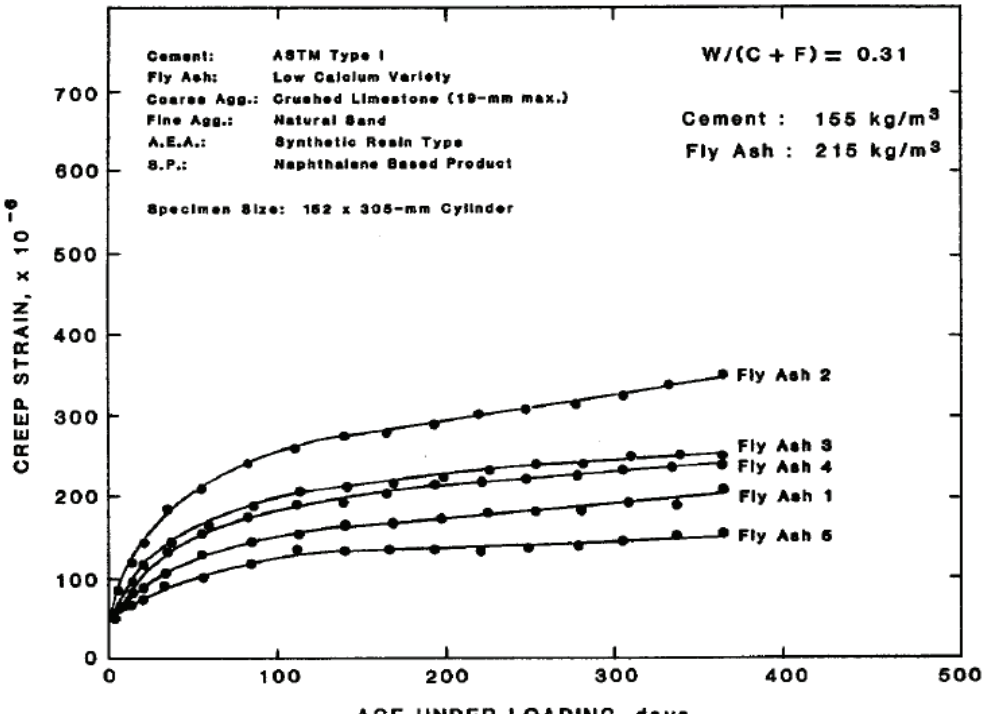

Figure 2.52. Creep strain behavior of the SCM concrete mixes that contained 155 kg/m^3 of cement (Sivasundaram, Carette, & Malhotra, 1991)

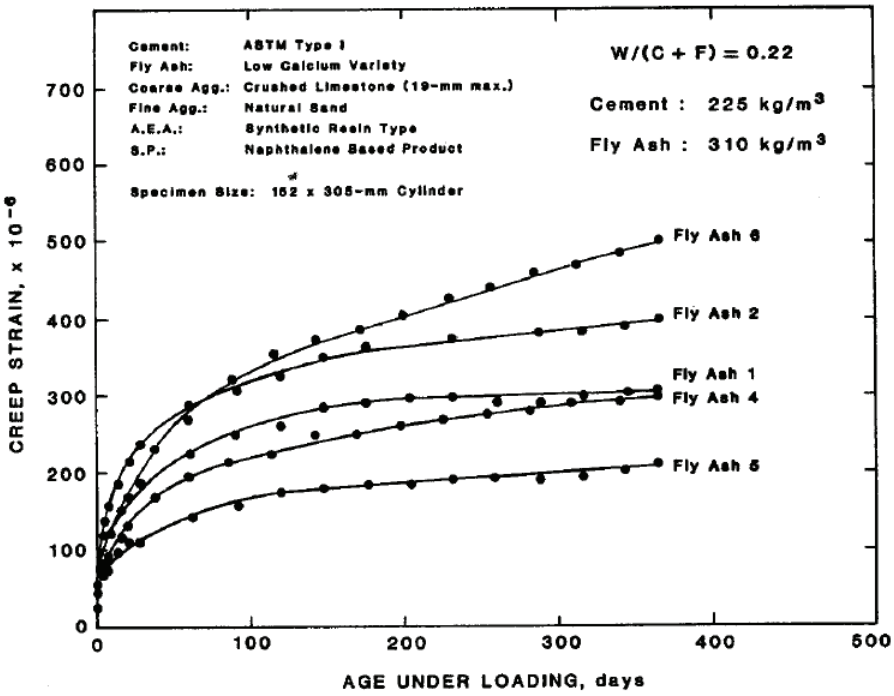

Figure 2.53. Creep strain behavior of the SCM concrete mixes that contained 225 kg/m^3 of cement (Sivasundaram, Carette, & Malhotra, 1991)

2.2.20.4 Conclusions

From this research the following conclusions were made:

1. High-volume fly ash concrete with good overall mechanical properties can be produced with Class F fly ashes covering a wide range of chemical compositions and fineness.

2. Generally, all the mixes developed higher compressive strength when the cement content was increased. However, the mix made with FA5 did not showed that trend, the increased cement content seemed not to contribute to the strength

3. Elastic modulus showed similar trend as the compressive strength results.

4. Creep strain of the SCM mixes was generally lower than conventional concrete. The mixes with higher cement content showed higher creep strain. The authors suggest the low creep strains are results of large portion of fly ash remaining unreacted in the concrete and thus acting as a fine aggregate, providing higher resistance against creep.

2.2.21 Tikalsky, Carrasquillo, & Carrasquillo, 1989

Strength and Durability Considerations Affecting Mix Proportioning of Concrete Containing Fly Ash

2.2.21.1 Research Objective

Tikalsky, et al. investigated both fresh and hardened properties of concrete containing fly ash and then uses the data to proportion high-quality concrete that will remain durable throughout the life of a structure

2.2.21.2 Material and Mix Design

ASTM Type I and Type IP Portland cements were selected and two fly ashes, Class C and Class F, were selected as SCM. Table 2.67 shows the physical properties and chemical analysis of the cements and fly ashes that were used in the research.

Table 2.67. Physical properties and chemical analysis (%) of cements and fly ashes (Tikalsky, Carrasquillo, & Carrasquillo, 1989)

Compounds	Shorthand notation	ASTM Type I	ASTM Type IP	Class C Fly ash	Class F Fly ash
Silicon Dioxide (SiO_2)	S	22.0	28.9	31.7	48.5
Aluminum Oxide (Al_2O_3)	A	4.1	7.9	20.2	23.5
Iron Oxide (Fe_2O_3)	F	3.1	3.8	5.1	6.4
$K_2O + Na_2O$	K+N	--	--	--	--
Sulphur Trioxide (SO_3)	$\bar{S}$	2.7	--	--	--
Calcium Oxide (CaO)	C	65.8	53.1	38.1	10.2
Magnesium Oxide (MgO)	M	0.9	0.1	6.8	1.7
Loss on Ignition	LOI	0.9	--	4.2	0.9
Specific gravity (g/cm^3)	SG	--	--	--	--
Active Silica	γ_s	--	--	--	--
Blaine specific surface (m^2/kg)	Blaine	331	303	--	319
Activity Index, 7 day (%)	7 AI	--	--	--	--
Activity Index, 28 day (%)	28 AI	--	--	97	106

Total of 5 basic mixes proportions were examined with total binder content varying from 307-391 kg/m^3 and the water content varied from 138-177 kg/m^3. In all cases the w/b ratio was kept constant at 0.45, the cement replacement varied from 0-35%.The proportioning of the mixes is summarized in Table 2.68. For determination of compressive strength and creep characteristics, 152x305 mm cylinders were cast and shrinkage strain was measured on 76x92x366 mm prisms.

Table 2.68.The basic mixture proportions of the concrete (Tikalsky, Carrasquillo, & Carrasquillo, 1989)

	Mix 1	Mix 2	Mix 3	Mix 4
Binder (kg/m^3)	307	335	363	391
Water (kg/m^3)	138	151	163	177
Fine Aggregate (kg/m^3)	632	576	520	464
Coarse Aggregate (kg/m^3)	1246	1246	1246	1246
Air (%)	5.0	5.0	5.0	5.0
w/b	0.45	0.45	0.45	0.45

2.2.21.3 Experiential Results

2.2.21.3.1 Compressive Strength

Figure 2.54 shows the compressive strength development of the concrete with binder content of 307 kg/m^3 (5.5 sacks per yd^3) using Class F fly ash as cement replacement and Figure 2.55 shows the same binder content using Class C fly ash as cement replacement. It can be seen from these figures that an optimum replacement level exists for different fly ash. At early-age, the control mix had always developed higher strength than the fly ash mixes. However,

the long-term strength of concrete containing fly ash was close to or exceeding the control mix (100% Portland cement). The authors state that the similar compressive strength behavior was observed for the other binder contents.

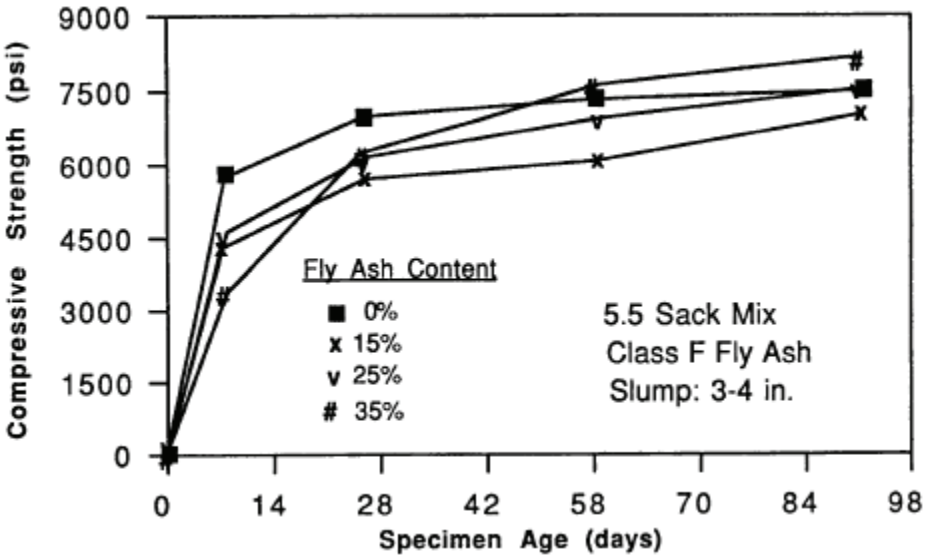

Figure 2.54. Compressive strength development of concrete containing Class F fly ash (1 psi =6895 Pa) (Tikalsky, Carrasquillo, & Carrasquillo, 1989)

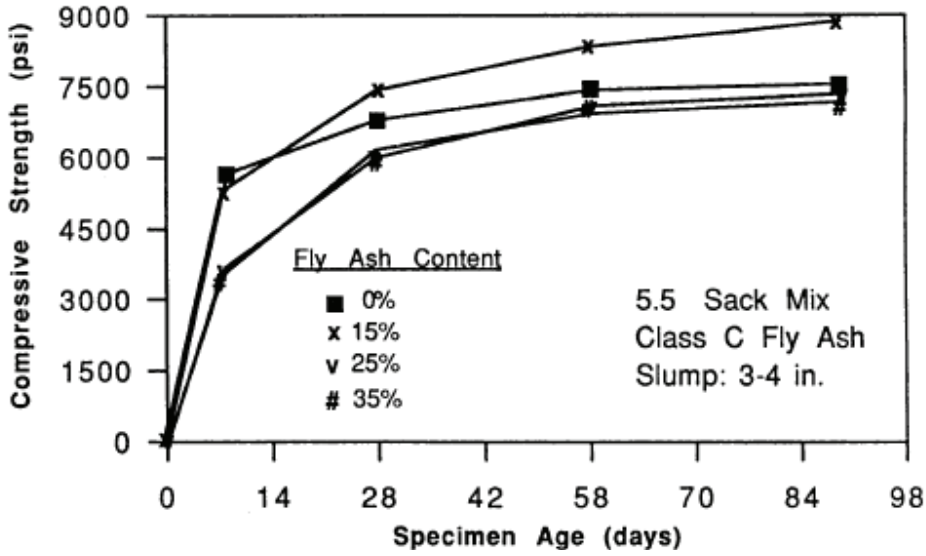

Figure 2.55. Compressive strength development of concrete containing Class C fly ash (1 psi =6895 Pa) (Tikalsky, Carrasquillo, & Carrasquillo, 1989)

2.2.21.3.2 Shrinkage and Creep Behavior

Shrinkage strain was monitored under hot-dry (38°C, 32% RH) and moderated conditions (24°C, 55% RH). The specimens tested under hot-dry condition were cured for 3 days before

testing and the specimens tested for moderate conditions were cured for 14 days before testing. The specimens that contained Class F fly ash showed lower shrinkage than the control mix under both hot-dry and moderated conditions. The specimens that contained Class C fly ash showed similar shrinkage as the control mix under both hot-dry and moderated conditions.

Figure 2.56 shows the creep behavior of the mixes that contained 35% cement replacement compared to the control mix. The Creep strain was tested after 28 days of curing under 0.34 to 0.40 stress/strength ratios. The mix that contains Class F fly ash shows less long-term creep strain than the control. However, the creep strains of the mix that contained Class F fly ash were higher than the control mix at early-ages. This is due to the slower strength gain at early-ages for concrete mixes that contains fly ash. Similarly, concrete containing Class C fly ash showed slightly less long-term creep strain than the control mix.

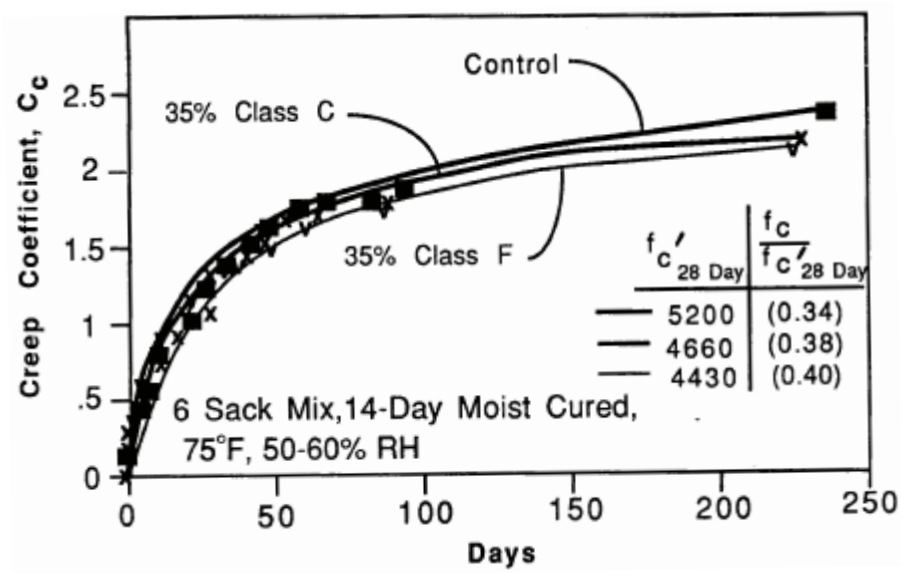

Figure 2.56. Creep of the concrete (Tikalsky, Carrasquillo, & Carrasquillo, 1989)

2.2.21.4 Conclusions

From this research the following conclusions were made:

1. The early-age strength development of the concrete mixes that contained fly ash was always lower than the control mix. However, as the curing period was extended the SCM mixes exceeded the control mix. It could be seen that an optimum replacement

level for each fly ash existed. Similar strength behavior was observed to all binder contents.

2. Reduction in shrinkage strains was observed when the concrete mix contained Class F fly ash. The specimens that contained Class C fly ash showed similar shrinkage strain as the control mix.

3. Similar, the concrete mix that contained Class F fly ash showed less long-term creep strain than the control mix. Although, the creep strain at early-age was higher than the control, the reason is due to the slower strength gain at early-ages for concrete mixes that contains fly ash. The concrete mix that contained Class C fly ash showed slightly less long-term creep strain than the control mix.

2.2.22 Valente, Vigneri, Bressan, Pasqualini, Bianchini, & Liberatore, 2010

Use of Fly Ash Concrete: Efficiency Factors of the Supplementary Cementing Material

2.2.22.1 Research Objective

Valente, et al. examined the efficiency factors of concrete that contains fly ash. According to EN 206-1 the k-value can be taken as 0.2 or 0.4, depending on type of cement. The authors want to demonstrate that EN 206-1 k-values are a lower bound, especially when referred to concrete at age 56-90 day.

2.2.22.2 Material and Mix Design

CEM Type I Portland cement was selected and one Class F fly ashes was used. The chemical composition for the cement was not provided, therefore standard values of CEM Type I were provided. Table 2.69 shows the physical properties and chemical analysis of the cement and FA that were used in the research.

Table 2.69. Physical properties and chemical analysis (%) of cement and fly ash (Valente, Vigneri, Bressan, Pasqualini, Bianchini, & Liberatore, 2010)

Compounds	Shorthand notation	CEM Type I*	Class F Fly ash
Silicon Dioxide (SiO_2)	S	20.7	50.3
Aluminum Oxide (Al_2O_3)	A	4.9	26.6
Iron Oxide (Fe_2O_3)	F	3.0	5.8
$K_2O + Na_2O$	K+N	0.9	--
Sulphur Trioxide (SO_3)	$\bar{S}$	2.3	--
Calcium Oxide (CaO)	C	61.8	5.3
Magnesium Oxide (MgO)	M	1.4	--
Loss on Ignition	LOI	--	5.1
Specific gravity (g/cm^3)	SG	--	--
Active Silica	γ_s	--	--
Blaine specific surface, m^2/kg	Blaine	--	--
Activity Index, 7 day (%)	7 AI	--	--
Activity Index, 28 day (%)	28 AI	--	--

*Typical values for CEM Type I – no chemical composition given

A total of 24 concrete mixes were prepared. Four were control mixes (100% Portland cement). The cement content in the fly ash mixes were 220, 270, 300 and 320 kg/m^3. The total binder content in the mixes varied from 240 to 490 kg/m^3. The water content was kept constant at 160 kg/m^3 for all the mixes. The resulting w/b ratio of the mixes varied from 0.33-0.67. The mixes had cement replacement from 0 to 35%. The proportioning and the properties of the mixes are summarized in Table 2.70. For determination of compressive strength, the mixes were cast in 150 mm cubes.

Table 2.70. Mixture proportions and properties of fresh concrete (Valente, Vigneri, Bressan, Pasqualini, Bianchini, & Liberatore, 2010)

Mixture no.	%	Cement (kg/m^3)	SCM[1] (kg/m^3)	Water (kg/m^3)	w/b	SP[2] (%)	Slump (mm)
1	0	260	0	160	0.62	0.50	190
2	0	320	0	160	0.50	0.50	210
3	0	360	0	160	0.44	0.50	230
4	0	400	0	160	0.40	0.50	220
5	8	220	20	160	0.67	0.50	210
6	15	220	40	160	0.62	0.50	210
7	21	220	60	160	0.57	0.50	220
8	27	220	80	160	0.53	0.50	220
9	35	220	120	160	0.47	0.50	210
10	10	270	30	160	0.53	0.50	210
11	16	270	50	160	0.50	0.50	230
12	23	270	80	160	0.46	0.50	230
13	29	270	110	160	0.42	0.50	210
14	34	270	140	160	0.39	0.60	220
15	12	300	40	160	0.47	0.50	210
16	17	300	60	160	0.44	0.50	220
17	25	300	100	160	0.40	0.60	200
18	30	300	130	160	0.37	0.60	220
19	35	300	160	160	0.35	0.70	220
20	14	320	50	160	0.43	0.50	190
21	20	320	80	160	0.40	0.50	200
22	27	320	120	160	0.36	0.60	200
23	31	320	145	160	0.34	0.65	210
24	35	320	170	160	0.33	0.70	210

[1]Fly ash, [2]Superplasticizer

2.2.22.3 Experimental Results

2.2.22.3.1 Compressive Strength

Table 2.71 summarizes the compressive strength results of this research. As expected, the strength gain of the control mixes at early-age have higher strength development than the SCM mixes. However, as the curing period was extended most of the SCM mixes exceeded the control mix. All the SCM mixes showed higher compressive strength when the cement content was increased.

Table 2.71. Compressive strength results of the mixes (Valente, Vigneri, Bressan, Pasqualini, Bianchini, & Liberatore, 2010)

Mixture no.	Measured Strength (MPa)					
	2 days	7 days	14 days	28 days	56 days	90 days
1	20.22	30.31	32.53	36.49	40.12	43.64
2	31.10	41.39	43.25	44.02	48.17	56.24
3	37.42	48.35	52.25	54.95	58.16	62.87
4	45.14	53.12	55.90	60.96	65.12	72.36
5	14.42	25.12	29.58	30.90	34.02	37.16
6	15.71	26.02	30.11	32.49	35.17	43.76
7	16.57	26.39	31.14	36.97	42.11	46.13
8	17.30	26.96	32.13	36.62	43.63	47.51
9	17.55	27.52	33.95	39.93	46.19	50.82
10	23.20	34.37	38.37	39.60	44.73	50.62
11	24.56	35.97	39.78	42.13	47.19	55.29
12	25.05	38.47	42.47	47.38	52.74	58.69
13	25.51	38.91	43.35	50.12	55.97	62.80
14	26.64	41.04	46.68	53.08	59.34	64.94
15	28.86	43.05	45.23	51.71	56.28	60.98
16	30.26	43.77	47.17	52.73	57.84	65.94
17	31.51	44.95	50.11	55.23	61.02	69.04
18	32.46	46.38	52.78	58.34	63.97	72.27
19	33.96	47.80	55.86	61.61	66.93	74.29
20	34.55	47.30	54.45	56.73	62.19	71.62
21	36.33	49.69	56.53	62.12	65.47	73.29
22	38.81	53.78	57.92	65.07	69.85	77.16
23	39.98	54.27	58.97	66.45	71.12	79.33
24	40.29	55.40	61.08	68.14	74.75	85.62

2.2.22.3.2 Efficiency Factor

Modified power strength equation was used to evaluate the efficiency (k-value) of the FA compared to the control mix. The equation is expressed as follows:

$$f_c = A_1 \left(\frac{w}{c + kP}\right)^{A_2} \tag{2.24}$$

where f_c is the compressive strength (MPa), w is the water content (kg/m^3), c is the cement content (kg/m^3), P is the fly ash content (kg/m^3), A_1 and A_2 are experimental parameters which depending on time of hydration and type of cement and can be determined on the control mix alone. Figure 2.57 and Figure 2.58 show the relationship between the efficiency factor and fly ash content by using Eq. (2.22) at 28 day and 90 day, respectively. From these figures it can be seen as the fly ash content increases the efficiency of the fly ash increases to peak efficiency, beyond that point increasing fly ash decreases the fly ash efficiency. Also,

increasing cement content increases the fly ash efficiency. The experimental data are much higher than the values that are EN 206-1 suggests, especially when referred to 56-90 day aged concrete. The values the standard suggests were reached after only two days.

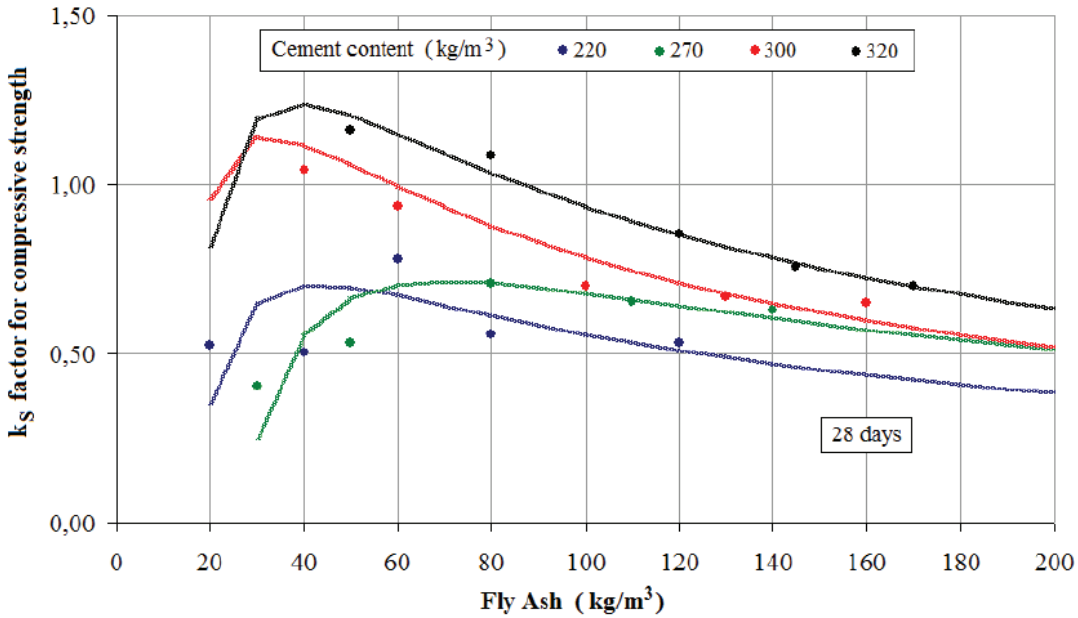

Figure 2.57. Efficiency factor versus fly ash content for 28 day compressive strength (Valente, Vigneri, Bressan, Pasqualini, Bianchini, & Liberatore, 2010)

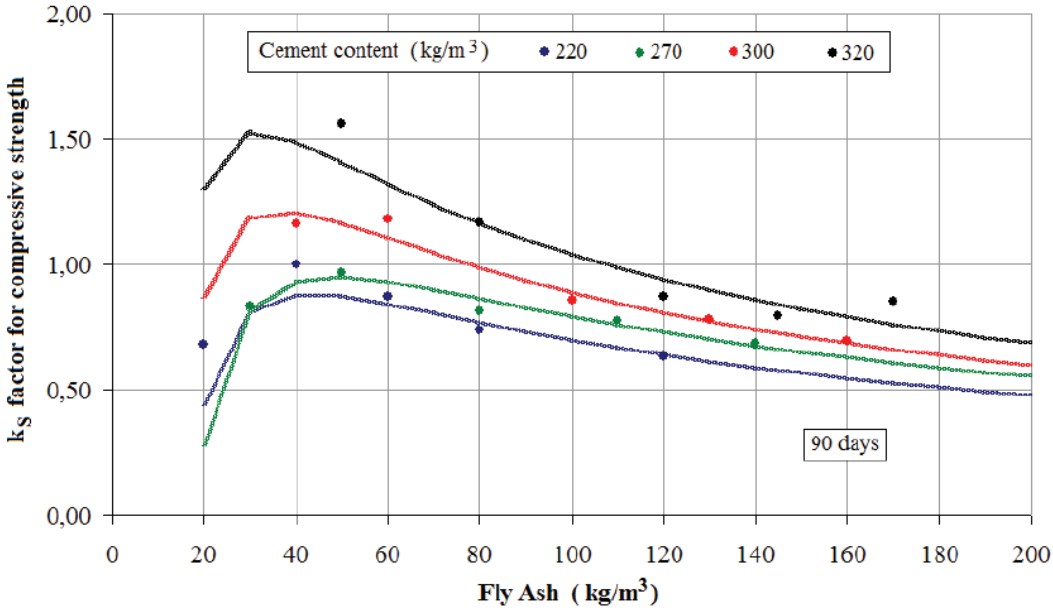

Figure 2.58. Efficiency factor versus fly ash content for 90 day compressive strength (Valente, Vigneri, Bressan, Pasqualini, Bianchini, & Liberatore, 2010)

Equivalent cement content (c_{eq}) of the fly ash can be calculated by multiplying the efficiency factor to the FA content. Figure 2.32 present total equivalent cement content ($c_{tot} = c+c_{eq}$) versus fly ash content at 28 and 90 days. From these figures it can be seen that c_{tot} increases with time, because efficiency of the FA increases with age, which was anticipated since pozzolanic reaction is slower than the hydraulic reaction.

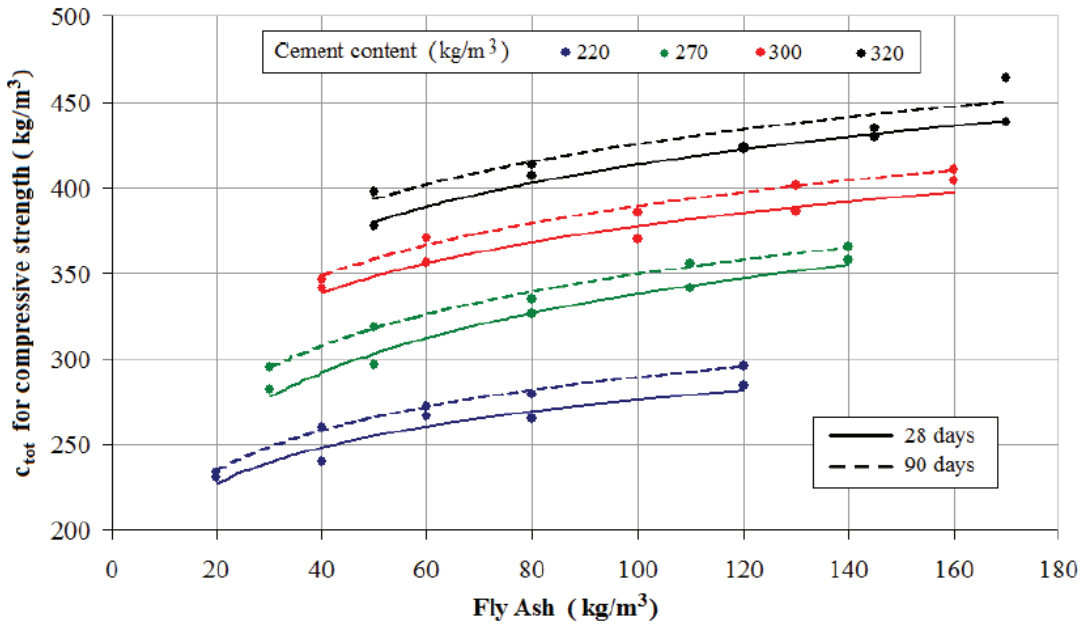

Figure 2.59. Total equivalent cement content versus fly ash content at 28 and 90 day (Valente, Vigneri, Bressan, Pasqualini, Bianchini, & Liberatore, 2010)

2.2.22.4 Conclusions

From this research the following conclusions were made:

1. The strength gain of the control mixes at early-age have higher strength development than the SCM mixes. However, as the curing period was extended most of the SCM mixes exceeded the control mix. All the SCM mixes showed higher compressive strength when the cement content was increased.

2. The experimental data are much higher than the values that are EN 206-1 suggests, especially when referred to 56-90 day aged concrete. The values the standard suggests were reached after only two days.

2.3 Summary

As can be seen a considerable amount of research has been done on concrete that contains SCMs. The main focus of the prior research has been on improving concrete mixes with the use of SCM. Number studies add SCM to the binder instead of replacing the cement content. Most authors have been looking for the optimum SCM amount in concrete so nearly all of the SCM is reacting, to obtain maximum strength. Most studies focus on use of binary mixes with fly ash as SCM, although slag has also been investigated. Fly ash has been investigated more frequently in part because there is more fly ash available. Additionally, the fly ash chemical composition is dependent on the coal or raw material that used in the plant and the operating conditions dictate the physical properties of the ash, such as the particle size. Regardless of the SCM used, typical replacement levels used in prior research are between 20-50%, and rarely exceed 70%. The prior research has shown that at small replacement levels (around 20%) that SCM, type or blend does not have much impact on the strength.

Not many researchers have examined SCC with high volume (≥ 60% cement replacement) of SCM. In this research focus will be more on the behavior of SCC with high volume (≥ 60% replacement) of fly ash (FA) and slag (SL), rather than maximizing strength. It is not necessary that all the SCM reacts with water; some can serve as filler, if the strength is sufficient. This research examines also the correlation between replacement, compressive strength and SCM's chemical compositions. This study will also examine the influence of high ternary replacement on creep- and shrinkage strain as well as elastic modulus.

Chapter 3: Test Matrix and Setup

The research was conducted to investigate the engineering characteristics of SCM concretes with a range of cement replacement by weight. Specifically, two phases were conducted. In the first Phase, four SCMs were used: one Class C fly ash, one Class F fly ash and two grade 100 slag. Concrete mixes were made with water-binder (w/b) ratio of 0.35 and were tested for compressive strength and initial time of set. In the second Phase, two SCMs were used: one Class C fly ash and one grade 100 slag. Concrete mixes were made with a water-binder (w/b) ratio of 0.40 and were tested for compressive strength, elastic modulus, shrinkage and creep.

3.1 Overview of Phase I and II

The first Phase mixes were cast in summer 2009. The objective of the first Phase was to examine the influence of high volume (≥ 60% replacement) of fly ash and slag on the compressive strength and time of set of self-consolidating concrete (SCC). The focus in the first Phase was to understand the compressive strength behavior with time rather than maximizing strength. It was not necessary that all the SCM would react with water; some could serve as filler, if the strength would be sufficient. In the first Phase, four locally available SCMs were used: one Class C fly ash, one Class F fly ash and two grade 100 slag. Twenty binary mixes (cement and one SCM) were made with 20%, 40%, 60%, 80% and 100% cement replacement. One control mix was established with only Portland cement. All of the mixes were made with w/b ratio of 0.35

The second Phase mixes were cast in summer 2010. The objective of the second Phase was to examine the influence of a high volume of ternary replacement on compressive strength, elastic modulus, shrinkage and creep of SCC. Two of the most promising SCMs from Phase I were used in the second Phase: one Class C fly ash and one grade 100 slag. A total of 16 mixtures were prepared; one control mixture, 6 binary mixtures and 9 ternary mixtures (cement and two SCM). Three different ratios of FA to SL in the ternary mixtures were determined to get wide range of $CaO/(SiO_2+Al_2O_3)$ ratio in the binder. The cement replacement levels by weight in the second Phase were 60%, 80% and 90%. All of the mixes were made with w/b ratio of 0.40.

3.1.1 Materials

A total of 5 cementitous materials were used for specified concrete mixes. The cement was ASTM I Portland Lafarge Cement (ASTM C 150, 2009). Two blast furnace slags (Seattle SL and St. Mary's SL) were used as SCM. The slags were classified as grade 100 (AASHTO M 302, 2006; ASTM C 989, 2009). Two sources of fly ash (Boardman FA and Centralia FA) were used as SCM. The Canadian standard (A23.1, 2004) classifies the Boardman FA and the Centralia FA as class CH (high calcium content) and class CI (Intermediate calcium content), respectively. Using the ASTM C 618 classification, the Boardman FA is classified as Class C fly ash and the Centralia is classified as Class F fly ash (ASTM C 618, 2008).

The chemical compositions of the materials were determined using X-ray fluorescence analysis (XRF). Table 3.1 shows the physical properties and chemical analysis of the cement and SCMs that were used in Phase I. Table 3.2 shows the same information for the materials used in Phase II. The concrete mixtures were SCC; therefore a low inter-particle friction was required. The maximum aggregate size was 9.53 mm (3/8 in).

Active silica, which is the reactive portion of the silica, is given in Table 3.1. Both SLs have almost all of the silica active (98-99%) whereas the FA has less active silica (70-79%). Activity index (AI) is used as quality control for the SCM and is given in Table 3.1 and Table 3.2. The AI for FA is determined by measuring a compressive strength of mortar with 20% SCM replacement and compared to a control with 100% Portland cement at days 7 and 28 (ASTM C 618, 2008). Similarly, the AI for SL is determined by measuring a compressive strength of mortar with 50% SCM replacement and compared to a control with 100% Portland cement at days 7 and 28 (ASTM C 989, 2009).

Table 3.1. Physical properties and chemical analysis (%) of cement, fly ash (FA) and slag (SL) in Phase I

Compounds	Shorthand notation	ASTM Type I	Boardman FA	Centralia FA	Seattle SL	St. Mary's SL
SiO_2	*S*	20.0	32.2	51.0	35.5	40.7
Al_2O_3	*A*	4.4	15.5	16.2	14.7	7.2
Fe_2O_3	*F*	3.3	7.5	6.2	--	--
$K_2O + Na_2O$	*K+N*	--	--	--	0.5	0.5
SO_3	$\overline{S}$	2.6	2.6	0.8	2.1	2.9
CaO	*C*	64.8	28.2	13.6	45.3	39.2
MgO	*M*	0.8	6.7	4.3	--	--
Loss on Ignition	*LOI*	2.6	--	0.2	--	--
Specific gravity (g/cm^3)	*SG*	3.15	2.58	2.63	2.89	2.89
Active SiO_2 (%)	γ_s	--	79	70	98	99
Activity Index, 7 day (%)	*7 AI*	--	91	85	88	86
Activity Index, 28 day (%)	*28 AI*	--	103	91	116	107

Table 3.2. Physical properties and chemical analysis (%) of cement, fly ash (FA) and slag (SL) in Phase II

Compounds	Shorthand notation	ASTM Type I	Boardman FA	Seattle SL
SiO_2	*S*	20.9	33.3	31.4
Al_2O_3	*A*	4.6	18.5	11.2
Fe_2O_3	*F*	3.1	5.3	1.2
$K_2O + Na_2O$	*K+N*	0.8	2.3	0.6
SO_3	$\overline{S}$	2.9	2.5	4.9
CaO	*C*	64.6	27.3	46.7
MgO	*M*	0.9	--	4.9
Loss on Ignition	*LOI*	--	0.4	--
Specific gravity (g/cm^3)	*SG*	3.15	2.58	2.89
Active SiO_2 (%)	γ_s	--	--	--
Activity Index, 7 day (%)	*7 AI*	--	92	88
Activity Index, 28 day (%)	*28 AI*	--	100	116

3.1.2 Mix Proportions

The mixes in Phase I and II were originally intended to have the same proportions of binder, water, aggregate, sand and admixture but a slight oversight in mixing in Phase II, lead to difference in mix proportions.

The total binder content in Phase I was kept constant at 473.8 kg/m^3 and the amount of sand was 807.1 kg/m^3. In Phase II the binder content was kept constant at 415.1 kg/m^3 and the amount of sand was 932.2 kg/m^3. Both phases had the same amount of water and aggregate, the water was approximately 167.9 kg/m^3 and the amount of aggregate was constant in all mixes in the amount of 819.5 kg/m^3. Therefore, Phase I had w/b ratio of 0.35 and Phase II

had w/b ratio of 0.40. The admixture used was a combination of accelerator-superplasticizer-viscosity and modifying chemical admixture (SIKA ViscoCrete 2100), which is typically used in SCC. The amount of water, binder, sand, aggregate and admixtures for the mixes are given in Table 3.3.

Table 3.3. Mix proportions of the specimens in Phase I and II

	Phase I	Phase II
Binder (kg/m^3)	473.8	415.1
Water (kg/m^3)	167.9	167.9
Sand, SSD (kg/m^3)	807.1	932.2
Aggregate 3/8 mm (kg/m^3)	819.5	819.5
Sika 2100 (L/m^3)	1.694	2.300
w/b	0.35	0.40

3.1.3 Specimens Preparation and Curing

Samples were mixed in a rotary drum mixer (Figure 3.1). First, the dry ingredients (aggregate, sand, cement and SCM, if applicable) were combined. Next, the wet ingredients (water and chemical admixture) were added and the ingredients were mixed until a homogeneous mixture was achieved. As needed, a small amount of additional water was added to control the rheology of the mixture so that the target inverted slump flow of 660 – 740 mm (ASTM C 1611, 2009) was attained. This range is typical for SCC mixes with good workability. Samples were cast into 101.6 x 203.2 mm (4x8 in) cylindrical molds (Figure 3.2) for determination of compressive strength and elastic modulus. For determination of creep and shrinkage strain the Samples were cast into 152.4 x 304.8 mm (6x12 in) cylindrical molds. Once sufficient strength was reached, the specimens were demolded and stored at 100% relative humidity until testing. Both ends of the cylinders were sulfur capped before testing, to ensure flat surface. Flat surface of the cylinders are required to minimize stress concentration and uneven loading, which reduces the compressive strength.

Figure 3.1. Photograph of a rotary drum mixer

Figure 3.2. Photograph of casting of cylinders

3.1.4 Test Matrix

From each concrete mixture, three cylinders were cast for compressive strength test. For determination of elastic modulus 2-3 cylinders were cast and 8 cylinders were cast for creep and shrinkage measurements.

In Phase I of the research, tests were made on binary mixtures with w/b of 0.35. Only compressive strength test was performed in the first Phase. Table 3.4 shows an overview of the tests that were performed in Phase I, the name convention and the casting ate.

Table 3.4. Phase I: Binary mixes and test overview

Mix name	C[1]	T[2]	E[3]	C&S[4]	Date of Cast
Base I	X	X			7/20/2009
20% Boardman FA–I	X	X			7/20/2009
40% Boardman FA–I	X	X			7/20/2009
60% Boardman FA–I	X	X			7/20/2009
80% Boardman FA–I	X	X			7/20/2009
100% Boardman FA–I	X	X			7/20/2009
20% Centralia FA–I	X	X			6/25/2009
40% Centralia FA–I	X	X			6/25/2009
60% Centralia FA–I	X	X			6/25/2009
80% Centralia FA–I	X	X			6/25/2009
100% Centralia FA–I	X	X			6/25/2009
20% Seattle SL–I	X	X			6/25/2009
40% Seattle SL–I	X	X			6/25/2009
60% Seattle SL–I	X	X			6/25/2009
80% Seattle SL–I	X	X			6/25/2009
100% Seattle SL–I	X	X			6/25/2009
20% St. Mary's SL–I	X	X			6/30/2009
40% St. Mary's SL–I	X	X			6/30/2009
60% St. Mary's SL–I	X	X			6/30/2009
80% St. Mary's SL–I	X	X			6/30/2009
100% St. Mary's SL–I	X	X			6/30/2009

[1]Compressive Test, [2]Time of set, [3]Elastic Modulus, [4]Creep and Shrinkage test

In Phase II of the research, tests were made on both binary and ternary mixtures with w/b ratio of 0.40. The compressive strength test as well as elastic modulus test, shrinkage and creep tests were performed in the second Phase. Table 3.5 shows an overview of the tests that were performed in the Phase II, the name convention and the casting date.

Table 3.5. Phase II: Binary and ternary mixes and test overview

Mix name	C[1]	T[2]	E[3]	C&S[4]	Date of Cast
Base II	X		X	X	6/25/2010
60% Boardman FA–II	X				6/25/2010
80% Boardman FA–II	X				6/25/2010
90% Boardman FA–II	X				5/21/2010
60% Seattle SL–II	X				7/15/2010
80% Seattle SL–II	X				7/15/2010
90% Seattle SL–II	X				5/21/2010
60% 25FA-75SL–II	X		X		5/6/2010
80% 25FA-75SL–II	X		X		5/6/2010
90% 25FA-75SL–II	X		X		5/18/2010
60% 50FA-50SL–II	X		X		5/12/2010
80% 50FA-50SL–II	X		X		5/12/2010
90% 50FA-50SL–II	X		X	X	5/28/2010
60% 75FA-25SL–II	X		X		5/6/2010
80% 75FA-25SL–II	X		X		5/18/2010
90% 75FA-25SL–II	X		X		5/18/2010

[1]Compressive Test, [2]Time of set, [3]Elastic Modulus, [4]Creep and Shrinkage test

3.2 Procedures and Setup

3.2.1 Initial Time of Set

The objective of this test is to measure the initial time of set of the concrete mixes. Time of set is an important parameter. It is mainly used to help regulate the time of mixing and transit, to gauge the effectiveness of various set-controlling admixtures (either retarding or accelerating agent) and to help plan the scheduling of finishing operations (Mindess, Young, & Darwin, 2003). The initial time of set was determined according to the ASTM C 403. The initial time of set test was performed on all of the SCM mixes in Phase I in this research.

3.2.1.1 Instrumentation

Figure 3.3 shows the equipment needed to perform the initial time of set test. Sieve No. 4 (4.75 mm) (Figure 3.3a) is used to removing the mortar fraction of the concrete. The mortar is placed in a container (Figure 3.3b). A removable needle (Figure 3.3c) with bearing area of 65 mm^2 (0.1 $in.^2$) is used to penetrate into the mortars. A hydraulic pressure gauge (Figure 3.3d) is used to measure the penetration resistance.

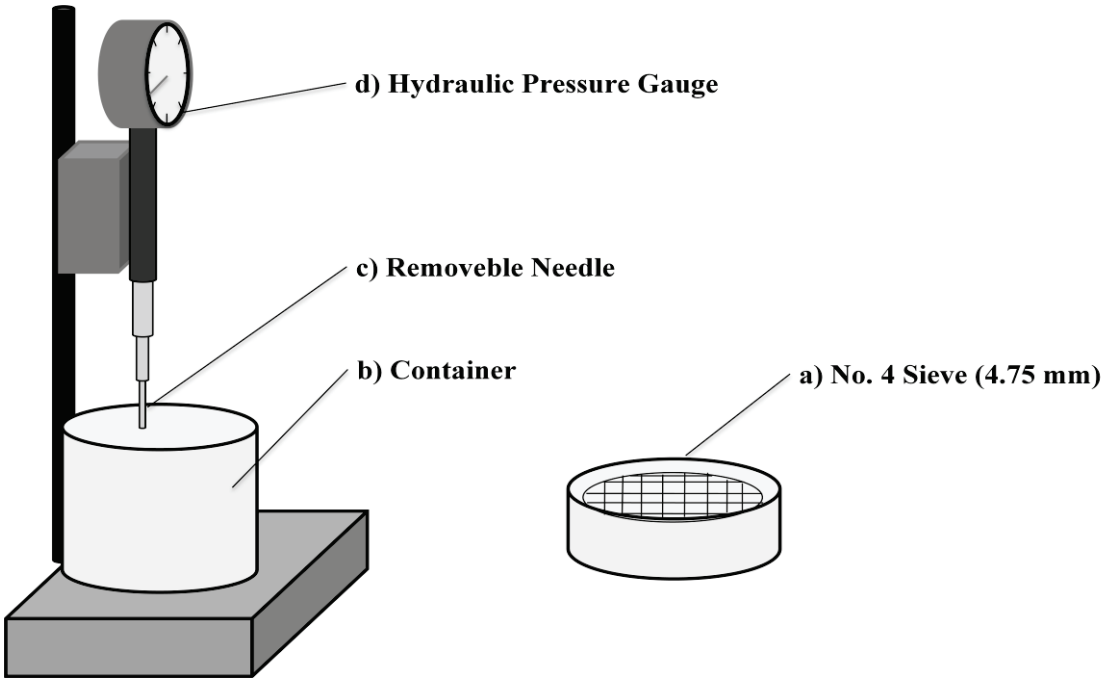

Figure 3.3. Instruments needed for initial time of set

3.2.1.2 Test setup

To set up the time of set test, the mortar fraction of the concrete is removed by passing it through a sieve No. 4. The mortar is sieved from the concrete mixture instead of using prepared mortar to simulate the mortar fraction of the concrete. It has been shown that the initial and final setting times may increase when using the prepared mortar (ASTM C 403, 2008). Finally, the sieved mortar is placed into container with diameter of 152 mm (6 in).

3.2.1.3 Procedure

After completing the test set up, as described in the Section 3.2.1.2, the force required to penetrate the needle 25.4 mm (1 in.) into the mortar is measured using the hydraulic pressure gauge. This process is repeated at regular intervals, and a curve of penetration resistance versus time is plotted. The initial time of set is defined as the time which the penetration resistance is 3.5 MPa (500 psi). The point 3.5 MPa corresponds approximately to the point at which the concrete will no longer become plastic under vibration (Mindess, Young, & Darwin, 2003).

3.2.2 Compressive Strength

The objective of this test is to measure the compressive strength of concrete mixes by applying axial load. The compressive strength test is primarily used to determine if the concrete mix meets the specified target strength. Since concrete has very little tensile strength, it is mainly used in a compressive mode, and therefore the compressive strength is very important in engineering practice. Furthermore, the compressive strength of concrete mixes increases with increasing curing period. It is therefore important to test the concrete mix at different days to capture the strength development. Compressive strength was measured according to ASTM C 39. The strength of the concrete mixtures was determined at 7, 14, 28, 56, 84, 112 and 168 days. The entire compressive test was performed at Lafarge North America except the 112 day test, which was performed at University of Washington.

3.2.2.1 Instrumentation

Figure 3.4 shows the apparatus needed to determine the compressive strength. It is very difficult to make sure that the ends of the specimens are exactly perpendicular to direction of applied load. To ensure loading with no eccentricity, a pivoting head (Figure 3.4a) is used. A safety door (Figure 3.4d) is kept closed during testing to prevent fly away particles. The apparatus is connected to a hydraulic testing machine that records only the maximum load that is applied.

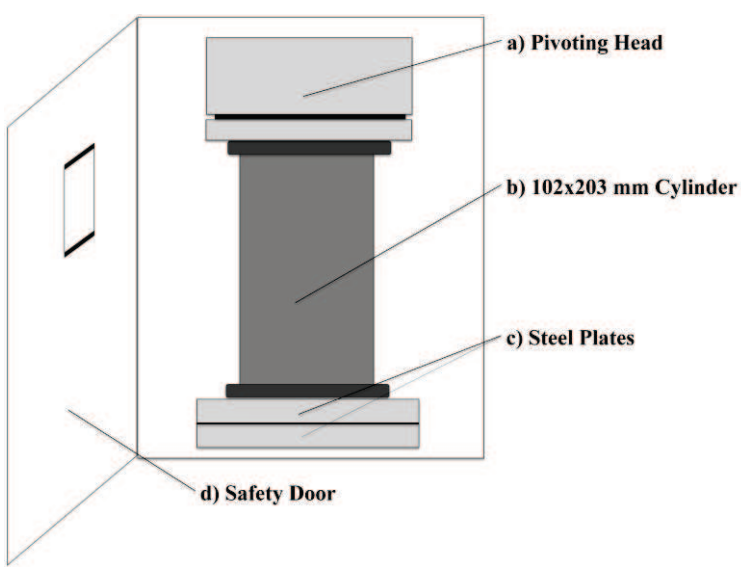

Figure 3.4. Compressive test setup

3.2.2.2 Test Setup

To set up the compressive test, 101.6 x 203.2 mm (4x8 in.) cylinder (Figure 3.4b) is placed in the apparatus (Figure 3.5). Steel plates (Figure 3.4c) are placed under the cylinder to elevate it, since the apparatus has limited axial displacement capacity.

Figure 3.5. Photograph of the compressive strength set up

3.2.2.3 Procedure

After completing the test set up, as described in the Section 3.2.2.1, the apparatus is turned on and the load reader is set to zero. The apparatus is set to record the peak load. Figure 3.6 and Figure 3.7 show photographs of the apparatus at Lafarge North America and University of Washington, respectively. The cylinder is then loaded to failure, at a rate of 0.25 +/- 0.05 MPa/s. Compression strength of the specimens is determined with equation (3.1):

$$f_c' = \frac{P_u}{A_c} \tag{3.1}$$

where f'_c is the compressive strength (MPa), P_u is the maximum sustained load (kN) and A_c is the original cross-sectional area of the specimen (mm^2).

At each age, three cylinders were tested for compressive strength. The strength of the mix was defined as average value of the three cylinders.

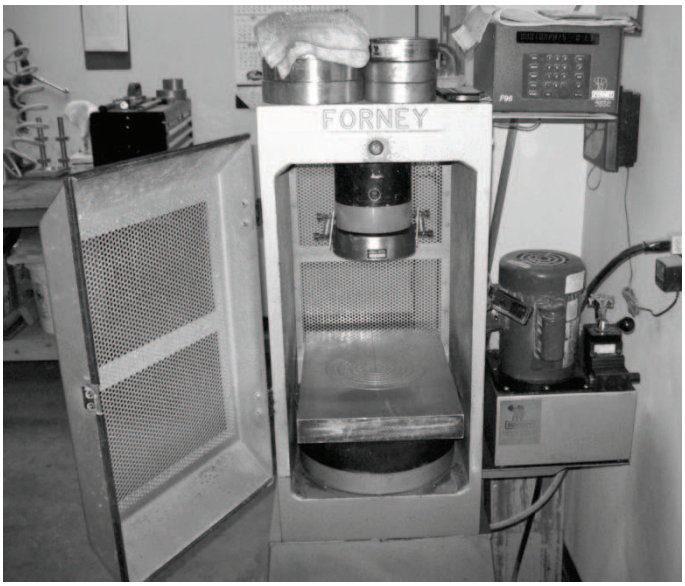

Figure 3.6. Photograph of the compressive apparatus at Lafarge North America

Figure 3.7. Photograph of the compressive test apparatus at University of Washington

3.2.3 Compressive Modulus of Elasticity

The objective of this test is to measure the elastic modulus of concrete mixes. Concrete is a highly complex heterogeneous material whose response to stress depends not only on the response of the individual components but also upon interaction between those components (Mindess, Young, & Darwin, 2003). This complexity leads to non-linear stress-strain response. However, to calculate the stiffness or expected deflection of structural concrete

members, it is necessary to obtain some estimation of the modulus of elasticity. The elastic modulus was measured according to ASTM C 469. The elastic modulus of the concrete mixtures was determined at age 7, 14, 28, 56 and 112 days.

3.2.3.1 Instrumentation

Figure 3.8 shows the setup of the compressometer that was used in the elastic modulus test. The compressometer consists of three yokes. The end yokes are rigidly attached to the cylinder (Figure 3.8f) each with 3 fasteners (Figure 3.8a). The middle yoke (Figure 3.8c) is attached at two diametrically opposite points (Figure 3.8g) so that the yoke is free to rotate. At one position on the circumference of the rotating yoke, a pivot rod (Figure 3.8b) is attached to maintain a constant distance between the two end yokes. On the opposite side from the rod on the circumference of the rotating yoke, a linear variable differential transformer (LVDT) (Figure 3.8e) is placed to read the displacement due to rotation of the middle yoke about the pivot rod. Figure 3.9 show the diagram of the displacement of the compressometer. Thus, when $e_g = e_r$ the effective gauge length doubles due to the rotation of the yoke. Two diametrically opposite steel plates (Figure 3.8d) were used to keep the effective gauge length of the compressometer at constant 127 mm (5 in.) to set up the test, but were removed during loading.

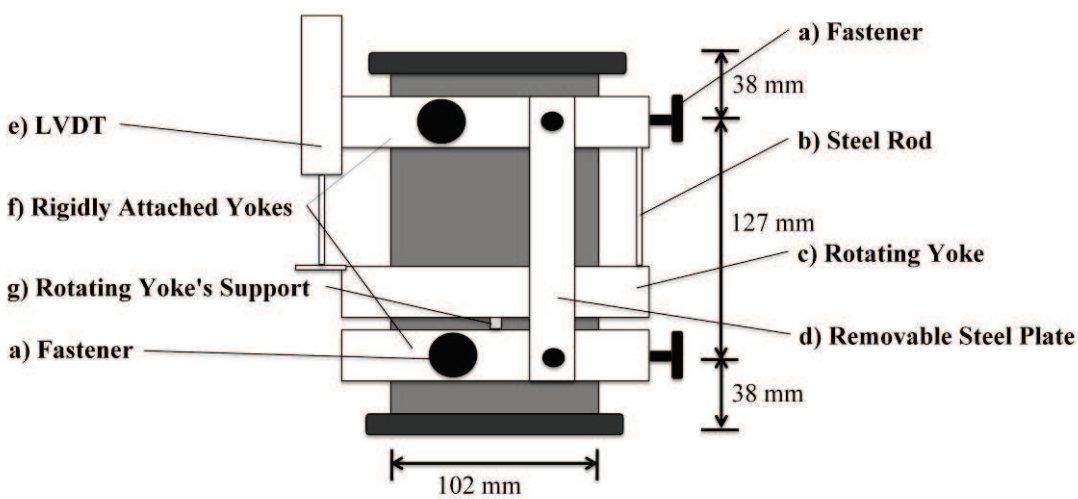

Figure 3.8. Compressometer

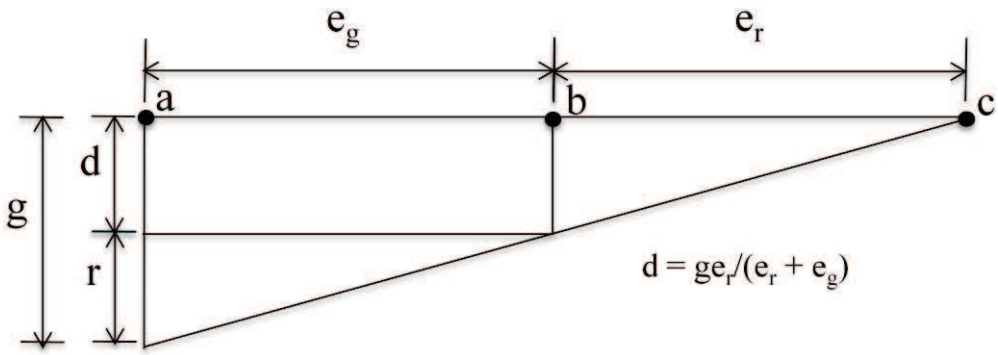

d) Displacement due to specimen deformation
r) Displacement due to rotation of the yoke about the pivot rod
a) Location of gauge
b) Support point of the rotating yoke
c) Location of pivot rod
g) Gauge reading
e_g) Perpendicular distance between points a) and b)
e_r) Perpendicular distance between points b) and c)

Figure 3.9. Diagram of displacement

The modulus of elasticity test was carried out in a hydraulic operated machine (Baldwin 300 kip machine, Figure 3.10). The Baldwin 300 kip machine and LVDT needs to be connected to computer so the stress and corresponding strain can be recorded. All the data was recorded by using Laboratory Virtual Instrumentation Engineering Workbench (LabVIEW) program

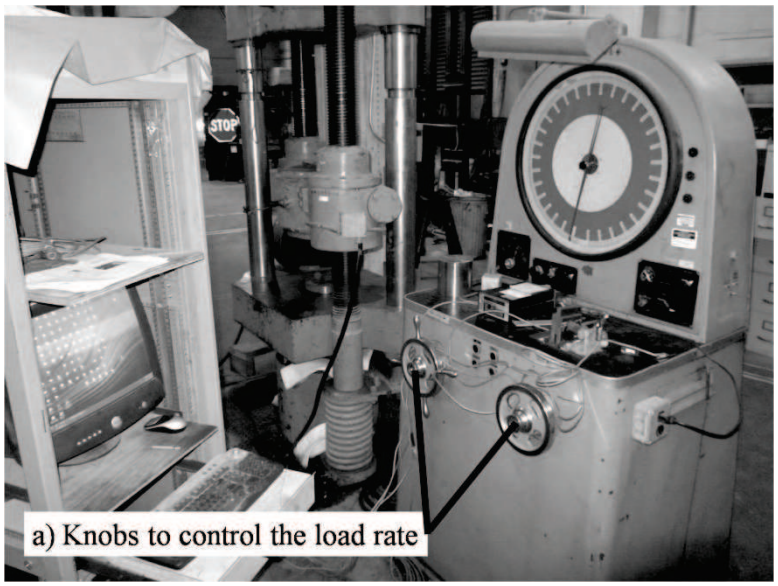

Figure 3.10. Photograph of Baldwin 300kip machine

3.2.3.2 Test Setup

To set up the elastic modulus test, 101.6 x 203.2 mm (4x8 in.) cylinder is placed in the compressometer (Figure 3.11). The compressometer was attached on the cylinder so that the space above and below the compressometer would be approximately equal. The cylinder needs to be in the center of the compressometer when it is attached. After attaching the compressometer on the cylinder, the cylinder is concentrically placed in the Baldwin 300 kip machine. A steel cylinder was placed on top of the concrete cylinder to prevent the LVDT from getting damaged during loading. Finally, the steel plates (Figure 3.8d) on the compressometer were removed

Figure 3.11. Photograph of the elastic modulus setup

3.2.3.3 Procedure

After completing the test set up, as described in the Section 3.2.3.2, the Baldwin 300 kip machine is turned on and both the load and displacement reader are set to zero in LabVIEW. The cylinder is then loaded to 40% of its ultimate strength, at a rate of 0.241 +/- 0.034MPa/s. The rate of loading is controlled by turning two knobs; one to unload and one to load (Figure 3.10a). Each specimen was loaded and unloaded three times. Only the last two cycles where

used for determining the elastic modulus, the first cycle is primarily to properly seat the test fixturing. The chord modulus of elasticity is calculated using equation (3.2):

$$E = \frac{S_1 - S_2}{\varepsilon_2 - 0.000050} \tag{3.2}$$

where E is the chord modulus of elasticity (MPa), S_2 is stress corresponding to 40% of ultimate load (MPa), S_1 is stress corresponding to a longitudinal strain ε_1 of 50 millionths (MPa) and ε_2 is longitudinal strain produced by stress S_2. Figure 3.12 shows schematic figure where the points are located on a typical concrete stress-strain diagram.

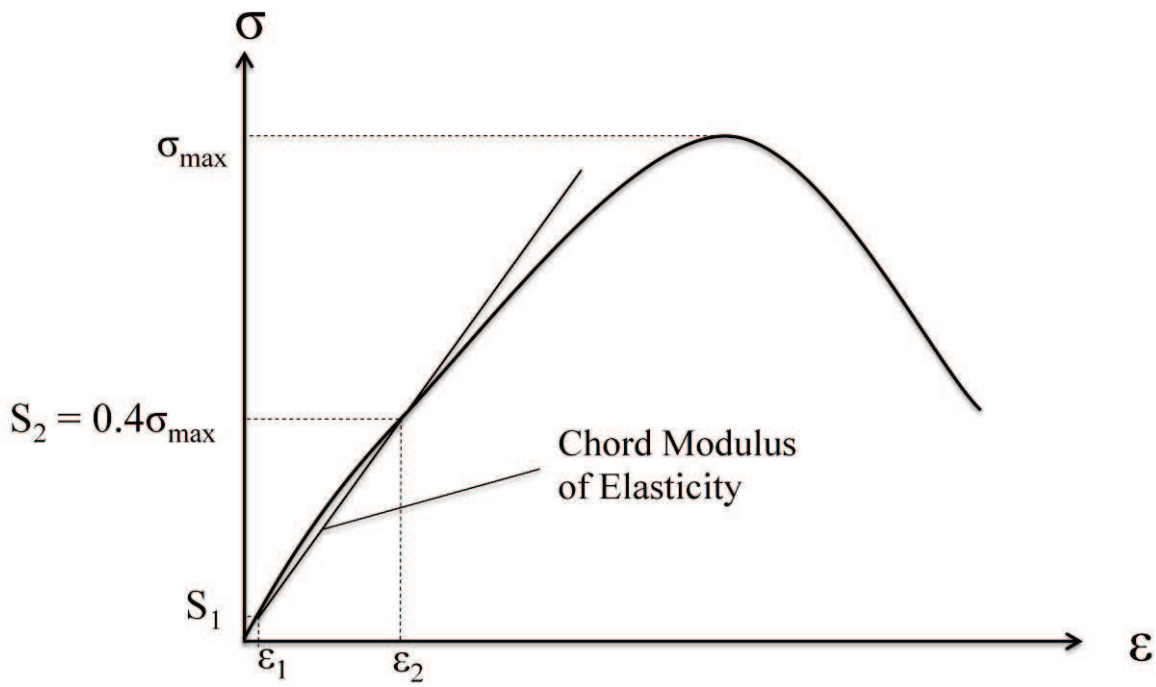

Figure 3.12. Typical stress-strain diagram for concrete and the points needed to determine the chord modulus of elasticity

For days 7 and 14 only two cylinders were used for determination of elastic modulus. Three cylinders were used to determine the elastic modulus of cylinders that were cured for 28 days and longer. The same three cylinders were used for testing at day 28, 56 and 168 since they were only loaded up to 40% of maximum strength (no micro cracks should form). Two sets of separate cylinders were used at day 7 and 14, since it was believed that they had not

developed enough strength to be loaded again even though the applied load was only 40% of maximum strength. The same three cylinders were used at day 28, 56 and 168 to get a better view of the elastic modulus development.

3.2.4 Creep and Shrinkage Monitoring

The objective of this test is to measure the creep and drying shrinkage strains of concrete mixes. Creep is a time-dependent deformation under a load and drying shrinkage occurs in a hardened concrete when free water evaporates. Creep and shrinkage strains can affect the serviceability and durability of structures. Creep strains increase the long-term deflections. In composite structures, too much creep strain can result such that the system is no longer acting together. In prestressed concrete elements, creep strain reduces prestress and causes redistribution of internal forces. However, concrete with high volume of SCM is not applicable in prestressed elements, since such elements require high early strength. Shrinkage can cause warping of slabs on grade due to differential drying and increased deflections of non-symmetrically reinforced concrete elements. Creep and shrinkage was measured according to ASTM C 512 after 7, 14 and 28 days of curing.

3.2.4.1 Instrumentation

Figure 3.13 shows the creep rig test setup. The rig is designed to apply a constant load to a series of cylinders. The creep rig consisted of 3 steel plates; a top plate (Figure 3.13a), a middle plate (Figure 3.13e) and a bottom plate (Figure 3.13g). The dimension of the top plate was 381x381x64 mm (15x15x2.5 in.) and the dimensions of the middle and bottom plate were 508x508x64 mm (20x20x2.5 in.). Four threaded 25-mm (1 in.) diameter A449 steel rods (Figure 3.13c) with an axial stiffness of approximately 175 kN/mm (1000 k/in) attached the steel plates to one another.

Each rig had 4 coil springs (Figure 3.13f) to maintain a nearly constant load as the specimens shortened. Section A-A in Figure 3.13 shows the layout of the springs, the springs were concentrically placed around 26 mm holes (Figure 3.13l) that accommodate steel rods; to ensure even distribution of the spring stiffness. Each spring had a maximum compression of 51 mm (2 in.), the outside-diameter of each spring was 117 mm (4-5/8 in.) and they had a

stiffness of 1.14 kN/mm (6.5 k/in). Therefore the total stiffness of the four springs was 4.56 kN/mm (26 k/in).

Four C 127 x 0.098 mm steel supports (Figure 3.13k) were used to elevate the creep rigs to accommodate a hydraulic jack under the rigs. A single 267-kN (60-kip) jack (Figure 3.13i) was used to apply the prescribed stress to the concrete cylinders in the creep rigs. A jacking plate (Figure 3.13j) with four 356 mm (14 in.) long threaded 25-mm diameter A449 steel rods and couplers (Figure 3.13h) was used elevate the jack. The dimension of the jacking plate was 371x358x51 mm (14.5x14x2 in). An electric lift was used to move the jack and the plate between rigs.

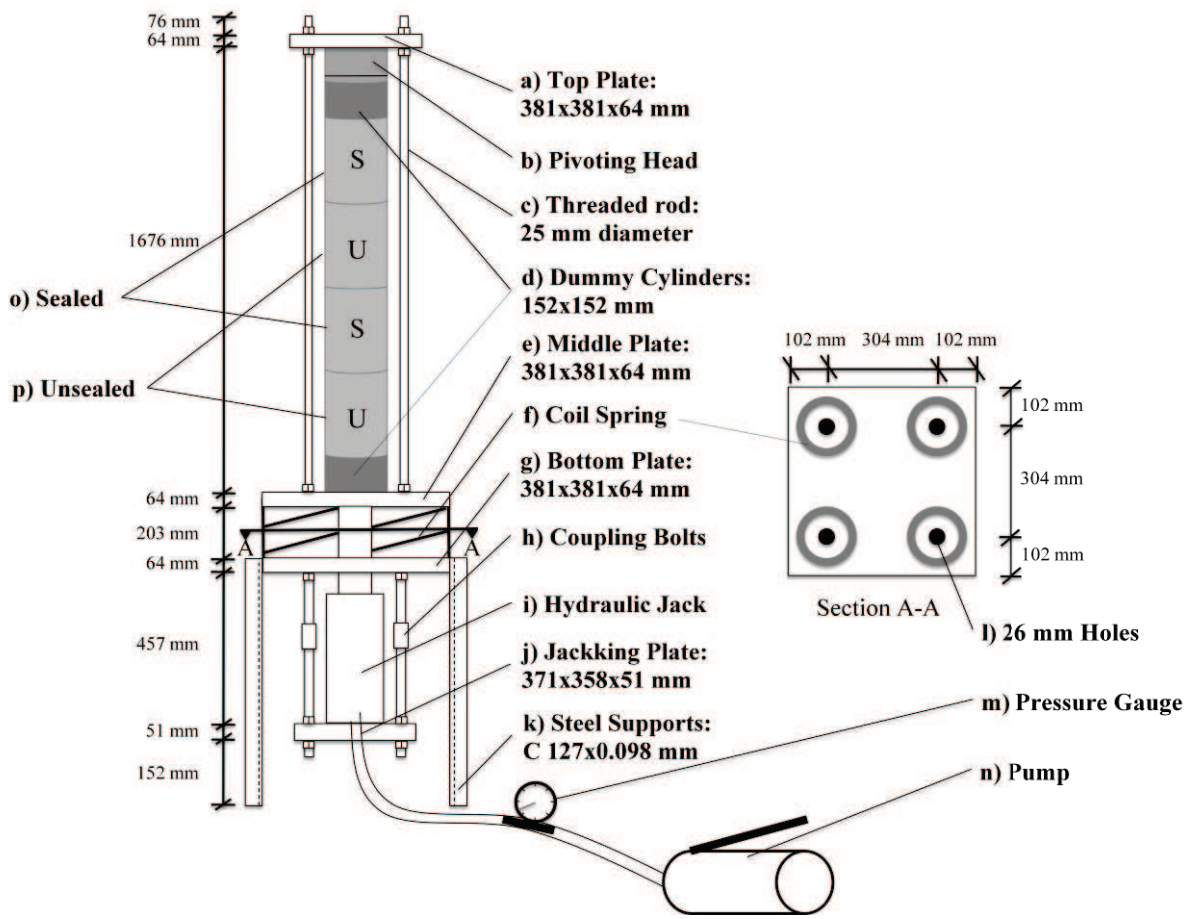

Figure 3.13. Creep rig

Figure 3.14 shows the detachable mechanical strain gauge (Whittemore Strain Gauge) that was used to measure the deformation of the specimens over time. The mechanical gauge reads increments of 2.54 μm (0.0001 in.) and has displacement capacity of 2.54 mm (0.1 in.).

The mechanical gauge has two dial gauges. The larger dial gauge (Figure 3.14a) has scale from 0 to 100 in. and the smaller dial gauge (Figure 3.14b) has scale from 0 to 900 in. Targets (Figure 3.14f) were constructed to be glued on concrete cylinders to set gauge length that could change over time. Targets were designed to have rivets to accommodate the conical steel studs (Figure 3.14c) on the mechanical gauge

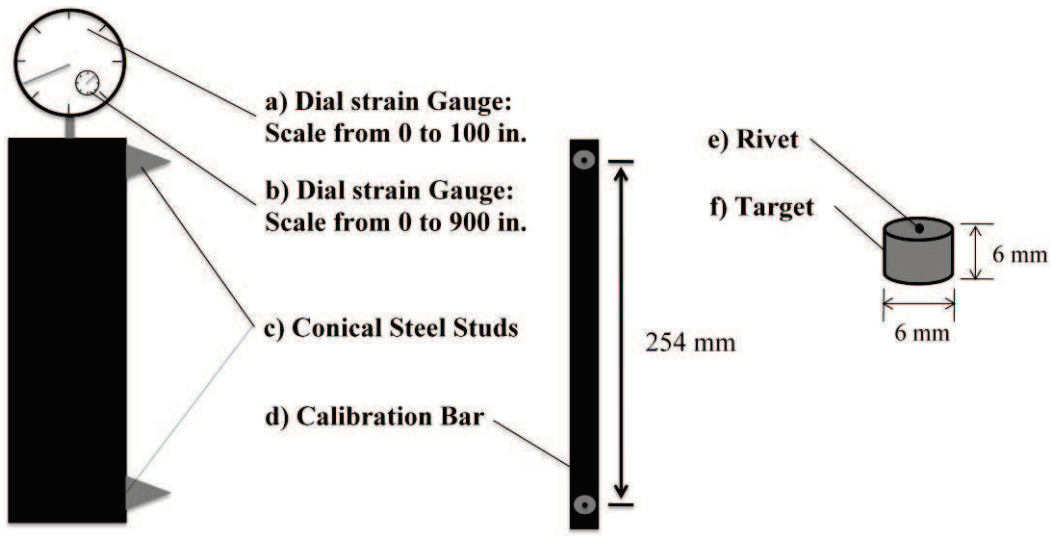

Figure 3.14. Whittemore strain gauge and target

3.2.4.2 Test Setup

A total of eight 152.4 x 304.8 mm (6x12 in.) cylinders were used in the creep and shrinkage test. The specimens were prepared the day before testing so the epoxy (System Three Epoxy) would be fully cured at day of testing. The required gauge length was 254 mm (10 in.), since the mechanical gauge had displacement capacity limited to only 2.54 mm (0.1 in.). The cylinders were instrumented with four sets of targets located diametrically at opposite sides of the specimens. Figure 3.15 and Figure 3.16 shows layout of the targets. The targets were spaced 254 mm (10 in.) apart. High viscous epoxy (Loctite Quick Set Epoxy) was used to glue the targets on the cylinders.

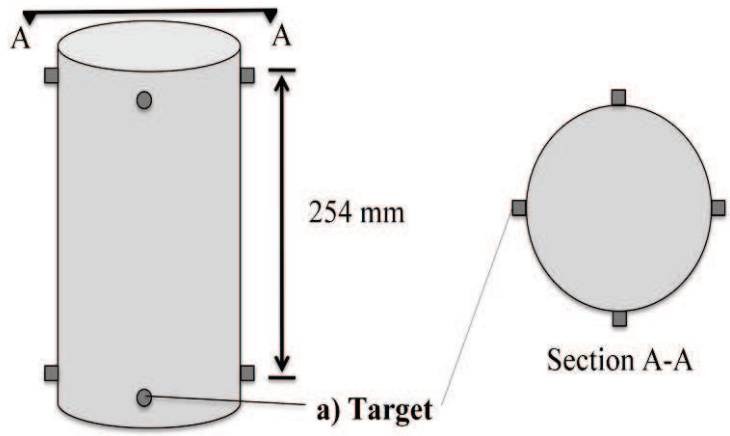

Figure 3.15. Target layout

Figure 3.16. Photograph of the target layout

After gluing the targets on the cylinders, 4 of the 8 cylinders were sealed with two layers of low viscous clear coat epoxy (System Three Epoxy). The epoxy needs to cure for 8 hours between layers. Low viscous epoxy was used to make the sealing of the cylinder easier. The second layer was allowed to cure for 24 hours before the test began.

On the day of testing 4 cylinders: 2 sealed and 2 unsealed, are stacked in the creep rig. Figure 3.17 shows a photograph of the creep rigs with all of the cylinders installed. The cylinders are stacked in order unsealed (U), sealed (S), unsealed (U), sealed (S) as shown in Figure 3.13. Before stacking the cylinders in the rig, 152.4x152.4 mm (6x6 in.) a dummy cylinder (Figure 3.13d) was placed between the steel bearing plates and the test specimens at each end of the stack so the tested cylinders would not touch the steel plates. A pivoting head (Figure

3.13b) was placed on the top of the stack to ensure loading with no eccentricity to the stack. Finally, the top plate (Figure 3.13a) was lowered until the plate was sitting on the stack. Then, the nuts on both sides of the top plate were incrementally hand tightened so the connection between the rod and the plate would be fixed. Since the connection is fixed, it provides increase bending resistance of the rods. The nuts below the bottom plate maintained the tension in the rods throughout the test. The nuts above the middle plate were kept lose; their purpose was to prevent the coil springs (Figure 3.13f) from extending in the event of unexpected cylinder failure.

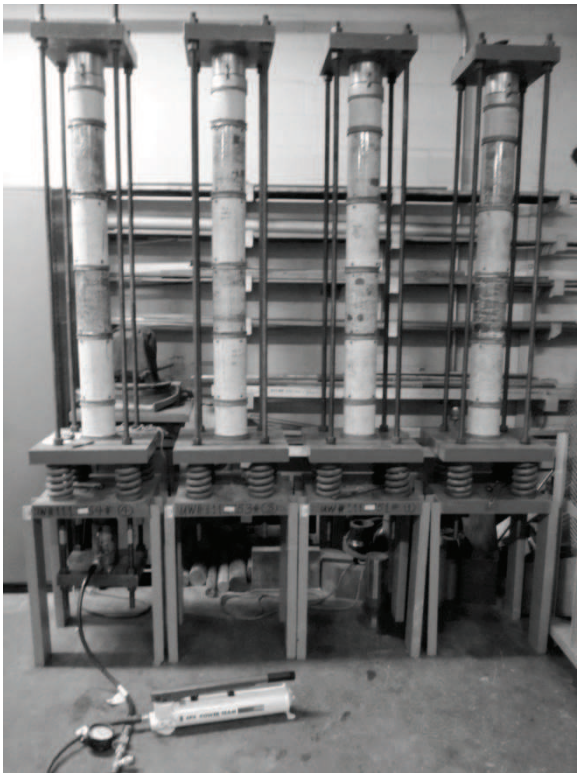

Figure 3.17. Photograph of the creep rigs with the installed cylinders

The other four cylinders, 2 sealed and 2 unsealed, were placed on a table so they would be at a similar height as the loaded cylinders. The cylinders on the table remained unloaded throughout the test and were used to determine the shrinkage strain. Figure 3.18 shows photograph of the shrinkage cylinders.

Figure 3.18. Photograph of the shrinkage cylinders

An environmentally controlled room was not available for the creep test. Instead, the creep rigs were placed in a region away from windows and doors, to minimize the change in temperature and humidity. The ambient temperature and humidity change during the test is graphically shown in Appendix A.

3.2.4.3 Procedure

After completing the test set up, as described in the Section 3.2.4.2, the rigs were loaded. To apply stress to the cylinders in the creep rig, the electric lift was wheeled under the rig, the lift was raised, the four rods of the jacking plate were connected to the rig rods using the couplers, the elevator was lowered, and a pump (Figure 3.13n) fitted with a pressure gauge (Figure 3.13i) connected to the jack. The pump was pumped until the correct load was reached and then the nuts below the bottom plate were hand tightened.

To take the strain reading, the two conical steel studs (Figure 3.14c) of the mechanical gauge are placed in the rivets of the target. Before taking a set of measurements, the mechanical gauge is calibrated with a mild steel calibration bar (Figure 3.14d). The calibration bar has the length 254 mm (10 in.) at 20°C, so if the ambient temperature is either higher or lower than 20°C the length must be corrected using the thermal expansion coefficient for mild steel. The correct length of the calibration bar can be evaluated using equations (3.3):

$$L_c = 254(1 + \Delta T \alpha_L) \tag{3.3}$$

where L_c is the corrected length of the calibration bar (mm), ΔT is the difference of ambient temperature from 20°C (°C) and α_L is the thermal expansion coefficient for mild steel and is equal to 0.0000126 1/°C. Equation (3.4) is used to find the distance between the targets relative to the calibration bar:

$$L_T = \left(\frac{\varepsilon_T - \varepsilon_c}{10000}\right) 25.4(mm) + L_c \tag{3.4}$$

where L_T is the distance between the targets (mm), ε_T is the strain value between the targets using the mechanical gauge (mm/mm) and ε_c is the strain value of the calibration bar using the mechanical gauge (mm/mm). Figure 3.19 shows photograph of the mechanical gauge used to measure the strains.

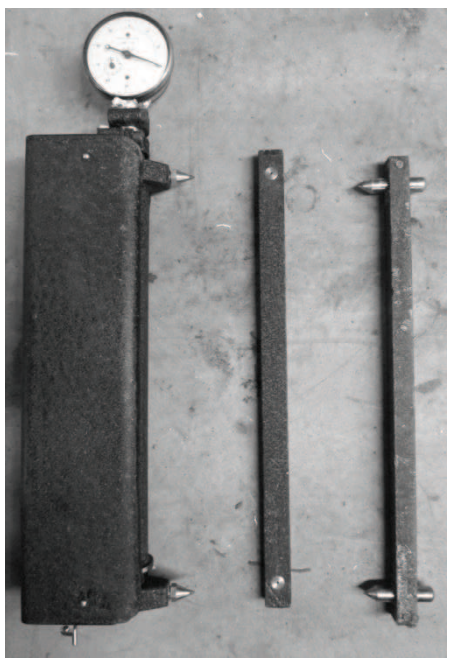

Figure 3.19. Photograph of the Whittemore strain gauge

Strain readings were taken immediately before and immediately after initial loading, and then again 2 hours later. Strain readings were taken daily for one week, then weekly for one month and then monthly. Before taking each strain reading, the applied load on the rig was adjusted with the hydraulic jack to the prescribe load. Strain readings on the shrinkage specimens were taken on the same schedule as the specimens placed in the creep rig.

Strain for each cylinder was obtained by taking the average of the four sides. Total creep was calculated with the following equation:

$$\varepsilon_{c,T} = \varepsilon_{l,UNS} - \varepsilon_{s,UNS} \quad \textbf{(3.5)}$$

where $\varepsilon_{c,T}$ is the total creep strain, $\varepsilon_{l,UNS}$ is the strain of the unsealed specimens under loading and $\varepsilon_{s,UNS}$ is the strain of the unsealed shrinkage specimens.

Similarly, basic creep was obtained with the following equation:

$$\varepsilon_{c,B} = \varepsilon_{l,S} - \varepsilon_{s,S} \quad \textbf{(3.6)}$$

where $\varepsilon_{c,B}$ is the basic creep strain, $\varepsilon_{l,S}$ is the strain of the sealed specimens under loading and $\varepsilon_{s,S}$ is the strain of the sealed shrinkage specimens.

Finally, drying creep was obtained with the following equation:

$$\varepsilon_{c,D} = \varepsilon_{c,T} - \varepsilon_{c,B} \quad \textbf{(3.7)}$$

where $\varepsilon_{c,D}$ is the drying creep strain

3.2.5 Active Silica

The objective of this test is to determine the quantity of the silica of the SCM that is reactive. The active silica plays a major role in the pozzolanic reaction and increases the C-S-H content in the binder. Thus, it is hypothesized that the active silica content would be a strong indicator of the SCM contribution to concrete strength development. The active silica was determined according to the European Standard EN 196-2. Active silica test was performed on all of the SCMs used in Phase I.

3.2.5.1 Instrumentation

Figure 3.20 shows the apparatus needed to evaporate the solution. Samples were evaporated in a porcelain dish (Figure 3.20b). A glass-stirring rod (Figure 3.20a) was used to stir

materials together and the flat end of the rod is used to crush the particles as needed to ensure decomposition was complete. The porcelain dish was surrounded by sand to ensure even heating. This assembly rested on a hot plate (Figure 3.20c) to evaporate the solution to dryness.

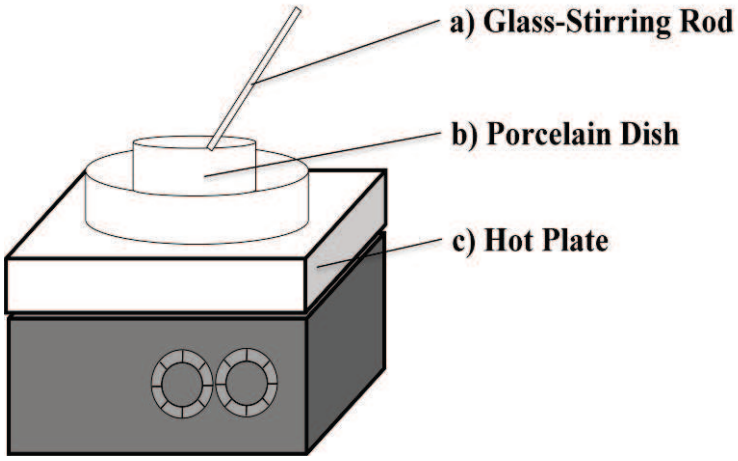

Figure 3.20. Hot plate

Figure 3.21 shows the test apparatus used to filter the solution. A funnel (Figure 3.21a) and filter paper is used to separate out the residue from the solution. A vacuum (Figure 3.21c) was used to assist with the filtering process. A 1000 ml flask (Figure 3.21b) captured the filtering liquid. Figure 3.22 shows the apparatus used to reflux the solution.

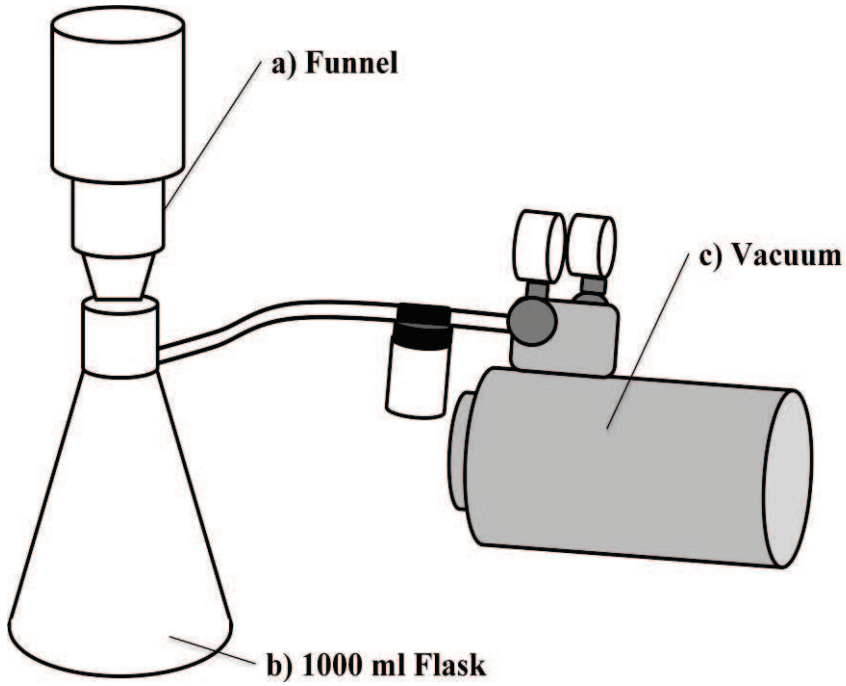

Figure 3.21. Filter apparatus

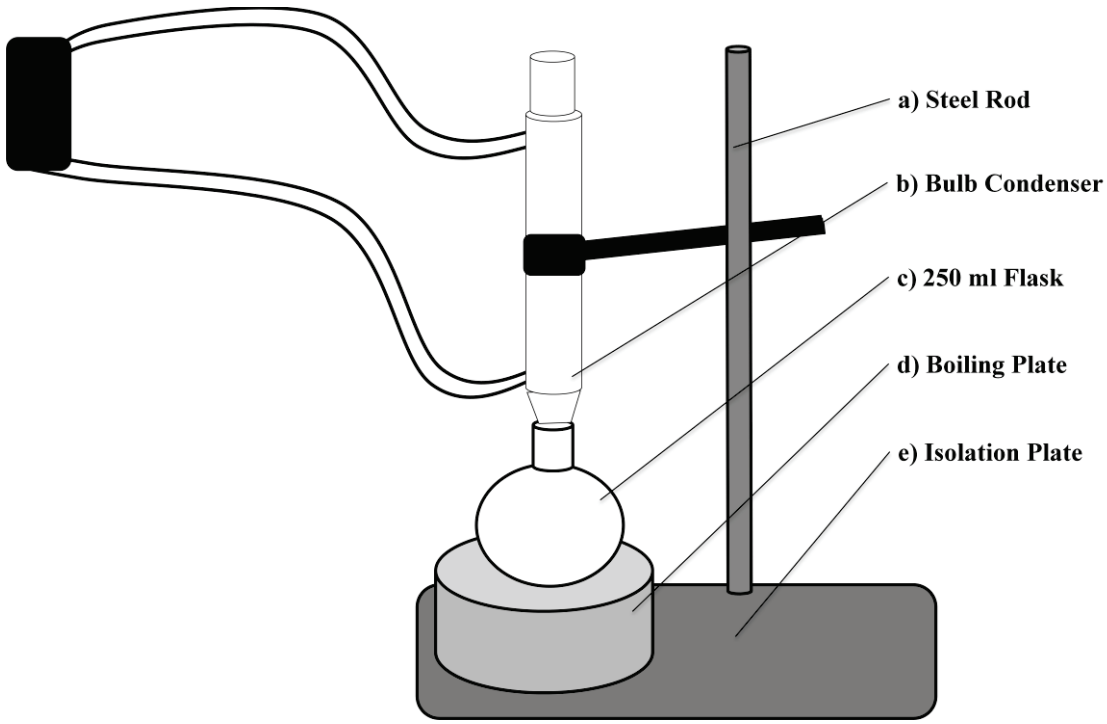

Figure 3.22. Reflux apparatus

3.2.5.2 Test Setup

First 1.00 ± 0.05 g of material is weighed (m_1) and placed with 25 ml of water in a porcelain dish. The two are mixed together by using a glass-stirring rod. Forty (40) ml of concentrated

hydrochloric acid was added. The porcelain dish was then placed on the hot plate (Figure 3.23).

Figure 3.23. Photograph of the evaporation setup

3.2.5.3 Procedure

After completing the test set up, as described in the Section 3.2.5.2, the solution in the porcelain dish was gently heated and the sample crushed with the flattened end of the glass-stirring rod until decomposition was complete. The solution was evaporated to dryness using the hot plate. This operation was performed three times with two additional 20 ml concentrated hydrochloric acid solutions added after evaporation to dryness.

The residue from the third evaporation was then treated with 100 ml of 25% hydrochloric acid. The solution was then reheated, filtered on a medium filter paper and washed with almost boiling water until it was free from chloride ions, and tested using chloride test strips (Chlroide QuanTab®, range 30-600 mg/l, 10-20 ppm detection).

The filter paper and its contents were then transferred to a 250 ml conical flask and 100 ml of potassium hydroxide was added. The solution was then allowed to stand for at least 16 hours at room temperature and then boiled under reflux for a minimum of 4 hours (Figure 3.24).

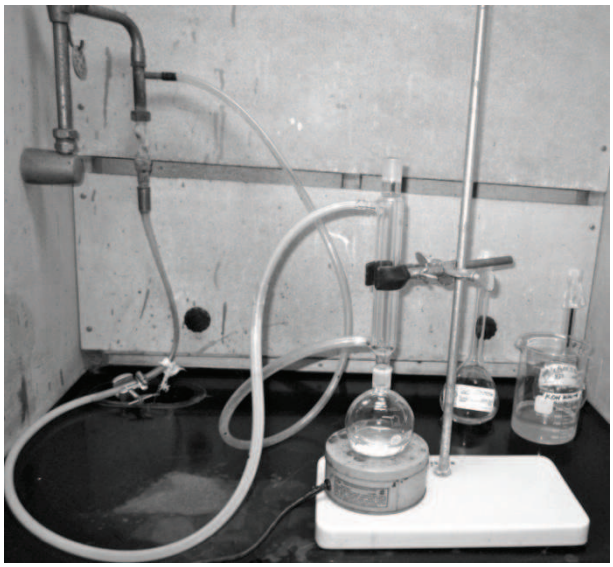

Figure 3.24. Photograph of the reflux setup

The solution was then filtered on a medium filter paper and washed with water with 10% hydrochloric acid solution and finally with almost boiling water until it was free from chloride ions, tested using chloride test strips. Then the solution was ignited at (950 ± 25) °C for at least 30 minutes, achieving a constant mass (m_2) (Figure 3.25).

Figure 3.25. Photograph of the filter setup

According to European Standard EN 197-1, active silica is defined as the fraction of the silicon dioxide that is soluble after treatment with hydrochloric acid and with boiling potassium hydroxide solution. Therefore, active silica is defined as the ratio of the difference

of amount of total silica and the silica present in the insoluble residue to with the total amount of silica. The total amount of silica was determined with XRF analysis (Table 3.1).

The insoluble residue was determined by the following equation:

$$IR = 100\frac{m_2}{m_1} \tag{3.8}$$

where *IR* is the insoluble residue, m_1 is the original mass (g) and m_2 is the mass of the ignited insoluble residue (g). The active silica was determined by the following equation:

$$\gamma_s = \frac{S - IR}{S} \tag{3.9}$$

where γ_s is the active silica fraction, *IR* is the insoluble residue (%) and *S* is the total amount of silica (%) determined by XRF analysis (Table 3.1).

Chapter 4: Measured Engineering Response of High Volume SCM Concrete

This chapter presents the results of the material testing program. The tests were performed in two phases. The primary objective of the first Phase was to study a broad spectrum of replacement levels of selected SCMs and compressive strength development of SCC. The concrete mixes of Phase I had water-binder-ratio (w/b) of 0.35. Compressive strength, initial time of set and air content was measured. Table 4.1 shows an overview the mixture proportions and the name convention of Phase I.

The second Phase focused on higher replacement levels (≥ 60 %) and examined both binary and ternary mixes. Two of the most promising SCMs from Phase I were used in the second Phase. The concrete mixes of Phase II had water-binder-ratio (w/b) of 0.40. In the second Phase elastic modulus, creep and shrinkage response as well as compressive strength was measured. Table 4.2 shows an overview the mixture proportions and the name convention of Phase II.

Table 4.1. Mixture proportions and name convention of Phase I

Mix name	%	C/(S+A)[1]	Cement (kg/m^3)	SCM (kg/m^3)	Water (kg/m^3)	w/b	SP[2] (mL/m^3)
Base I	0	2.66	474	0	168	0.35	169
20% Boardman FA–I	20	1.98	379	95	168	0.35	169
40% Boardman FA–I	40	1.49	284	190	168	0.35	169
60% Boardman FA–I	60	1.12	190	284	168	0.35	169
80% Boardman FA–I	80	0.83	95	379	168	0.35	169
100% Boardman FA–I	100	0.59	0	474	168	0.35	169
20% Centralia FA–I	20	1.66	379	95	168	0.35	169
40% Centralia FA–I	40	1.07	284	190	168	0.35	169
60% Centralia FA–I	60	0.68	190	284	168	0.35	169
80% Centralia FA–I	80	0.41	95	379	168	0.35	169
100% Centralia FA–I	100	0.20	0	474	168	0.35	169
20% Seattle SL–I	20	2.06	379	95	168	0.35	169
40% Seattle SL–I	40	1.64	284	190	168	0.35	169
60% Seattle SL–I	60	1.33	190	284	168	0.35	169
80% Seattle SL–I	80	1.09	95	379	168	0.35	169
100% Seattle SL–I	100	0.90	0	474	168	0.35	169
20% St. Mary's SL–I	20	2.05	379	95	168	0.35	169
40% St. Mary's SL–I	40	1.61	284	190	168	0.35	169
60% St. Mary's SL–I	60	1.28	190	284	168	0.35	169
80% St. Mary's SL–I	80	1.02	95	379	168	0.35	169
100% St. Mary's SL–I	100	0.82	0	474	168	0.35	169

[1]$CaO/(SiO_2+Al_2O_3)$ of total binder, [2]Superplasticizer

Table 4.2. Mixture proportions and name convention of Phase II

Mix name	%	C/(S+A)[1]	Cement (kg/m^3)	SCM (kg/m^3)	Water (kg/m^3)	w/b	SP[2] (mL/m^3)
Base II	0	2.53	415	0	168	0.40	230
60% Boardman FA–II	60	1.02	166	249	168	0.40	230
80% Boardman FA–II	80	0.75	83	332	168	0.40	230
90% Boardman FA–II	90	0.63	42	374	168	0.40	230
60% Seattle SL–II	60	1.50	166	249	168	0.40	230
80% Seattle SL–II	80	1.28	83	332	168	0.40	230
90% Seattle SL–II	90	1.18	42	374	168	0.40	230
60% 25FA-75SL–II	60	1.37	166	249	168	0.40	230
80% 25FA-75SL–II	80	1.13	83	332	168	0.40	230
90% 25FA-75SL–II	90	1.03	42	374	168	0.40	230
60% 50FA-50SL–II	60	1.25	166	249	168	0.40	230
80% 50FA-50SL–II	80	0.99	83	332	168	0.40	230
90% 50FA-50SL–II	90	0.88	42	374	168	0.40	230
60% 75FA-25SL–II	60	1.13	166	249	168	0.40	230
80% 75FA-25SL–II	80	0.86	83	332	168	0.40	230
90% 75FA-25SL–II	90	0.75	42	374	168	0.40	230

[1]$CaO/(SiO_2+Al_2O_3)$ of total binder, [2]Superplasticizer

4.1 Initial Time of Set and Air Content

Table 4.3 presents the air content and initial time of set for the mixtures in Phase I. Air content of the mixes was determined using the pressure method (ASTM C 231, 2008). This method measures the change in volume of the concrete when subjected to a given pressure. This change in volume is assumed to be caused entirely by compression of air. The air content of the mixes varied from 1.5-1.9%, which is typical for SCCs. Figure 4.1, displays the time of set the SCM mixes as a function of percent replacement. The time of set is generally greater, or close to, the time of set of the base mix except for high replacement (60-100%) of the Boardman FA. For the high Boardman FA replacement, the setting time decreases rapidly. Decreased time of set at high replacement levels of Class C fly ash has been previously reported (Cross & Stephens, 2005; Naik & Singh, 1997). The rapid setting that is only associated with Class C fly ash (not Class F fly ash) results from the high amount of CaO. At higher cement replacement with Class C fly ash, the concentration of gypsum in the mixture is low, which results in reduced retarding characteristic of the mixture. Set retarding agents can be used to control the time of set as needed. In slag (a more regulated material); gypsum is usually grinded with the material to prevent this problem.

Table 4.3.The air content in the mixes and the initial time of set with fly ash (FA) or slag (SL) as cement replacement

	Replacement (%)	0	20	40	60	80	100
Boardman FA	Air Content (%)	1.80	1.60	1.70	1.70	1.50	1.50
	Time of set (min)	270	440	315	175	55	20
Centralia FA	Air Content (%)	1.80	1.50	1.50	1.87	1.90	1.50
	Time of set (min)	270	445	420	300	280	210
Seattle SL	Air Content (%)	1.80	1.60	1.90	1.80	1.60	1.60
	Time of set (min)	270	285	290	300	365	385
St. Mary's SL	Air Content (%)	1.80	1.80	1.50	1.87	1.70	1.40
	Time of set (min)	270	300	275	260	340	220

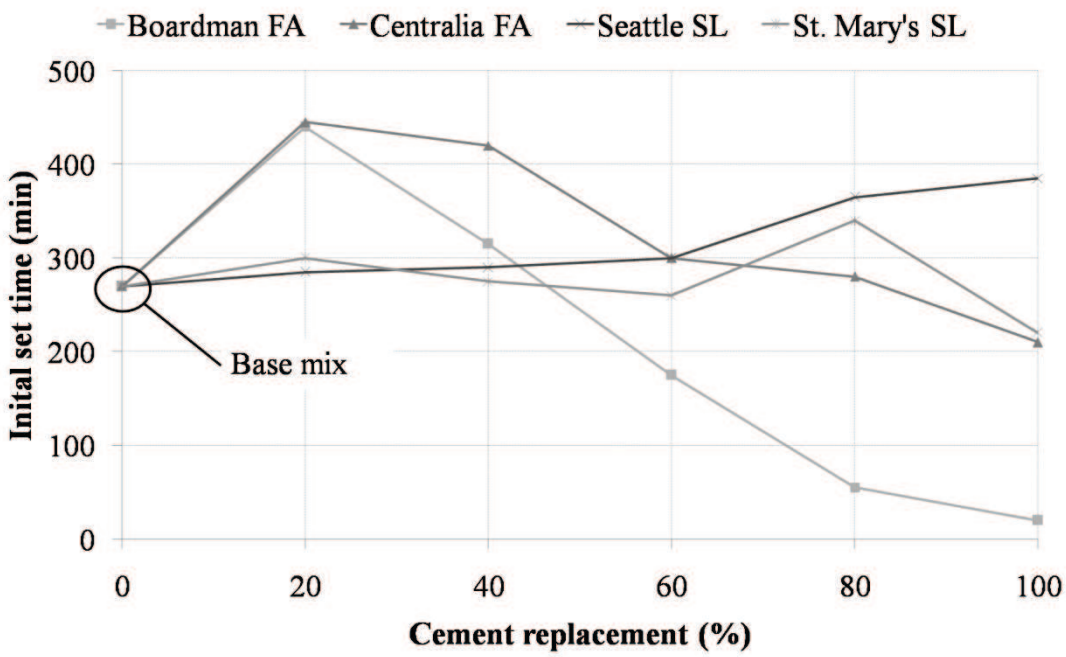

Figure 4.1. The initial time of set of the binary SCM mixes (w/b = 0.35).

4.2 Compressive Strength Behavior

Compressive strength was determined in two phases. The first Phase had 20 binary mixes and one base mix; the mixes had water-binder-ratio of 0.35. The second Phase had 6 binary mixes, 9 ternary mixes and one base mix; the mixes had w/b = 0.40. The compressive strength test was performed as described in Chapter 3, Section 3.2.2. Compressive strength data for each cylinder is presented in Appendix B.

4.2.1 Phase I

Table 4.4 summarizes the average compressive strength values and standard deviations, for all of the Phase I mixes (w/b = 0.35). Figure 4.2 through Figure 4.6, exhibit SCMs concrete

compressive strength gain compared with Base I, with cement replacement of 20%, 40%, 60%, 80% and 100%, respectively. Figure 4.7 shows the compressive strength at 56 days as function of cement replacement percentage. The following observations are made:

- The early-age strength (≤ 14 days) of all of the SL-concrete mixtures is less than the control mixture. The early-age strength is less for the FA-concrete mixtures than the control mixture, if the replacement is 40% or higher.
- At later ages (> 14 days), both SL and FA concrete mixtures with replacement of 60% or less have higher compressive strength than the control mixture.
- The lower early strength and higher long-term strength of the SCM mixes are a result of the delay in calcium-silicate-hydrate (C-S-H) formation since the pozzolanic reaction is the primary reaction for increased cement replacement (see Chapter 1 for details about pozzolanic and hydraulic reaction).
- The strength gain of the SCMs differs significantly for a lower (20-60%) and higher (80% and 100%) replacement levels.
- At 80% and 100% cement replacement levels, the strength performance depends more significantly on the SCM used. However, all of the SCM mixtures with replacement up to 80% have strengths over 45 MPa (~6500 psi) at 56 days, which is a desired strength for structural applications. Furthermore, the 80% Boardman FA has higher strength than the control mixture at 168 days.
- All of the SCM mixtures had very low strength for 100% replacement. This trend was expected since pozzolanic reaction depends on the available calcium hydroxide and at 100% replacement level, the amount of CaO in the binder is low, which results in less formation of calcium hydroxide. It was expected that the 100% Centralia FA mix would have the lowest strength since it has the lowest amount of CaO in the binder and thus, the least hydraulic reactivity.

Table 4.4. Compressive strength of SCC, with standard deviation, with fly ash (F) or slag (S) as cement replacement (w/b = 0.35)

Mix Name	Compressive Strength (MPA)					
	7 Day	14 Day	28 Day	56 Day	84 Day	168 Day
Base I	64.6±0.8	73.8±1.3	80±0.1	81.5±0.6	83.3±0.3	85.1±0.6
20% Boardman FA–I	64.6±0.5	70.7±0.8	80±0.1.0	88.6±0.3	91.9±1.0	94.1±0.6
40% Boardman FA–I	62.7±1.4	72.1±0.9	83.5±0.4	91.2±0.6	100.6±0.5	102.2±0.8
60% Boardman FA–I	50.7±0.6	63.3±0.7	75.7±0.5	86.6±0.4	91.3±0.8	94.7±0.4
80% Boardman FA–I	6.1±0.3	7.6±1.1	35.1±1.7	67.3±1.0	74.3±1.1	88.0±0.7
100% Boardman FA–I	4.8±0.2	6.4±0.1	7.0±0.3	8.9±0.2	10.6±0.4	18.3±0.5
20% Centralia FA–I	67.9±0.3	79.2±0.5	84.2±0.7	94.8±0.6	96.0±1.3	98.5±0.4
40% Centralia FA–I	65.3±0.2	70.5±0.6	87.0±0.6	94.9±0.6	96.7±0.5	97.6±0.4
60% Centralia FA–I	44.2±1.8	52.9±2.4	63.5±0.3	77.7±1.4	84.6±1.3	90.3±0.2
80% Centralia FA–I	19.0±0.5	21.0±0.7	32.0±0.7	45.6±0.8	49.2±1.1	65.6±0.6
100% Centralia FA–I	1.2±0.0	1.5±0.1	1.8±0.1	1.9±0.0	2.2±0.2	2.9±0.2
20% Seattle SL–I	53.2±0.7	61.8±6.3	71.8±1.8	80.8±0.2	82.5±0.5	86.6±0.6
40% Seattle SL–I	51.9±1.2	63.0±1.4	76.6±1.2	82.3±0.7	88.2±0.4	90.1±0.3
60% Seattle SL–I	43.7±1.2	55.2±0.4	66.4±0.4	77.3±0.9	86.1±0.8	90.3±0.7
80% Seattle SL–I	36.8±0.2	46.3±1.0	54.9±1.2	67.7±1.1	70.1±0.2	76.6±0.9
100% Seattle SL–I	12.1±0.7	16.6±0.3	20.4±0.2	26.6±0.6	32.3±0.9	38.0±0.8
20% St. Mary's SL–I	62.8±0.6	66±17.8	85.0±2.3	93.6±0.9	95.8±0.7	97.5±0.3
40% St. Mary's SL–I	51.1±0.1	66.1±1.1	83.5±3.4	88.5±0.4	94.9±0.6	97.2±1.0
60% St. Mary's SL–I	37.3±0.2	58.0±0.9	75.8±0.5	85.0±0.4	89.9±0.3	90.5±0.6
80% St. Mary's SL–I	28.7±0.9	43.1±0.9	51.0±1.2	53.2±0.4	55.6±0.7	60.0±0.7
100% St. Mary's SL–I	12.1±0.2	13.9±0.4	18.9±0.8	21.0±0.1	24.0±0.5	28.3±0.6

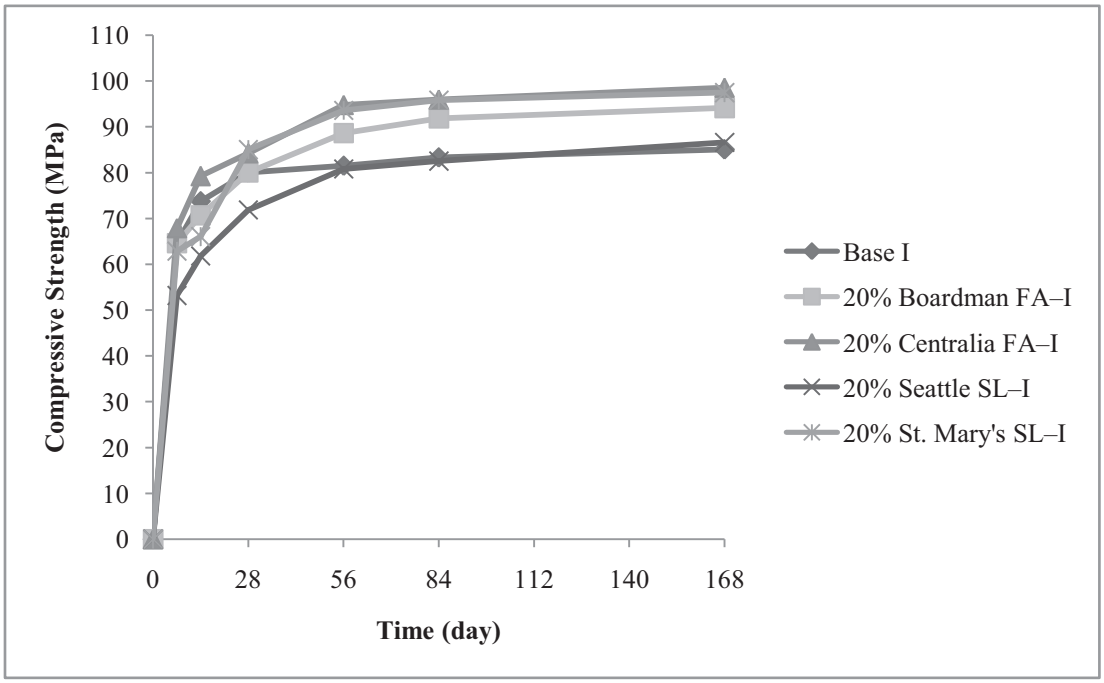

Figure 4.2. Strength development of the 20% SCM mixes and the Base I (w/b = 0.35)

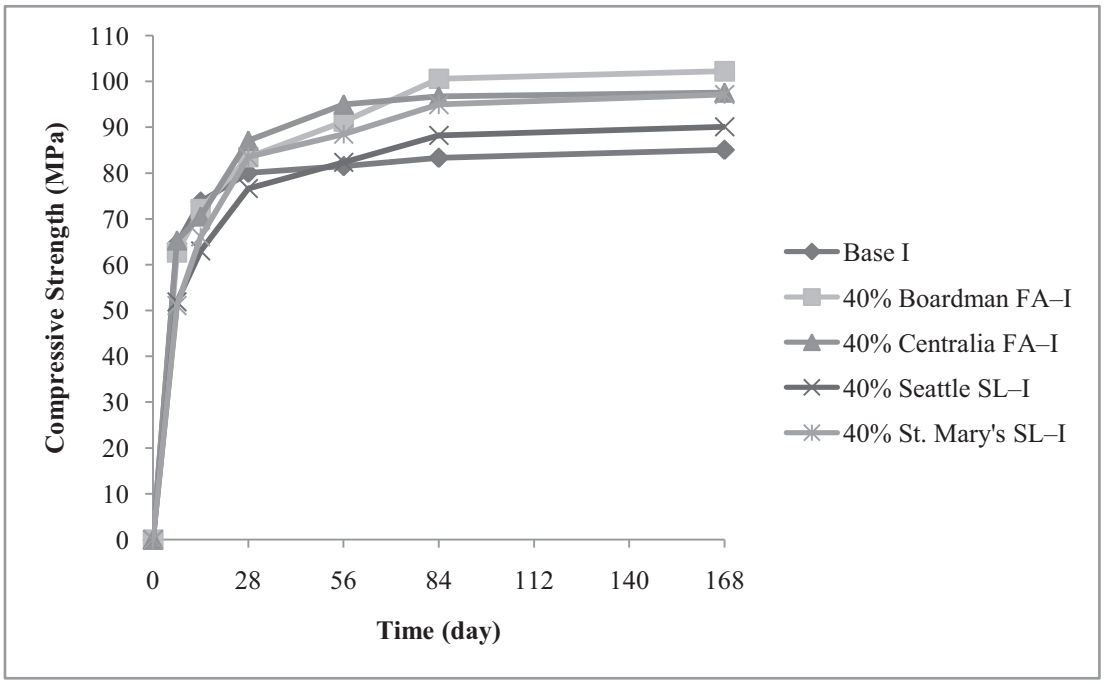

Figure 4.3. Strength development of the 40% SCM mixes and the Base I (w/b = 0.35)

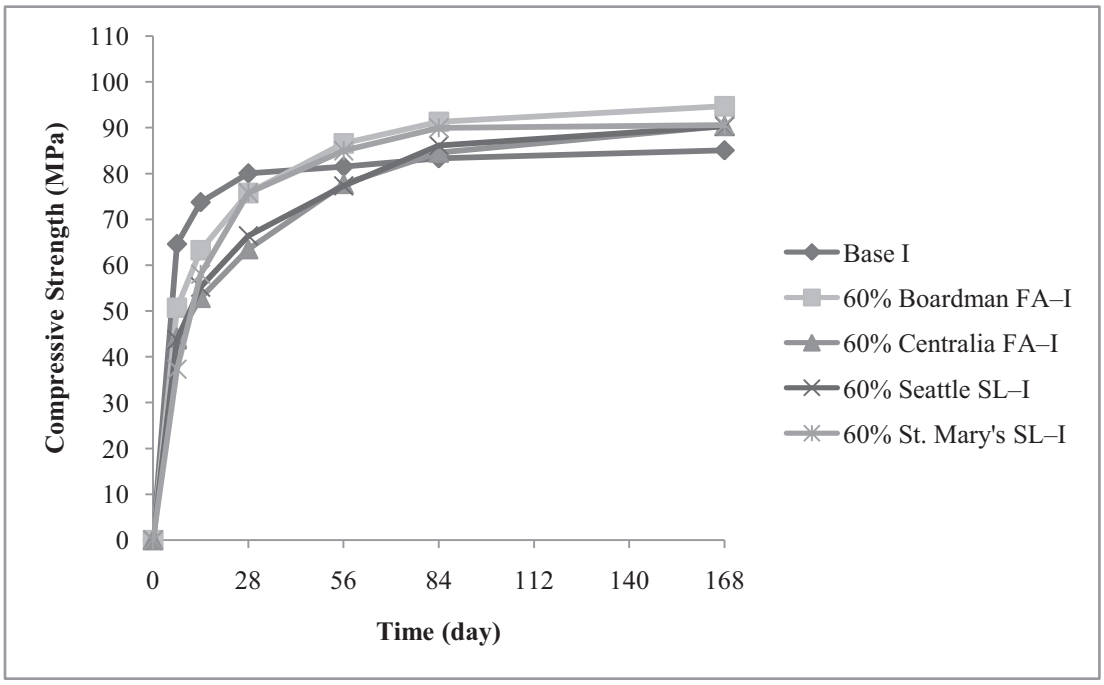

Figure 4.4. Strength development of the 60% SCM mixes and the Base I (w/b = 0.35)

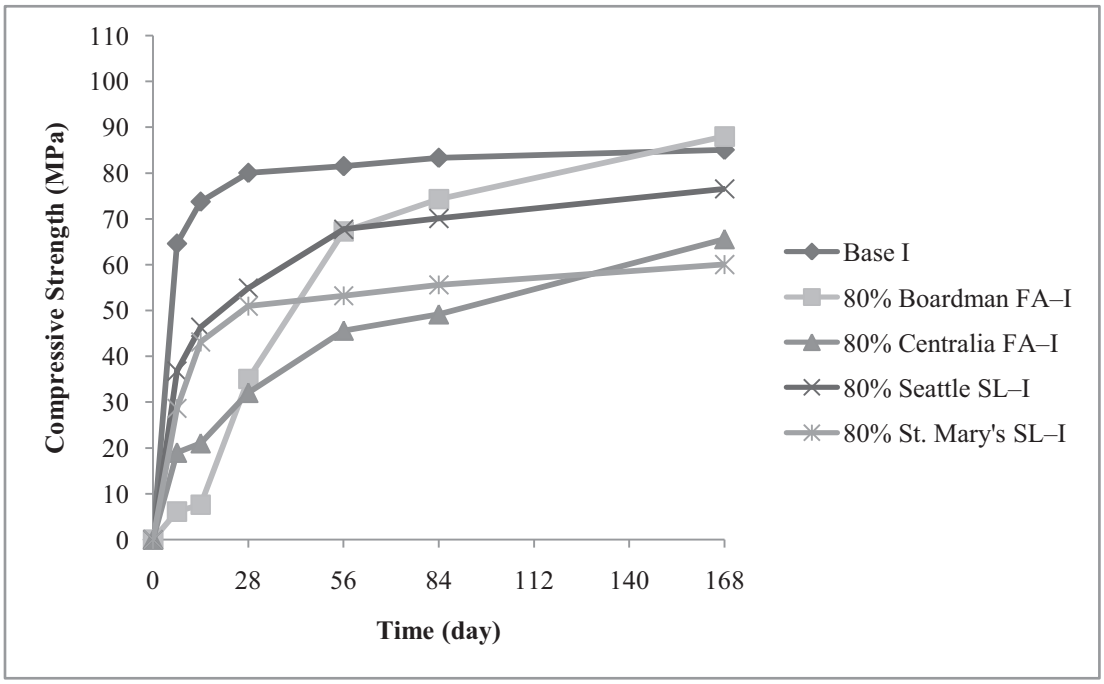

Figure 4.5. Strength development of the 80% SCM mixes and the Base I (w/b = 0.35)

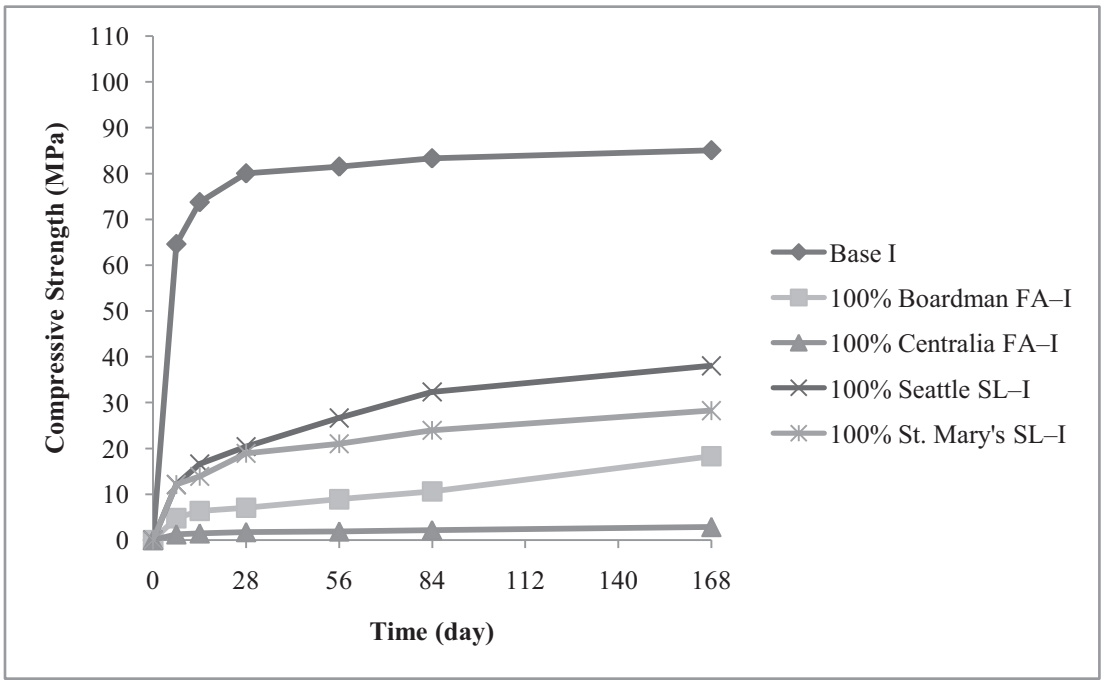

Figure 4.6. Strength development of the 100% SCM mixes and the Base I (w/b = 0.35)

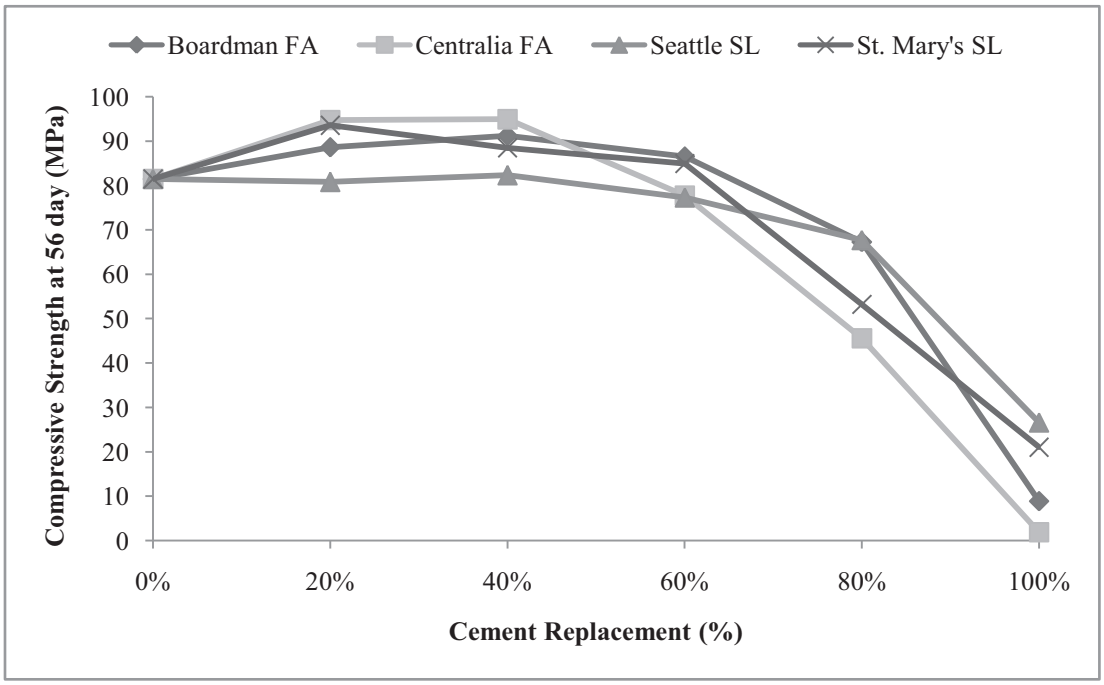

Figure 4.7. Compressive strength at 56 days versus cement replacement percentage

4.2.2 Phase II

Table 4.5 summarizes the average compressive strength values and standard deviations, for all of the Phase II mixes (w/b = 0.40). Figure 4.8 shows compressive strength development of Base I and Base II mixes. Base I had always higher strength than Base II. This was expected since Base I has lower w/b ratio than Base II. Figure 4.9 through Figure 4.11 exhibit the SCMs concrete compressive strength gain compared with Base II, with replacement levels of 60%, 80% and 90%, respectively. Figure 4.12 shows ternary mixes and the Base II mix. The following observations are made:

- Early-age strength development of Base II is superior relative to the SCM mixes; however, at later ages (≥ 112 days) the strength of the SCM mixes approximates that of the Base II mix (within 18%).
- Early-age compressive strength of both ternary and binary mixes increases with increasing SL content.
- The ternary mixes at given replacement level nearly always had higher compressive strength (except the 80% 75FA-25SL-II mix) than the comparable FA binary mix.

This behavior was expected since the SL increases the CaO content and, hence, the hydraulic reaction.

- Both the binary and ternary mixes need additional time to gain the same strength, relative to the Base II mix. This trend was anticipated because slow strength gain is often associated with concrete mixes with high volume of SCM since the pozzolanic reaction becomes the major reaction as the cement replacement increases.
- Two of the ternary mixes with 60% replacement exhibited higher strengths than the binary mixes at age 112 day, which suggest that synergy between the fly ash and slag has taken place.
- This synergy at 90% replacement is more prominent. The 90% 25FA-75SL-II mix always outperforms the binary mixes. At 56 days all of the ternary mixes are exhibiting higher strength than the binary mixes.
- The ternary mix with 75:25 FA to SL ratio ternary mixes at 80% cement replacement (80% 75FA-25SL-II) has lower compressive strength than both binary mixes. This is surprising since that mix has a higher CaO content than the binary FA mix.

Table 4.5. Compressive strength of SCC, with standard deviation, with fly ash (F) or slag (S) as cement replacement (w/b = 0.40)

Mix Name	%	Compressive Strength (MPa)					
		7 Day	14 Day	28 Day	56 Day	112 Day	168 Day
Base II	0	51.9±0.2	62.1±1.0	67.3±1.4	71.6±0.9	71.8±3.6	--
60% Boardman FA–II	60	26.8±0.5	32.4±0.4	34.1±0.9	44.3±1.3	--	--
80% Boardman FA–II	80	17.0±0.7	25.8±0.3	40.0±0.4	50.7±0.5	--	--
90% Boardman FA–II	90	3.3±0.4	5.0±0.1	10.9±0.1	22.1±0.2	28.9±0.6	32.8±0.7
60% Seattle SL–II	60	39.6±0.6	49.3±0.8	52.3±0.8	66.1±0.8	66.9±3.0	--
80% Seattle SL–II	80	37.9±0.3	47.1±0.2	57.6±0.5	76.8±0.5	74.4±5.2	--
90% Seattle SL–II	90	23.1±0.5	28.3±0.4	37.9±0.8	45.9±0.7	52.6±1.1	49.9±1.6
60% 25FA-75SL–II	60	30.9±0.9	41.8±0.6	54.2±0.5	64.0±0.5	72.4±5.2	75.3±1.1
80% 25FA-75SL–II	80	30.5±0.6	38.1±0.5	63.0±0.4	65.3±0.5	71.9±8.6	76.8±1.1
90% 25FA-75SL–II	90	25.8±0.4	38.4±1.1	47.2±0.2	58.4±0.5	66.6±1.2	68.6±1.4
60% 50FA-50SL–II	60	34.0±0.3	45.2±0.8	56.0±0.3	72.1±0.4	72.9±6.0	84.5±1.2
80% 50FA-50SL–II	80	20.6±0.4	30.5±0.6	41.4±0.5	59.8±0.3	64.0±6.6	74.1±0.9
90% 50FA-50SL–II	90	11.5±0.7	20.5±0.6	33.0±0.3	47.4±0.6	61.1±2.1	60.3±0.8
60% 75FA-25SL–II	60	25.4±0.4	36.0±0.6	49.0±0.9	56.4±0.6	63.8±5.5	68.3±0.6
80% 75FA-25SL–II	80	14.3±0.3	21.2±0.7	28.0±0.2	42.2±0.3	59.1±2.4	76.8±1.1
90% 75FA-25SL–II	90	11.3±0.4	18.1±0.5	32.0±0.3	48.5±0.3	59.8±2.0	61.9±1.0

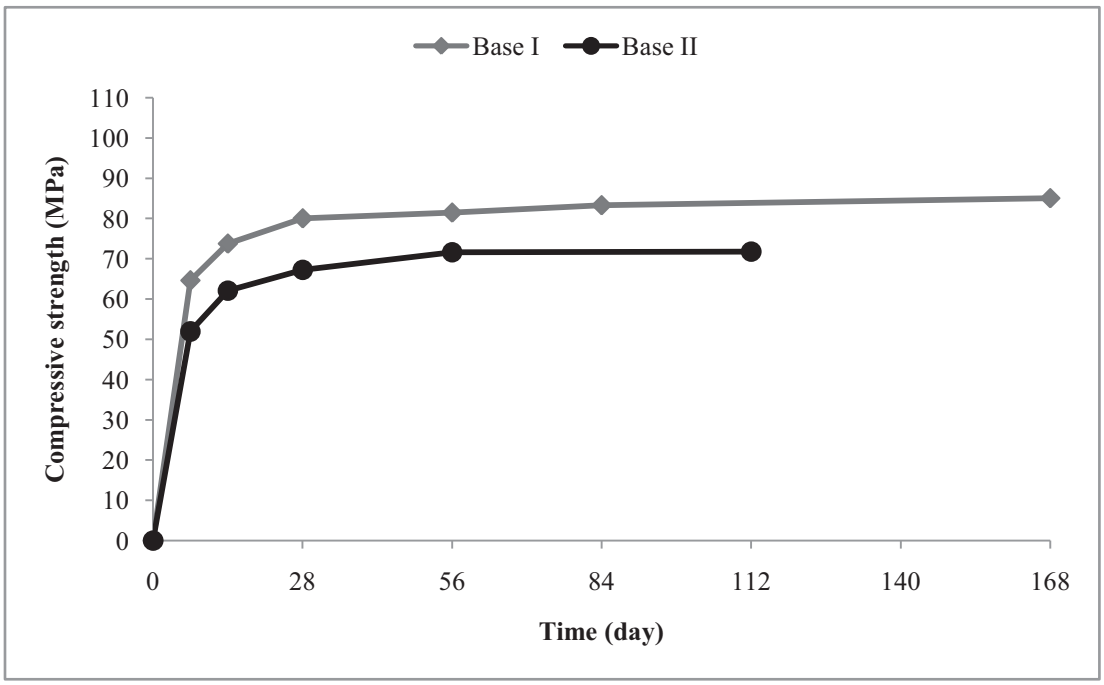

Figure 4.8. Comparison of Base I and Base II

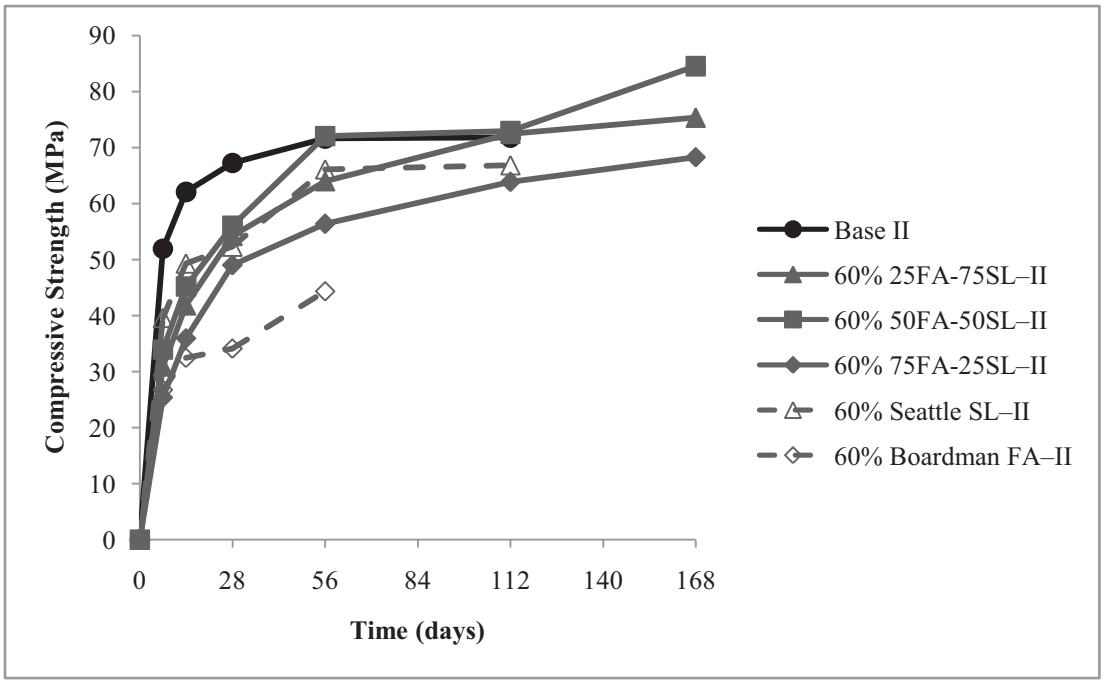

Figure 4.9. Strength development of the 60% SCM mixes and the Base II (w/b = 0.40)

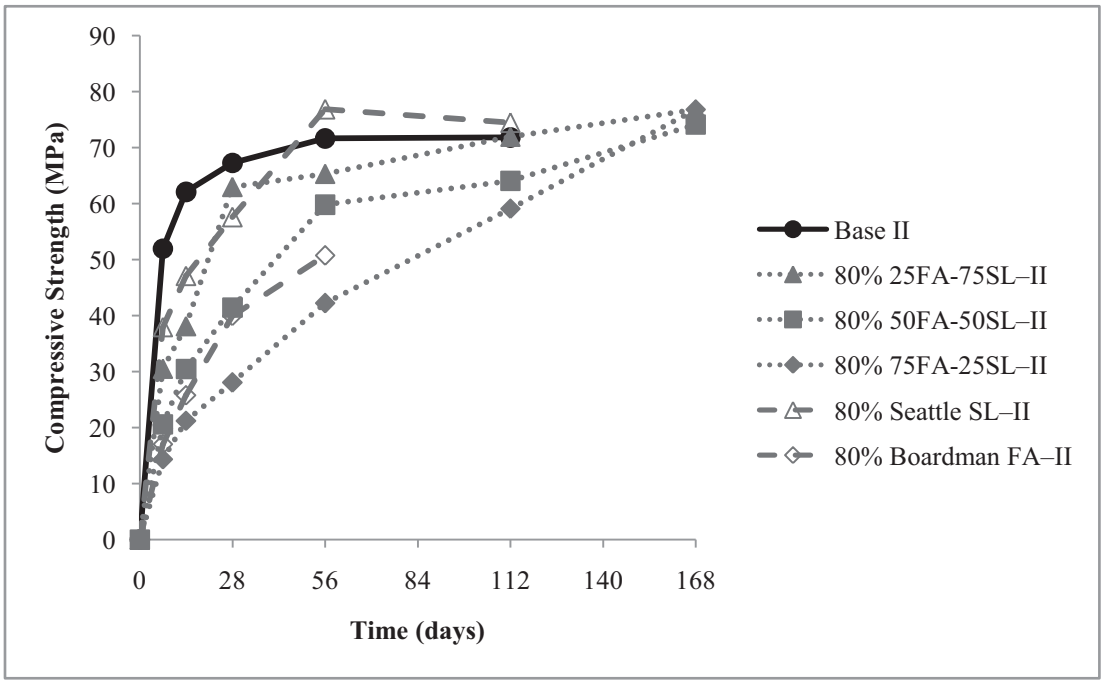

Figure 4.10. Strength development of the 80% SCM mixes and the Base II (w/b = 0.40)

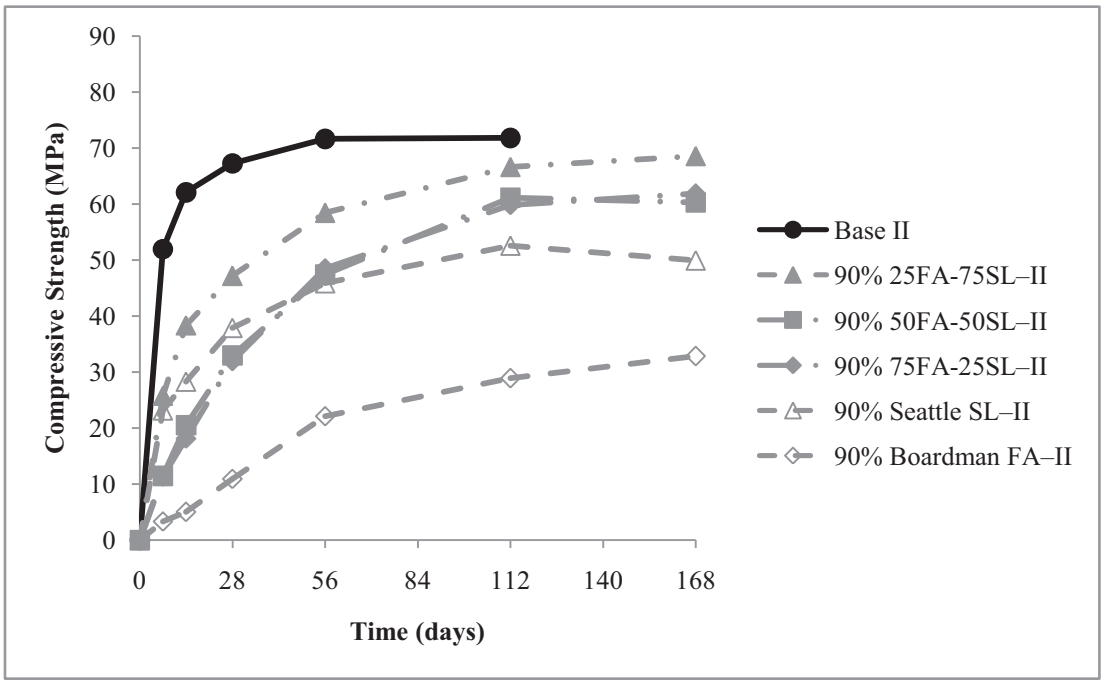

Figure 4.11. Strength development of the 90% SCM mixes and the Base II (w/b = 0.40)

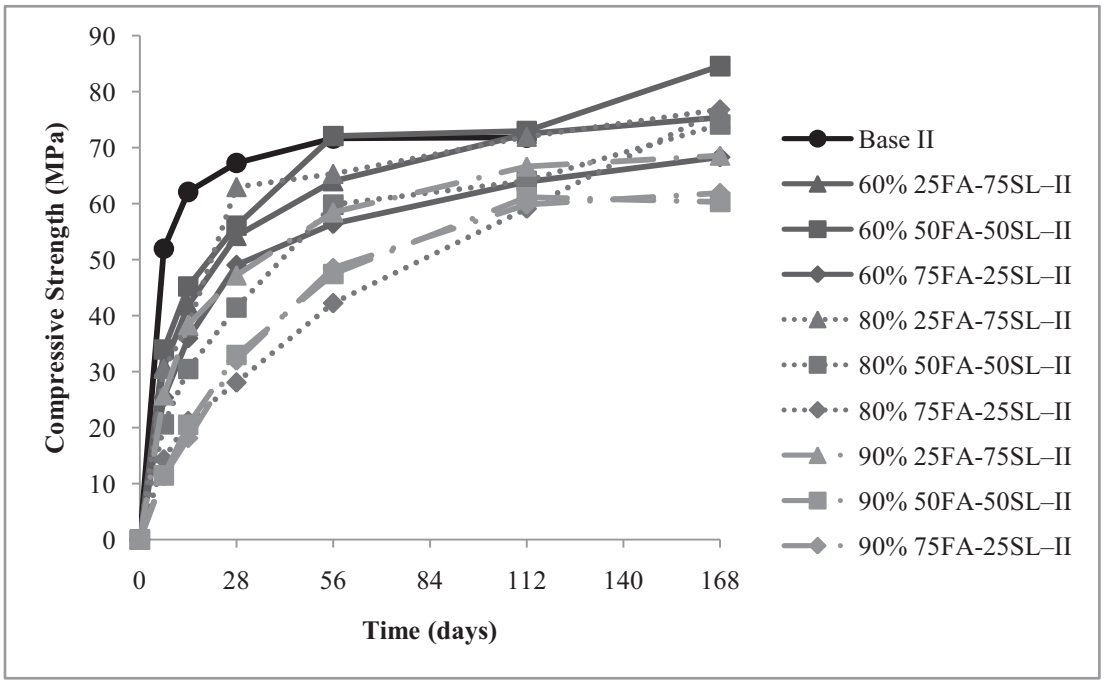

Figure 4.12. Strength development of the ternary mixes to the Base II (w/b = 0.40)

4.3 Elastic Modulus

Nine ternary mixes with 60%, 80% and 90% replacement of cement by weight and one control mix with only cement (Base II) were used to examine the time dependent development of the elastic modulus. The elastic modulus of the concrete mixtures was measured at the following times: 7, 14, 28, 56 and 112 days. The elastic modulus test was performed as described in Chapter 3, Section 3.2.3. Elastic modulus data for each cylinder are presented in Appendix C.

Table 4.6 summarizes the average elastic modulus values and standard deviations of the ternary mixes from Phase II compared with the Base II. Figure 4.13 through Figure 4.15 provides the elastic modulus of the SCM and the control mixes, with cement replacement of 60%, 80% and 90%, respectively.

Table 4.6. Elastic modulus of SCC, with standard deviation, with Boardman fly ash (BF) and Seattle slag (SS) as cement replacement (w/b = 0.40)

Mix name	Elastic Modulus (GPa)				
	7 day	14 day	28 day	56 day	112 day
Base II	47±0	45±2	46±4	49±3	46±1
60% 25FA-75SL-II	34±1	34±2	38±2	46±0	47±3
60% 50FA-50SL-II	32±1	37±1	41±5	54±2	55±4
60% 75FA-25SL-II	30±0	34±2	38±4	46±3	44±3
80% 25FA-75SL-II	28±2	31±1	40±3	49±2	49±2
80% 50FA-50SL-II	26±3	36±0	41±1	52±2	62±3
80% 75FA-25SL-II	27±1	36±1	37±2	43±1	49±5
90% 25FA-75SL-II	28±1	32±1	39±1	46±3	46±1
90% 50FA-50SL-II	28±1	28±0	40±4	45±3	53±11
90% 75FA-25SL-II	27±1	32±3	40±3	45±1	51±1

The results indicated that at high replacement levels (≥ 60%) the elastic modulus is less sensitive to increased cement replacement when compared to compressive strength. This could be a result of the reduced porosity, which results from C-S-H formation of the pozzolanic reaction. Elastic modulus is sensitive to porosity in the concrete. Lower porosity results in higher elastic modulus (Mindess, Young, & Darwin, 2003; Brandt, 1995). All of the ternary mixes had similar elastic modulus values at a given age and the elastic modulus of all of the ternary SCM mixes increased gradually up to day 56. The difference in the elastic modulus of the SCM mixes at age 56 and 112 day is approximately equal, with the exception of the mix with 80% SCM and 50:50 FA to SL ratio (80% 50FA-50SL-II). This suggests that the SCM mixes have developed their long-term modulus by day 56. On average the elastic modulus, of the SCM mixes increased by 40% day 7 to day 112. On the other hand the Base II mix develops the majority of its long-term modulus in the first week. The data clearly show that the elastic modulus of the ternary mixes (replacement of 60% or larger) are all lower than the Base II mix prior to 56 days, but was equal to or exceeding the Base II mix at day 56. This constant elastic modulus value of the control mix and the gradual increase of the elastic modulus of SCM mixes have previously been reported (Naik, Singh, & Ramme, 1998).

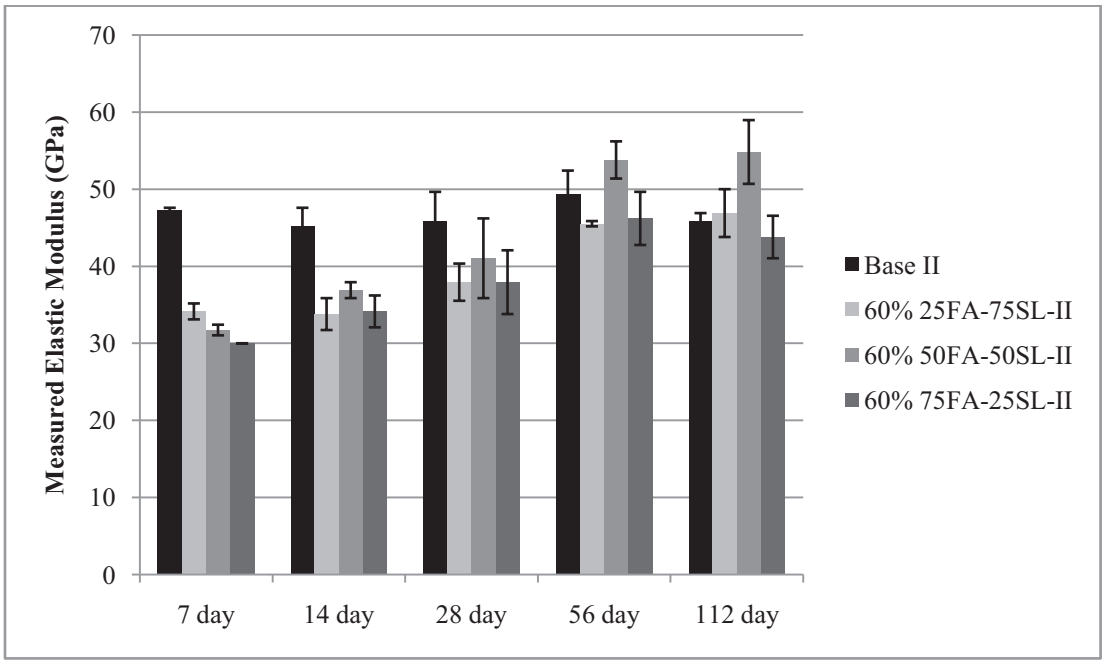

Figure 4.13. Elastic modulus of the 60% ternary SCM mixes and Base II (w/b = 0.40)

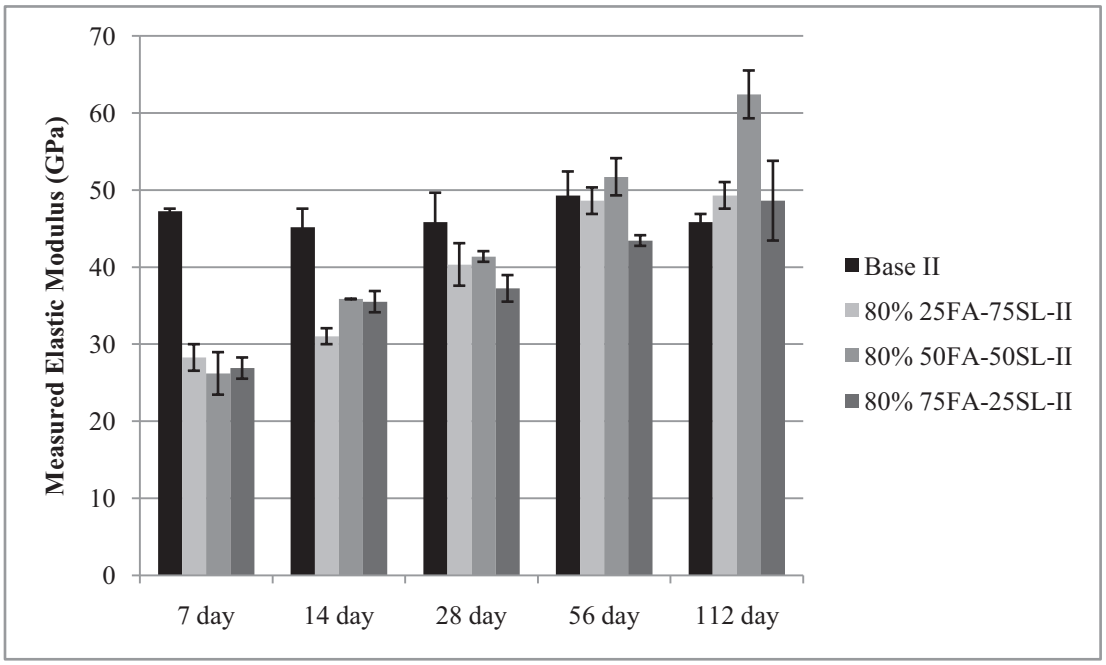

Figure 4.14. Elastic modulus of the 80% ternary SCM mixes and Base II (w/b = 0.40)

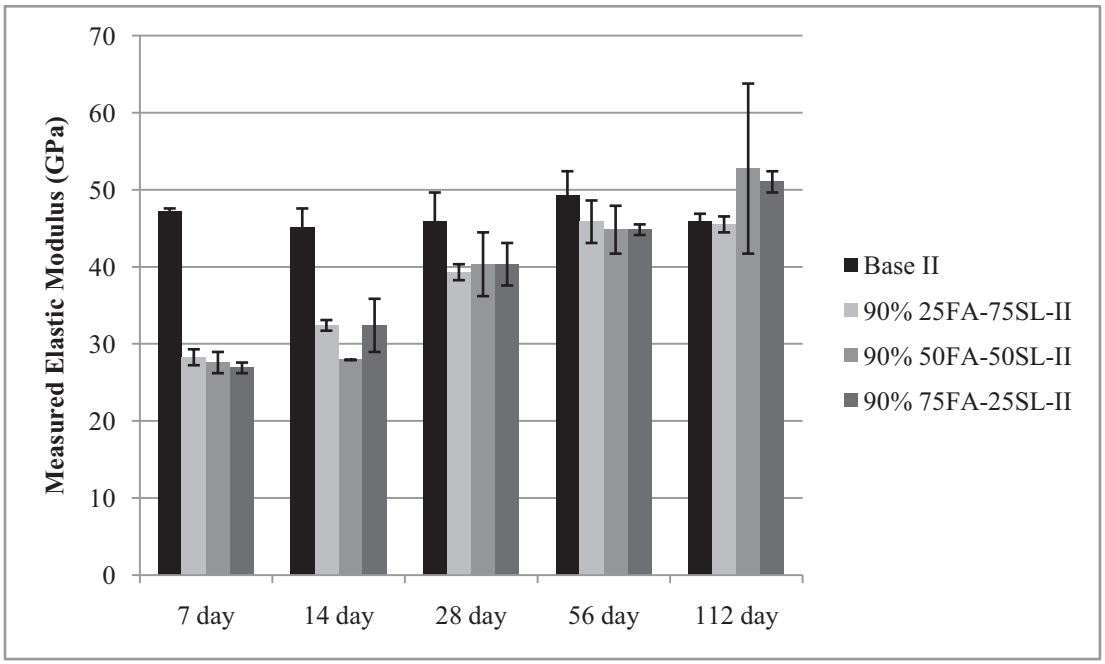

Figure 4.15. Elastic modulus of the 90% ternary SCM mixes and Base II (w/b = 0.40)

4.4 Creep and Shrinkage Response

Ternary mix with 90% replacement of cement by weight with the ratio of FA to SL as 50-50 (90% 50FA-50SL-II) was tested to determine their creep and shrinkage behavior. The creep behavior of the ternary mixture was determined after 7, 14 and 28 days of curing in 100% relative humidity prior loading. In addition, Base II mix was also tested for creep behavior and was loaded after 7 days of curing. The creep and shrinkage tests were performed both on sealed and unsealed specimens. The tests were performed as described in Chapter 3, Section 3.2.4. Each quarter point of the cylinder was measured three times, and then averaged. The average of the measurement is provided in Appendix D.

All the rigs were loaded with the same load of 4.14MPa (600 psi). This load approximated the stress demand from dead load in construction (0.1 f'_c) for concrete with design strength of 41.37 MPa (6000 psi). Table 4.7 shows the stress/strength ratio of cylinders at day of loading in each rig and name convention.

Table 4.7. Stress/Strength ratio in the creep test

Creep Rig	Mix name	Day of Loading	Short hand Notation	Stress (MPa)	Strength[1] (MPa)	Stress/ Strength
1	90% 50FA-50SL-II	7	7 SCM	4.14	11.46	0.36
2	90% 50FA-50SL-II	14	14 SCM	4.14	20.52	0.20
3	90% 50FA-50SL-II	28	28 SCM	4.14	32.97	0.13
4	Base II	7	7 Base II	4.14	51.95	0.08

[1]Compressive strength at day of loading

4.4.1 Total Strain

Total strain is the sum of the elastic, creep and shrinkage strain. The total strains of the unsealed and sealed loaded specimens are shown in Figure 4.16 and Figure 4.17, respectively. The plot shows the average total strain of two sets of cylinders. Total strain for each cylinder was obtained by taking the average strain at the four quarter points. 'Time' refers to the time elapsed since the corresponding rig was loaded.

As expected, the plots of total strain are characterized by an initial strain (elastic concrete response) followed by a gradual increase in strain with time. As expected the total strain of the unsealed cylinders was larger than the sealed cylinders. Less shrinkage occurs in the sealed cylinders because excess water in the concrete cannot evaporate. Furthermore, as expected, higher stress/strength ratio resulted in higher total strain. The 90% 50FA-50SL-II mix that was loaded after 28 days exhibits a total strain that is approximately equal; their respective stress/strength ratios were 0.13 and 0.08.

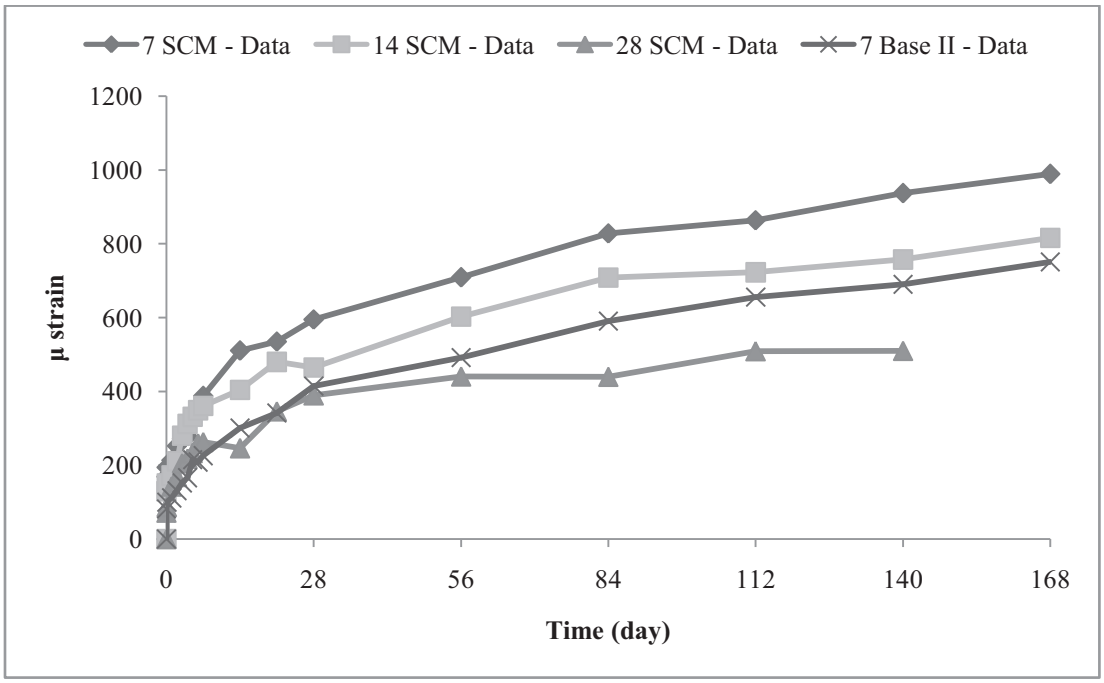

Figure 4.16. Total strain of the unsealed cylinders

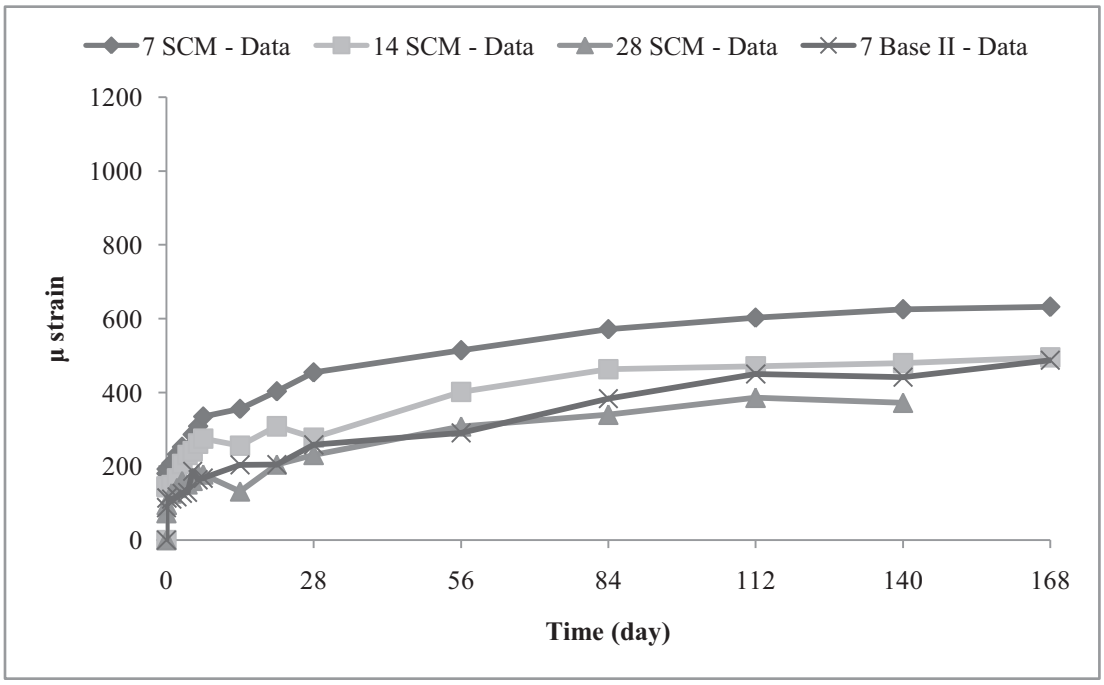

Figure 4.17. Total strain of the sealed cylinders

4.4.2 Shrinkage Strain

The shrinkage strains in the unsealed and sealed specimens are shown in Figure 4.16 and Figure 4.17, respectively. The plot shows the average shrinkage strain of two of cylinders.

Shrinkage strain for each cylinder was obtained by taking the average strain at the four quarter points. 'Time' refers to the time elapsed since the cylinder was removed from the fog room (100% humidity) and stored next to the loaded specimens.

As expected, the unsealed specimens exhibit more shrinkage than the sealed specimens (the epoxy prevents the majority of the free water from evaporating). There is little difference between mixes and curing periods.

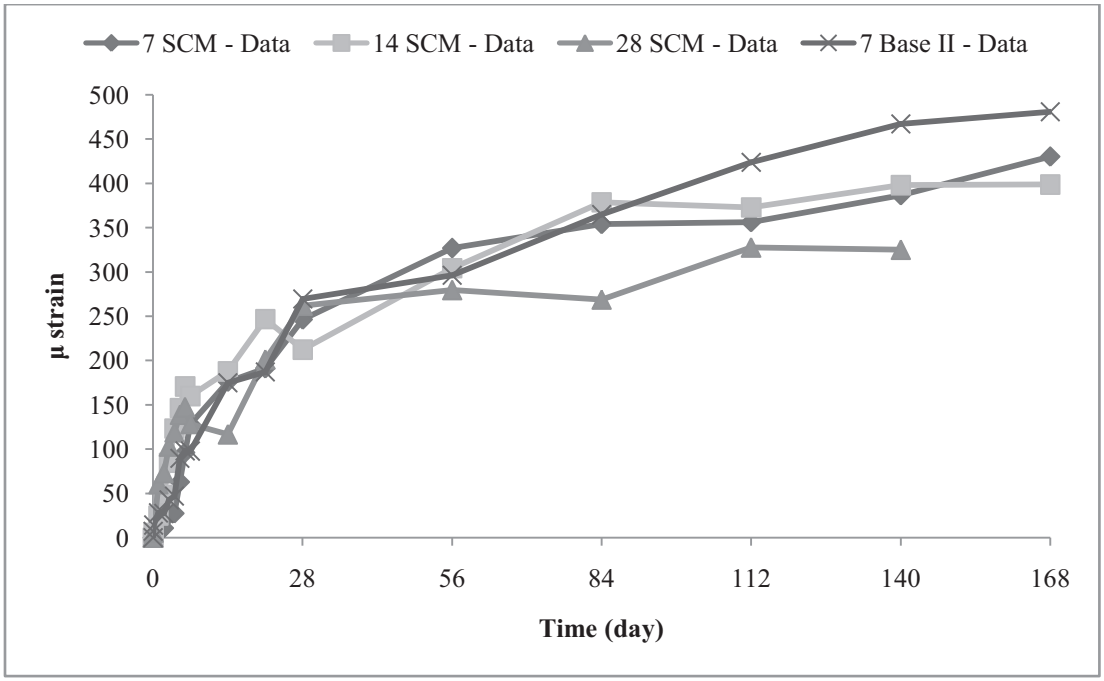

Figure 4.18. Shrinkage strain of the unsealed cylinders since removal from fog room

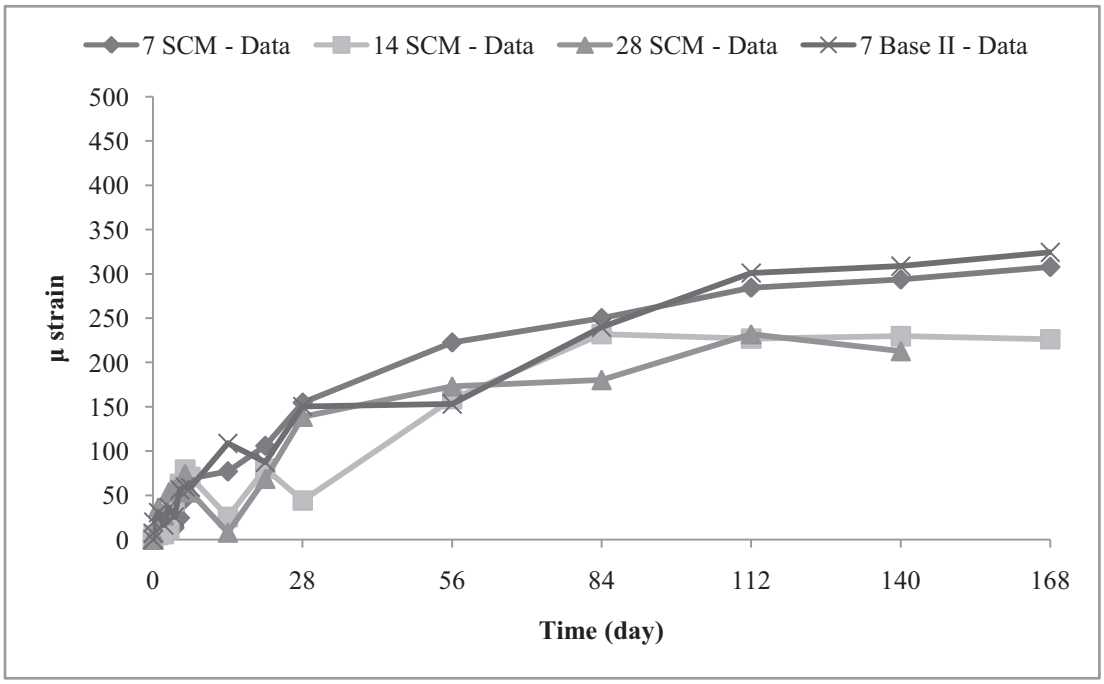

Figure 4.19. Shrinkage strain of the sealed cylinders since removal from fog room

4.4.3 Total, Drying and Basic Creep

The creep and elastic strains in the unsealed and sealed cylinders are displayed in Figure 4.20 and Figure 4.21, respectively. Figure 4.22 and Figure 4.23 exhibit the creep strains in the unsealed and sealed cylinders, respectively. Figure 4.24 shows the drying creep. Table 4.8 summarizes the results. Total creep, basic creep and drying creep were obtained as described in Section 3.2.4.3. Specific creep strain is defined as the creep strain per unit of stress.

Table 4.8. Creep results of the concrete mixtures

Concrete	Age of loading	Cylinder	Applied Stress (MPa)	Creep strain (10^{-6})	Duration of loading (days)	Elastic and Creep strain (10^{-6})	Specific Creep strain (10^{-6}/MPa)	Creep Coefficient $\varphi(t,t_0)$
SCM	7 day	Unsealed	4.14	381	168	559	92	3.2
		Sealed	4.14	149	168	331	36	1.8
SCM	14 day	Unsealed	4.14	280	168	417	68	3.0
		Sealed	4.14	128	168	269	31	1.9
SCM	28 day	Unsealed	4.14	108	140	185	26	2.4
		Sealed	4.14	79	140	159	19	2.0
Base II	7 day	Unsealed	4.14	190	168	270	46	3.4
		Sealed	4.14	76	168	163	18	1.9

The total creep strains (unsealed cylinders) are larger than the basic creep strains (sealed cylinders), since less water has evaporated from the sealed specimens. This is expected since

the free water in capillary pores increases creep resistance (Mindess, Young, & Darwin, 2003). Thus, less free water reduces creep resistance. Higher stress/strength ratio resulted in higher creep strain.

For the total creep, the 90% 50FA-50SL mix that was loaded after 28 day (28 day SCM) exhibited strains that was slightly less than Base II mix that was loaded after 7 days (7 day Base II) for unsealed cylinder. The stress/strength ratios of the concrete mixes were approximately the same. However, the creep strains of the 28 day SCM and the 7 day Base II mixes are almost identical when the sealed cylinders are compared. This behavior suggests that the Base II loaded after 7 days had more free water than the 28 day SCM; this is rational since the SCM mix had longer time to cure. Figure 4.24 shows that the drying creep of the 28 day SCM is very small (negligible), whereas the 7 day Base II is showing higher drying creep, which again supports this theory. Longer curing periods decreased the drying creep.

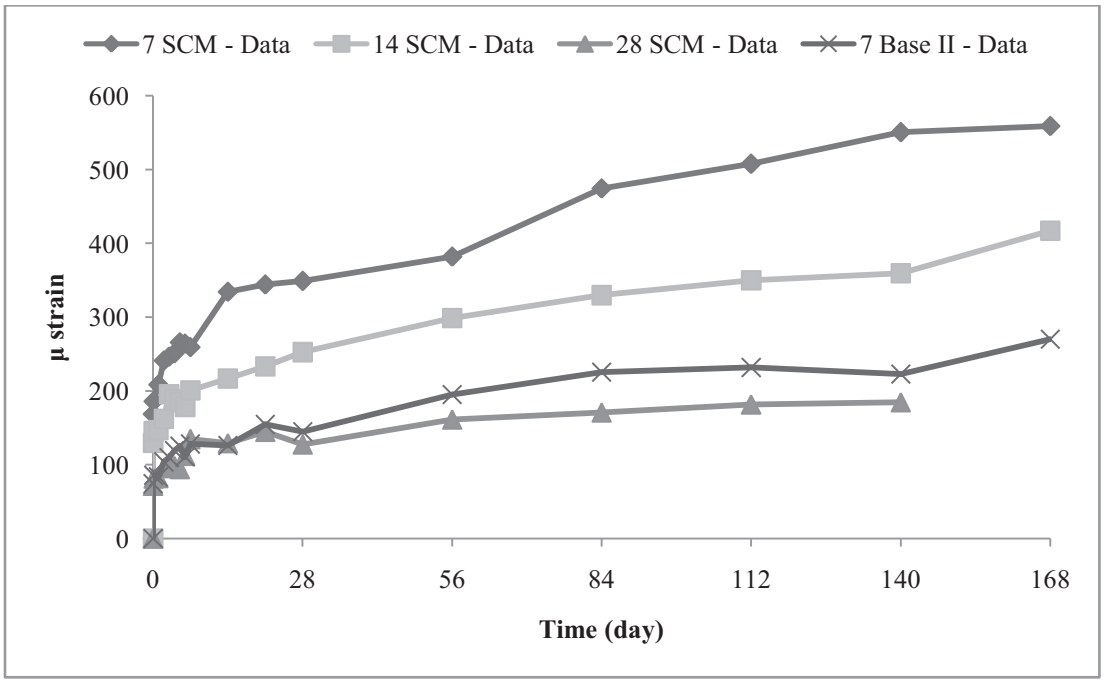

Figure 4.20. Elastic and creep strain of the unsealed cylinders since loading

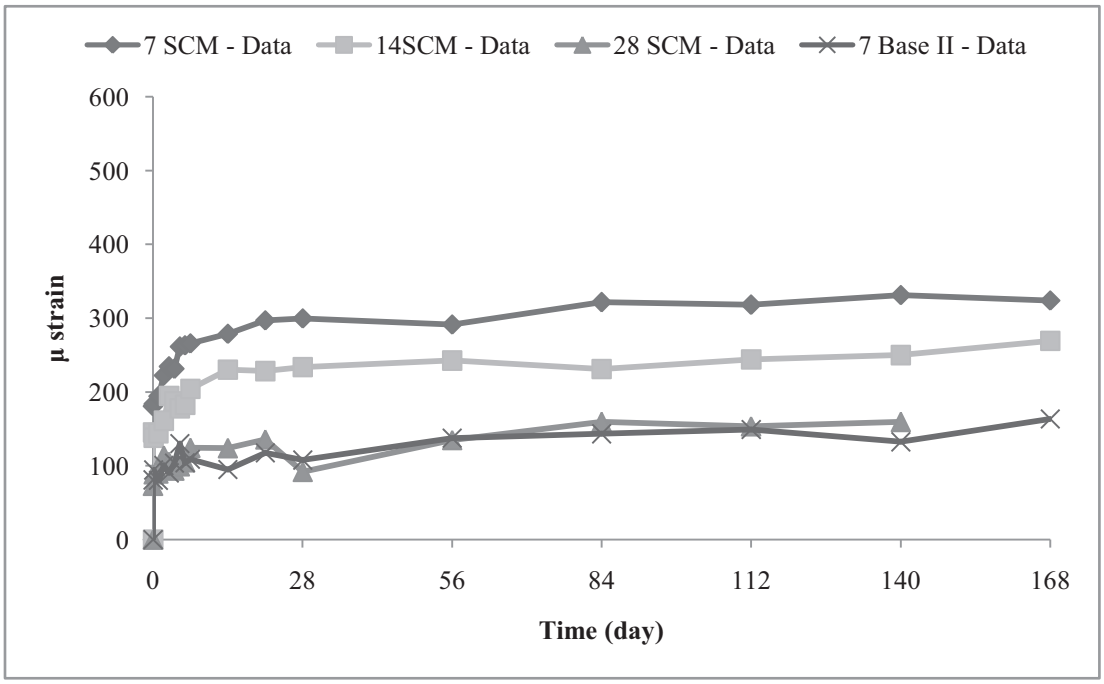

Figure 4.21. Elastic and creep strain of the sealed cylinders since loading

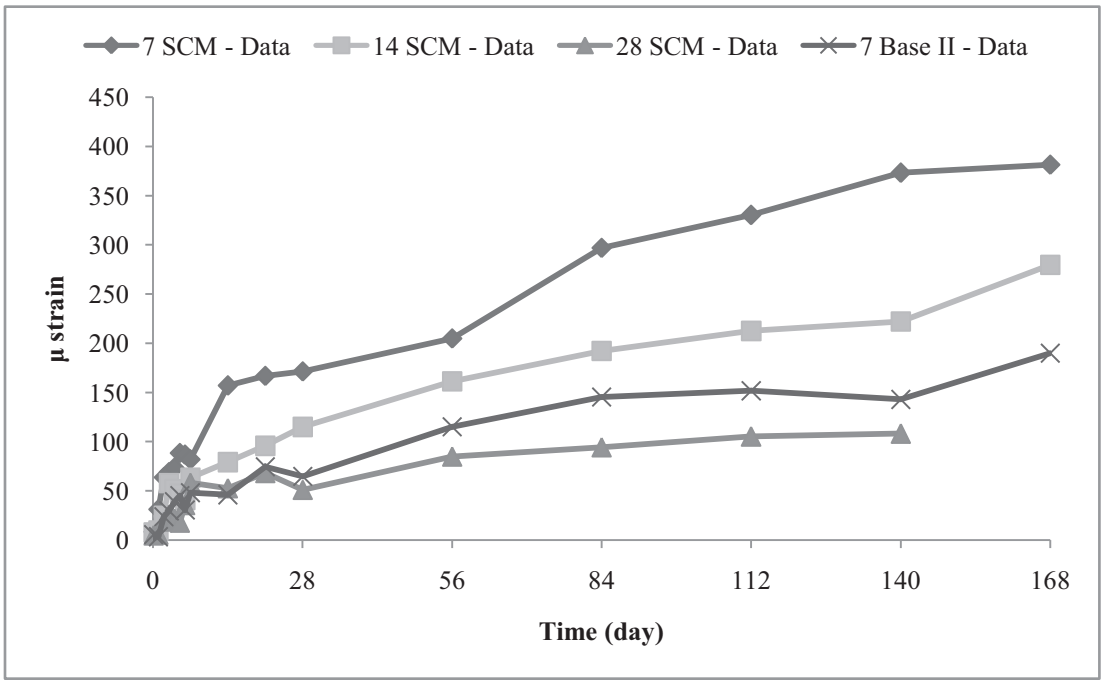

Figure 4.22. Creep strain of the unsealed cylinders since loading (total creep)

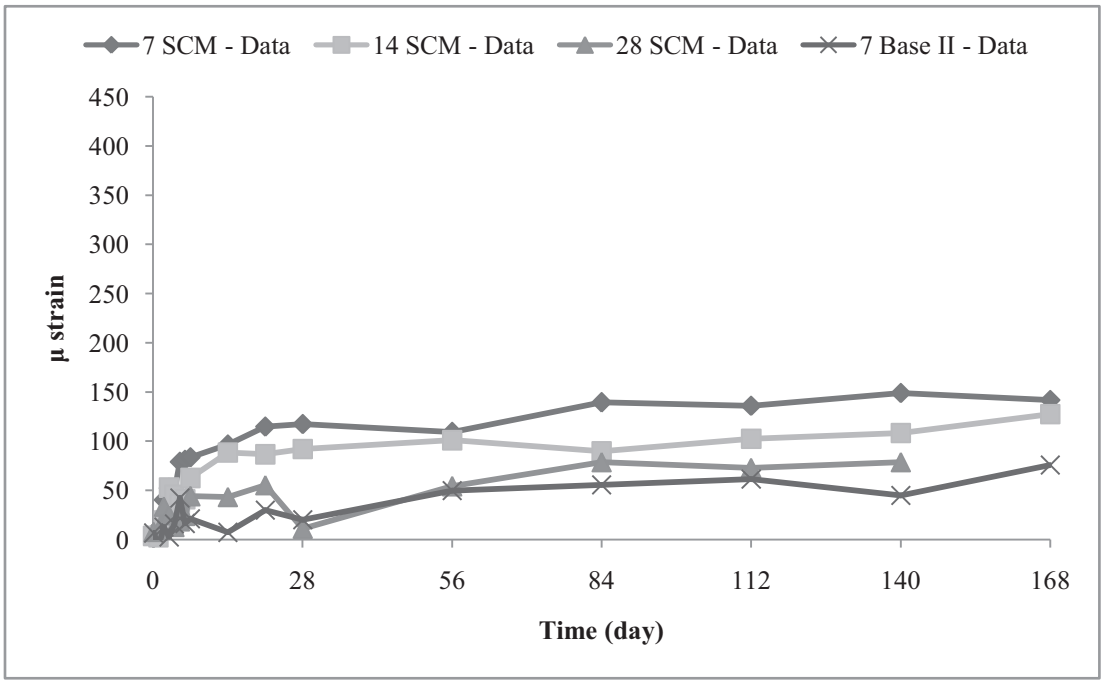

Figure 4.23. Creep strain of the sealed cylinders since loading (basic creep)

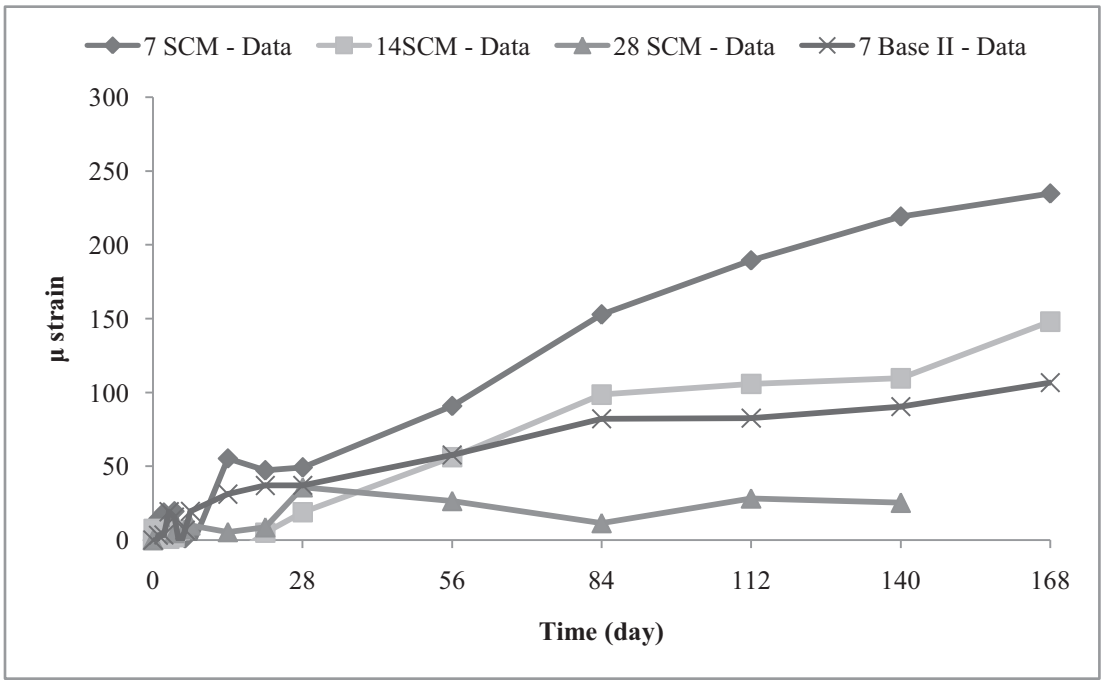

Figure 4.24. Drying creep strain of the cylinders since loading

The ratio of creep strain after very long time to the elastic strain is called creep coefficient, φ. Figure 4.25 and Figure 4.26 display the creep coefficient of the unsealed and sealed cylinders, respectively. The unsealed cylinders exhibit higher creep coefficient than the

sealed cylinders. This was expected since the unsealed cylinders exhibited higher creep strain than the sealed cylinders. There is little difference between mixes and curing periods. The creep coefficients for each mix are given in Table 4.8. The creep coefficient of concrete after 70 years with an effective thickness of 152.4 mm (12 in.) loaded after 7 and 28 days according to CEB can be taken as 3 and 2.4, respectively (CEB, 1993). These values are comparable to the creep coefficients of the unsealed cylinders. However, the sealed cylinders exhibit lower creep coefficients than the values from CEB.

In general, all of the creep strains are lower than the literature review (Chapter 2). The mixes previously tested for creep behavior also had lower replacement levels than this research. The lower creep strains might result from the larger unreacted portion of fly ash and slag which act as a fine aggregate, providing higher creep resistance.

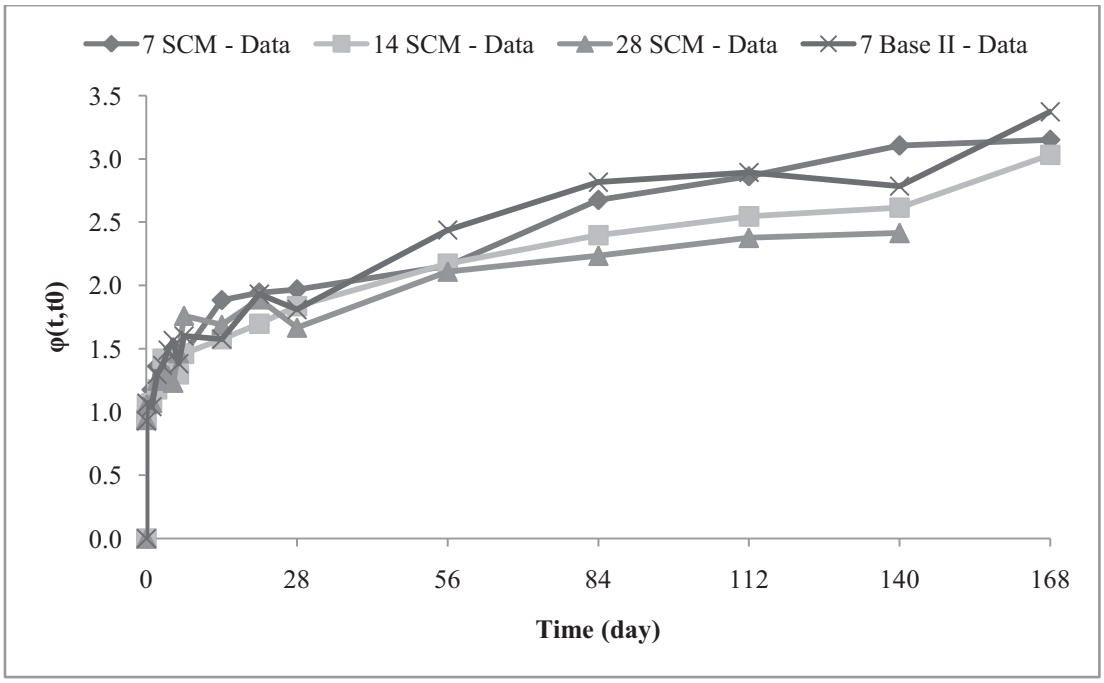

Figure 4.25. Creep coefficient of the unsealed cylinders since loading since loading

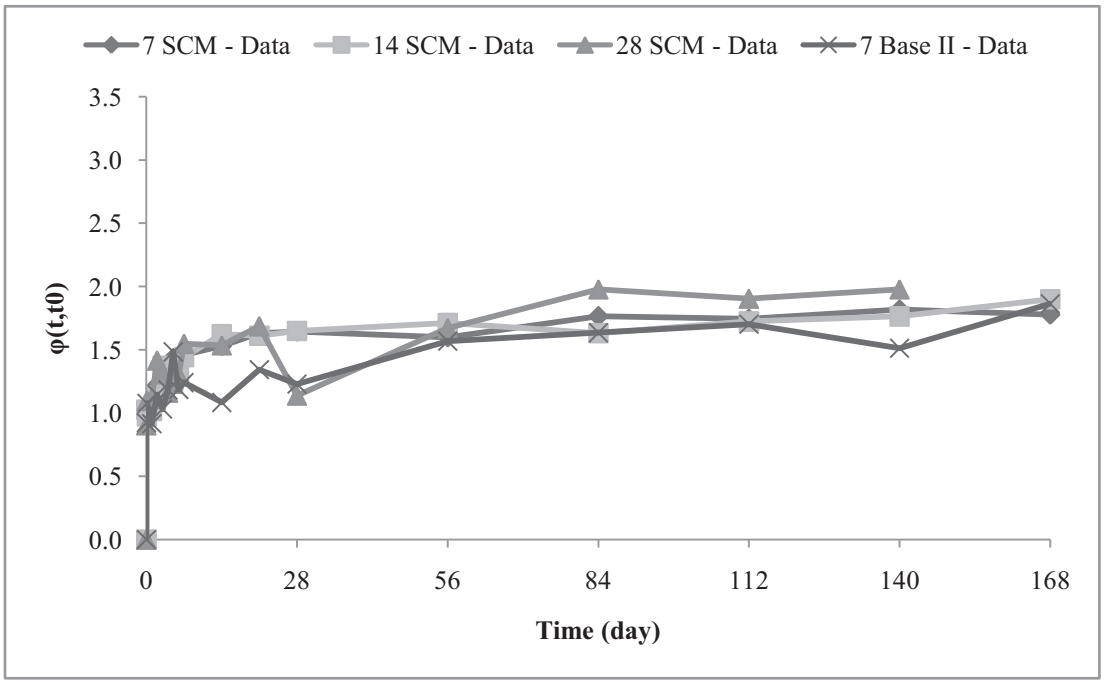

Figure 4.26. Creep coefficient of the sealed cylinders since loading since loading

Chapter 5: Analytical Expressions for Mechanical Properties

Analytical expressions were developed to estimate the mechanical properties of the SCM rich concretes. The compressive strength was estimated using efficiency factor expression based on the chemical composition of the total binder, for use in the modified Bolomey equation. Two equations for estimating the elastic modulus are compared; the commonly used ACI equation and an equation from the European code and recommendations are made. Finally the combined Bingham-Maxwell model is used to model the creep response.

5.1 Compressive Strength

One of the primary objectives of the research was to develop a compressive strength equation that is capable of predicting the strength at any time. The modified Bolomey equation was adopted. Prior efficiency factor (k-value) expressions were compared. The experimental data was examined and a new k-value expression was developed, which was compared with prior compressive strength results.

5.1.1 Equivalent Cement Content

Efficiency factors (*k*-values) were evaluated using concrete's compressive strength and Eq. (2.4). For a *k*-value equal to one, the SCMs are considered to be equivalent to cement. Figure 5.1 through Figure 5.4 present the equivalent cement content (*kP*) versus the SCM content for binary mixes with w/b ratio of 0.35 for Centralia FA, Boardman FA, Seattle SL and St. Mary's SL, respectively. The results show that fly ash has an optimum SCM content of approximately 284 kg/m^3 (60% replacement) where the slag has an optimum SCM content between 284 and 379 kg/m^3 (60 and 80% replacement). At day 168, all of the mixes with replacement levels of 60% or less, have *kP* greater than one suggesting an efficiency exceeding the Base II mix.

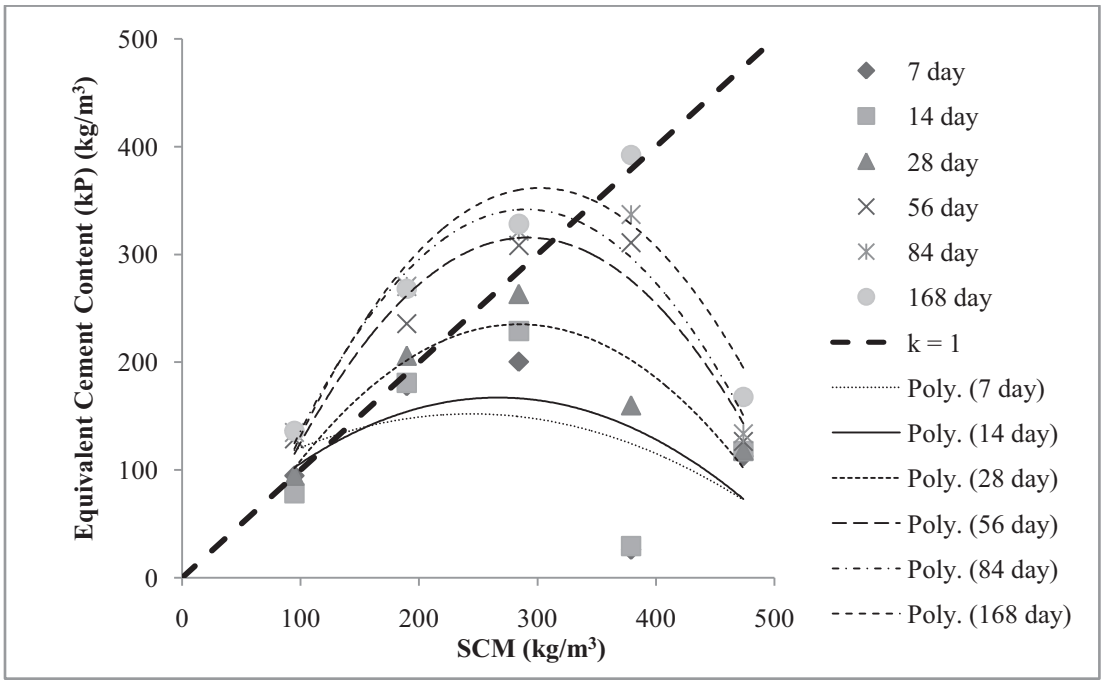

Figure 5.1. Equivalent cement content versus cement replacement – Boardman FA (w/b = 0.35)

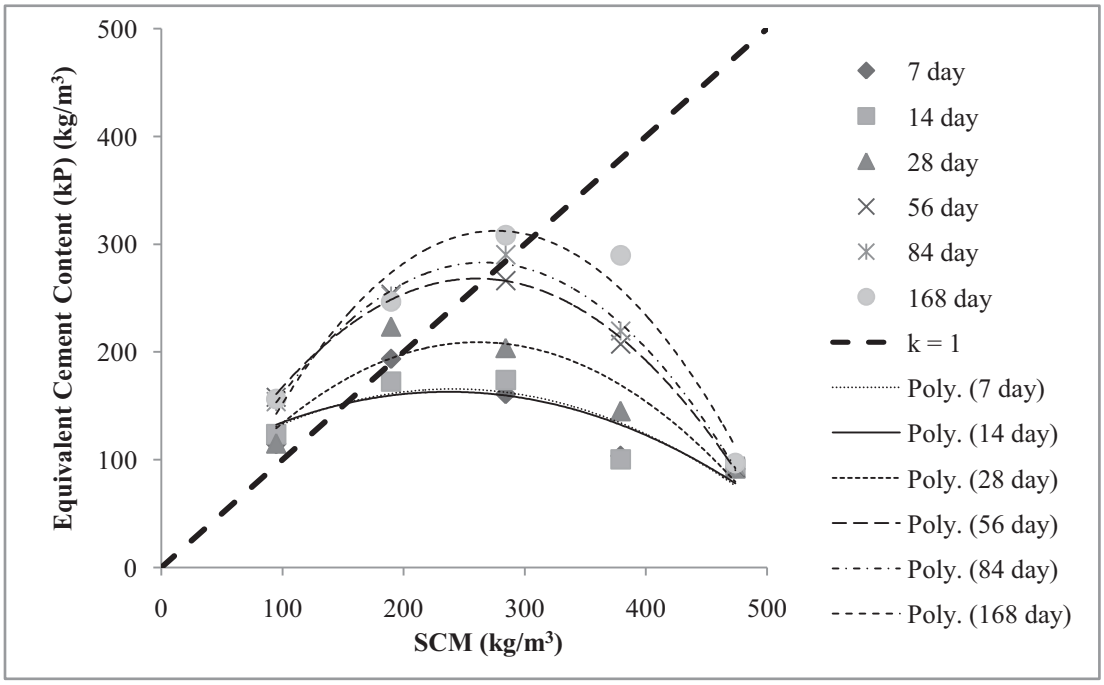

Figure 5.2. Equivalent cement content versus cement replacement – Centralia FA (w/b = 0.35)

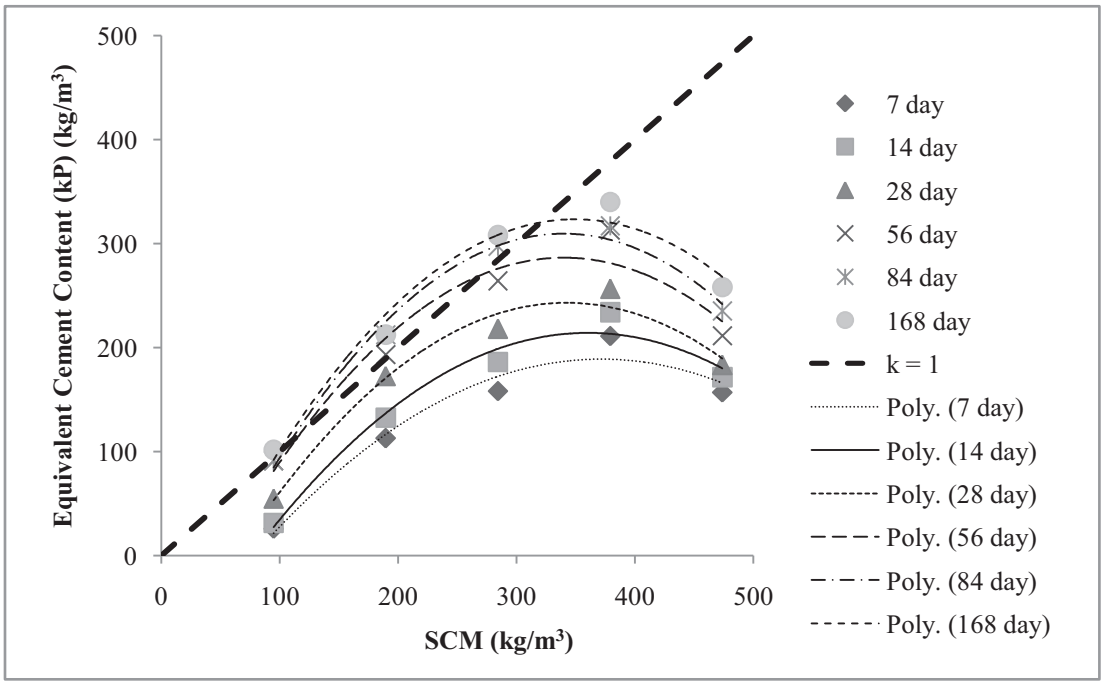

Figure 5.3. Equivalent cement content versus cement replacement – Seattle SL (w/b = 0.35)

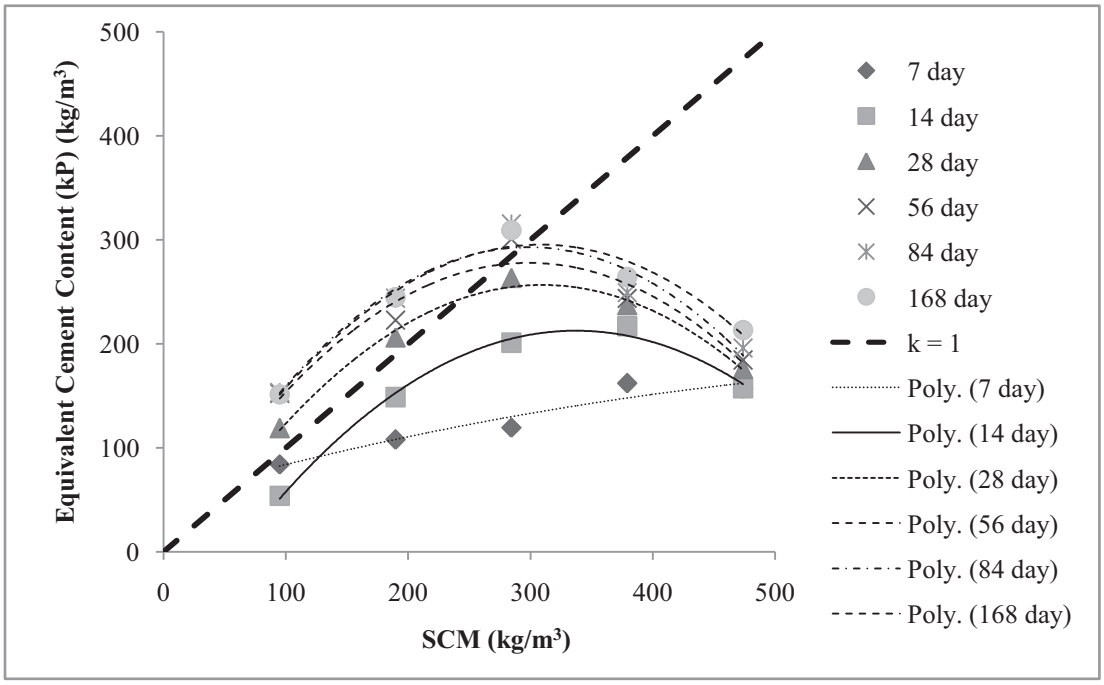

Figure 5.4. Equivalent cement content versus cement replacement – St. Mary's SL (w/b = 0.35)

Second-order polynomial regression equations were developed from the data shown on Figure 5.1 through Figure 5.4, to fit the following expression: $kP = aP^2 + bP + c$. This methodology, relating equivalent cement content to cement replacement by using second-

order polynomial regression, has been used in other research as well (Pekmezci & Akyüz, 2004; Oner, Akyuz, & Yildiz, 2005; Oner & Akyuz, 2007). Table 5.1 provides value for the coefficients and the R^2-values. The R^2 values show that second-order polynomial equation is a reasonable approximation with the exception of the Boardman FA at age 7 and 14 days. The outsider is at 80% replacement level for the binary Boardman FA mix. The mixes fit the polynomials better as the concrete gets older (R^2 value approaches one). The SL mixes have a better fit (R^2 values close to one) than FA mixes at early age (≤ 14 days).

The polynomial expressions were then used to calculate the equivalent cement content and compressive strength. Figure 5.5 shows the calculated versus measured compressive strength using these expression. In general, good agreement is seen between the calculated and experimental data, except when the SCM mixes had compressive strength less than 17.2 MPa (non structural concrete according to ACI) (ACI Committee 318, 2008). Eighty-six percent of the data fell within 20% of the measured strength.

Table 5.1. Coefficients of second-order polynomial regression and R^2 values for Bolomey strength equations (FA = fly ash and SL = slag)

Cementitious Material	Day	$kP = aP^2 + bP + c$			
		a	b	c	R^2
Boardman FA	7	-0.002	0.736	62.318	0.202
	14	-0.002	1.171	10.970	0.237
	28	-0.004	2.114	-65.295	0.844
	56	-0.005	3.027	-125.352	0.927
	84	-0.006	3.296	-136.668	0.935
	168	-0.006	3.404	-152.126	0.856
Centralia FA	7	-0.002	0.794	70.104	0.666
	14	-0.002	0.715	78.372	0.727
	28	-0.003	1.502	12.701	0.855
	56	-0.004	2.034	3.176	0.996
	84	-0.004	2.353	-30.055	0.994
	168	-0.005	2.844	-80.811	0.934
Seattle SL	7	-0.002	1.622	-112.358	0.958
	14	-0.003	1.909	-129.726	0.970
	28	-0.003	2.119	-119.590	0.975
	56	-0.003	2.322	-107.935	0.939
	84	-0.004	2.549	-123.201	0.986
	168	-0.004	2.495	-112.400	0.972
St. Mary's SL	7	0.000	0.332	52.938	0.923
	14	-0.003	1.854	-99.624	0.991
	28	-0.003	1.875	-33.307	0.988
	56	-0.003	1.873	-1.738	0.915
	84	-0.003	2.018	-8.035	0.924
	168	-0.003	1.951	-5.160	0.961

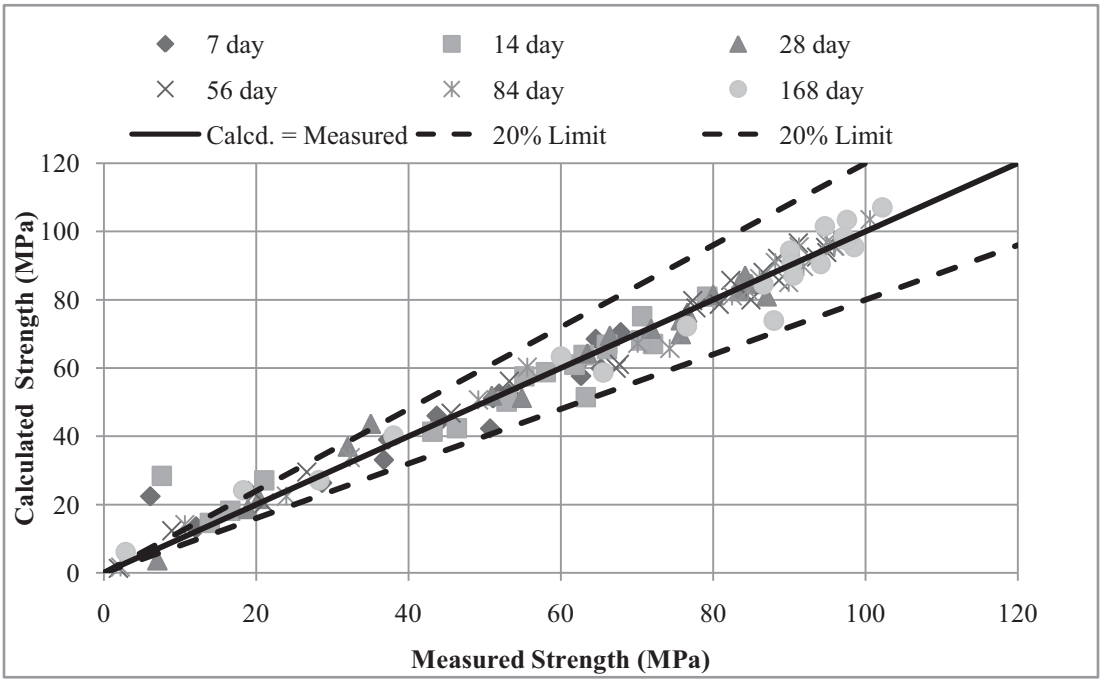

Figure 5.5. Calculated versus measured compressive strength of the binary SCM (w/b = 0.35), using the Bolomey strength equation and calibrated kP expression (Table 5.1)

This method is not practical since all of the strength data is needed to develop and expression for kP. Other expressions from published literature (Chapter 2) such as relating the strength to Blaine specific surface (fineness) (Hwang, Noguchi, & Tomosawa, 2004; Das & Yudhbir, 2006), were not used since the fineness of the SCM used were not determined. The expression from Rajamane, et al. 2007, was not used either since that expression is limited to fly ash as sand replacement.

The expression from Papadakis, et al. 2002, Eq. (2.21), to evaluate the k-value based on the active silica content of the SCM was used to estimate the k-values at age 28 day for the binary mixes with w/b = 0.35. Table 5.2 shows the calculated and measured k-values using this expression. This expression approximates the efficiency of the fly ash at 20 and 40% replacement levels reasonably well, whereas it over estimates the efficiency of the slag in all cases. The expression does a poor job of evaluating the efficiency at 80% replacement and at 100% replacement the expression does not work because the cement content is zero (dividing with zero). This expression has been used in published literature (Antiohos, Papadakis, Chaniotakis, & Tsimas, 2007; Papadakis, Antiohos, & Tsimas, 2002) to estimate the efficiency factor. In these research programs the expression did a good job of estimating the

efficiency of the SCMs; however the cement replacement was limited to only 20-30%. Therefore, an alternative methodology was investigated. Figure 5.6 shows the calculated versus measured strength using the k-values from Table 5.2 and using the modified Bolomey strength equation, Eq. (2.4).

Table 5.2. Measured and calculated k-values using Eq. (2.21) at an age of 28 days

SCM	Measured k-value					Calculated k-value				
	20%	40%	60%	80%	100%	20%	40%	60%	80%	100%
Boardman FA	1.00	1.09	0.93	0.42	0.25	0.99	0.90	0.71	0.14	NAN
Centralia FA	1.22	1.18	0.72	0.38	0.20	1.39	1.26	0.99	0.20	NAN
Seattle SL	0.58	0.91	0.77	0.68	0.39	1.35	1.23	0.97	0.20	NAN
St. Mary's SL	1.26	1.09	0.93	0.63	0.37	1.57	1.42	1.12	0.23	NAN

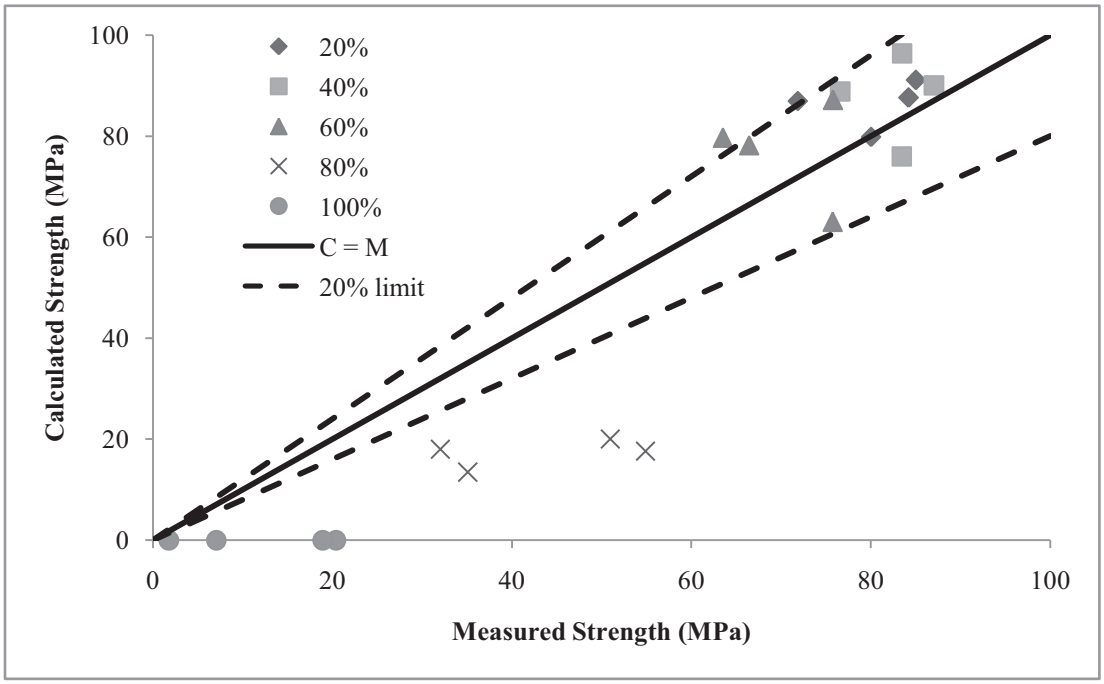

Figure 5.6. Measured and calculated strength using k-values from Table 5.2

5.1.2 Chemical Composition Effect

The results show an importance of several aspects of the chemical compositions of the SCMs and cement. It is postulated that not just the amount but the relative amount of the CaO (early strength, hydraulic reaction) and SiO_2 + Al_2O_3 (long-term strength, pozzolanic reaction) is critical. Thus, the objective is to go beyond amount of replacement, since the efficiency is not equal for all SCMs. The efficiency depends on the material source and on operating condition. Material variability is especially important for fly ash, since the requirements for

quality control is typically less than for slag. Hence, the objective was to consider only the chemical compositions (XRF analysis) part readily available to predict time-dependant compressive strength without testing.

It is known that the pozzolanic reaction (which is the major chemical reaction of SCM) is slow. For example, this is demonstrate with the 80% replacement Boardman FA mix, which has much lower strength than the control prior to day 28 but exceeds the strength of the control mix at day 168 (Figure 4.5). Chapter 1 describes the compounds that need to be available in the binder for the pozzolanic and hydraulic reaction to occur. Calcium hydroxide is produced by the hydration of Portland cement and is consumed by the pozzolanic reaction. The pozzolanic reaction can only take place after the hydraulic reaction starts.

The C_3S reaction is faster than the C_2S reaction, and as a result, is the major reaction at early-ages. The amount of CaO (C) enhances of C_3S reaction and therefore is beneficial to developing strength at early-ages. C_2S hydration and the pozzolanic reaction are considered to be similar; both are slow and affect the concrete's final strength. The amount of silica (S) contributes to the C_2S reaction and both silica and aluminum oxide (A) play an important role in the pozzolanic reaction. The amount of silica and aluminum oxide are associated with the long-term strength. Since theses three chemical compounds are critical to early and long-term strength, the compressive strength of the specimens was examined relative to the total ratio of CaO to the sum of SiO_2 and Al_2O_3.

Figure 5.7 and Figure 5.8 present strength versus the total C/(S+A) ratio, for 28 and 56-days strength for w/b = 0.35 and w/b = 0.40, respectively. For the ratio of C/(S+A) exceeding 1.5, the mixture's strength is approximately constant. As the ratio C/(S+A) decreases, the strength decreases approximately linearly. Similar trends were observed at other ages (Appendix E). The difference between concrete ages it that the slope, between 0-1.5 C/(S+A), becomes steeper and when C/(S+A) is greater than 1.5 the constant portion takes on a larger values. The trend is noted for both w/b ratios.

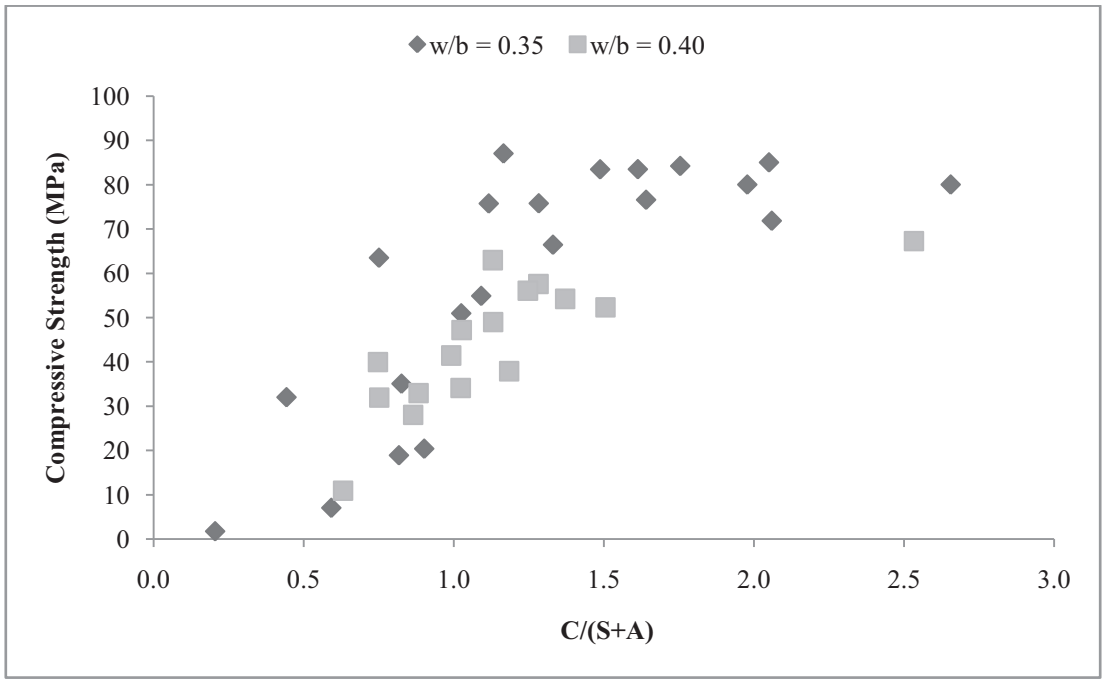

Figure 5.7. Relationship between the total C/(S+A) ratio and the 28-day strength

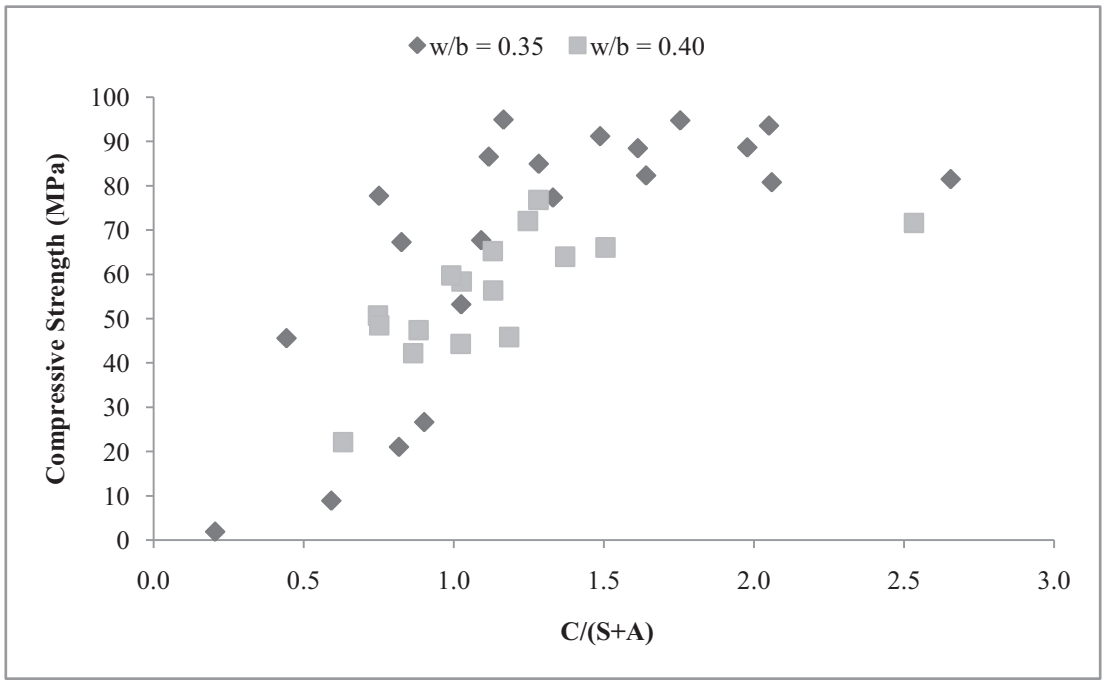

Figure 5.8. Relationship between the total C/(S+A) ratio and the 56-day strength

The equivalent cement content (kP) was compared to the total C/(S+A) ratio. It was observed that the kP versus C/(S+A) ratio had a second-order polynomial behavior (Appendix E). Thus, the second-order polynomial regression was used. Figure 5.9 and Figure 5.10, show the

equivalent cement content versus C/(S+A), for 28 and 56-days strength for w/b = 0.35 and w/b = 0.40, respectively. The optimum amount of C/(S+A) was computed by taking the derivative of the 2nd order equation and setting it equal to zero. The optimum C/(S+A) was found to be approximately 1.2 for both 28 and 56 days.

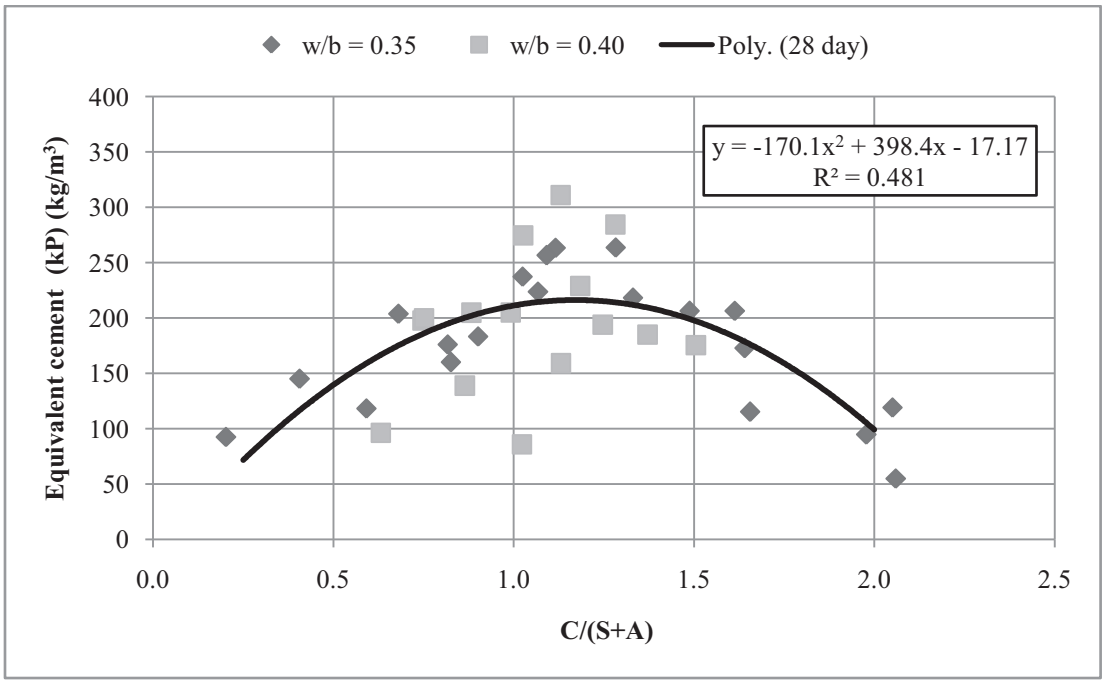

Figure 5.9. Equivalent cement content versus the total C/(S+A) at an age of 28 days

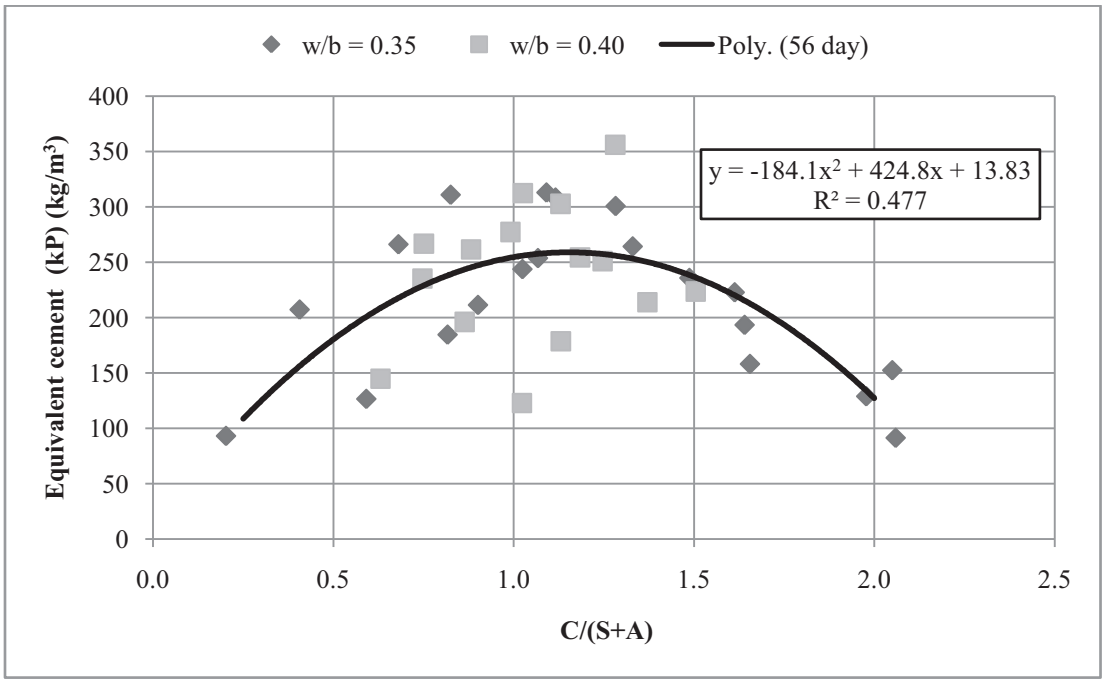

Figure 5.10. Equivalent cement content versus the total C/(S+A) at an age of 56 days

The efficiency factor (k-value) was also compared to the C/(S+A) ratio. Figure 5.11 through Figure 5.14 show the concrete's efficiency factors (*k*-value) as a function of the total C/(S+A) ratio in the binder at 7, 14, 28 and 56 days, respectively. For each plot a linear regression line was determined. Table 5.3 summarizes the values of the slope of the linear regression fit for each day and the R^2-values. The data show that the relationship between the k-values and the total C/(S+A) ratio in the binder is independent of w/b ratio. As the concrete ages, the slope increases and the coefficient of determination (R^2) increases.

Table 5.3. Slope at each age, standard error, R^2-value and number of data points

Age (day)	H (Slope)	Standard Error	R^2	Data Points
7	0.4	0.2	0.40	35
14	0.5	0.2	0.36	35
28	0.6	0.2	0.53	35
56	0.7	0.2	0.61	35
84	0.8	0.3	0.62	20
112	0.8	0.1	0.45	13
168	0.8	0.3	0.60	20

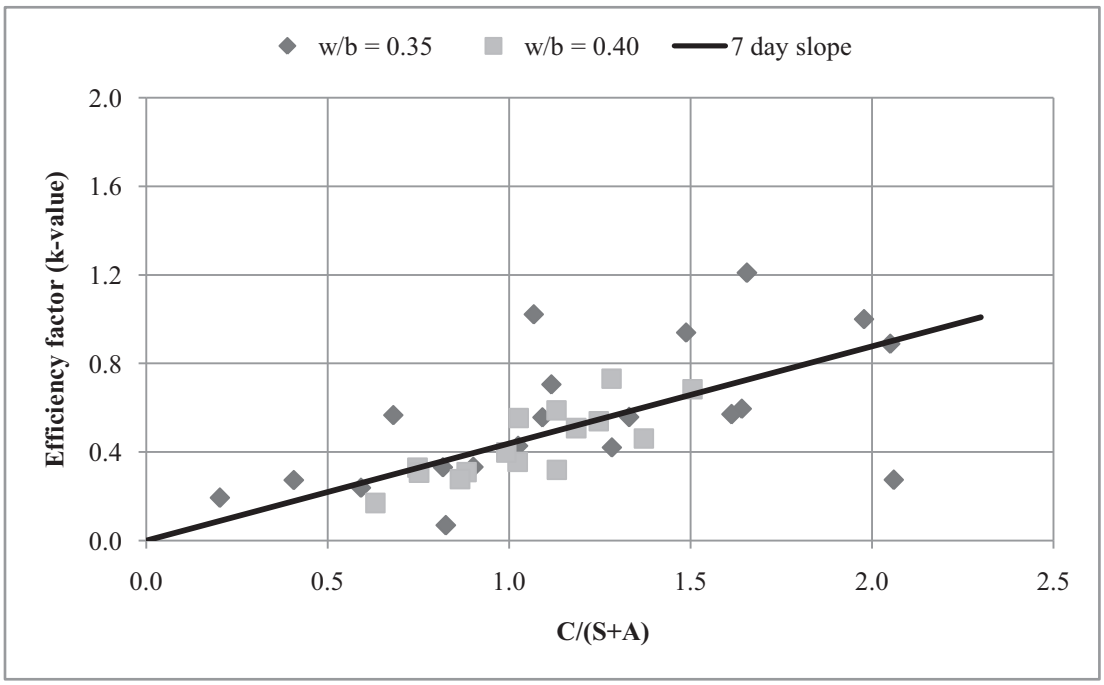

Figure 5.11. Efficiency factor (k-value) versus the total C/(S+A) at an age of 7 days

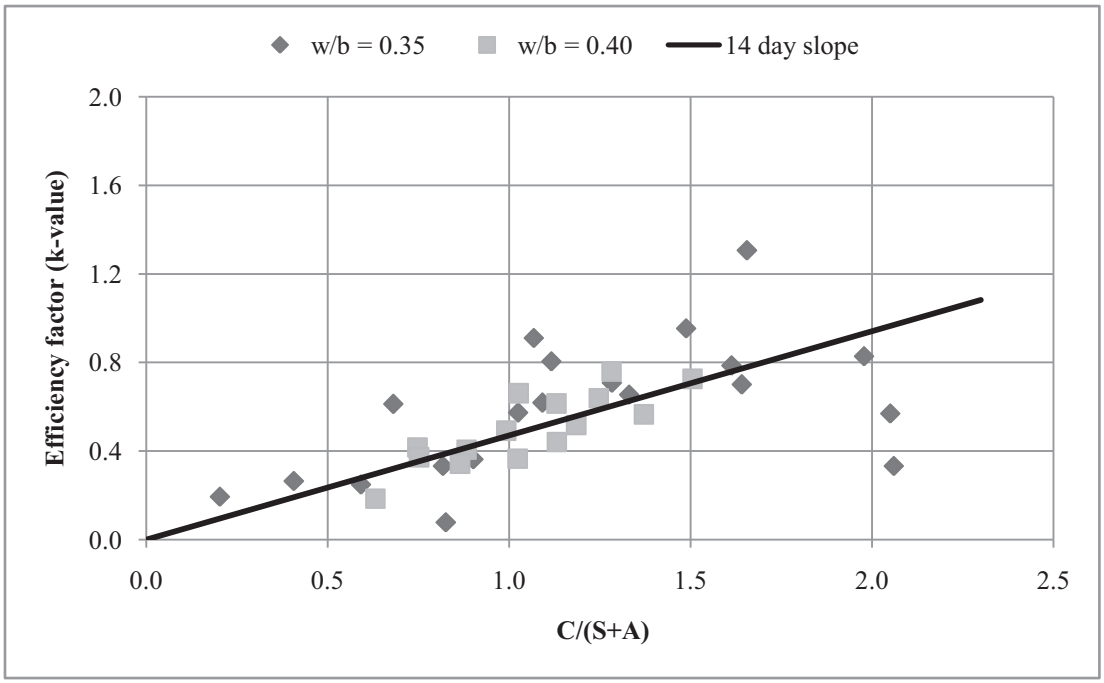

Figure 5.12. Efficiency factor (k-value) versus the total C/(S+A) at an age of 14 days

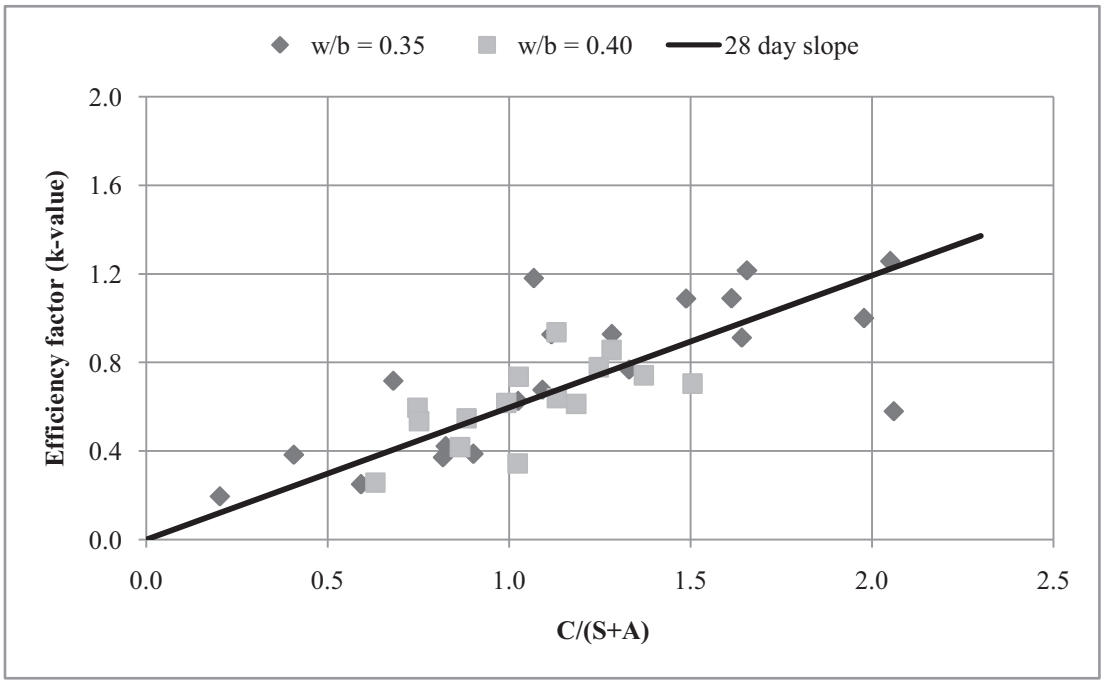

Figure 5.13. Efficiency factor (k-value) versus the total C/(S+A) at an age of 28 days

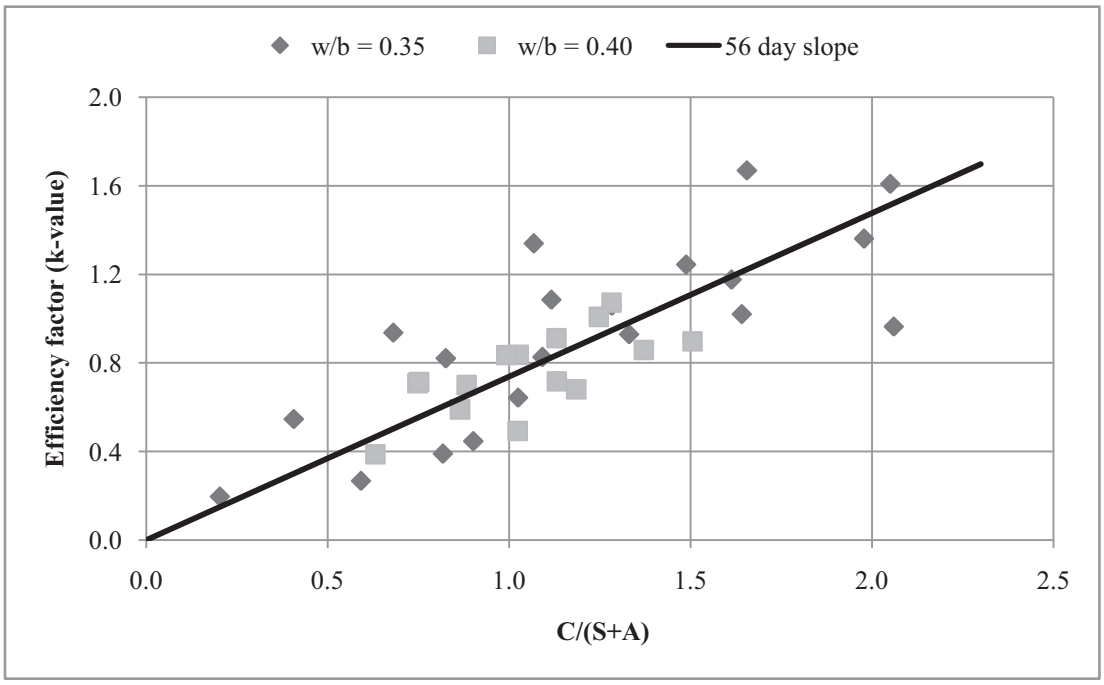

Figure 5.14. Efficiency factor (k-value) versus the total C/(S+A) at an age of 56 days

The slope data were used to relate the efficiency factor to the total C/(S+A) ratio in the binder (Table 5.3 and Figure 5.11 - Figure 5.14) using Eq. (5.1):

$$k(t) = H(t)\frac{C}{(S+A)} \tag{5.1}$$

where, *k(t)* is the efficiency factor at day t, *H(t)* is the slope between k and C/(S+A) at day *t*, *C/(S+A)* is the total ratio of the binder. Figure 5.15 displays the *H(t)* correlation and the standard error as a function of curing time.

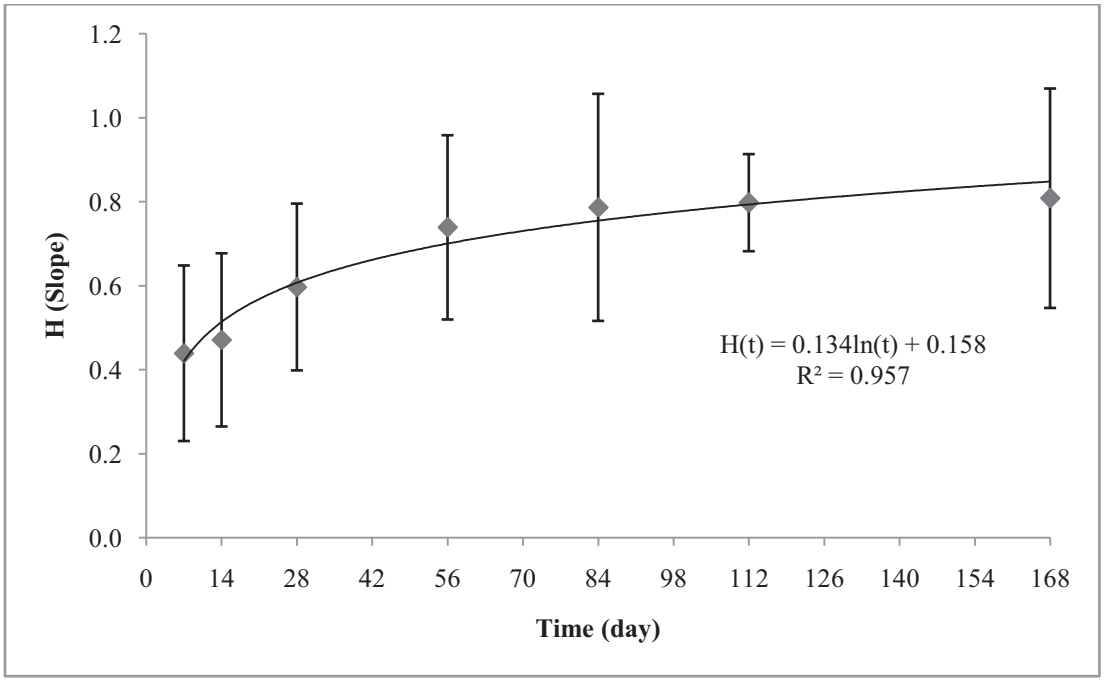

Figure 5.15. The correlation between the slope, H(t), and time

Eq. (5.1) provides an estimation of the efficiency of the SCM based solely on the total chemical composition of the binder. To use Eq. (5.1), K_B values of the modified Bolomey equation, Eq. (2.4), must be determined based on the base mix. Appendix E provides the measured strengths, calculated k-values and calculated strengths for this research program. Figure 5.16 shows the calculated versus measured strength of all of the mixes tested in this research program (w/b = 0.35 and w/b = 0.40). Figure 5.17 shows the same results as a function of replacement percentage. The calculated values are generally within 20% of the measured strength for replacement percentage less than 60%. At higher replacement percentage the calculated values exceed the 20% limit, especially for low strengths.

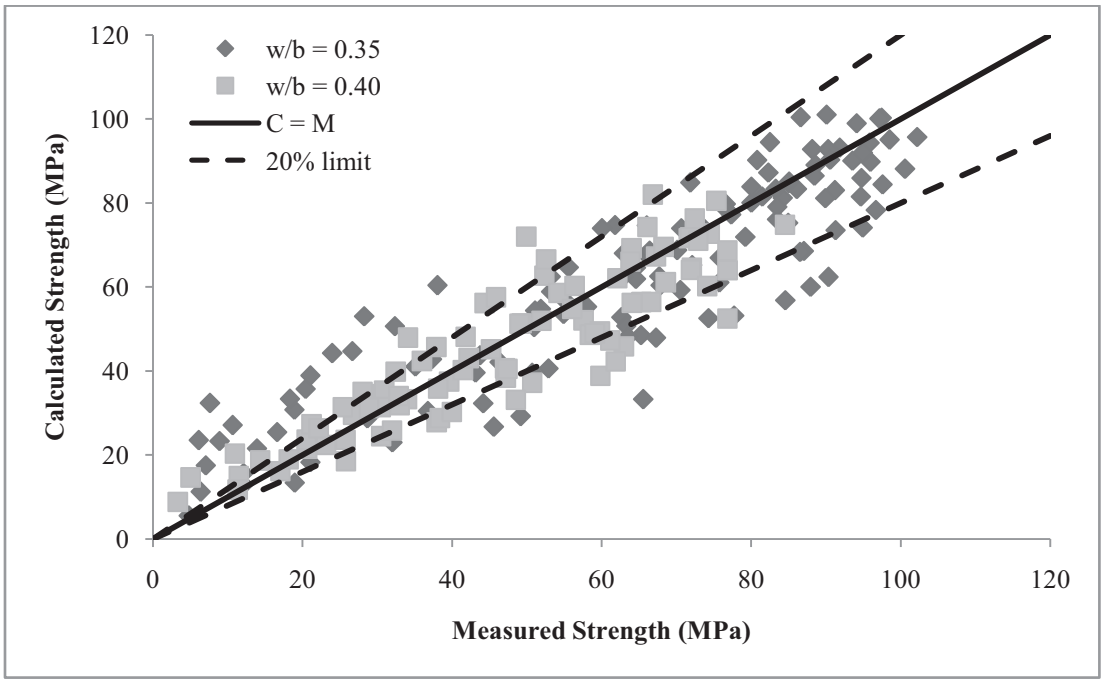

Figure 5.16. Calculated versus measured compressive using proposed efficiency expression

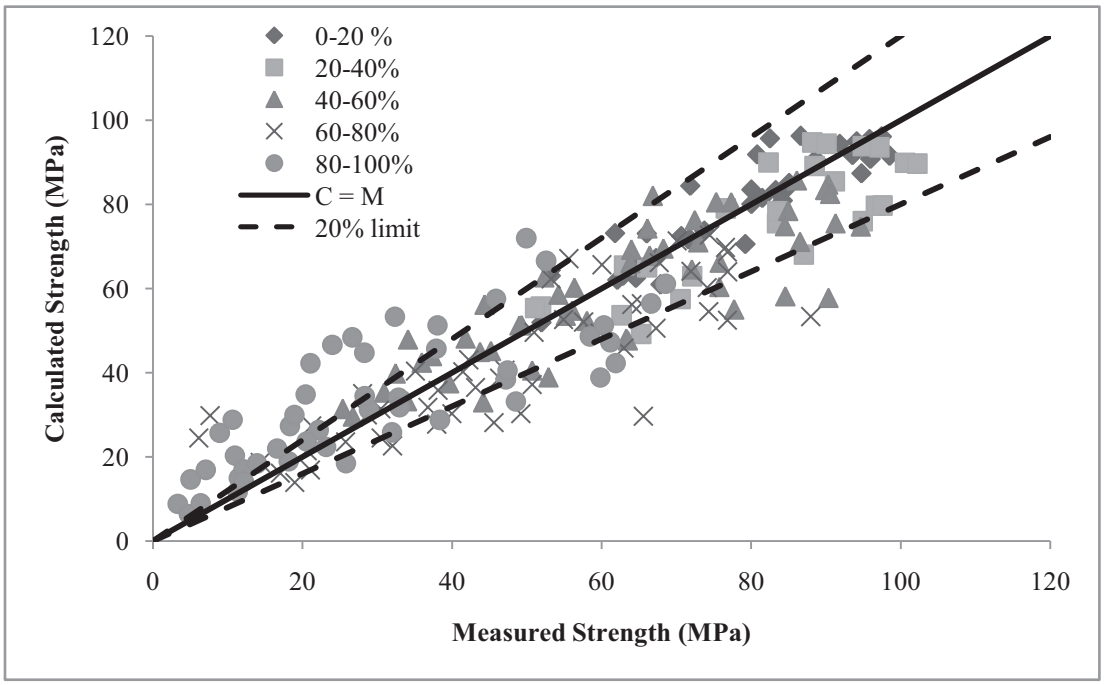

Figure 5.17. Calculated versus measured compressive strength using proposed efficiency expression (separated with replacement percentage)

Compressive strength of prior research data (presented in Chapter 2), in which the mix design and chemical composition of the SCM was provided, was calculated using the modified Bolomey strength equation. The proposed expression was used to evaluate the

efficiency of the SCMs. For each data set, the $K_B(t)$ and C/(S+A) was determined. Appendix F provides the measured strengths, calculated k-values and calculated strengths for the prior data. Figure 5.18 shows the calculated versus measured strength of prior data. All of the calculated data is close to or within 20% of the measured strength with the exception of one research program (Naik, Singh, & Ramme, 1998). For these strength values the calculated strength is a lot lower than the measured strength. The reason might be due to the unusually low strength values from the base mix in that research program. The low strength values might be the result of difference of coarse aggregate and admixture dosages of the base mix compared to the SCM mixes, which resulted in lower K_B value than usual. Therefore, it was decided to leave that strength data out. Figure 5.19 shows the same results without the strength data from Naik, et al. 1998.

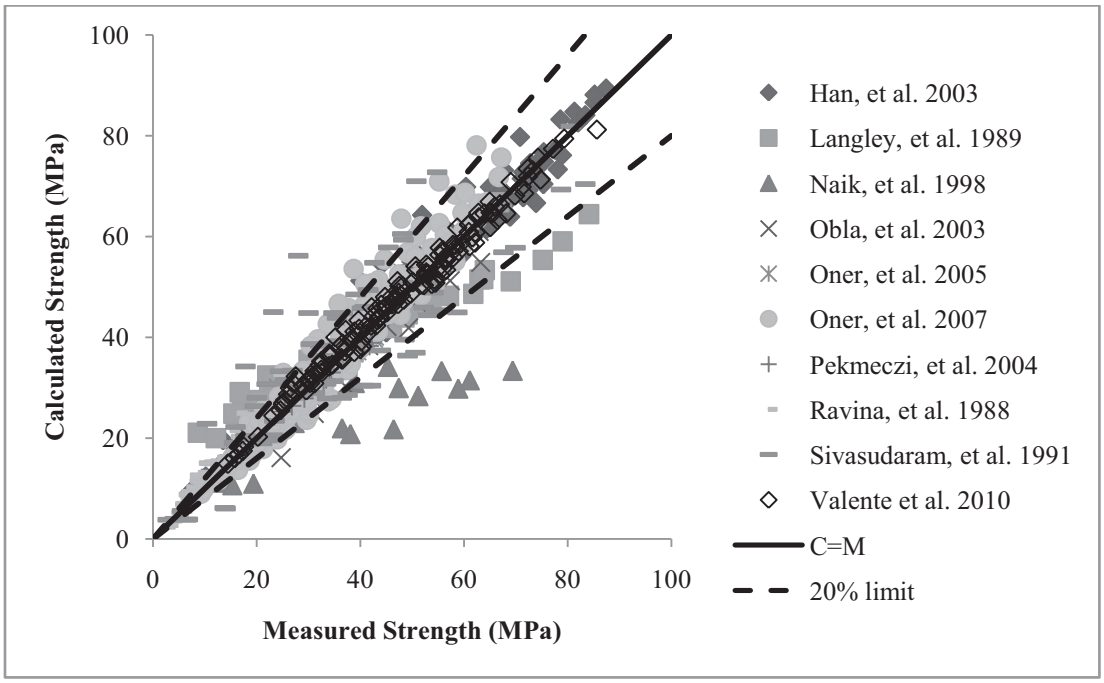

Figure 5.18. Calculated versus measured compressive strength from the prior research using proposed efficiency expression

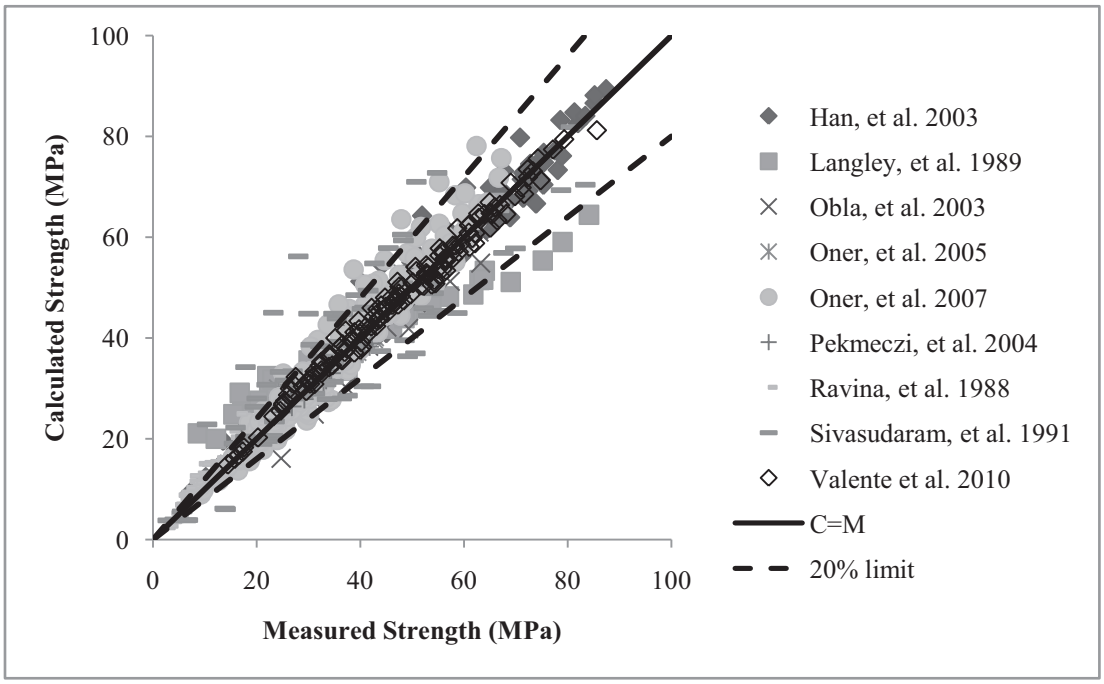

Figure 5.19. Calculated versus measured compressive strength from the prior research using proposed efficiency expression without the data from Naik, et al. 1998

Figure 5.20 shows the same results separated with replacement level. The calculated values are generally within 20% of the measured strength for replacement levels less than 40%. There was no strength data available for the 80 to 100% replacement level. Figure 5.21 shows the calculated/measured strength at 28 days from prior result as function of w/b ratio. This figure shows that the proposed efficiency equation works for wide w/b ratios, which suggest that the efficiency equation is independent of w/b ratio. Although, this is a simple relationship and does not consider any physical properties (such as fineness, active silica, or specific gravity), the data implies that relating the total C/(S+A) ratio in the binder is an excellent first approximation to evaluate the SCM's efficiency and to predict strength without test data.

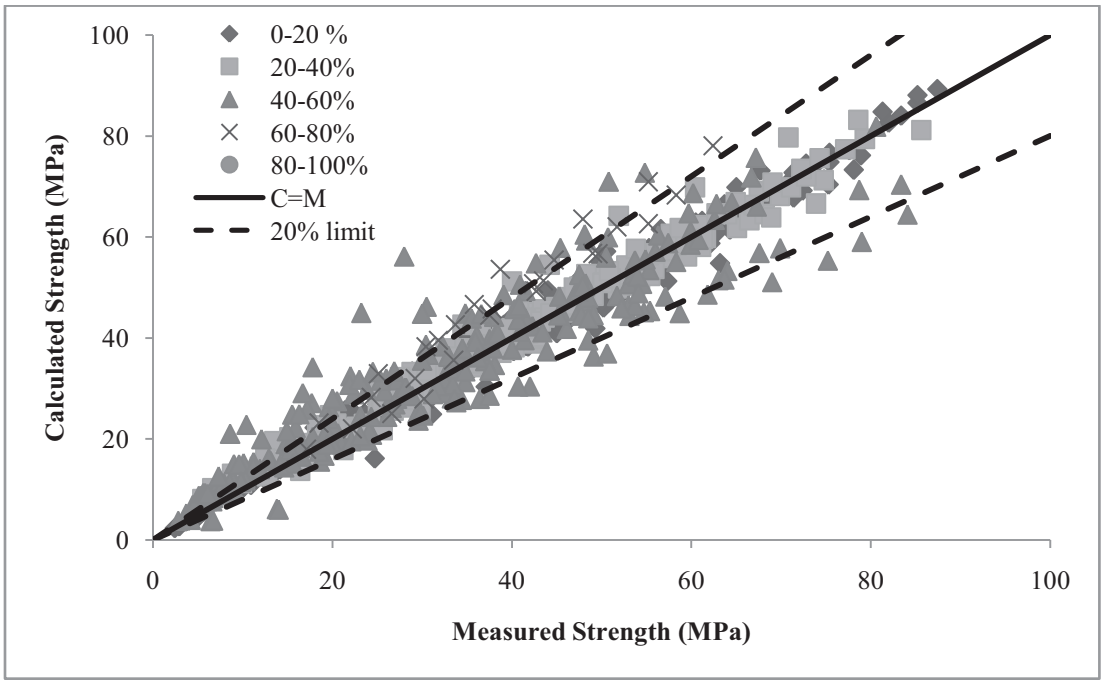

Figure 5.20. Calculated versus measured compressive strength from the prior research using proposed efficiency expression (separated with replacement percentage)

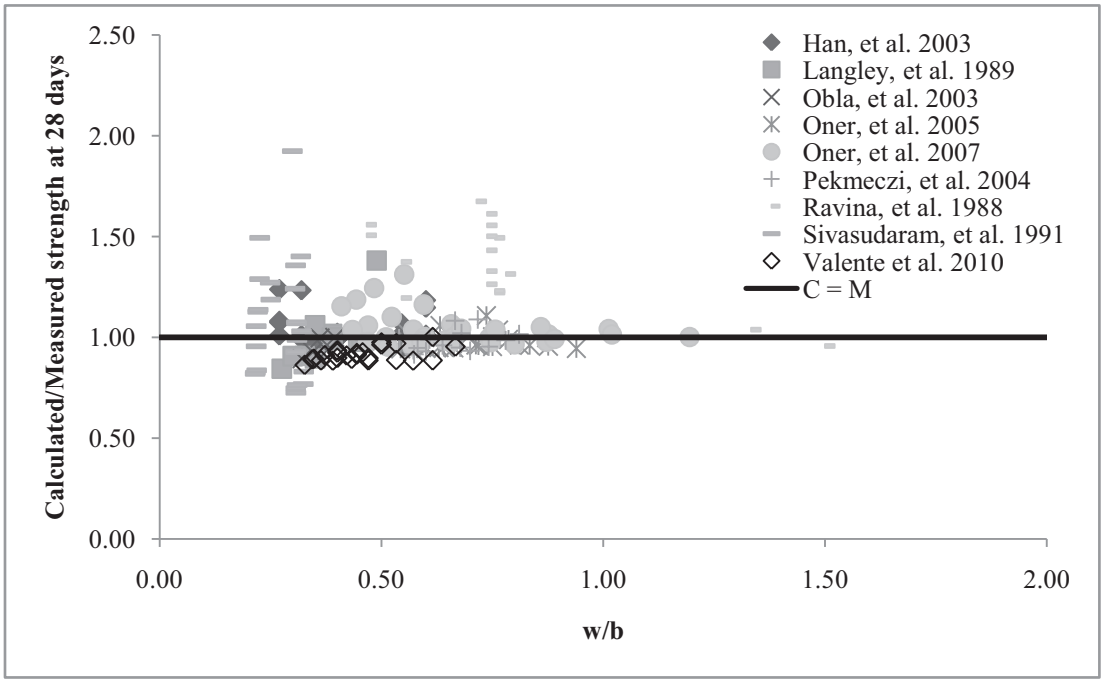

Figure 5.21. Calculated/Measured strength at 28 days versus w/b ratio from the prior research

5.2 Modulus of Elasticity

Typical design expressions for the modulus of elasticity are based on the compressive strength. For normal weight concrete with density of 2323 kg/m^3 (145 lb/ft^3), ACI 318 Section 8.5.1 gives the modulus of elasticity as (ACI Committee 318, 2008):

$$E = 4730\sqrt{f_c'} \tag{5.2}$$

where, E is the elastic modulus (MPa) and f'_c is the compressive strength (MPa). Figure 5.22 shows the calculated versus measured elastic modulus for the concrete mixes using Eq. (5.2). The calculated modulus is always less than the measured modulus, on average 20% lower. ACI 318 Section R8.5.1 states that measured values range typically 120 to 80 percent from the specific value from Eq. (5.2). Therefore all the calculated values should be within the 20% limit; however the measured data deviates from this.

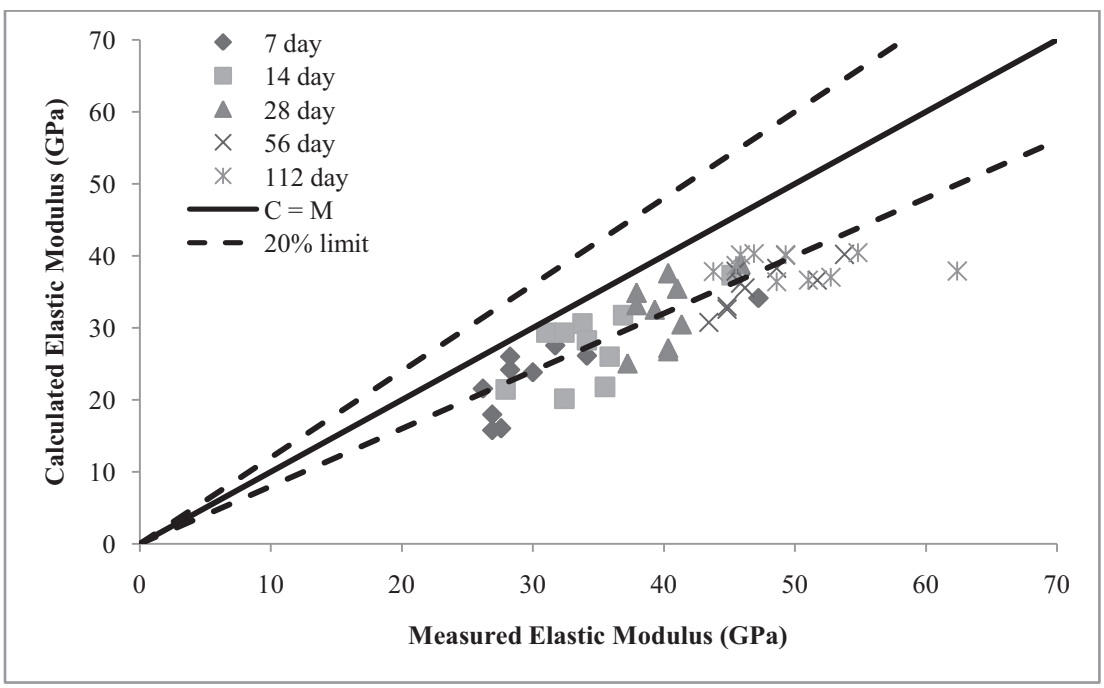

Figure 5.22. Calculated versus measured elastic modulus by using the ACI equation, Eq. (5.2)

European standard provides the following expression to calculate the elastic modulus (CEB, 1997):

$$E = 10000(f_c' + 8)^{0.33} \quad \textbf{(5.3)}$$

Figure 5.23 shows the calculated versus measured elastic modulus data. All the calculated values at age 56 day and less are within 20% of the measured value. At age 112 days few of the calculated values exceeds the 20% limit. One mix (80% SCM with 50:50 FA to SL ratio) is far from the calculated value. Over all, when the expressions from the ACI and the European standard are compared, the calculated values from the European standard are closer to the measured values. Form this data it can be concluded that it is better to use the equation from the European standard to estimate elastic modulus of SCC with high volume of SCM.

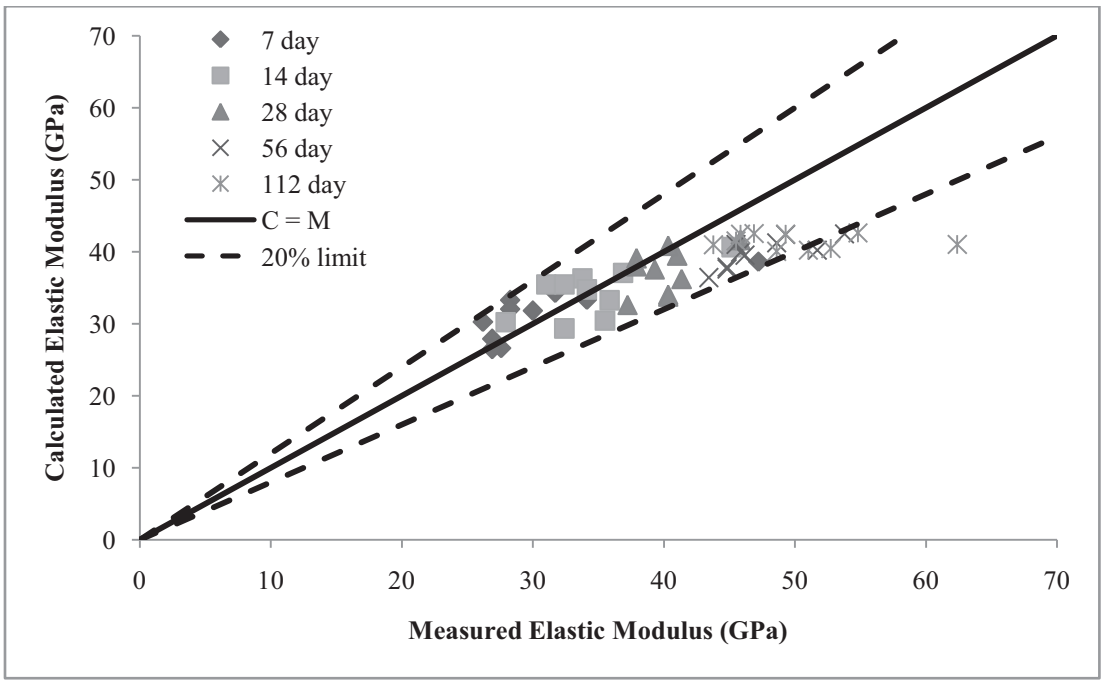

Figure 5.23. Calculated versus measured elastic modulus by using the CEM equation, Eq. (5.3)

5.3 Rheological Model for Creep

A one dimensional model consisting of two springs and one dashpot was used to model creep. Figure 5.24 illustrates the model. Where σ denotes the total stress, the E_0 and E_1 are spring constants and the viscosity in the (linear) dashpot is τ. The variable ε denotes the total strain, where ε^e is the strain in the spring and ε^v is the strain in the dashpot.

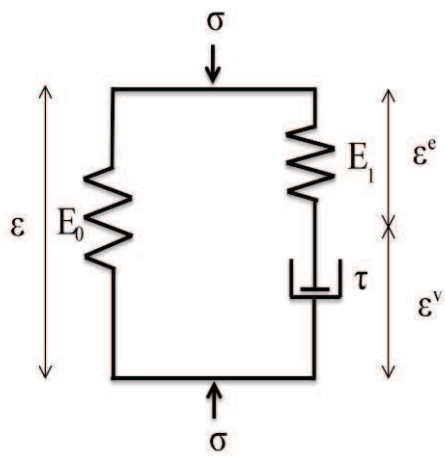

Figure 5.24. One dimensional mechanical device

The governing equation of the model is derived using the internal variables in Figure 5.24. The governing equation must satisfy equilibrium, kinematics and constitutive relation. The external force form the applied stress (σ) must in equilibrium with the internal forces. Since model is one dimensional (has unit width), the external stress (σ) is in equilibrium with the internal stress (σ_0 and σ_1):

$$\sigma = \sigma_0 + \sigma_1 \tag{5.4}$$

where, σ_0 and σ_1 are the stresses in the springs. Using the kinematics of the device the following equation is obtained:

$$\varepsilon = \varepsilon^e + \varepsilon^v \tag{5.5}$$

Taking derivative of Eq. (5.5) with respect with time the following equation is obtained:

$$\frac{d\varepsilon}{dt} = \dot{\varepsilon} = \dot{\varepsilon}^e + \dot{\varepsilon}^v \tag{5.6}$$

The constitutive relations are:

$$\sigma_0 = E_o \varepsilon \tag{5.7}$$

$$\sigma_1 = E_1 \varepsilon^e = \tau E_1 \dot{\varepsilon}^v \tag{5.8}$$

The governing equation for the device is achieved by combining Eqs. (5.4) through (5.8)

$$\tau(E_1 + E_0)\dot{\varepsilon} + E_0 \varepsilon = \sigma + \dot{\sigma}\tau \tag{5.9}$$

Eq. (5.9) is a differential equation and can be solved for either constant stress or constant strain. The constant stress case simulates the creep behavior of a material. Constant strain would be the case if strain is restrained, then a stress relaxation will occur as a result of creep behavior.

5.3.1 Creep model – Constant Stress

Eq. (5.9) is solved for constant stress to model creep behavior of concrete:

$$\varepsilon(t) = \left(\frac{\sigma}{(E_0 + E_1)} - \frac{\sigma}{E_0}\right) exp\left(\frac{-E_0 t}{\tau(E_0 + E_1)}\right) + \frac{\sigma}{E_0} \tag{5.10}$$

where, ε(t) is the creep strain at time t (m/m), t is the time since load is applied (day), σ is the constant applied stress (MPa), (E_0 + E_1) is the instantaneous elastic modulus of the concrete (MPa), E_0 is the elastic modulus of the concrete at time infinity (MPa) and τ is the relaxation time of the concrete (day)

The data from the creep test were used to calibrate the coefficients in Eq. (5.10). Table 5.4 summarizes the value of the constants, in addition comparison of the (E_0 + E_1) and measured elastic modulus (from Table 4.6). The (E_0 + E_1) values compares reasonably well with the measured values with the exception of the SCM concrete loaded at 7 day, which was lower, and 28 day, which is somewhat higher.

Figure 5.25 and Figure 5.26 compares the model with the test data of the unsealed and sealed specimens. The model accurately captures the creep behavior of the specimens. However, this model must be calibrated to experimental data, which may not be practical.

Table 5.4. Material constants for creep model

Concrete	Age of loading	Cylinder	Eo (GPa)	E1 (GPa)	τ (day)	Eo + E1 (GPa)	E - test (GPa)
SCM	7 day	Unsealed	7	16	15	23	28
		Sealed	12	10	16	23	
SCM	14 day	Unsealed	10	20	21	30	28
		Sealed	15	14	16	29	
SCM	28 day	Unsealed	21	33	20	54	40
		Sealed	26	25	9	51	
Base II	7 day	Unsealed	15	35	21	49	47
		Sealed	25	20	20	45	

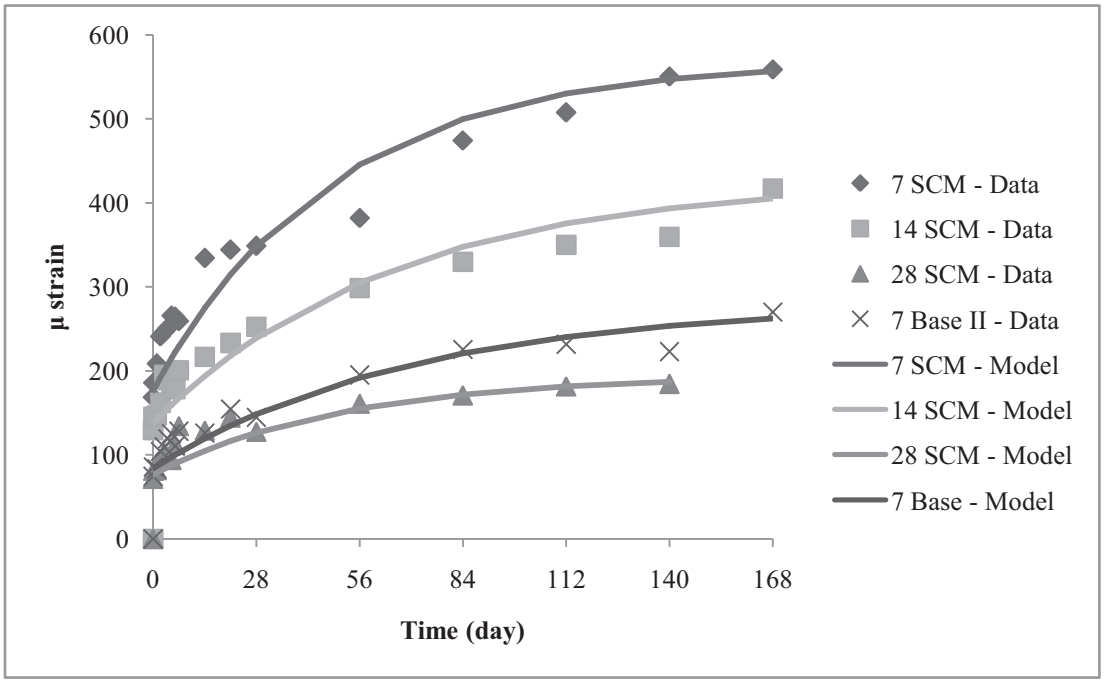

Figure 5.25. Comparison of test data and model for unsealed cylinders (total creep)

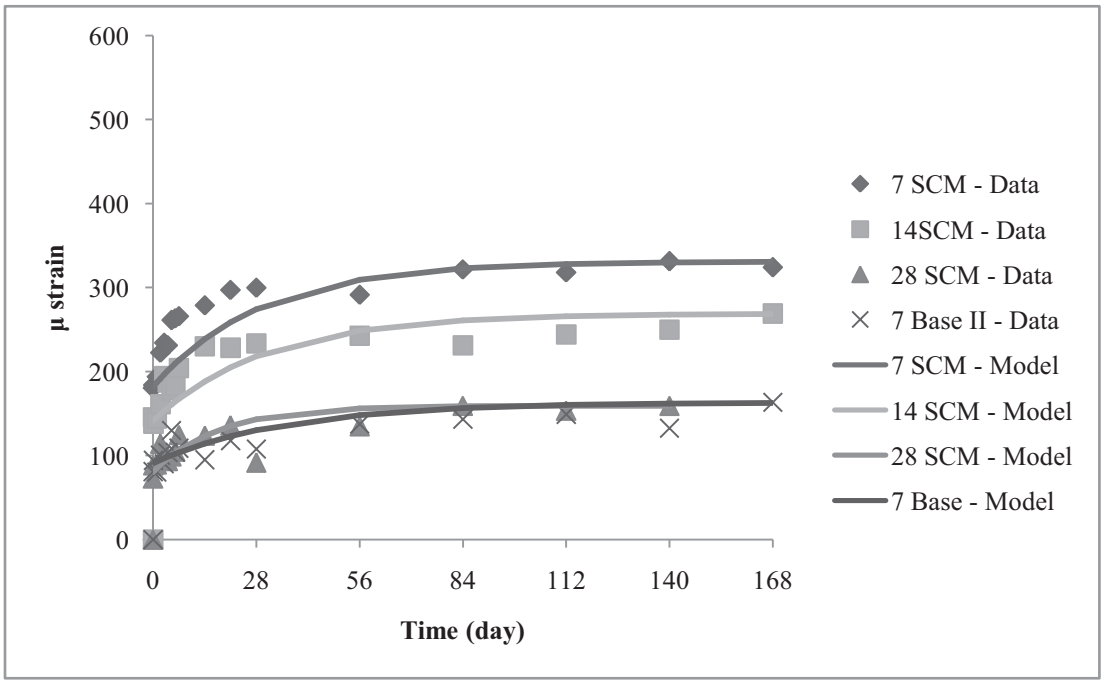

Figure 5.26. Comparison of test data and model for sealed cylinders (basic creep)

5.3.2 Relaxation model – Constant Strain

Eq. (5.9) needs to be solved for constant strain, to model stress relaxation of concrete. The solution is:

$$\sigma(t) = (\sigma - E_0\varepsilon_0)exp(-t/\tau) + E_o\varepsilon_0 \tag{5.11}$$

where, σ(t) is the stress in the concrete at time t (MPa), σ is the initial constant applied stress (MPa), ε_0 is the restrained strain (constant) (m/m), E_0 is the elastic modulus of the concrete at time infinity (MPa) and τ is the characteristic time of the concrete, the time it takes strain to reach a constant value (day)

The same coefficients can be used to model creep behavior and stress relaxation. The coefficients in Table 5.4 can therefore be used to model stress relaxation of the concrete. Applications for this model would be for the case if strain is restrained. For example, in a concrete filled tube where the outer steel jacket restrains the deformation of the concrete, then a stress relaxation will occur as a result of creep behavior, and the stress demand on the steel jacket increases.

Chapter 6: Conclusions and Recommendations

A research program was undertaken to determine the mechanical properties of SCC with the research emphasized on high-cement replacement ratios (60-90%) as they have had limited attention in the literature. This research was performed in two phases. Phase I had concrete with water-binder-ratio of 0.35 and focused on binary concretes with different SCMs. In the first Phase, compressive strength, initial time of set and air content were measured. Phase II had concrete with water-binder-ratio of 0.40. This Phase developed binary and ternary mixes using two SCMs. In the second Phase, elastic modulus, creep and shrinkage strains as well as compressive strength were measured

One of the primary objectives was to develop practical methods to predict the time dependent mechanical properties of SCM rich concretes. There is a high material variability associated with SCM which affects their efficiency and concrete containing high SCM dosages affect the compressive strength relative to a conventional concrete, particularly at ages less than 28 days. Compressive strength and efficiency factors were related to information that is readily available for designers from XRF chemical analysis. Models were also developed to predict the long-term compressive (creep) strain.

6.1 Conclusions

6.1.1 Time of Set

- The setting time was generally close to the setting time of the base mix, except for high replacement ratios (60-100%) of the Class C Boardman FA, where the setting time decreased significantly. Set retarding agents can be used to control the time of set as needed.

6.1.2 Compressive Strength

6.1.2.1 Binary Compressive Strength

- The results showed that fly ash has an optimum replacement of approximately 60% where the slag has an optimum replacement between 60 and 80%.

- The early-age (≤14 days) compressive strength development of the SCM mixtures is normally less than that of the control mixture. This trend was expected since the pozzolanic reaction is slower than the hydraulic reaction.

- As the curing period is extended the SCM binary mixtures, with replacement of 60% and less, had a higher strength than the base mix.

- At 80% and 100% cement replacement levels, the strength performance varies significantly based on the SCM used. The SL-mixes had higher and more reliable strength development than the FA-mixes at early ages. However, as the curing period was extended the FA-mixes exhibit more strength development than the SL-mixes.

- The compressive strength of the 100% replacement is quite low, which indicates that some cement needs to be present in the binder so the pozzolanic reaction can occur. The difference in strength depends on SCM type and the amount of CaO.

6.1.2.2 Ternary Compressive Strength

- The ternary mixes in Phase II always showed higher compressive strength than binary FA mix for a given replacement level with the exception of the SCM ternary mix with 75:25 FA to SL ratio at 80% cement replacement (80% 75FA-25SL-II). It was expected that the ternary mixes would show higher strength since it had a higher CaO content in the binder.

- Two of the ternary mixes in Phase II with 60% replacement exhibit higher strength than both binary mixes at age 112 day, which indicates that synergy between the fly ash and slag, has taken place. The synergy between the fly ash and slag is more prominent at 90% replacement level.

- In general, the ternary mixes with 50:50 fly ash to slag ratio, had the most reliable strength development.

6.1.2.3 Analytical Expressions for the Compressive Strength

- Using second-order polynomial regression to relate equivalent cement content to the SCM content with the modified Bolomey strength equation gives good results for

structural grade concrete (strength greater than 17.2 MPa). Eighty-six percent of the data fell within 20% of the measured strength by using the Bolomey equation. However, all the strength data needs to exist in order to use this method.

- Relating the ratio C/(S+A) in the binders to the efficiency factor (*k*-value), gives the impression that it might be applicable for predicting compressive strength. The proposed efficiency equation proves to be independent of w/b ratio of the mix. If this relationship holds true for all SCMs, then the ratio of C/(S+A) can be used to estimate how efficient the SCM is for certain cement replacement levels and w/b ratio.

6.1.3 Elastic Modulus

- Elastic modulus was not impacted as much as the compressive strength with increasing SCM replacement level. It was observed that all the SCM mixes had similar elastic moduli that gradually increase up to age 56 days. Beyond that age, the modulus is somewhat constant indicating that the SCM mixes have developed their long-term modulus. On average the elastic modulus of the SCM mixes increase by 40% between 7 to 112 days.

- The Base II mix (100% cement) exhibits a constant elastic modulus behavior between days. This trend indicates that it has developed the majority of its long-term modulus in the first week. The elastic modulus of the Base II mix is almost time independent.

- All the elastic modulus values are rather high compared to the strength values and are probably the result of the unhydrated fly ash and slag particles acting as fine aggregate.

6.1.3.1 Analytical Expressions for Elastic Modulus

- Two equations for estimating the elastic modulus are compared; the commonly used ACI equation and an equation from the European code

- It was observed that the ACI expression underestimated the elastic modulus in all cases. Using the expression from the European standard led to calculated values that were generally within 20% of the measured value. From these data it can be

concluded that it is better to use the equation from the European standard to estimate elastic modulus of SCC with high volume of SCM.

6.1.4 Creep and Shrinkage Strains

6.1.4.1 Shrinkage strains

- Shrinkage strains of the unsealed specimens were less than the sealed specimens. This trend was expected since less water evaporation occurs in the sealed specimens. Strains in both sealed and unsealed specimens show little difference between mixes and curing periods.

6.1.4.2 Creep strains

- The creep strains of the sealed specimens were less than the unsealed specimens. This trend was expected since less water evaporation occurs in the sealed specimens. The same mix with higher stress/strength ratio showed higher creep strains, which was also expected.

- The 90% 50FA-50SL-II mix that is loaded after 28 days showed creep strain that is similar to the Base II mix that was loaded after 7 days, even though it has a slightly higher stress/strength ratio. Their respective stress/strength ratios were 0.13 and 0.08.

- In general all the creep strains were low which is probably due to a large portion of fly ash and slag remaining unreacted in the concrete and, therefore, acting as a fine aggregate providing higher resistance against creep.

6.1.4.3 Analytical Expressions for Creep

- A one dimensional model consisting of two springs and one dashpot was used to model the creep behavior of the specimens. The model did a good job of capturing the creep behavior of the specimens. However, this method needs experimental data in order to calibrate all the material coefficients in the model.

6.2 Recommendations for Further Research

Based on this investigation, a few recommendations for future research can be made:

- Different w/b ratio and different SCMs should be tested for compressive strength to evaluate if the proposed efficiency equation works.
- Further research should also be done on the creep behavior of concrete containing high volumes of SCM.
- Concrete mixes at different replacement levels and at higher loads should be evaluated.
- Expressions that predict long-term creep strain and elastic modulus values without performing tests are also needed.

This research focused only on the mechanical properties of concrete at material levels. Future work would include testing the high replacement levels concrete in a full scale structural applications. Possible composite components that could be tested include concrete filled tubes for structural columns and dual skin composite shear walls to resist gravity and seismic loadings. An advantage of using a high-volume SCM concrete in these applications is that early strength is not required from the concrete, since the steel jacket is capable of supporting the initial construction load and formwork is not removed (as would be required for a reinforced concrete component). Therefore, concrete containing high volume of SCM can be more readily used in composite construction, even though a low early strength (≤ 14 days) is often associated with such concrete.

Reference

A23.1. (2004). *Concrete materials and methods of concrete construction/Methods of test and standard practices for concrete.* Ontario: Canadian Standards Association.

AASHTO M 302. (2006). *Standard Specification for Ground Granulated Blast-Furnace Slag for Use in Concrete and Mortars.*

ACI Committee 318. (2008). *Building Code Requirements for Structural Concrete and Commentary.* Farmington Hills: ACI.

Antiohos, S. K., Papadakis, V. G., Chaniotakis, E., & Tsimas, S. (2007). Improving the performance of ternary blended cements by mixing different types of fly ashes. *Cement and Concrete Research* , 877-885.

Antiohos, S. K., Papageorgiou, A., Papadakis, V. G., & Tsimas, S. (2008). Influence of quicklime addition on the mechanical properties and hydration degree of blended cements containing different fly ashes. *Construction and Building Materials , 27*, 1191-1200.

ASTM C 150. (2009). *Standard Specification for Portland Cement* (Vol. 04.01). ASTM Comittee C09.

ASTM C 1611. (2009). *Standard Test Method for Slump Flow of Self-Consolidating Concrete* (Vol. 04.02). ASTM Comittee C09.

ASTM C 231. (2008). *tandard Test Method for Air Content of Freshly Mixed Concrete by the Pressure Method.* ASTM Comittee C09.

ASTM C 403. (2008). *Standard Test Method for Time of Setting of Concrete Mixtures by Penetration Resistance* (Vol. 04.02). ASTM Comittee C09.

ASTM C 618. (2008). *Standard Specification for Coal Fly ash and Raw or Calcined Natural Pozzolan for use in Concrete* (Vol. 04.02). ASTM Comittee C09.

ASTM C 989. (2009). *Standard Specification for Slag Cement for Use in Concrete and Mortars* (Vol. 04.02). ASTM Comittee C09.

Babu, K. G., & Kumar, V. S. (2000). Efficiency of GGBS in concrete. *Cement and Concrete Research , 30*, 1031-1036.

Brandt, A. (1995). Cement based composites: materials, properties and performance. *E and FN SPON* .

Carette, G., Bilodeau, A., Chevrier, R. L., & Malhotra, V. M. (1993). Mechanical Properties of Concrete Incorporating High Volumes of Fly Ash from Sources in the U.S. *ACI Materials Journal , 90*, 535-544.

CEB. (1993). *CEB-FIP Model Code 1990.* London: Thomas Telford Service Ltd.

CEB. (1997). *European Standard for Design of Concrete Structures.* London: Thomas Telford Service Ltd.

CEMBUREAU. (2009). *Activity Report 2008.* Brussels: CEMBUREAU.

Cross, D., & Stephens, J. (2005). An Alternative to Portland Cement Concrete. *Proceedings of The Third International Conference on Construction Materials: Performance, Innovations and Structural Implications and Mindess Symposium.* Vancouver.

Cross, D., Stephens, J., & Berry, M. (2010). Sustainable Construction Contributions from the Treasure State. *Concrete international* , 41-46.

Das, S. K., & Yudhbir. (2006). A simplified model for prediction of pozzolanic characteristics of fly ash, based on chemical composition. *Cement and Concrete Research , 36*, 1827-1832.

Dhir, R. K., McCarthy, M. J., & Title, P. A. (1994, May). Use of conditioned PFA as fine aggregate in concrete. *Indian Concrete Journal* , 278-282.

European Standard EN 196-2. (2005). *Methods of testing cement - Part 2: Chemical analysis of cement.* Brussels: CEN.

European Standard EN 197-1. (2000). *Cement - Part 1: Composition, specifications and conformity criteria for common cements.* Brussels: CEN.

Han, S.-H., Kim, J.-K., & Park, Y.-D. (2003). Prediction of compressive strength of fly ash concrete by new apparent activation energy function. *Cement and Concrete Research , 33*, 965-971.

Hwang, K., Noguchi, T., & Tomosawa, F. (2004). Prediction model of compressive strength development of fly-ash concrete. *Cement and Concrete Research , 34*, 2269-2276.

Langley, W. S., Carette, G. F., & Malhotra, V. M. (1989). Structural Concrete Incorporating High Volumes of ASTM Class F Fly Ash. *ACI Materials Journal , 86*, 507-514.

Malhotra, V. M. (2006, September). Reducing CO2 Emissions - The role of fly ash and other supplementary cementitious materials. *Concrete international* , 42-45.

Mangaraj, B. K., & Krishnamoorthy, S. (1994, May). Use of pond fly ash as part replacement for mortar and concrete. *Indian Concrete Journal* , 279-282.

Mehta, P. K. (2009, February). Global Concrete Industry Sustainability - Tools for moving forward to cut carbon emissions. *Concrete international* , 45-48.

Mindess, S., Young, J. F., & Darwin, D. (2003). *Concrete - Second Edition.* Upper Saddle River: Pearson Education, Inc.

Naik, T. R., & Singh, S. S. (1997). Influence of Fly Ash on Setting and Hardening. *ACI materials journal , 94*, 355-360.

Naik, T. R., Singh, S., & Ramme, B. (1998). Mechanical Properties and Durability of Concrete Made with Blended Fly Ash. *ACI Materials Journal , 95*, 454-462.

Nasser, K. W., & Al-Manaseer, A. A. (1986). Creep of Concrete Containing Fly Ash and Superplasticizer at Different Stress/Strength Ratios. *ACI Journal* , 668-673.

Obla, K. H., Hill, R. L., Thomas, M. D., Shashiprakash, S. G., & Perebatova, O. (2003). Properties of Concrete Containing Ultra-Fine Fly Ash. *ACI Materials Journal , 100*, 426-433.

Oner, A., & Akyuz, S. (2007). An experimental study on optimum usage of GGBS for the compressive strength of concrete. *Cement & Concrete Composites , 29*, 505-514.

Oner, A., Akyuz, S., & Yildiz, R. (2005). An experimental study on strength development of concrete containing fly ash and optimum usage of fly ash in concrete. *Cement and Concrete Research , 35*, 1165-1171.

Papadakis, V. G., & Tsimas, S. (2002). Supplementary cementing materials in concrete Part I: efficiency and design. *Cement and Concrete Research , 32*, 1525-1532.

Papadakis, V. G., Antiohos, S., & Tsimas, S. (2002). Supplementary cementing materials in concrete Part II: A fundamental estimation of the efficiency factor. *Cement and Concrete Research* , 1533-1538.

Pekmezci, B. Y., & Akyüz, S. (2004). Optimum usage of a natural pozzolan for the maximum compressive strength of concrete. *Cement and Concrete Research , 34*, 2175-2179.

Rafat, S. (2003). Effect of fine aggregate replacement with Class F fly ash on mechanical properties of concrete. *Cement and Concrete Research , 33*, 539-547.

Rajamane, N. P., Peter, J. A., & Ambily, P. S. (2007). Prediction of compressive strength of concrete with fly ash as sand replacement. *Cement & Concrete Composites , 29*, 218-223.

Ravina, D., & Mehta, P. K. (1988). Compressive strenght of low cement/high fly ash concrete. *Cement and Concrete Research , 18*, 571-583.

Sivasundaram, V., Carette, G. G., & Malhotra, V. M. (1991). Mechanical Properties, Creep and Resistance to Diffusion of Chloride Ions of Concretes Incorporating High Volumes of ASTM Class F Fly Ashes from Seven Different Sources. *ACI Materials Journal , 88*, 407-416.

Tikalsky, P. J., Carrasquillo, P. M., & Carrasquillo, R. L. (1989). Strength and Durability Considerations Affecting Mix Proportioning of Concrete Containing Fly Ash. *ACI Materials Journal* , 505-511.

Valente, M., Vigneri, M., Bressan, M., Pasqualini, A., Bianchini, S., & Liberatore, F. M. (2010). Use of Fly Ash in Concrete: Efficiency Factors of the Supplementary Cementing Material. *Second International Conference on Sustainable Construction Materials and Technologies* .

Appendix A – Temperature and Humidity Report

As discussed in Chapter 3, an environmental control room was not available for the creep and shrinkage test. Instead the ambient temperature and relative humidity change was recorded during the test. Both temperature and humidity was recorded using two meters (Planet Waves Meters). Only the highest and the lowest values were recorded. Figure A-1 and A-2, display the average value of the two meters during the test. The temperature ranged from 18.9 to 27.8°C and the relative humidity ranged from 20 to 74%. Table A-1 summarizes the beginning of each creep test.

Table A-1: Date of beginning for each test

Name of Test	Date of Start
7-day SCM	June 4th, 2010
14-day SCM	June 10th, 2010
28-day SCM	June 17th, 2010
7-day Base	June 13th, 2010

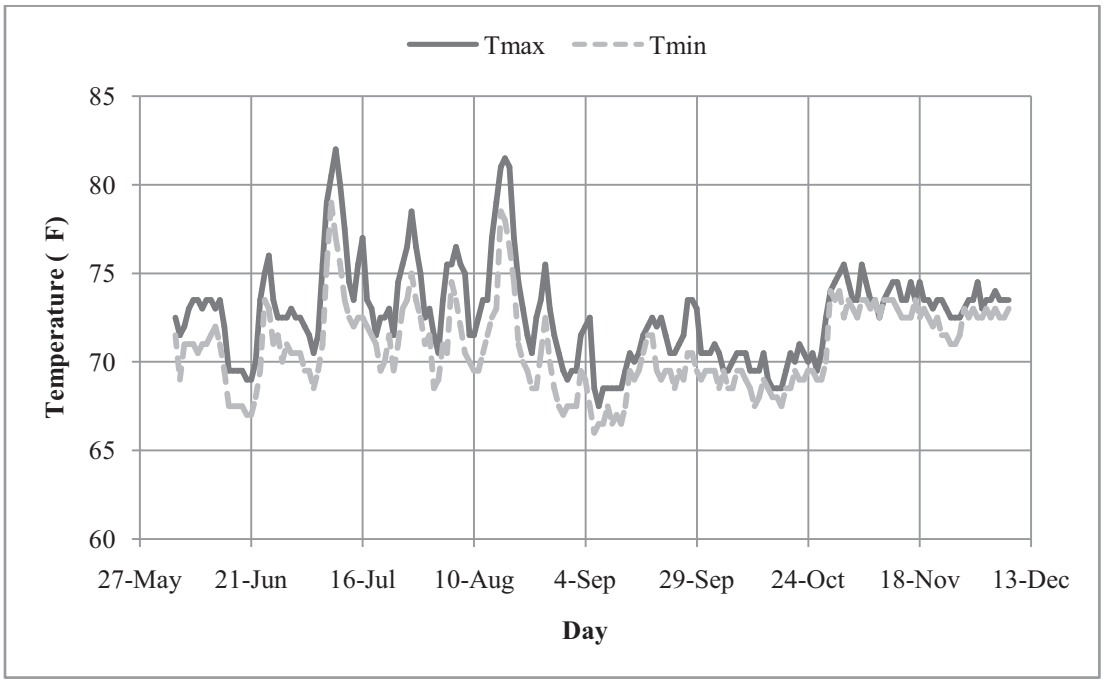

Figure A-1: Room temperature measurement during creep test

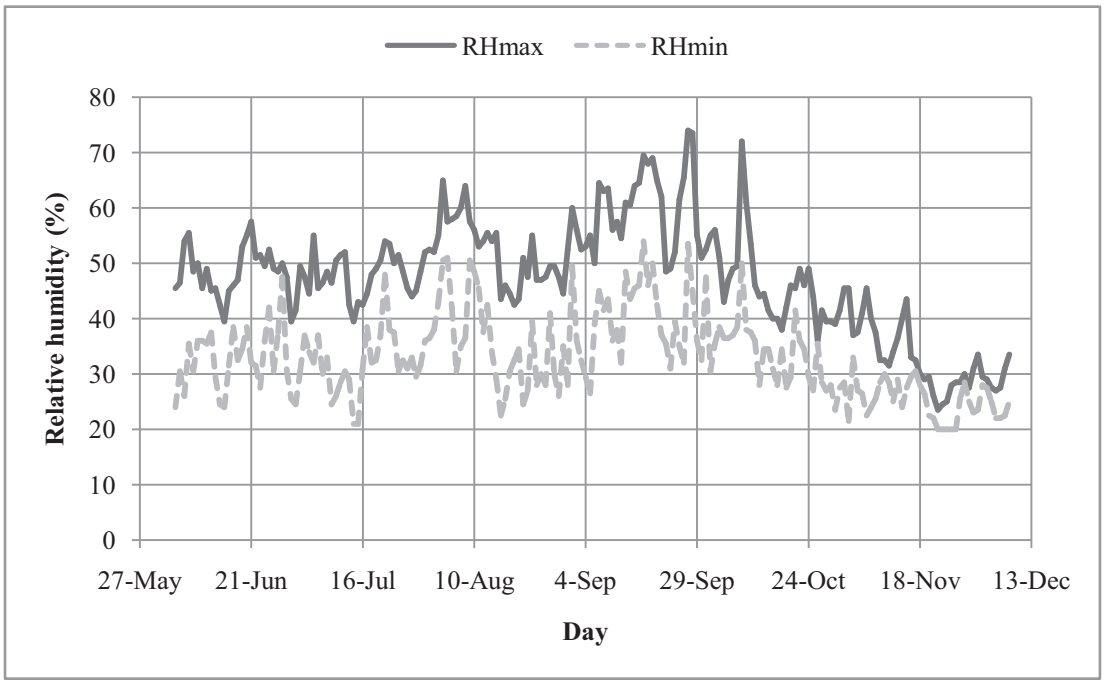

Figure A-2: Humidity measurement during creep test

Appendix B – Compressive Strength Data

As discussed in Chapter 3, the compressive strength test was performed in two phases. The compressive strength was obtained according to ASTM C 39.

The first Phase mixes were cast in the summer of 2009 with all mixes made with w/b ratio of 0.35. Tables B-1 through B-5, present the compressive strength of each concrete cylinder in Phase I.

The second Phase mixes were cast in the summer of 2010 with all mixes made with w/b ratio of 0.40. Tables B-6 through B-11, present the compressive strength of each concrete cylinder in Phase II.

Phase I

Table B-1: The compressive strength trials of the Boardman FA in Phase I

Boardman Fly Ash Trials					
Days of Curing	Compressive Strength (MPa)				
	20%	40%	60%	80%	100%
7	64.54	63.86	50.02	6.37	4.56
7	65.12	62.96	51.01	5.83	4.98
7	64.12	61.20	51.11	6.12	4.85
14	71.00	72.73	63.37	6.84	6.23
14	71.20	72.50	63.90	8.88	6.52
14	69.80	71.10	62.58	7.13	6.36
28	79.85	83.48	76.06	33.23	6.74
28	80.09	83.01	75.17	36.48	7.14
28	80.12	83.88	76.01	35.50	7.25
56	88.94	91.45	86.23	68.41	8.69
56	88.30	90.45	86.41	67.02	8.99
56	88.69	91.66	87.02	66.39	9.03
84	90.67	100.44	91.65	74.68	10.65
84	92.33	101.10	90.33	73.02	10.22
84	92.55	100.21	91.89	75.22	11.01
168	93.56	101.33	94.20	88.60	17.70
168	94.66	102.50	94.80	88.10	18.55
168	94.11	102.80	95.00	87.20	18.66

Table B-2: The compressive strength trials of the Centralia FA in Phase I

Centralia Fly Ash Trials					
Days of Curing	Compressive Strength (MPa)				
	20%	40%	60%	80%	100%
7	68.22	65.27	45.82	19.53	1.24
7	67.59	65.06	42.20	18.82	1.25
7	67.80	65.50	44.50	18.52	1.25
14	79.80	70.52	54.26	21.71	1.48
14	78.80	70.00	50.10	20.30	1.56
14	79.10	71.10	54.30	21.12	1.42
28	83.62	87.70	63.71	32.84	1.64
28	83.99	86.76	63.21	31.55	1.77
28	85.04	86.66	63.58	31.65	1.85
56	94.57	95.57	76.25	46.50	1.90
56	95.47	94.71	79.06	45.29	1.88
56	94.22	94.51	77.88	44.98	1.95
84	94.50	96.23	84.17	47.89	1.99
84	97.10	96.55	83.55	50.01	2.22
84	96.30	97.30	86.01	49.66	2.30
168	98.22	97.88	90.12	65.08	2.65
168	99.01	97.11	90.55	66.25	2.88
168	98.33	97.69	90.36	65.39	3.02

Table B-3: The compressive strength trials of the St. Mary's SL in Phase I

St. Mary's Slag Ash Trials					
Days of Curing	Compressive Strength (MPa)				
	20%	40%	60%	80%	100%
7	63.09	51.00	37.29	29.65	11.94
7	63.25	51.07	37.12	27.80	12.29
7	62.20	51.20	37.50	28.50	12.10
14	76.24	66.45	58.86	43.43	13.50
14	45.50	66.89	57.02	43.85	13.98
14	76.38	64.87	58.23	42.11	14.21
28	87.02	81.86	76.39	51.97	19.48
28	82.58	87.36	75.55	51.25	18.02
28	85.47	81.25	75.41	49.63	19.22
56	92.78	88.12	84.50	53.07	20.96
56	94.58	88.92	85.39	53.66	21.04
56	93.33	88.37	84.98	52.96	21.13
84	95.00	94.40	89.70	55.60	24.50
84	96.20	94.80	90.20	56.30	23.60
84	96.30	95.60	89.90	54.90	23.80
168	97.18	98.22	90.05	59.28	27.55
168	97.66	96.98	91.22	60.23	28.66
168	97.55	96.25	90.35	60.58	28.54

Table B-4: The compressive strength trials of the Seattle SL in Phase I

Seattle Slag Ash Trials					
Days of Curing	Compressive Strength (MPa)				
	20%	40%	60%	80%	100%
7	52.48	51.59	44.35	36.90	11.64
7	53.78	50.85	44.52	36.89	12.87
7	53.30	53.22	42.30	36.50	11.85
14	65.65	64.23	55.59	46.93	16.93
14	54.50	61.50	54.89	46.90	16.34
14	65.21	63.30	55.12	45.20	16.52
28	73.41	78.01	66.62	55.96	20.50
28	69.88	75.77	66.03	53.59	20.48
28	72.25	75.98	66.66	55.12	20.20
56	81.04	82.33	77.71	67.22	25.93
56	80.79	83.01	76.26	68.99	26.99
56	80.55	81.61	78.01	66.89	27.02
84	81.95	88.61	86.30	70.02	31.33
84	82.56	87.90	85.30	7.04	32.66
84	83.02	88.03	86.77	69.89	33.02
168	86.03	89.71	89.68	75.55	37.20
168	87.22	90.22	90.23	76.89	38.66
168	86.55	90.33	90.98	77.21	38.25

Table B-5: The compressive strength trials of the Base mix in Phase I

Portland Cement Trials	
Days of Curing	Compressive Strength (MPa) 0%
7	65.05
7	65.10
7	63.61
14	74.73
14	72.32
14	74.20
28	79.97
28	80.11
28	80.00
56	81.50
56	80.90
56	82.10
84	83.22
84	82.99
84	83.66
168	84.97
168	84.55
168	85.66

Phase II

Table B-6: The compressive strength trials of the Boardman FA in Phase II

Boardman Fly Ash Trials			
Days of Curing	Compressive Strength (MPa) 60%	80%	90%
7	27.03	16.27	3.23
7	26.12	17.72	2.99
7	27.11	17.06	3.69
14	32.88	25.39	5.02
14	32.01	25.88	5.13
14	32.45	26.01	4.89
28	33.16	39.53	10.81
28	34.26	40.11	11.02
28	34.88	40.23	10.95
56	43.06	50.58	22.00
56	45.66	51.22	22.10
56	44.25	50.33	22.30
112	--	--	28.20
112	--	--	29.02
112	--	--	29.41
168	--	--	32.24
168	--	--	33.55
168	--	--	32.69

Table B-7: The compressive strength trials of the Seattle SL in Phase II

Seattle Slag Trials			
Days of Curing	Compressive Strength (MPa)		
	60%	80%	90%
7	38.99	37.60	23.14
7	39.66	38.22	22.58
7	40.12	37.98	23.66
14	50.22	47.29	27.82
14	48.99	46.89	28.66
14	48.69	47.03	28.41
28	51.51	57.53	37.00
28	52.33	58.06	38.22
28	53.11	57.11	38.45
56	65.31	77.09	45.06
56	66.89	76.25	46.20
56	66.12	77.15	46.33
112	68.60	74.67	52.92
112	68.53	69.08	51.35
112	63.42	79.54	53.43
168	--	--	48.15
168	--	--	51.22
168	--	--	50.36

Table B-8: The compressive strength trials of the ternary 25FA-75SL mix in Phase II

25FA-75SL Trials			
Days of Curing	Compressive Strength (MPa)		
	60%	80%	90%
7	30.26	30.07	26.15
7	30.55	30.25	25.88
7	31.89	31.22	25.32
14	41.22	38.02	37.07
14	42.33	38.69	38.95
14	41.88	37.66	39.03
28	54.78	63.32	47.00
28	53.69	62.59	47.17
28	54.21	63.00	47.33
56	64.40	64.80	58.18
56	63.50	65.30	58.12
56	64.10	65.80	59.00
112	77.03	81.46	65.18
112	73.47	69.43	67.41
112	66.80	64.87	67.26
168	75.46	76.53	68.51
168	74.22	77.98	67.22
168	76.33	75.89	69.98

Table B-9: The compressive strength trials of the ternary 50FA-50SL mix in Phase II

50FA-50SL Trials			
Days of Curing	Compressive Strength (MPa)		
	60%	80%	90%
7	34.06	20.37	10.63
7	33.58	21.05	11.74
7	34.22	20.35	12.01
14	44.29	29.79	19.89
14	45.63	30.56	21.02
14	45.69	31.05	20.66
28	55.80	41.15	33.06
28	56.32	42.03	32.59
28	56.02	41.11	33.25
56	72.29	59.60	46.73
56	72.33	60.11	47.88
56	71.55	59.65	47.62
112	79.65	56.66	61.38
112	71.03	65.90	58.90
112	68.10	69.56	63.15
168	84.70	74.10	59.70
168	85.66	73.22	61.25
168	83.22	75.03	59.88

Table B-10: The compressive strength trials of the ternary 75FA-25SL mix in Phase II

75FA-25SL Trials			
Days of Curing	Compressive Strength (MPa)		
	60%	80%	90%
7	24.96	14.10	10.96
7	25.68	14.66	11.25
7	25.44	14.22	11.69
14	35.31	20.37	17.71
14	36.02	21.56	18.66
14	36.55	21.66	18.01
28	48.66	28.06	31.64
28	50.01	28.15	32.25
28	48.33	27.85	31.97
56	55.85	42.02	48.80
56	56.95	42.00	48.56
56	56.33	42.60	48.21
112	57.59	56.43	57.56
112	66.32	61.09	61.14
112	67.63	59.69	60.77
168	67.77	76.53	61.25
168	68.95	77.98	63.02
168	68.12	75.89	61.33

Table B-11: The compressive strength trials of the Base mix in Phase II

Portland Cement Trials	
Days of Curing	Compressive Strength (MPa) 0%
7	51.66
7	52.07
7	52.11
14	63.11
14	61.02
14	62.11
28	65.66
28	67.88
28	68.22
56	71.22
56	70.99
56	72.66
112	73.35
112	67.70
112	74.33
168	--
168	--
168	--

Appendix C – Elastic Modulus Data

As discussed in Chapter 3, the elastic modulus was found by using the chord modulus according to ASTM C 469. Elastic modulus was only performed on the Base II mix and ternary mixes in Phase II. Tables C-1 through C-5, presents the elastic modulus of each concrete cylinder at age 7, 14, 28, 56 and 112 days.

Table C-1: Elastic modulus trials at age 7 days

7 day - Elastic Moduli according to ASTM C 469						
Mix	σ_{max} (psi)	S_2 (psi)	S_1 (psi)	ε_2 (in/in)	ε_1 (in/in)	E (ksi)
Base II	7534	3014	205	0.000463	0.00005	6798
	7534	3014	270	0.000448	0.00005	6885
60% 25-75	4410	1764	166	0.00036	0.00005	5091
	4410	1544	182	0.00033	0.00005	4856
60% 50-50	4905	1962	145	0.00044	0.00005	4658
	4905	1962	113	0.00046	0.00005	4503
60% 75-25	3672	1469	162	0.00035	0.00005	4345
	3672	1469	168	0.00035	0.00005	4324
80% 25-75	4374	1750	119	0.00047	0.00005	3894
	4374	1750	170	0.00042	0.00005	4263
80% 50-50	3003	1201	112	0.00032	0.00005	4095
	3003	1201	106	0.00036	0.00005	3542
80% 75-25	2085	834	139	0.00023	0.00005	3773
	2085	834	215	0.00020	0.00005	4055
90% 25-75	3773	1509	56	0.00041	0.00005	4019
	3773	1509	149	0.00037	0.00005	4218
90% 50-50	1662	665	189	0.00016	0.00005	4159
	1662	665	137	0.00019	0.00005	3848
90% 75-25	1611	644	162	0.00017	0.00005	3955
	1611	644	177	0.00017	0.00005	3843

Table C-2: Elastic modulus trials at age 14 days

14 day - Elastic Moduli according to ASTM C 469						
Mix	σ_{max} (psi)	S_2 (psi)	S_1 (psi)	ε_2 (in/in)	ε_1 (in/in)	E (ksi)
Base II	9003	3601	116	0.000565	0.00005	6772
	9003	3601	194	0.000592	0.00005	6286
60% 25-75	6059	2424	210	0.00048	0.00005	5108
	6059	2424	129	0.00054	0.00005	4707
60% 50-50	6520	2608	218	0.00050	0.00005	5258
	6520	2608	246	0.00048	0.00005	5489
60% 75-25	5173	2069	142	0.00046	0.00005	4721
	5173	2069	122	0.00043	0.00005	5144
80% 25-75	5563	2225	160	0.00052	0.00005	4391
	5563	2225	144	0.00050	0.00005	4588
80% 50-50	4376	1750	233	0.00034	0.00005	5186
	4376	1750	220	0.00034	0.00005	5219
80% 75-25	3075	1230	182	0.00026	0.00005	5010
	3075	1230	244	0.00024	0.00005	5275
90% 25-75	5562	2225	182	0.00049	0.00005	4627
	5562	2225	189	0.00047	0.00005	4799
90% 50-50	2976	1190	178	0.00030	0.00005	4063
	2976	1190	136	0.00031	0.00005	4046
90% 75-25	2630	1052	208	0.00024	0.00005	4352
	2630	1052	259	0.00021	0.00005	5053

Table C-3: Elastic modulus trials at age 28 days

28 day - Elastic Moduli according to ASTM C 469						
Mix	σ_{max} (psi)	S_2 (psi)	S_1 (psi)	ε_2 (in/in)	ε_1 (in/in)	E (ksi)
Base II	9753	3901	184	0.00066	0.00005	6077
	9753	3901	185	0.00057	0.00005	7182
	9753	3901	177	0.00061	0.00005	6692
60% 25-75	7865	3146	223	0.00056	0.00005	5690
	7865	3146	178	0.00057	0.00005	5664
	7865	3146	137	0.00064	0.00005	5080
60% 50-50	8129	3252	166	0.00060	0.00005	5600
	8129	3252	223	0.00049	0.00005	6819
	8129	3252	262	0.00060	0.00005	5449
60% 75-25	7107	2843	272	0.00058	0.00005	4877
	7107	2843	182	0.00053	0.00005	5542
	7107	2843	293	0.00047	0.00005	6086
80% 25-75	9133	3653	157	0.00070	0.00005	5375
	9133	3653	147	0.00062	0.00005	6113
	9133	3653	244	0.00061	0.00005	6041
80% 50-50	6009	2404	160	0.00042	0.00005	6062
	6009	2404	234	0.00041	0.00005	6103
	6009	2404	263	0.00041	0.00005	5895
80% 75-25	4064	1626	269	0.00032	0.00005	5115
	4064	1626	280	0.00029	0.00005	5536
	4064	1626	227	0.00030	0.00005	5581
90% 25-75	6841	2736	149	0.00049	0.00005	5853
	6841	2736	187	0.00051	0.00005	5561
	6841	2736	180	0.00049	0.00005	5747
90% 50-50	4782	1913	268	0.00031	0.00005	6216
	4782	1913	192	0.00038	0.00005	5164
	4782	1913	245	0.00032	0.00005	6171
90% 75-25	4634	1854	270	0.00033	0.00005	5578
	4634	1854	281	0.00031	0.00005	6110
	4634	1854	305	0.00029	0.00005	6386

Table C-4: Elastic modulus trials at age 56 days

56 day - Elastic Moduli according to ASTM C 469						
Mix	σ_{max} (psi)	S_2 (psi)	S_1 (psi)	ε_2 (in/in)	ε_1 (in/in)	E (ksi)
Base II	10388	4155	375	0.00055	0.00005	7518
	10388	4155	275	0.00058	0.00005	7355
	10388	4155	265	0.00064	0.00005	6642
60% 25-75	9282	3713	282	0.00057	0.00005	6603
	9282	3713	216	0.00058	0.00005	6615
	9282	3713	270	0.00058	0.00005	6525
60% 50-50	10451	4180	364	0.00052	0.00005	8158
	10451	4180	314	0.00057	0.00005	7505
	10451	4180	279	0.00056	0.00005	7680
60% 75-25	8177	3271	216	0.00048	0.00005	7133
	8177	3271	301	0.00049	0.00005	6815
	8177	3271	253	0.00054	0.00005	6139
80% 25-75	9471	3788	230	0.00053	0.00005	7359
	9471	3788	351	0.00054	0.00005	6944
	9471	3788	371	0.00055	0.00005	6896
80% 50-50	8672	3469	167	0.00051	0.00005	7105
	8672	3469	315	0.00046	0.00005	7642
	8672	3469	293	0.00046	0.00005	7826
80% 75-25	6122	2449	261	0.00039	0.00005	6366
	6122	2449	263	0.00040	0.00005	6232
	6122	2449	404	0.00037	0.00005	6359
90% 25-75	8474	3390	333	0.00051	0.00005	6635
	8474	3390	392	0.00048	0.00005	7051
	8474	3390	242	0.00055	0.00005	6256
90% 50-50	6876	2750	361	0.00044	0.00005	6153
	6876	2750	322	0.00045	0.00005	6123
	6876	2750	344	0.00040	0.00005	6925
90% 75-25	7037	2815	367	0.00043	0.00005	6496
	7037	2815	402	0.00042	0.00005	6515
	7037	2815	392	0.00043	0.00005	6335

Table C-5: Elastic modulus trials at age 112 days

112 day - Elastic Moduli according to ASTM C 469						
Mix	σ_{max} (psi)	S_2 (psi)	S_1 (psi)	ε_2 (in/in)	ε_1 (in/in)	E (ksi)
Base II	10413	4165	204	0.00066	0.00005	6506
	10413	4165	50	0.00065	0.00005	6813
	10413	4165	196	0.00065	0.00005	6576
60% 25-75	10506	4202	234	0.00060	0.00005	7197
	10506	4202	223	0.00063	0.00005	6835
	10506	4202	355	0.00066	0.00005	6304
60% 50-50	10578	4231	339	0.00051	0.00005	8399
	10578	4231	290	0.00059	0.00005	7272
	10578	4231	281	0.00054	0.00005	8138
60% 75-25	9260	3704	200	0.00064	0.00005	5914
	9260	3704	450	0.00054	0.00005	6666
	9260	3704	266	0.00058	0.00005	6482
80% 25-75	10431	4172	258	0.00058	0.00005	7442
	10431	4172	253	0.00061	0.00005	7048
	10431	4172	411	0.00059	0.00005	6950
80% 50-50	9288	3715	589	0.00038	0.00005	9550
	9288	3715	328	0.00044	0.00005	8715
	9288	3715	271	0.00044	0.00005	8937
80% 75-25	8568	3427	341	0.00047	0.00005	7308
	8568	3427	329	0.00055	0.00005	6167
	8568	3427	290	0.00046	0.00005	7611
90% 25-75	9662	3865	239	0.00061	0.00005	6428
	9662	3865	294	0.00058	0.00005	6769
	9662	3865	295	0.00059	0.00005	6632
90% 50-50	8867	3547	197	0.00062	0.00005	5846
	8867	3547	287	0.00044	0.00005	8297
	8867	3547	138	0.00044	0.00005	8821
90% 75-25	8676	3470	406	0.00047	0.00005	7223
	8676	3470	232	0.00048	0.00005	7599
	8676	3470	339	0.00048	0.00005	7205

Appendix D – Creep and Shrinkage Data

As discussed in Chapter 3, the creep and shrinkage strain was obtained according to ASTM C 512. Table D-1 through Table D-4, presents the average creep and shrinkage strain values. The average values were obtained by taking the average strain of four sides.

Strains of the loaded cylinders in the rig were measured with RAM ON and RAM OFF. RAM ON refers to strain readings when both the hydraulic jack and the nuts under the bottom plate carry the load and RAM OFF refers to strain reading without the hydraulic jack (the nuts under the bottom plate carry all the load). Both RAM ON and RAM OFF should have the same strain values if there would be no stress relaxation when only the nuts carry the load. The difference between RAM ON and RAM OFF was found to negligible, that is very little stress relaxation occurs when only the nuts carry the load.

Table D-1: Creep and shrinkage data of the 90% 50FA-50SL mix that were cured for 7 days, where RAM ON is strain readings with the jack on, RAM OFF is strain reading without the jack (the nuts hold the stress) and shrinkage are the unloaded cylinders

	Loaded after 7 day (90% 50-50) - Ram ON μ strain				Loaded after 7 day (90% 50-50) - Ram OFF μ strain				Cured for 7 day (90% 50-50) - Shrinkage μ strain			
Day	Unsealed 1	Sealed 1	Unsealed 2	Sealed 2	Unsealed 1	Sealed 1	Unsealed 2	Sealed 2	Unsealed 1	Sealed 1	Unsealed 2	Sealed 2
0	0	0	0	0	0	0	0	0	0	0	0	0
0	206	184	168	179	173	180	164	181	0	0	0	0
0.08	203	201	176	186	206	198	183	187	15	12	2	5
1	230	212	201	202	224	214	204	202	8	27	2	2
2	252	247	241	218	257	246	247	219	12	18	10	3
3	275	265	263	238	274	263	271	241	26	29	26	7
4	279	254	266	239	286	254	271	235	28	16	27	10
5	345	300	314	270	346	296	311	275	64	29	62	20
6	378	318	337	300	381	314	340	304	97	51	95	41
7	404	337	365	331	408	340	367	329	126	74	130	64
14	540	365	493	358	534	357	487	354	174	82	179	72
21	569	404	514	422	562	391	509	415	186	104	196	108
28	618	449	577	457	615	449	575	460	248	148	244	161
56	736	520	692	519	732	518	686	510	314	231	340	215
84	863	574	788	574	866	571	790	571	355	268	353	232
112	894	608	827	595	898	604	830	601	354	294	358	275
140	963	632	906	621	976	633	898	616	375	288	398	299

Table D-2: Creep and shrinkage data of the 90% 50FA-50SL mix that were cured for 14 days, where RAM ON is strain readings with the jack on, RAM OFF is strain reading without the jack (the nuts hold the stress) and shrinkage are the unloaded cylinders

	Loaded after 14 day (90% 50-50) - Ram ON μ strain				Loaded after 14 day (90% 50-50) - Ram OFF μ strain				Cured for 14 day (90% 50-50) - Shrinkage μ strain			
Day	Unsealed 1	Sealed 1	Unsealed 2	Sealed 2	Unsealed 1	Sealed 1	Unsealed 2	Sealed 2	Unsealed 1	Sealed 1	Unsealed 2	Sealed 2
0	0	0	0	0	0	0	0	0	0	0	0	0
0	132	123	118	133	131	134	132	134	0	0	0	0
0.08	158	148	171	149	161	137	176	149	8	7	3	3
1	175	133	194	155	176	141	197	157	23	7	27	3
2	215	147	246	171	206	161	245	174	45	6	52	6
3	278	203	323	213	270	206	309	207	78	20	91	3
4	293	227	338	236	299	225	343	236	117	55	129	32
5	334	239	372	253	327	239	359	243	143	75	150	50
6	347	258	387	263	346	264	379	259	170	89	171	69
7	365	278	390	270	364	280	383	269	165	85	155	57
14	418	266	446	243	413	274	434	237	190	17	185	34
21	493	309	532	289	483	335	527	282	248	77	245	83
28	467	295	497	244	467	309	494	247	225	35	199	54
56	605	435	653	362	603	448	643	354	308	148	301	169
84	708	497	746	444	703	490	743	437	374	234	384	230
112	717	495	749	443	723	495	751	448	359	234	387	220
140	757	502	780	455	763	503	782	456	393	226	403	233

Table D-3: Creep and shrinkage data of the 90% 50FA-50SL mix that were cured for 28 days, where RAM ON is strain readings with the jack on, RAM OFF is strain reading without the jack (the nuts hold the stress) and shrinkage are the unloaded cylinders

	Loaded after 28 day (90% 50-50) - Ram ON μ strain				Loaded after 28 day (90% 50-50) - Ram OFF μ strain				Cured for 28 day (90% 50-50) - Shrinkage μ strain			
Day	Unsealed 1	Sealed 1	Unsealed 2	Sealed 2	Unsealed 1	Sealed 1	Unsealed 2	Sealed 2	Unsealed 1	Sealed 1	Unsealed 2	Sealed 2
0	0	0	0	0	0	0	0	0	0	0	0	0
0	59	53	72	86	62	54	82	91	0	0	0	0
0.08	75	77	92	111	78	80	96	111	8	7	3	8
1	131	117	154	127	134	122	151	131	52	42	69	32
2	165	149	185	143	157	145	180	138	63	35	83	20
3	205	156	210	145	199	159	212	159	86	59	120	49
4	207	160	234	148	202	153	232	148	103	58	135	56
5	222	170	252	160	218	165	248	155	122	66	156	56
6	250	204	274	163	249	199	270	159	136	79	159	69
7	248	196	279	160	249	196	277	160	109	62	147	45
14	225	135	267	127	225	136	267	128	93	14	140	2
21	333	211	358	202	334	206	358	203	173	85	230	52
28	375	231	411	240	371	224	408	237	239	148	284	130
56	425	337	462	290	421	329	461	287	261	176	298	171
84	429	379	456	303	422	377	457	302	255	196	283	164
112	489	411	528	369	492	408	527	363	309	239	346	225
140	498	388	531	353	491	391	528	353	318	226	333	200

Table D-4: Creep and shrinkage data of the Base II mix that were cured for 7 days, where RAM ON is strain readings with the jack on, RAM OFF is strain reading without the jack (the nuts hold the stress) and shrinkage are the unloaded cylinders

	Loaded after 7 day (Base II) - Ram ON μ strain				Loaded after 7 day (Base II) - Ram OFF μ strain				Cured for 7 day (Base II) - Shrinkage μ strain			
Day	Unsealed 1	Sealed 1	Unsealed 2	Sealed 2	Unsealed 1	Sealed 1	Unsealed 2	Sealed 2	Unsealed 1	Sealed 1	Unsealed 2	Sealed 2
0	0	0	0	0	0	0	0	0	0	0	0	0
0	90	96	78	91	90	91	73	85	7	7	7	7
0.08	119	126	94	116	111	121	89	107	10	19	19	21
1	136	130	89	95	133	127	90	95	28	40	29	21
2	138	139	125	109	143	132	119	102	31	31	24	2
3	174	132	138	121	170	132	134	121	51	47	34	25
4	184	149	146	115	187	148	145	110	61	42	33	9
5	243	188	211	195	229	181	201	192	103	74	77	38
6	225	182	192	152	226	183	191	144	119	79	77	40
7	258	205	205	136	248	201	204	135	112	71	84	47
14	316	237	289	180	314	232	288	176	187	122	163	96
21	357	239	326	188	359	238	324	172	199	92	176	83
28	439	288	397	235	434	292	395	225	282	148	257	152
56	515	307	483	280	512	305	471	276	303	158	290	148
84	614	412	576	359	610	409	570	358	377	254	353	226
112	658	475	657	435	658	471	653	430	441	314	406	288
140	690	471	689	415	691	467	689	416	483	289	452	328

Appendix E – Measured and Calculated strength from this research

Figure E-1 through Figure E-8 show the relationship between C/(S+A) ratio of the total binder and the compressive strength at days 7, 14, 28 and 56, respectively.

The base mix for each Phase was used to calibrate the Bolomey strength equation (2.1) and the proposed efficiency equation (5.1) was used to evaluate the efficiency of the SCM in this research program. The compressive strength of the SCM mixes was calculated using equation (2.4). Table E-1 through Table E-4 presents the measured strength, calculated k-values and calculated strength.

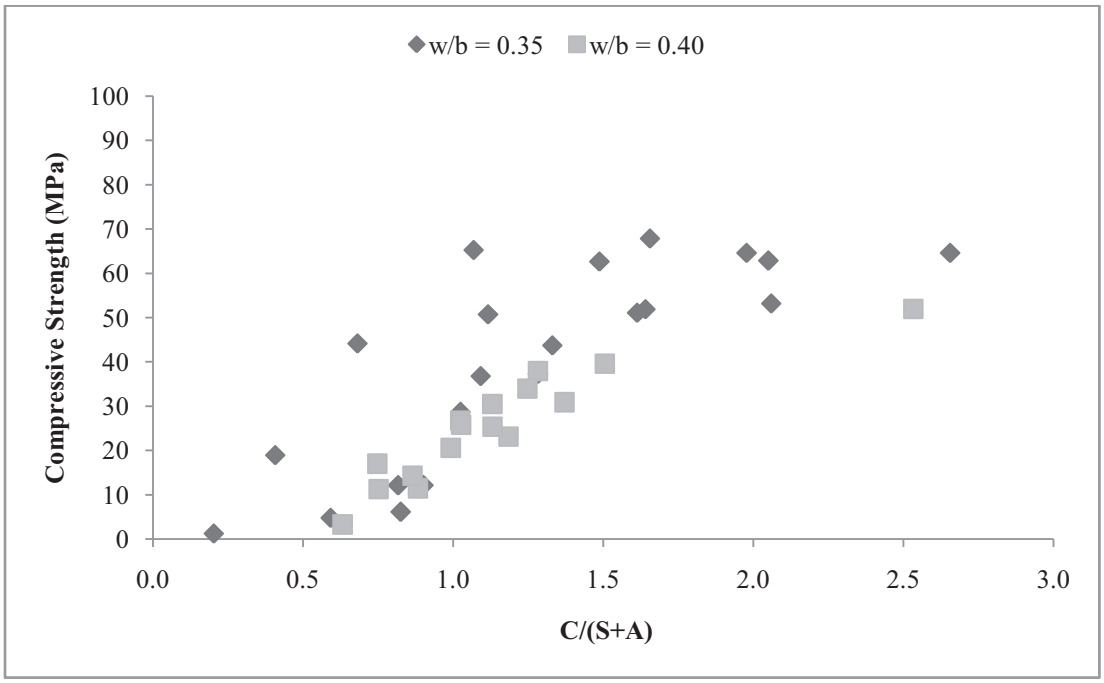

Figure E-1: Relationship between the total C/(S+A) ratio and the 7-day strength

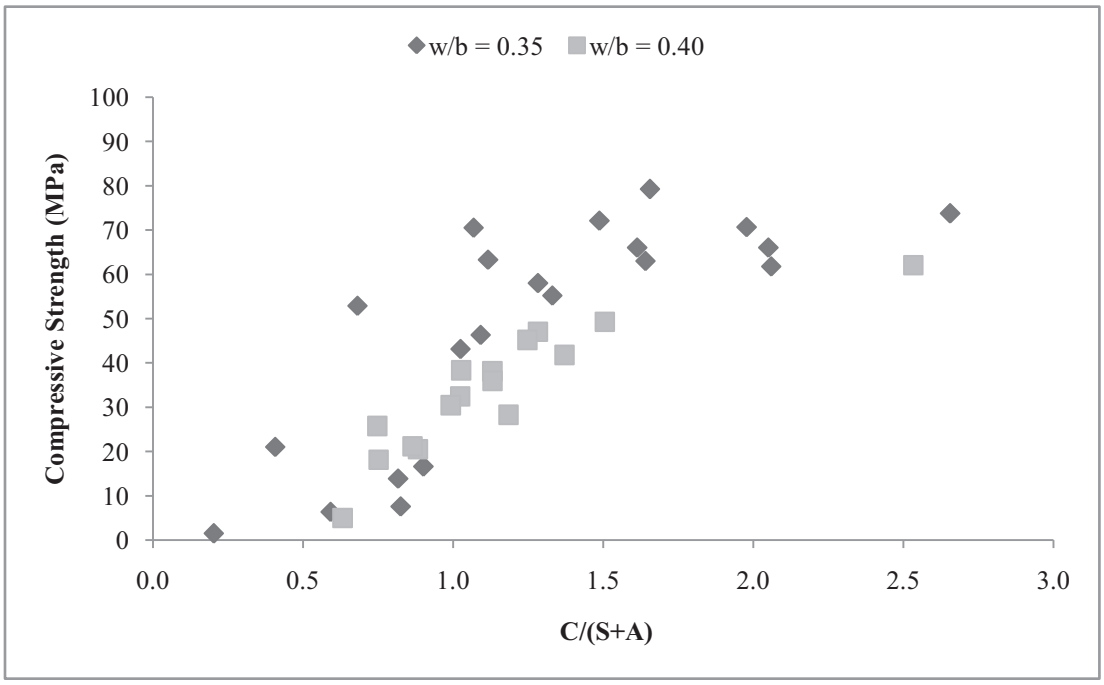

Figure E-2: Relationship between the total C/(S+A) ratio and the 14-day strength

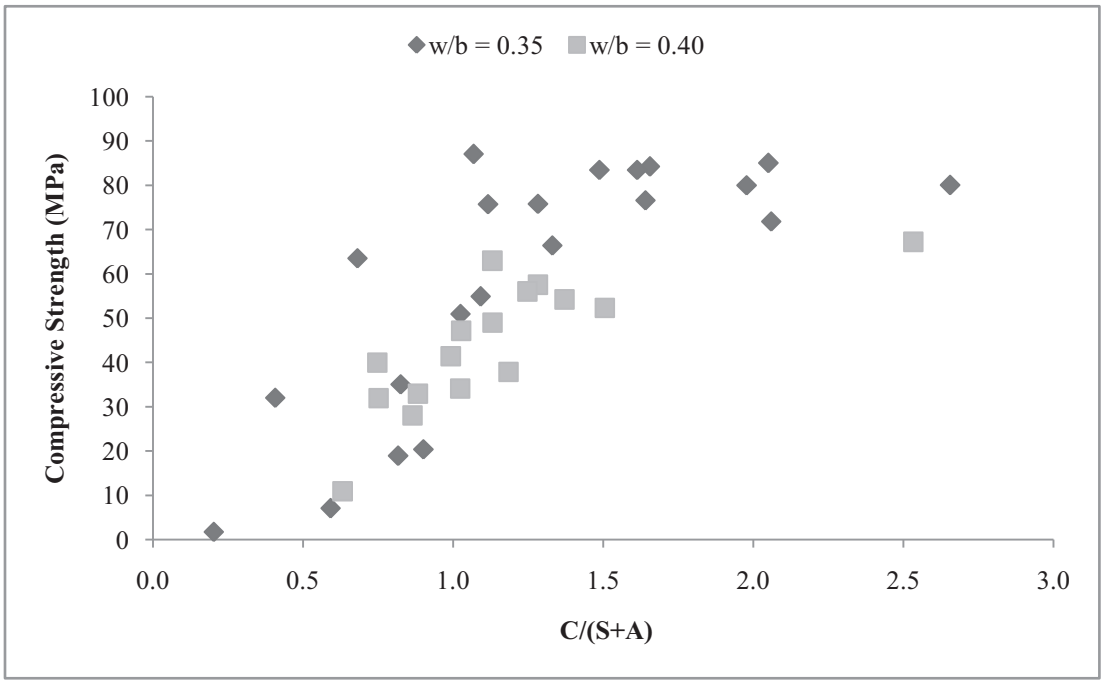

Figure E-3: Relationship between the total C/(S+A) ratio and the 28-day strength

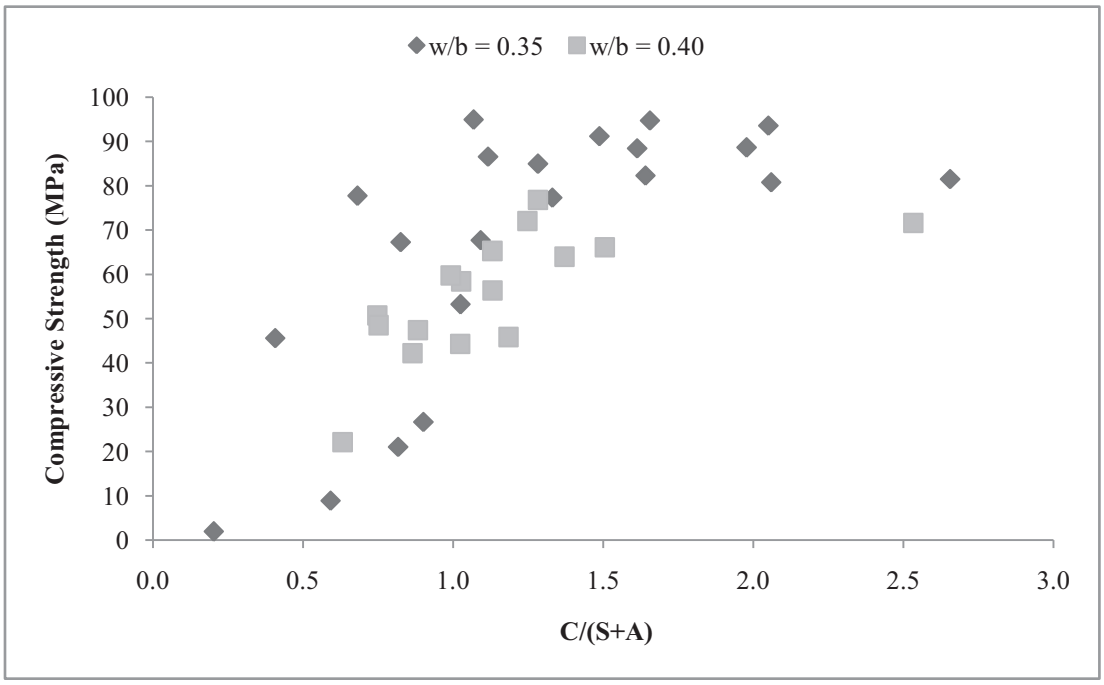

Figure E-4: Relationship between the total C/(S+A) ratio and the 56-day strength

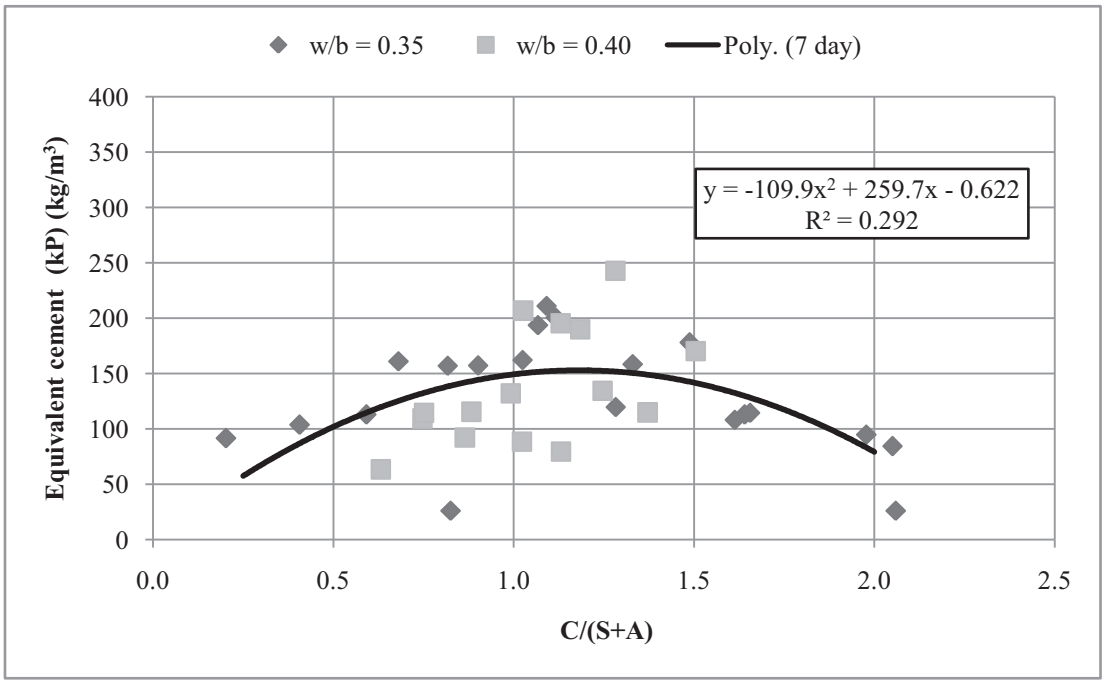

Figure E-5: Equivalent cement content versus the total C/(S+A) at an age of 7 days

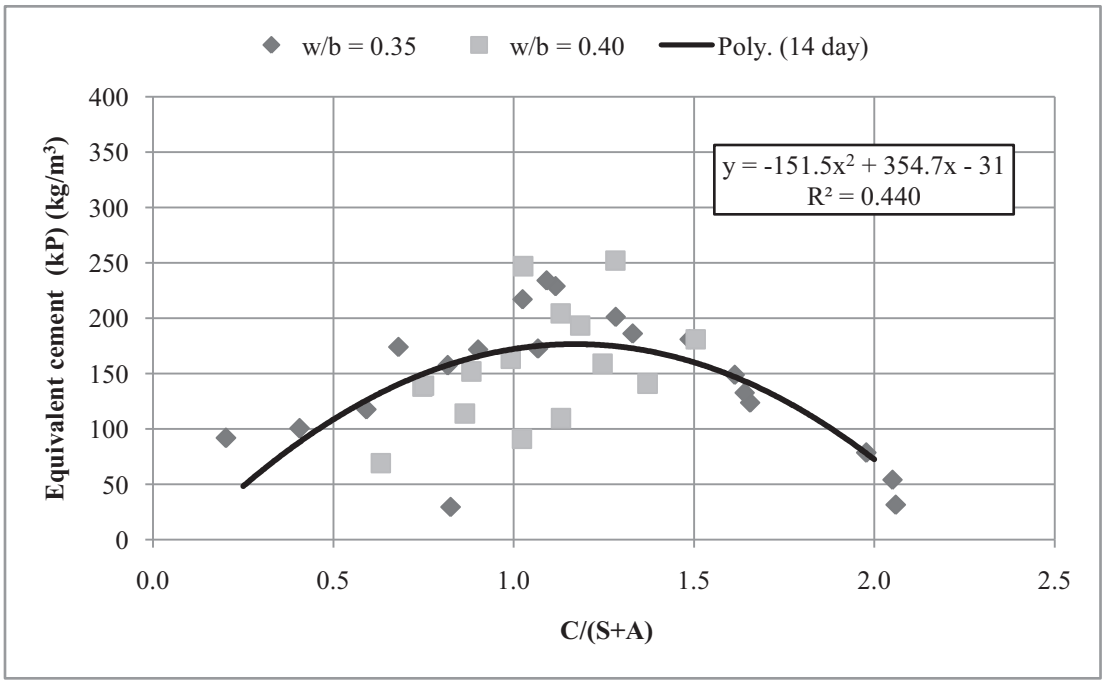

Figure E-6: Equivalent cement content versus the total C/(S+A) at an age of 14 days

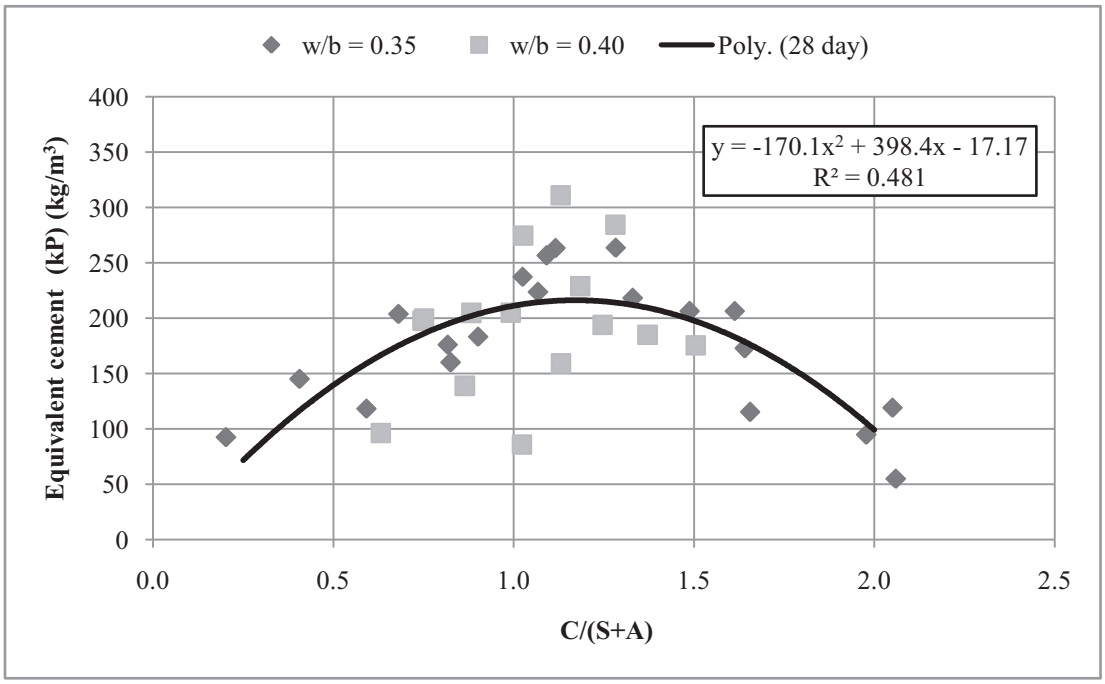

Figure E-7: Equivalent cement content versus the total C/(S+A) at an age of 28 days

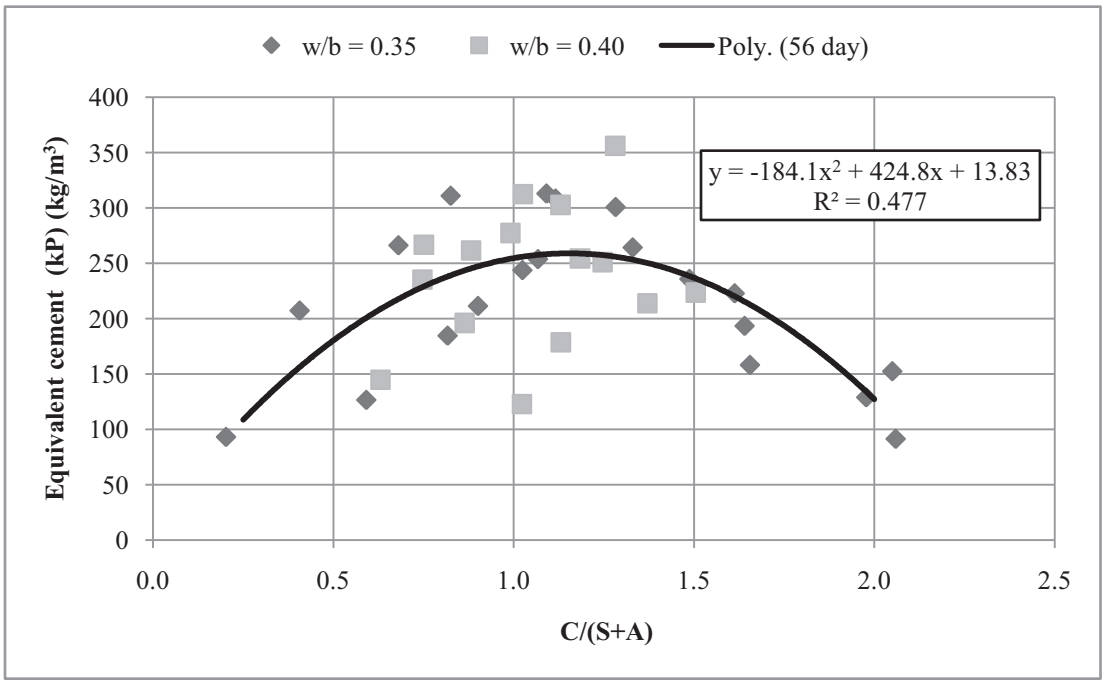

Figure E-8: Equivalent cement content versus the total C/(S+A) at an age of 56 days

Table E-1: K_B and B for the Bolomey equation determined based on the Base I mix (w/b = 0.35)

	7 days	14 days	28 days	56 days	84 days	168 days
K_B	27.83	31.77	34.48	35.11	35.88	36.65
a(t)	-0.50	-0.50	-0.50	-0.50	-0.50	-0.50

Table E-2: Measured strength calculated k-value and calculated strength for Phase I (w/b = 0.35)

SCM	%	C/(S+A)	Measured Strength (MPa)						Calculated k-value						Calculated Strength (MPa)					
			7	14	28	56	84	168	7	14	28	56	84	168	7	14	28	56	84	168
Boardman FA	20	1.98	64.59	70.67	80.02	88.64	91.85	94.11	0.83	1.01	1.20	1.38	1.49	1.67	61.91	73.99	83.86	89.04	93.18	98.96
	40	1.49	62.67	72.11	83.46	91.19	100.58	102.21	0.62	0.76	0.90	1.04	1.12	1.26	52.76	65.20	76.13	83.01	88.10	95.69
	60	1.12	50.71	63.28	75.75	86.55	91.29	94.67	0.47	0.57	0.67	0.78	0.84	0.94	39.52	50.70	61.07	68.35	73.54	81.53
	80	0.83	6.11	7.62	35.07	67.27	74.31	87.97	0.35	0.42	0.50	0.58	0.62	0.70	23.50	32.34	41.06	47.89	52.57	60.03
	100	0.59	4.80	6.37	7.04	8.90	10.63	18.30	0.25	0.30	0.36	0.41	0.44	0.50	5.53	11.25	17.55	23.31	27.08	33.34
Centralia FA	20	1.75	67.87	79.23	84.22	94.75	95.97	98.52	0.73	0.90	1.06	1.22	1.32	1.48	60.44	71.94	81.23	85.96	89.77	95.05
	40	1.17	65.28	70.54	87.04	94.93	96.69	97.56	0.49	0.60	0.70	0.81	0.88	0.98	48.53	59.29	68.55	74.10	78.29	84.44
	60	0.75	44.17	52.89	63.50	77.73	84.58	90.34	0.31	0.38	0.45	0.52	0.56	0.63	32.30	40.63	48.15	53.18	56.83	62.36
	80	0.44	18.96	21.04	32.01	45.59	49.19	65.57	0.19	0.23	0.27	0.31	0.33	0.37	13.42	18.27	23.02	26.70	29.23	33.25
	100	0.20	1.25	1.49	1.75	1.91	2.17	2.85	0.09	0.10	0.12	0.14	0.15	0.17	-7.20	-6.52	-5.23	-3.45	-2.40	-0.49
Seattle SL	20	2.06	53.19	61.79	71.85	80.79	82.51	86.60	0.86	1.05	1.24	1.44	1.55	1.74	62.45	74.74	84.82	90.17	94.42	100.38
	40	1.64	51.89	63.01	76.59	82.32	88.18	90.09	0.69	0.84	0.99	1.14	1.23	1.39	54.78	68.01	79.73	87.24	92.77	101.04
	60	1.33	43.72	55.20	66.44	77.33	86.12	90.30	0.56	0.68	0.80	0.93	1.00	1.12	43.74	56.59	68.62	77.23	83.31	92.75
	80	1.09	36.76	46.34	54.89	67.70	70.09	76.55	0.46	0.56	0.66	0.76	0.82	0.92	30.49	42.09	53.56	62.57	68.75	78.59
	100	0.90	12.12	16.60	20.39	26.65	32.34	38.04	0.38	0.46	0.54	0.63	0.68	0.76	15.72	25.45	35.76	44.71	50.65	60.38
St. Mary's SL	20	2.05	62.85	66.04	85.02	93.56	95.83	97.46	0.86	1.05	1.24	1.43	1.54	1.73	62.39	74.65	84.71	90.04	94.28	100.22
	40	1.61	51.09	66.07	83.49	88.47	94.93	97.15	0.68	0.83	0.98	1.12	1.21	1.36	54.42	67.51	79.09	86.48	91.93	100.08
	60	1.28	37.30	58.04	75.78	84.96	89.93	90.54	0.54	0.66	0.78	0.89	0.96	1.08	42.80	55.29	66.95	75.26	81.15	90.27
	80	1.02	28.65	43.13	50.95	53.23	55.60	60.03	0.43	0.52	0.62	0.71	0.77	0.87	28.74	39.64	50.42	58.89	64.69	73.94
	100	0.82	12.11	13.90	18.91	21.04	23.97	28.25	0.34	0.42	0.49	0.57	0.61	0.69	12.94	21.58	30.80	38.89	44.23	53.02

Table E-3: K_B and B for the Bolomey equation determined based on the Base II mix (w/b = 0.40)

	7 days	14 days	28 days	56 days	112 days	168 days
K_B	26.34	31.48	34.10	36.31	36.40	--
a(t)	-0.50	-0.50	-0.50	-0.50	-0.50	--

Table E-4: Measured strength calculated k-value and calculated strength for Phase II (w/b = 0.40)

SCM	%	C/(S+A)	Measured Strength (MPa)						Calculated k-value						Calculated Strength (MPa)					
			7	14	28	56	112	168	7	14	28	56	112	168	7	14	28	56	112	168
60% Bordman FA - B	60	1.02	26.75	32.45	34.10	44.32	--	--	0.43	0.52	0.62	0.71	0.81	0.86	29.61	39.82	47.95	56.18	--	--
80% Bordman FA - B	80	0.75	17.02	25.76	39.96	50.71	--	--	0.31	0.38	0.45	0.52	0.59	0.63	16.15	23.62	30.26	37.21	--	--
90% Bordman FA - B	90	0.63	3.30	5.01	10.93	22.13	28.88	32.83	0.26	0.32	0.38	0.44	0.50	0.53	8.83	14.66	20.33	26.38	31.19	--
60% Seattle SL - B	60	1.50	39.59	49.30	52.32	66.11	66.85	--	0.63	0.77	0.91	1.05	1.19	1.27	37.50	51.33	62.68	74.28	82.01	86.62
80% Seattle SL - B	80	1.28	37.93	47.07	57.57	76.83	74.43	--	0.54	0.66	0.77	0.89	1.01	1.08	27.81	40.65	52.07	64.00	72.72	--
90% Seattle SL - B	90	1.18	23.13	28.30	37.89	45.86	52.56	49.91	0.50	0.61	0.72	0.83	0.94	1.00	22.40	34.48	45.70	57.55	66.60	--
60% 25FA-75SL - B	60	1.37	30.90	41.81	54.23	64.00	72.43	75.34	0.57	0.70	0.83	0.96	1.08	1.16	35.31	48.14	58.59	69.26	76.29	80.50
80% 25FA-75SL - B	80	1.13	30.51	38.12	62.97	65.30	71.92	76.80	0.47	0.58	0.68	0.79	0.89	0.95	24.51	35.82	45.89	56.41	64.10	68.68
90% 25FA-75SL - B	90	1.03	25.78	38.35	47.17	58.43	66.61	68.57	0.43	0.52	0.62	0.72	0.81	0.87	18.52	28.81	38.44	48.64	56.47	61.13
60% 50FA-50SL - B	60	1.25	33.95	45.20	56.05	72.06	72.93	84.53	0.52	0.64	0.75	0.87	0.99	1.05	33.27	45.17	54.79	64.59	70.99	74.82
80% 50FA-50SL - B	80	0.99	20.59	30.47	41.43	59.79	64.04	74.12	0.42	0.51	0.60	0.69	0.78	0.84	21.48	31.41	40.23	49.46	56.21	60.23
90% 50FA-50SL - B	90	0.88	11.46	20.52	32.97	47.41	61.14	60.28	0.37	0.45	0.53	0.62	0.70	0.75	15.00	23.66	31.85	40.54	47.27	51.28
60% 75FA-25SL - B	60	1.13	25.36	35.96	49.00	56.38	63.85	68.28	0.47	0.58	0.68	0.79	0.89	0.96	31.38	42.40	51.25	60.24	66.05	69.53
80% 75FA-25SL - B	80	0.86	14.33	21.20	28.02	42.21	59.07	76.80	0.36	0.44	0.52	0.60	0.68	0.73	18.71	27.35	35.04	43.09	48.97	52.47
90% 75FA-25SL - B	90	0.75	11.30	18.13	31.95	48.52	59.82	61.87	0.31	0.38	0.45	0.52	0.59	0.63	11.78	18.96	25.84	33.15	38.88	42.29

Appendix F – Measured and Calculated Compressive Strength from Prior Research

As discussed in Chapter 5, papers with information about mix design and chemical composition of the SCM, were used to predict the compressive strength. Table F-1 summarizes the research papers that were used to predict the strength, the type of specimen tested and type of SCM used.

Table F-1: Research paper used to predict the compressive strength and the type of specimens tested

Authors	Year	%	Specimen	SCM
Han, et al.	2003	0-30	100x200 mm cylinders	Fly ash
Langley, et al.	1989	55-56	150x300 mm cylinders	Fly ash
Naik, et al.	1998	0-40	150x300 mm cylinders	Fly ash
Obla, et al.	2003	0-11	102x203 mm cylinders	Fly ash
Oner, et al.	2005	0-37	150 mm cubes	Fly ash
Oner, et al.	2007	0-61	150 mm cubes	Slag
Pekmezci, et al.	2004	0-29	50 mm cubes	Natural Pozzolan
Ravina, et al.	1988	0-60	76x152 mm cylinders	Fly ash
Sivasundaram, et al.	1991	58	152x305 mm cylinders	Fly ash
Valente, et al.	2010	0-35	150 mm cubes	Fly ash

The base mix in each paper was used to calibrate the Bolomey strength equation (2.1) and the proposed efficiency equation (5.1) was used to evaluate the efficiency of the SCM. The compressive strength of the SCM mixes was calculated using equation (2.4). Table F-2 through Table F-22 presents the measured strength, calculated k-values and calculated strength from the papers in Table F-1.

Table F-2: K_B and B for the Bolomey equation determined based on the base mix using data from Han, et al. 2003

	3 days	7 days	28 days	90 days	180 days	365 days
K_B	20.63	18.76	19.22	17.34	19.48	19.81
a(t)	-0.87	-0.33	0.07	0.58	0.54	0.54

Table F-3: Measured strength calculated k-value and calculated strength using data from Han, et al. 2003 and Eq. (5.1)

Mixture no.	%	C/(S+A)	Measured Strength (MPa)						Calculated k-value						Calculated Strength (MPa)					
			3	7	28	90	180	365	3	7	28	90	180	365	3	7	28	90	180	365
WC60-0	0	2.52	15.4	23.6	32.9	38.6	41.6	42.5	0.77	1.06	1.52	1.92	2.15	2.39	16.4	25.0	33.3	38.9	42.9	43.7
WC60-10	10	1.81	13.1	21.8	33.8	40.3	45.4	47.6	0.55	0.76	1.10	1.38	1.55	1.72	14.9	24.2	33.6	40.0	44.7	46.1
WC60-20	20	1.34	10.2	18.0	28.0	37.2	41.6	44.8	0.41	0.56	0.81	1.02	1.15	1.28	12.4	22.3	32.1	39.1	43.9	45.5
WC60-30	30	1.01	7.2	13.5	25.0	36.0	40.1	43.2	0.31	0.43	0.61	0.77	0.87	0.96	9.3	19.6	29.6	36.9	41.6	43.3
WC55-0	0	2.52	18.7	26.6	36.1	40.2	46.3	46.5	0.77	1.06	1.52	1.92	2.15	2.39	19.4	27.7	36.1	41.5	45.8	46.6
WC55-10	10	1.81	16.0	25.4	38.3	45.8	49.6	51.8	0.55	0.76	1.10	1.38	1.55	1.72	17.8	26.9	36.5	42.7	47.7	49.2
WC55-20	20	1.34	14.6	22.6	33.8	43.5	50.0	52.1	0.41	0.56	0.81	1.02	1.15	1.28	15.0	24.8	34.8	41.6	46.8	48.6
WC55-30	28	1.06	12.7	18.3	30.9	39.3	47.0	48.2	0.33	0.45	0.64	0.81	0.91	1.01	12.7	22.7	33.0	40.1	45.3	47.1
WC40-0	0	2.52	34.0	43.6	49.7	56.3	60.4	61.9	0.77	1.06	1.52	1.92	2.15	2.39	33.6	40.6	49.3	53.4	59.2	60.2
WC40-10	10	1.81	31.5	42.1	50.3	57.5	62.8	66.5	0.55	0.76	1.10	1.38	1.55	1.72	31.3	39.5	49.8	55.0	61.8	63.7
WC40-20	20	1.34	29.4	38.0	48.0	56.5	61.4	65.4	0.41	0.56	0.81	1.02	1.15	1.28	27.5	36.5	47.5	53.6	60.6	62.9
WC40-30	30	1.01	24.2	33.7	42.8	53.5	57.6	61.3	0.31	0.43	0.61	0.77	0.87	0.96	22.9	32.5	43.8	50.4	57.2	59.6
WC35-0	0	2.52	45.0	49.1	56.3	59.7	66.6	68.8	0.77	1.06	1.52	1.92	2.15	2.39	41.0	47.3	56.2	59.6	66.1	67.3
WC35-10	10	1.81	39.5	50.2	55.7	64.3	72.4	74.8	0.55	0.76	1.10	1.38	1.55	1.72	38.3	46.0	56.7	61.4	69.2	71.3
WC35-20	20	1.34	34.1	44.9	56.0	61.3	71.4	75.3	0.41	0.56	0.81	1.02	1.15	1.28	34.0	42.6	54.1	59.8	67.8	70.4
WC35-30	30	1.01	27.0	39.1	51.8	59.5	68.9	73.9	0.31	0.43	0.61	0.77	0.87	0.96	28.8	38.1	49.8	56.2	63.9	66.6
WC32-0	0	2.52	45.9	52.2	62.1	63.3	71.2	71.4	0.77	1.06	1.52	1.92	2.15	2.39	46.6	52.5	61.5	64.3	71.5	72.7
WC32-10	10	1.81	43.4	51.9	61.7	65.3	75.4	77.6	0.55	0.76	1.10	1.38	1.55	1.72	43.8	51.1	62.1	66.4	74.8	77.2
WC32-20	20	1.34	39.6	46.6	58.6	66.1	78.1	78.9	0.41	0.56	0.81	1.02	1.15	1.28	39.0	47.3	59.2	64.6	73.3	76.1
WC32-30	30	1.01	28.8	36.5	44.2	57.7	67.5	72.8	0.31	0.43	0.61	0.77	0.87	0.96	33.3	42.3	54.5	60.6	69.0	72.0
WC27-0	0	2.52	56.5	61.2	71.8	73.8	82.0	83.4	0.77	1.06	1.52	1.92	2.15	2.39	58.4	63.2	72.5	74.2	82.6	84.0
WC27-10	10	1.81	49.9	56.6	67.7	75.4	85.2	87.4	0.55	0.76	1.10	1.38	1.55	1.72	55.0	61.5	73.1	76.7	86.6	89.3
WC27-20	20	1.34	44.0	50.5	65.0	72.8	81.3	85.2	0.41	0.56	0.81	1.02	1.15	1.28	49.4	57.1	69.8	74.5	84.8	88.1
WC27-30	30	1.01	34.5	40.0	51.9	60.4	70.8	78.6	0.31	0.43	0.61	0.77	0.87	0.96	42.6	51.2	64.2	69.9	79.7	83.2

Table F-4: K_B and B for the Bolomey equation determined based on the Base I mix using data from Langley, et al. 1989

	1 days	3 days	7 days	28 days	91 days	365 days
K_B-I	42.37	8.78	16.31	15.70	15.38	22.18
a(t)-I	-2.14	1.29	0.04	0.71	1.04	0.16

Table F-5: K_B and B for the Bolomey equation determined based on the Base III mix using data from Langley, et al. 1989

	1 days	3 days	7 days	28 days	91 days	365 days
K_B-III	40.37	12.94	20.86	34.06	21.12	35.90
a(t)-III	-0.50	0.70	-0.23	-0.84	0.22	-0.72

Table F-6: Measured strength, calculated k-value and calculated strength using data from Langley, et al. 1989 and Eq. (5.1)

Cement Type	Mixture no.	%	C/(S+A)	Measured Strength (MPa)						Calculated k-value						Calculated Strength (MPa)					
				1	3	7	28	91	365	1	3	7	28	91	365	1	3	7	28	91	365
I	1	55	0.60	13.7	22.4	34.2	57.1	75.2	--	0.10	0.18	0.25	0.36	0.46	0.57	--	28.9	35.5	48.2	55.3	--
	1C	0	2.41	27.3	35.6	44.6	52.3	54.0	--	0.38	0.74	1.01	1.46	1.84	2.29	--	33.9	42.6	51.6	55.7	--
	2	56	0.58	0.6	17.7	26.0	49.1	63.0	79.0	0.09	0.18	0.25	0.35	0.45	0.56	--	27.1	32.0	44.6	51.5	59.0
	2C	0	2.41	10.2	32.2	40.4	50.7	57.3	--	0.38	0.74	1.01	1.46	1.84	2.29	--	33.9	42.6	51.6	55.7	--
	3	56	0.58	16.5	17.2	25.8	46.1	61.8	--	0.09	0.18	0.25	0.35	0.45	0.56	--	25.8	29.5	41.8	48.6	--
	3C	0	2.41	2.7	31.0	38.7	47.2	51.3	--	0.38	0.74	1.01	1.46	1.84	2.29	--	30.9	37.0	46.2	50.4	--
	4	56	0.58	20.5	15.5	20.5	37.5	53.0	69.0	0.09	0.18	0.25	0.35	0.45	0.56	--	24.9	27.5	39.8	46.4	51.1
	4C	0	2.41	4.0	30.5	34.9	44.7	49.1	52.2	0.38	0.74	1.01	1.46	1.84	2.29	--	30.6	36.4	45.6	49.9	52.2
	5	56	0.59	--	8.6	12.1	23.0	37.9	--	0.09	0.18	0.25	0.36	0.45	0.56	--	21.1	20.0	31.8	37.9	--
III	6	56	0.59	30.5	22.0	30.0	48.5	64.0	84.1	0.09	0.18	0.25	0.36	0.45	0.56	--	32.4	35.5	43.9	53.3	64.5
	6C	0	2.41	5.7	42.4	49.0	59.0	59.0	66.8	0.38	0.74	1.01	1.46	1.84	2.29	--	42.4	49.0	59.0	59.0	66.8
	7	56	0.59	30.7	16.7	23.8	37.5	53.7	63.7	0.09	0.18	0.25	0.36	0.45	0.56	--	29.1	29.8	33.6	46.4	51.6
	7C	0	2.41	--	37.5	41.1	46.1	51.0	53.2	0.38	0.74	1.01	1.46	1.84	2.29	--	37.5	41.1	46.1	51.0	53.2

Table F-7: K_B and B for the Bolomey equation determined based on the base mix using data from Naik, et al. 1998

	1 day	7 day	28 day	91 day	365 day
K_B	6.47	10.05	11.92	11.96	--
a(t)	-0.50	-0.50	-0.50	-0.50	--

Table F-8: Measured strength, calculated k-value and calculated strength using data from Naik, et al. 1998 and Eq. (5.1)

Mix no.	%	C/(S+A)	Measured Strength (MPa)					Calculated k-value					Calculated Strength (MPa)				
			1	7	28	91	365	1	7	28	91	365	1	7	28	91	365
C1	0	2.99	18.3	28.4	33.7	33.8	--	0.48	1.25	1.81	2.28	2.84	18.3	28.4	33.7	33.8	--
C2	35	1.68	12.3	36.5	47.4	55.7	70.6	0.27	0.71	1.02	1.28	1.60	11.2	22.0	29.9	33.4	--
B1	40	1.40	19.4	46.4	58.9	69.4	76.1	0.22	0.59	0.85	1.07	1.33	11.0	21.8	29.9	33.4	--
B2	40	1.28	15.3	38.1	51.2	61.1	63.8	0.20	0.54	0.77	0.98	1.21	10.7	20.8	28.3	31.5	--
B3	40	1.17	9.5	27.3	38.9	45.3	52.0	0.19	0.49	0.71	0.89	1.11	12.1	23.0	30.9	34.1	--

Table F-9: K_B and B for the Bolomey equation determined based on the base mix using data from Obla, et al. 2003

	1 day	3 day	7 day	28 day	90 day	180 day
K_B	6.83	12.33	16.51	19.26	22.75	23.54
a(t)	-0.50	-0.50	-0.50	-0.50	-0.50	-0.50

Table F-10: Measured strength, calculated k-value and calculated strength using data from Obla, et al. 2003 and Eq. (5.1)

Mix no.	%	C/(S+A)	Measured Strength (MPa)						Calculated k-value						Calculated Strength (MPa)					
			1	3	7	28	90	180	1	3	7	28	90	180	1	3	7	28	90	180
360 C	0	2.53	13.9	25.1	33.6	39.2	46.3	47.9	0.40	0.77	1.06	1.53	1.93	2.16	13.9	25.1	33.6	39.2	46.3	47.9
360 SF8	8	--	13.4	26.4	40.8	47.9	53.9	56.6	--	--	--	--	--	--	--	--	--	--	--	--
360 UF12.1	11	1.85	12.7	31.1	36.8	45.1	53.6	63.2	0.29	0.57	0.78	1.12	1.41	1.58	13.2	24.9	34.4	42.2	51.8	54.8
360 UF8	8	2.02	14.2	29.3	36.9	44.8	54.6	55.9	0.32	0.62	0.85	1.23	1.54	1.73	14.5	26.9	36.9	44.7	54.4	57.2
360 UF12.2	11	1.85	15.0	30.8	41.6	50.7	56.9	62.9	0.29	0.57	0.78	1.12	1.41	1.58	14.8	27.8	38.4	47.0	57.7	61.0
360 UF12.3	11	1.85	24.7	37.1	49.3	57.3	60.5	63.7	0.29	0.57	0.78	1.12	1.41	1.58	16.1	30.4	41.9	51.2	62.9	66.5

Table F-11: K_B and B for the Bolomey equation determined based on the base mix using data from Oner, et al. 2005

	28 day	180 day
K_B	34.96	40.67
a(t)	-0.49	-0.49

Table F-12: Measured strength, calculated k-value and calculated strength using data from Oner, et al. 2005 and Eq. (5.1)

Mixture no.	%	C/(S+A)	Measured strength (MPa)		Calculated k-value		Calculated strength (MPa)	
			28	180	28	180	28	180
C250FA00	0	2.42	23.1	26.6	1.46	2.06	23.1	26.6
C200FA30	13	1.64	21.3	25.0	0.99	1.40	20.1	25.5
C200FA50	20	1.35	22.4	26.7	0.82	1.15	21.4	27.8
C200FA65	25	1.19	22.9	27.2	0.72	1.02	22.0	29.0
C200FA85	30	1.03	22.7	27.1	0.63	0.88	22.5	29.9
C200FA100	33	0.94	21.4	25.7	0.57	0.80	22.2	29.8
C200FA115	37	0.86	20.0	24.2	0.52	0.74	22.1	29.9
C300FA00	0	2.42	29.5	34.2	1.46	2.06	29.6	34.2
C240FA35	13	1.65	27.1	32.2	1.00	1.41	26.1	32.8
C240FA60	20	1.35	29.2	34.6	0.82	1.15	27.9	35.9
C240FA80	25	1.18	29.6	35.3	0.71	1.01	28.5	37.1
C240FA100	29	1.04	29.8	35.6	0.63	0.89	28.8	37.9
C240FA120	33	0.94	28.5	34.2	0.57	0.80	28.6	37.9
C240FA140	37	0.85	26.9	32.6	0.52	0.73	28.5	38.0
C350FA00	0	2.42	35.7	41.4	1.46	2.06	35.7	41.3
C280FA40	13	1.66	33.0	38.9	1.01	1.42	31.6	39.5
C280FA70	20	1.35	35.6	42.2	0.82	1.15	33.8	43.2
C280FA95	25	1.17	36.2	43.3	0.71	1.00	34.4	44.5
C280FA120	30	1.03	36.5	43.4	0.62	0.88	34.6	45.3
C280FA140	33	0.94	35.5	42.5	0.57	0.80	34.3	45.1
C280FA165	37	0.85	33.6	40.8	0.51	0.73	34.2	45.3
C400FA00	0	2.42	41.5	48.0	1.46	2.06	41.5	48.0
C320FA50	14	1.61	39.3	46.3	0.98	1.38	37.4	46.7
C320FA80	20	1.35	41.4	49.3	0.82	1.15	39.1	49.8
C320FA105	25	1.19	42.5	50.7	0.72	1.01	39.8	51.3
C320FA135	30	1.04	42.7	50.9	0.63	0.89	40.2	52.4
C320FA160	33	0.94	41.2	49.7	0.57	0.80	40.2	52.6
C320FA185	37	0.86	39.5	48.3	0.52	0.73	40.0	52.7

Table F-13: K_B and B for the Bolomey equation determined based on the base mix using data from Oner and Akyüz 2007

	7 day	14 day	28 day	63 day	119 day	180 day	365 day
K_B	23.74	27.12	32.84	33.82	34.49	35.90	38.07
a(t)	-0.46	-0.48	-0.44	-0.44	-0.44	-0.45	-0.45

Table F-14: Measured strength, calculated k-value and calculated strength using data from Oner and Akyüz 2007 and Eq. (5.1)

Mixture no.	%	C/(S+A)	Measured Strength (MPa)							Calculated k-value							Calculated Strength (MPa)						
			7	14	28	63	119	180	365	7	14	28	63	119	180	365	7	14	28	63	119	180	365
C250GGBS00.0	0	2.42	15.3	17.6	22.7	23.2	23.7	24.6	25.9	1.01	1.24	1.46	1.72	1.93	2.06	2.29	16.2	18.1	23.0	23.6	24.1	24.9	26.1
C175GGBS00.0	0	2.42	9.2	9.7	13.0	13.3	13.6	14.1	14.5	1.01	1.24	1.46	1.72	1.93	2.06	2.29	9.0	9.8	13.0	13.3	13.6	14.0	14.6
C175GGBS37.5	18	1.90	12.7	13.4	18.1	19.3	20.0	20.5	21.4	0.80	0.98	1.15	1.36	1.52	1.63	1.81	11.7	13.8	18.8	20.5	21.9	23.3	25.7
C175GGBS75.0	30	1.62	16.4	17.4	23.5	26.8	28.1	29.0	30.5	0.68	0.83	0.98	1.16	1.30	1.39	1.54	13.7	16.6	23.0	25.6	27.8	29.9	33.4
C175GGBS125.0	42	1.40	18.6	20.2	27.0	31.7	34.8	36.2	38.4	0.59	0.72	0.85	1.00	1.12	1.20	1.33	15.5	19.3	26.9	30.5	33.4	36.2	40.9
C175GGBS175.0	50	1.26	19.1	20.6	27.8	33.1	36.5	38.2	40.8	0.53	0.65	0.76	0.90	1.01	1.08	1.20	16.7	21.1	29.6	33.9	37.4	40.7	46.4
C175GGBS225.0	56	1.17	18.5	20.1	27.2	32.9	36.1	38.0	40.9	0.49	0.60	0.71	0.83	0.93	1.00	1.11	17.5	22.4	31.6	36.5	40.5	44.2	50.6
C175GGBS275.0	61	1.10	17.1	18.5	25.1	30.4	33.7	35.8	38.7	0.46	0.56	0.67	0.79	0.88	0.94	1.04	18.0	23.2	32.9	38.3	42.6	46.7	53.6
C300GGBS00	0	2.42	19.9	22.7	28.9	29.8	30.4	31.5	33.1	1.01	1.24	1.46	1.72	1.93	2.06	2.29	20.7	23.3	29.3	30.1	30.7	31.8	33.4
C210GGBS00.0	0	2.42	12.4	13.7	17.5	18.0	18.3	18.8	19.8	1.01	1.24	1.46	1.72	1.93	2.06	2.29	12.4	13.7	17.7	18.2	18.5	19.2	20.0
C210GGBS45.0	18	1.90	16.7	18.3	23.6	25.0	26.7	27.6	28.9	0.80	0.98	1.15	1.36	1.52	1.63	1.81	15.7	18.5	24.8	26.9	28.6	30.4	33.3
C210GGBS90.0	30	1.62	21.2	23.1	30.0	33.0	35.8	37.1	39.1	0.68	0.83	0.98	1.16	1.30	1.39	1.54	17.8	21.6	29.3	32.4	35.0	37.6	41.9
C210GGBS150.0	42	1.40	23.9	26.1	34.0	40.0	43.4	45.2	47.9	0.59	0.72	0.85	1.00	1.12	1.20	1.33	19.7	24.4	33.5	37.7	41.1	44.5	50.2
C210GGBS210.0	50	1.26	24.4	26.6	34.9	40.9	45.4	47.4	50.5	0.53	0.65	0.76	0.90	1.01	1.08	1.20	20.9	26.2	36.2	41.3	45.3	49.2	55.9
C210GGBS270.0	56	1.17	24.1	26.3	34.5	40.7	45.3	47.5	50.7	0.49	0.60	0.71	0.83	0.93	1.00	1.11	21.5	27.3	38.0	43.6	48.2	52.5	59.9
C210GGBS330.0	61	1.10	22.2	24.3	31.8	37.8	42.4	44.7	47.9	0.46	0.56	0.67	0.79	0.88	0.94	1.04	22.0	28.2	39.6	45.8	50.8	55.5	63.5
C350GGBS00	0	2.42	24.9	27.8	35.0	35.9	36.5	37.9	40.0	1.01	1.24	1.46	1.72	1.93	2.06	2.29	24.9	28.0	35.1	36.0	36.7	38.1	40.1
C245GGBS00.0	0	2.42	16.1	17.9	22.6	23.0	23.5	24.3	25.6	1.01	1.24	1.46	1.72	1.93	2.06	2.29	15.8	17.6	22.4	23.0	23.5	24.3	25.5
C245GGBS52.5	18	1.90	20.8	22.9	29.0	30.3	33.0	34.3	36.2	0.80	0.98	1.15	1.36	1.52	1.63	1.81	19.4	22.8	30.1	32.5	34.5	36.6	40.2
C245GGBS105.0	30	1.62	25.6	28.3	36.1	39.2	42.5	44.3	46.9	0.68	0.83	0.98	1.16	1.30	1.39	1.54	21.8	26.3	35.2	38.9	41.9	44.9	50.0
C245GGBS175.0	42	1.40	29.6	32.4	41.4	47.7	51.7	54.0	57.4	0.59	0.72	0.85	1.00	1.12	1.20	1.33	23.6	29.2	39.6	44.4	48.3	52.2	58.8
C245GGBS245.0	50	1.26	30.1	33.0	42.3	48.5	53.5	56.0	59.7	0.53	0.65	0.76	0.90	1.01	1.08	1.20	24.7	30.9	42.3	48.0	52.6	57.1	64.7
C245GGBS315.0	56	1.17	29.5	32.4	41.5	48.1	53.7	56.3	60.2	0.49	0.60	0.71	0.83	0.93	1.00	1.11	25.1	31.8	43.9	50.3	55.4	60.3	68.7
C245GGBS385.0	61	1.10	26.6	29.2	37.5	43.5	49.0	51.7	55.2	0.46	0.56	0.67	0.79	0.88	0.94	1.04	25.0	32.0	44.5	51.3	56.8	62.0	70.9
C400GGBS00	0	2.42	29.1	32.6	40.4	41.5	42.4	44.0	46.3	1.01	1.24	1.46	1.72	1.93	2.06	2.29	28.8	32.5	40.5	41.6	42.4	44.0	46.4
C280GGBS00.0	0	2.42	19.6	21.9	27.5	28.3	28.9	29.8	31.2	1.01	1.24	1.46	1.72	1.93	2.06	2.29	18.8	21.0	26.6	27.3	27.8	28.8	30.3
C280GGBS60.0	18	1.90	24.0	26.7	33.7	35.2	37.8	39.1	41.1	0.80	0.98	1.15	1.36	1.52	1.63	1.81	22.8	26.8	35.2	37.9	40.1	42.6	46.7
C280GGBS120	30	1.62	29.8	33.1	41.8	45.9	49.1	51.0	53.8	0.68	0.83	0.98	1.16	1.30	1.39	1.54	25.5	30.8	40.9	45.0	48.4	51.9	57.7
C280GGBS200	42	1.40	33.8	37.5	47.5	54.5	58.3	60.8	64.5	0.59	0.72	0.85	1.00	1.12	1.20	1.33	27.3	33.6	45.3	50.7	55.1	59.4	66.8
C280GGBS280	50	1.26	34.4	38.1	48.4	55.3	59.9	62.6	66.7	0.53	0.65	0.76	0.90	1.01	1.08	1.20	27.8	34.7	47.2	53.5	58.5	63.4	71.8
C280GGBS360	56	1.17	33.3	37.0	47.0	54.9	59.9	62.8	67.2	0.49	0.60	0.71	0.83	0.93	1.00	1.11	28.1	35.4	48.7	55.6	61.1	66.5	75.7
C280GGBS440	61	1.10	30.2	33.5	42.7	49.6	55.2	58.3	62.4	0.46	0.56	0.67	0.79	0.88	0.94	1.04	28.0	35.6	49.3	56.7	62.6	68.3	78.1

Table F-15: K_B and B for the Bolomey equation determined based on the base mix using data from Pekmeczi and Akyüz 2004

	28 day
K_B	27.18
a(t)	-0.31

Table F-16: Measured strength, calculated k-value and calculated strength using data from Pekmeczi and Akyüz 2004 and Eq. (5.1)

Mixture no.	%	C/(S+A)	Measured Strength (MPa)	Calculated k-value	Calculated Strength (MPa)
			28	28	28
C300T00	0	2.46	26.8	1.49	26.4
C250T40	14	1.68	24.8	1.02	25.2
C250T50	17	1.56	29.2	0.94	27.9
C250T75	23	1.32	25.4	0.80	27.7
C250T100	29	1.15	26.6	0.69	28.8
C350T00	0	2.46	30.9	1.49	31.5
C300T40	12	1.78	32.9	1.07	30.7
C300T50	14	1.66	33.4	1.01	31.7
C300T75	20	1.43	34.4	0.87	33.0
C300T100	25	1.26	34	0.76	33.6
C400T00	0	2.46	42.1	1.49	41.9
C350T40	10	1.85	40.2	1.12	37.4
C350T50	12	1.74	40.8	1.06	38.6
C350T75	18	1.52	41.8	0.92	38.3
C350T100	22	1.35	42.2	0.81	38.9

Table F-17: K_B and B for the Bolomey equation determined based on the base mix using data from Ravina and Mehta 1988

	7 day	14 day	28 day	56 day	180 day	400 day
K_B	14.98	17.85	20.13	23.43	27.88	--
a(t)	-0.51	-0.51	-0.48	-0.48	-0.51	--

Table F-18: Measured strength, calculated k-value and calculated strength using data from Ravina and Mehta 1988 and Eq. (5.1)

Mixture no.	%	C/(S+A)	Measured Strength (MPa)						Calculated k-value						Calculated Strength (MPa)					
			7	14	28	56	180	400	7	14	28	56	180	400	7	14	28	56	180	400
Reference	0	2.46	10.9	12.9	15.3	17.8	20.4	20.5	1.03	1.26	1.49	1.72	2.10	2.37	10.9	12.9	15.3	17.7	20.3	--
Control - A	0	2.46	3.6	4.0	5.3	5.9	6.3	--	1.03	1.26	1.49	1.72	2.10	2.37	3.6	4.2	5.5	6.4	6.8	--
A-FA1	34	0.98	6.0	7.6	9.6	13.6	18.3	25.0	0.41	0.50	0.59	0.68	0.84	0.94	7.7	9.8	12.6	15.6	19.6	--
A-FA2	34	0.94	5.5	6.6	8.8	12.5	15.2	18.0	0.40	0.48	0.57	0.66	0.81	0.91	8.1	10.3	13.1	16.2	20.3	--
A-FA3	34	1.20	7.5	9.9	11.9	17.9	20.4	20.9	0.50	0.61	0.73	0.84	1.02	1.15	8.8	11.3	14.5	18.1	23.1	--
A-FA4	34	1.35	7.8	10.1	12.5	17.8	19.7	20.4	0.57	0.69	0.82	0.94	1.16	1.30	9.3	12.0	15.4	19.2	24.7	--
A2-FA1	51	0.63	8.7	10.3	13.1	19.9	29.8	--	0.26	0.32	0.38	0.44	0.54	0.60	9.6	12.2	15.7	19.5	24.9	--
A2-FA2	51	0.60	7.6	8.9	11.2	15.5	24.3	--	0.25	0.31	0.37	0.42	0.52	0.58	9.4	12.0	15.4	19.1	24.4	--
Control - B	0	2.46	2.4	2.9	4.0	4.8	4.9	--	1.03	1.26	1.49	1.72	2.10	2.37	2.4	2.7	3.8	4.4	4.5	--
B-FA1	43	0.78	4.5	5.3	7.4	11.2	16.4	24.0	0.33	0.40	0.47	0.54	0.67	0.75	6.8	8.8	11.5	14.3	18.3	--
B-FA2	43	0.75	4.8	5.9	7.9	11.9	15.3	23.4	0.32	0.39	0.45	0.52	0.64	0.72	6.7	8.6	11.3	14.1	17.9	--
B-FA3	43	1.01	6.6	9.0	10.4	16.6	19.3	25.5	0.42	0.52	0.61	0.71	0.86	0.97	7.7	10.0	13.1	16.5	21.5	--
B-FA4	43	1.17	5.1	7.2	9.0	14.8	16.3	18.0	0.49	0.60	0.71	0.82	1.00	1.13	8.8	11.5	15.1	19.0	24.9	--
B2-FA1	60	0.48	7.1	9.0	10.1	16.6	23.1	31.6	0.20	0.25	0.29	0.34	0.41	0.46	9.1	11.8	15.2	19.0	24.6	--
B2-FA2	60	0.47	6.9	8.9	9.6	15.2	19.6	27.3	0.20	0.24	0.28	0.33	0.40	0.45	9.0	11.6	15.0	18.7	24.0	--
C-FA1	50	0.64	3.7	4.4	5.8	10.3	15.6	21.9	0.27	0.33	0.39	0.45	0.55	0.62	5.3	6.9	9.4	11.8	15.2	--
C-FA2	50	0.62	--	4.6	6.1	9.8	14.1	20.8	0.26	0.32	0.38	0.43	0.53	0.60	--	6.8	9.2	11.5	14.8	--
C-FA3	50	0.88	5.3	6.7	8.5	14.6	19.4	27.8	0.37	0.45	0.53	0.61	0.75	0.84	6.3	8.4	11.3	14.4	18.9	--
C-FA4	50	1.04	4.7	5.6	7.3	12.9	14.9	19.8	0.44	0.53	0.63	0.73	0.89	1.00	7.0	9.4	12.6	16.2	21.5	--

Table F-19: K_B and B for the Bolomey equation determined based on the base mix using data from Sivasundaram, et al. 1991

	1 day	3 day	7 day	28 day	91 day	365 day
K_B	3.66	--	15.31	19.56	22.83	25.19
a(t)	-0.50	--	-0.50	-0.50	-0.50	-0.50

Table F-20: Measured strength, calculated k-value and calculated strength using data from Sivasundaram, et al. 1991 and Eq. (5.1)

Mixture series	FA source	Batch	%	C/(S+A)	Measured Strength (MPa)						Calculated k-value						Calculated Strength (MPa)					
					1	3	7	28	91	365	1	3	7	28	91	365	1	3	7	28	91	365
1	1	A	58	0.53	13.8	--	34.8	54.7	69.9	83.4	0.08	0.16	0.22	0.32	0.40	0.50	6.1	--	31.3	45.1	57.8	70.4
		B	58	0.53	--	--	--	55.4	--	--	0.08	0.16	0.22	0.32	0.40	0.50	--	--	--	45.4	--	--
		C	58	0.53	6.4	--	19	31.2	43.9	52.2	0.08	0.16	0.22	0.32	0.40	0.50	3.8	--	19.8	28.9	37.4	45.9
		D	58	0.53	--	--	--	28.9	--		0.08	0.16	0.22	0.32	0.40	0.50	--	--	--	28.5	--	--
		E	58	0.53	14	--	33.4	53.1	67.6	78.7	0.08	0.16	0.22	0.32	0.40	0.50	6.0	--	30.8	44.4	56.9	69.3
2	2	A	58	0.72	--	21.1	33	53	67.3	80.6	0.11	0.22	0.30	0.43	0.55	0.68	--	--	34.2	50.7	66.0	81.8
		B	58	0.72	--	--	--	48.2	--	--	0.11	0.22	0.30	0.44	0.55	0.68	--	--	--	50.8	--	--
		C	58	0.72	4.2	--	15.9	26.9	35.5	42.7	0.11	0.22	0.30	0.44	0.55	0.68	4.0	--	22.2	33.4	43.9	54.8
		D	58	0.72	--	--	--	24.5	--	--	0.11	0.22	0.30	0.44	0.55	0.68	--	--	--	33.3	--	--
		E	58	0.72	--	9.1	10.4	17.8	23.2	28	0.11	0.22	0.30	0.43	0.55	0.68	--	--	22.8	34.2	45.0	56.1
3	3	C	58	0.58	--	14	21	36.4	49.1	58.7	0.09	0.18	0.24	0.35	0.44	0.55	--	--	19.0	28.0	36.4	44.9
		D	58	0.58	--	--	--	33.6	--	--	0.09	0.18	0.24	0.35	0.44	0.55	--	--	--	27.9	--	--
4	4	A	58	0.59	--	13.5	21.9	34.8	45.4	50.8	0.09	0.18	0.25	0.36	0.45	0.56	--	--	30.7	44.8	57.9	71.0
		B	58	0.59	--	--	--	30	--	--	0.09	0.18	0.25	0.36	0.45	0.56	--	--	--	44.8	--	--
		C	58	0.60	2.8	--	17.8	28.2	35.9	39.1	0.09	0.18	0.25	0.36	0.45	0.57	3.8	--	20.4	30.2	39.2	48.5
		D	58	0.59	--	--	--	28.1	--	--	0.09	0.18	0.25	0.36	0.45	0.56	--	--	--	30.2	--	--
5	5	A	58	0.59	--	19.1	25.4	40.8	48.3	54.8	0.09	0.18	0.25	0.36	0.45	0.56	--	--	31.6	46.0	59.3	72.8
		B	58	0.59	--	--	--	40.3	--	--	0.09	0.18	0.25	0.36	0.45	0.56	--	--	--	45.8	--	--
		C	58	0.59	6.7	--	23.1	40.7	48.5	54.1	0.09	0.18	0.25	0.36	0.45	0.56	3.9	--	20.6	30.4	39.5	48.9
		D	58	0.60	--	--	--	42	--	--	0.09	0.18	0.25	0.36	0.46	0.57	--	--	--	30.4	--	--
6	6	A	58	0.55	--	15.9	19.6	32.3	41.5	48.1	0.09	0.17	0.23	0.34	0.42	0.53	--	--	26.4	38.3	49.4	60.5
		B	58	0.55	--	--	--	30.4	--	--	0.09	0.17	0.23	0.34	0.42	0.53	--	--	--	38.6	--	--
		C	58	0.56	--	12.3	15.6	27.2	32.9	36.6	0.09	0.17	0.23	0.34	0.42	0.53	--	--	19.0	28.0	36.3	44.8
		D	58	0.55	--	--	--	20	--	--	0.09	0.17	0.23	0.34	0.42	0.53	--	--	--	28.0	--	--
7	7	C	58	0.53	--	16.9	22.1	37.5	50.6		0.08	0.16	0.22	0.32	0.40	0.50	--	--	19.6	28.6	36.9	--
8	Control	A	0	2.46	5.6		23.4	29.9	34.9	38.5	0.39	0.75	1.03	1.49	1.88	2.33	5.6	--	23.4	29.9	34.9	38.5

Table F-21: K_B and B for the Bolomey equation determined based on the base mix using data from Valente, et al. 2010

	2 days	7 days	14 days	28 days	56 days	90 days
KB	28.21	26.43	27.68	29.00	29.24	32.28
a(t)	-0.91	-0.46	-0.43	-0.40	-0.28	-0.27

Table F-22: Measured strength, calculated k-value and calculated strength using data from Valente, et al. 2010 and Eq. (5.1)

Mixture no.	%	C/(S+A)	Measured Strength (MPa)						Calculated k-value						Calculated Strength (MPa)					
			2	7	14	28	56	90	2	7	14	28	56	90	2	7	14	28	56	90
1	0	2.42	20.2	30.3	32.5	36.5	40.1	43.6	0.61	1.01	1.24	1.46	1.69	1.84	20.2	30.9	33.0	35.5	39.2	43.6
2	0	2.42	31.1	41.4	43.3	44.0	48.2	56.2	0.61	1.01	1.24	1.46	1.69	1.84	30.8	40.8	43.4	46.4	50.2	55.8
3	0	2.42	37.4	48.4	52.3	55.0	58.2	62.9	0.61	1.01	1.24	1.46	1.69	1.84	37.9	47.4	50.3	53.6	57.5	63.8
4	0	2.42	45.1	53.1	55.9	61.0	65.1	72.4	0.61	1.01	1.24	1.46	1.69	1.84	44.9	54.0	57.2	60.9	64.8	71.9
5	8	1.91	14.4	25.1	29.6	30.9	34.0	37.2	0.48	0.80	0.98	1.16	1.34	1.46	14.9	26.9	29.5	32.5	36.8	41.5
6	15	1.59	15.7	26.0	30.1	32.5	35.2	43.8	0.40	0.67	0.81	0.96	1.11	1.21	16.0	28.7	31.7	35.2	40.0	45.3
7	21	1.36	16.6	26.4	31.1	37.0	42.1	46.1	0.34	0.57	0.70	0.82	0.95	1.04	16.8	29.9	33.3	37.2	42.3	48.1
8	27	1.19	17.3	27.0	32.1	36.6	43.6	47.5	0.30	0.50	0.61	0.72	0.83	0.91	17.4	30.9	34.5	38.7	44.0	50.2
9	35	0.96	17.6	27.5	34.0	39.9	46.2	50.8	0.24	0.40	0.49	0.58	0.67	0.73	18.3	32.3	36.3	40.9	46.6	53.3
10	10	1.83	23.2	34.4	38.4	39.6	44.7	50.6	0.46	0.77	0.94	1.11	1.28	1.39	24.4	36.4	39.6	43.3	48.0	54.1
11	16	1.58	24.6	36.0	39.8	42.1	47.2	55.3	0.40	0.66	0.81	0.95	1.10	1.20	25.5	38.0	41.7	46.0	51.1	57.8
12	23	1.31	25.1	38.5	42.5	47.4	52.7	58.7	0.33	0.55	0.67	0.79	0.92	1.00	26.7	39.8	44.0	48.8	54.4	61.8
13	29	1.12	25.5	38.9	43.4	50.1	56.0	62.8	0.28	0.47	0.58	0.68	0.79	0.86	27.5	41.1	45.7	50.9	56.8	64.7
14	34	0.99	26.6	41.0	46.7	53.1	59.3	64.9	0.25	0.41	0.51	0.60	0.69	0.75	28.1	42.1	47.0	52.5	58.6	66.9
15	12	1.74	28.9	43.1	45.2	51.7	56.3	61.0	0.44	0.73	0.89	1.06	1.22	1.33	30.4	42.3	46.1	50.4	55.4	62.4
16	17	1.53	30.3	43.8	47.2	52.7	57.8	65.9	0.39	0.64	0.79	0.93	1.07	1.17	31.4	43.9	48.1	52.9	58.3	65.9
17	25	1.24	31.5	45.0	50.1	55.2	61.0	69.0	0.31	0.52	0.64	0.75	0.87	0.95	32.8	46.1	50.9	56.4	62.3	70.8
18	30	1.09	32.5	46.4	52.8	58.3	64.0	72.3	0.27	0.46	0.56	0.66	0.76	0.83	33.6	47.3	52.5	58.3	64.6	73.5
19	35	0.97	34.0	47.8	55.9	61.6	66.9	74.3	0.24	0.41	0.50	0.59	0.68	0.74	34.2	48.3	53.7	59.8	66.3	75.6
20	14	1.67	34.6	47.3	54.5	56.7	62.2	71.6	0.42	0.70	0.85	1.01	1.16	1.27	34.5	46.6	50.8	55.5	60.8	68.6
21	20	1.41	36.3	49.7	56.5	62.1	65.5	73.3	0.35	0.59	0.72	0.85	0.98	1.07	35.8	48.6	53.4	58.8	64.5	73.1
22	27	1.17	38.8	53.8	57.9	65.1	69.9	77.2	0.30	0.49	0.60	0.71	0.82	0.89	37.1	50.6	55.9	61.8	68.1	77.4
23	31	1.06	40.0	54.3	59.0	66.5	71.1	79.3	0.27	0.45	0.54	0.64	0.74	0.81	37.7	51.5	57.1	63.3	69.8	79.4
24	35	0.97	40.3	55.4	61.1	68.1	74.8	85.6	0.25	0.41	0.50	0.59	0.68	0.74	38.2	52.3	58.1	64.5	71.3	81.2